Electrochemical Society

GLC Anodes Are CUSTOM MADE for JEFFERSON CHEMICALS

The Jefferson Chemical Company Inc., chlor-alkali cell room at Port Neches, Texas

ACCELERATE your cost reduction program by putting GLC custom made anodes to work in your electrolytic cells.

OUR TECHNICAL PERSONNEL can help gear GLC anode characteristics to the goals of longer anode life, longer diaphragm life, reduced power and labor costs.

PRODUCTS ELECTRODE GLC DIVISION YOU CAN TRUST

GREAT LAKES CARBON CORPORATION

18 EAST 48TH STREET, NEW YORK 17, N.Y. OFFICES IN PRINCIPAL CITIES

EDITORIAL STAFF

C. L. Faust, Chairman, Publication Committee
Cecil V. King, Editor
Norman Hackerman, Technical Editor
Ruth G. Sterns, Managing Editor
U. B. Thomas, News Editor
H. W. Salzberg, Book Review Editor
Natalie Michalski, Assistant Editor

DIVISIONAL EDITORS

W. C. Vosburgh, Battery
Milton Stern, Corrosion
R. T. Foley, Corrosion
Louis J. Frisco, Electric Insulation
Seymour Senderoff, Electrodeposition
H. C. Froelich, Electronics
Ephraim Banks, Electronics
Ernest Paskell, Electronics—Semiconductors
D. R. Frankl, Electronics—Semiconductors
Sherlock Swann, Jr., Electro-Organic
Stanley Wawzonek, Electro-Organic
John M. Blocher, Jr., Electrothermics and Metallurgy
J. H. Westbrook, Electrothermics and Metallurgy
N. J. Johnson, Industrial Electrolytic
C. W. Tobias, Theoretical Electrochemistry
A. J. deBethune, Theoretical Electrochemistry
R. M. Hurd, Theoretical Electrochemistry

ADVERTISING OFFICE

ECS

1860 Broadway, New York 23, N. Y.

ECS OFFICERS

Henry B. Linford, President
Columbia University, New York, N. Y.

F. L. LaQue, Vice-President
International Nickel Co., Inc.,
New York, N. Y.

W. J. Hamer, Vice-President
National Bureau of Standards,
Washington, D. C.

Lyle I. Gilbertson, Vice-President
Air Reduction Co., Murray Hill, N. J.

Ernest G. Enck, Treasurer
Felicity Farm,
Gwynedd Valley, Pa.

Ivor E. Campbell, Secretary
National Steel Corp., Weirton, W. Va.

Robert K. Shannon, Executive Secretary
National Headquarters, The ECS,
1860 Broadway, New York 23, N. Y.

Manuscripts submitted to the Journal should be sent, in triplicate, to the Editorial Office at 1860 Broadway, New York 23, N. Y. They should conform to the revised Instructions to Authors, last published on pp. 145C-146C of the July 1961 issue. Manuscripts so submitted become the property of The Electrochemical Society and may not be published elsewhere, in whole or in part, unless permission is requested of and granted by the Editor.

The Electrochemical Society does not maintain a supply of reprints of papers appearing in its Journal. A photoprint copy of any particular paper, however, may be obtained by corresponding direct with the Engineering Societies Library, 29 W. 39 St., New York 18, N. Y.

Inquiries re positive microfilm copies of volumes should be addressed to University Microfilms, Inc., 313 N. First St., Ann Arbor, Mich.

Walter J. Johnson, Inc., 111 Fifth Ave., New York 3, N. Y., have reprint rights to out-of-print volumes of the Journal, and also have available for sale back volumes and single issues, with the exception of the current calendar year. Anyone interested in securing back copies should correspond direct with them.

Journal of the Electrochemical Society

AUGUST 1961 **VOL. 108 • NO. 8**

CONTENTS

Editorial

"Growing up Absurd" 148C

Technical Papers

High Energy: Weight Ratio, Nickel Cadmium Cells. *J. C. Duddy and A. J. Salkind* 717
Electrochemical Corrosion of Platinum in Hydrochloric Acid Solutions. *J. Llopis and A. Sancho* 720
The Anodic Surface Oxidation of Gold. *H. A. Laitinen and M. S. Chao* 726
The Influence of Iodide Ions and Carbon Monoxide on the Anodic Dissolution of Active Iron. *K. E. Heusler and G. H. Cartledge* 732
Anodic Polarization of Stainless Steel in Chloride Solutions. *G. M. Schmid and Norman Hackerman* 741
Thermodynamics of the Interaction of Niobium and Tantalum with Oxygen and Nitrogen at Temperatures near the Melting Point. *J. P. Pemsler* 744
Niobium Solid Electrolytic Capacitors. *N. Schwartz, M. Gresh, and S. Karlik* 750
Mechanism of Addition Agent Reaction in Bright and Leveling Nickel Deposition, I. Studies with Radioactive Sodium Allyl Sulfonate. *S. E. Beacom and B. J. Riley* 758
The Electrophoretic Deposition and Recrystallization of Synthetic Fluorphlogopite Mica. *W. McNeill, J. E. Chrostowski, and T. J. Mackus* 763
Electroless Deposition of Gold from Aqueous Solution on Base Metals of Nickel and Iron-Nickel-Cobalt Alloys. *R. F. Walton* 767
Porosity Measurements on Gold Plated Copper. *M. S. Frant* 774
Influence of Thiourea on the Deposition Reactions of Iron and Nickel. *R. D. DeMars* 779
Some Factors Affecting the Surface Chromium Content of Electrochemically Treated Tin Plate. *P. R. Carter* 782
Crystal Growth and Structural Study of the Barium-Titanium-Phosphate Phosphor. *D. E. Harrison and G. Shirane* 788
Photoetching and Plating of Gallium Arsenide. *R. W. Haisty* 790
Boron Diffusion in Silicon. *E. L. Williams* 795
Lead Dioxide Anode in the Preparation of Perchlorates. *K. C. Narasimham, S. Sundararajan, and H. V. K. Udupa* 798
Electrolytic Production of Sintered Titanium from Titanium Tetrachloride at a Contact Cathode. *R. B. Head* 806

Technical Notes

Cordierite-Indialite; A New Manganese-Activated Phosphor. *F. A. Hummel* 809
Thermal Coefficients of EMF of the Silver (I) and the Silver (II) Oxide-Zinc-45% Potassium Hydroxide Systems. *S. Hills* 810

Brief Communication

Transport Numbers in Pure Fused Cesium Chloride. *E. D. Wolf* 811

Detroit Meeting Program **155C-186C**

Current Affairs **187C-202C**

Published monthly by The Electrochemical Society, Inc., from Manchester, N. H., **Executive Offices, Editorial Office** and **Circulation Dept.,** and **Advertising Office** at 1860 Broadway, New York 23, N. Y., combining the JOURNAL and TRANSACTIONS OF THE ELECTROCHEMICAL SOCIETY. Statements and opinions given in articles and papers in the JOURNAL OF THE ELECTROCHEMICAL SOCIETY are those of the contributors, and The Electrochemical Society assumes no responsibility for them. Subscription to members as part of membership service; subscription to nonmembers $24.00. Single copies $1.70 to members, $2.25 to nonmembers.

Copyright 1961 by The Electrochemical Society, Inc.

Entered as second-class matter at the Post Office at Manchester, N. H., under the act of August 24, 1912.

Editorial

"Growing up Absurd"

GROWING UP ABSURD is the title of a recent book by Paul Goodman, whose thesis is that the American economic system does not provide a satisfactory life for a great many of its young people (or adults either), or give them adequate opportunity to develop their fullest capabilities. Dr. Goodman's attitude is far too pessimistic, we think, but he does discuss problems which need continual airing and consideration by public officials, responsible laymen, and authoritative community groups.

1. Many juvenile delinquents come from crowded city slums, quarreling and indifferent parents; have no interest or ability in schools which offer them little; have no spending money or opportunity to earn any; drift into gang activities, petty stealing, and more serious crime. Social workers try to keep them out of trouble and ameliorate their home life, cannot really help much with the present lack of adequate planning.

2. Delinquents come from well-to-do homes too; they steal cars ("take them for joy-rides"), break into homes, learn to use narcotics, organize illicit parties. The reasons are, in part, lack of parental supervision and, especially, the fact that our System and Organization does not really need young people unless as customers for its plethora of goods and services. They are expected to occupy themselves with school and its associated activities, they can do nothing essential in sustaining life or well-being, they cannot even earn money in an honorable way.

3. The Beatniks are the more intelligent and educated young men who have learned enough of the System and Organization to decide they do not like it.

4. Suppose that a boy finishes high school chiefly because the local rules forbid keeping him back; he wants a job and he wants to get married, the latter partly because of the insistence of his prospective father-in-law. He achieves both objectives promptly; but the job is more boring than school, he tends a machine but no one told him what he is making. His wife is a slovenly creature, the kitchen and the child are equally dirty and unkempt. The pay isn't enough. What happens; does he become a resigned Conformist? Could the community work out a better formula for such young men?

5. Finally, consider the bright young man who graduates from college and shows promise as a professional business man, as some kind of writer or designer. He drifts into writing copy extolling the virtues of something that dissolves faster or cleans four ways better, and puts some of these things into jingles which really sell cheap chemicals at high prices. Being rather cynical and not over-scrupulous, he does not object to going as far as the regulatory agencies allow if the commissions are good.

The above paragraphs give an idea of the tenor of "Growing up Absurd." Whatever the author may think, we do not believe his argument constitutes a valid indictment of our way of life. But, in keeping with his attitude, let us comment on a recent speech by Vice-President Johnson, who suggested that we should call on "Madison Avenue," which has been so successful in selling American goods to American people, to take a greater part in selling our virtues and good-will abroad. Is it really like selling wheaties to kiddies? For the Singing Commercial, we know that billions rhymes with millions, but who has a good rhyme for "Yanqui go home"?

—CVK

Germanium *and other semiconductors from* **EAGLE-PICHER**

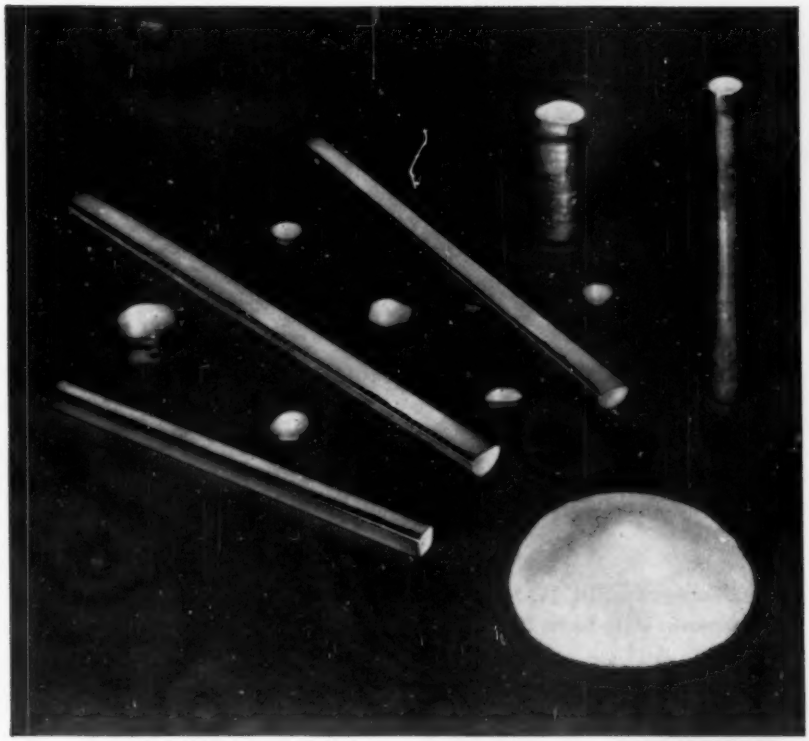

Eagle-Picher Rare Metals and Semiconductors

GERMANIUM DIOXIDE, minimum purity 99.999%.

FIRST REDUCTION GERMANIUM METAL, minimum resistivity 5 ohm-cm.

INTRINSIC GERMANIUM METAL, minimum resistivity 40 ohm-cm.

SINGLE CRYSTAL GERMANIUM [undoped] minimum resistivity 30 ohm-cm.

SINGLE CRYSTAL GERMANIUM [doped] to customers' specified resistivity.

SPECIAL SHAPES, INTRINSIC GERMANIUM METAL, for horizontal or vertical crystal growing. Wide variety in stock, other shapes furnished to customers' specifications.

SCRAP GERMANIUM PLAN, scrap Germanium may be returned for economical reprocessing under a toll arrangement.

— also immediately available

CADMIUM SULFIDE

GALLIUM, ultra pure.
Metallic crystals, minimum purity 99.9999%.
Metallic crystals, minimum purity 99.999%.

GALLIUM SESQUIOXIDE

Eagle-Picher, pioneer in Germanium, is an acknowledged leader in dependable production to meet the precise demands of the semiconductor industry. We offer a complete line of Germanium products and in addition, reprocess customers' *scrap Germanium* under our new low-cost toll arrangement.

FREE! An interesting, new brochure, "EAGLE - PICHER GERMANIUM" is now available. Write for your copy today.

EAGLE EP PICHER

Since 1843

THE EAGLE-PICHER COMPANY

Chemical Division, Dept. JES-861

GENERAL OFFICES: CINCINNATI 1, OHIO

FUTURE MEETINGS OF
The Electrochemical Society

Detroit, Mich., October 1, 2, 3, 4, and 5, 1961
Headquarters at the Statler Hotel
Sessions will be scheduled on
Batteries, Corrosion (including a Symposium on Surface Structure vs. Corrosion Behavior), Battery–Corrosion Joint Symposium on Fused Salt Corrosion, Electrodeposition (including symposia on Addition Agents and on Electrodeposited Magnetic Films), Electronics (Semiconductors), Electro-Organics, and Electrothermics and Metallurgy
(*See* pp. 155C-186C for complete program)

★ ★ ★

Los Angeles, Calif., May 6, 7, 8, 9, and 10, 1962
Headquarters at the Statler Hilton Hotel
Sessions probably will be scheduled on
Electric Insulation, Electronics (including Luminescence and Semiconductors), Electrothermics and Metallurgy, Industrial Electrolytics, and Theoretical Electrochemistry

★ ★ ★

Boston, Mass., September 16, 17, 18, 19, and 20, 1962
Headquarters at the Statler Hilton Hotel

★ ★ ★

Pittsburgh, Pa., April 14, 15, 16, 17, and 18, 1963
Headquarters at the Penn Sheraton Hotel

★ ★ ★

New York, N. Y., September 29, 30, and October 1, 2, and 3, 1963
Headquarters at the New Yorker Hotel

★ ★ ★

Toronto, Ont., Canada, May 3, 4, 5, 6, and 7, 1964
Headquarters at the Royal York Hotel

Papers are now being solicited for the meeting to be held in Los Angeles, Calif., May 6-10, 1962. Triplicate copies of each abstract (*not exceeding 75 words in length*) are due at Society Headquarters, 1860 Broadway, New York 23, N. Y., *not later than December 15, 1961* in order to be included in the program. *Please indicate on abstract for which Division's symposium the paper is to be scheduled, and underline the name of the author who will present the paper.* No paper will be placed on the program unless one of the authors, or a qualified person designated by the authors, has agreed to present it in person. An author who wishes his paper considered for publication in the JOURNAL should send triplicate copies of the manuscript to the Managing Editor of the JOURNAL, 1860 Broadway, New York 23, N. Y.

Presentation of a paper at a technical meeting of the Society does not guarantee publication in the JOURNAL. However, all papers so presented become the property of The Electrochemical Society, and may not be published elsewhere, either in whole or in part, unless permission for release is requested of and granted by the Editor. Papers already published elsewhere, or submitted for publication elsewhere, are not acceptable for oral presentation except on invitation by a Divisional program Chairman.

how do you look at ANODES?

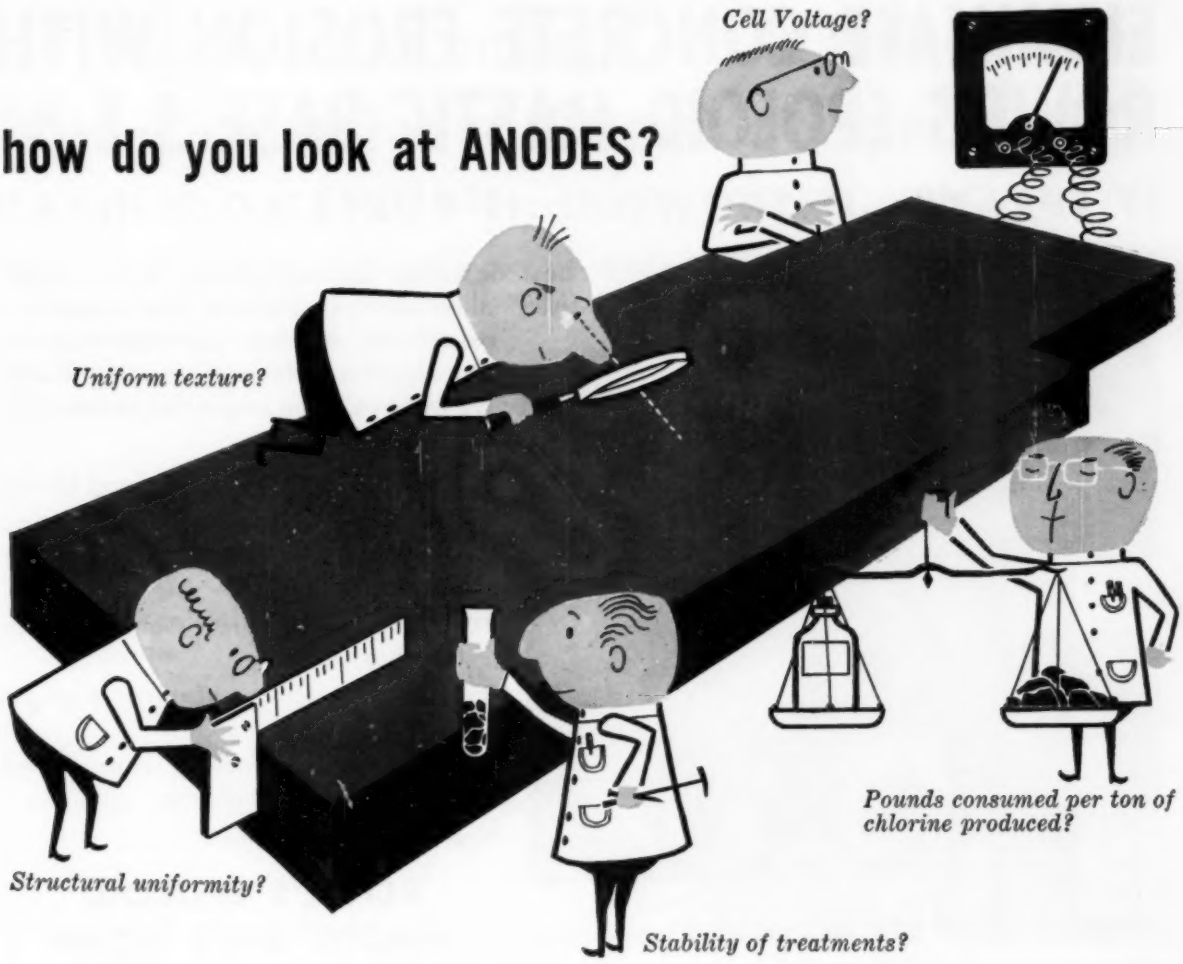

Judged by Cell Maintenance Costs Alone,

the highly stable impregnants used in Stackpole GraphAnode reduce diaphragm clogging to a bare minimum. The graphite is consumed slowly and evenly. Because GraphAnode anodes present uniform, low-porosity surfaces to the electrolyte, the graphite does not slough off to clog the diaphragm or to contaminate the cell.

Judged by Anode Cost and Performance,

Stackpole GraphAnode proves second to none whether you figure in terms of anode life, or in tons of chlorine produced per pound of graphite consumed. You get maximum anode life . . . and with the added advantage of low cell voltages. Stackpole engineers stand ready to offer a convincing demonstration on your equipment.

Stackpole Carbon Company, St. Marys, Pa.

STACKPOLE
GraphAnode®

ELECTROCHEMICAL ANODES FOR DIAPHRAGM, MERCURY, MANGANESE DIOXIDE, & SODIUM CHLORATE CELLS. OTHER TYPES FOR CATHODIC PICKLING, ALUMINUM ANODIZING, AND OTHER USES.

CATHODIC PROTECTION ANODES • FLUXING & DE-GASSING TUBES • SALT BATH RECTIFICATION RODS • ROCKET NOZZLES • RISER RODS • GRAPHITE BEARINGS & SEAL RINGS • ELECTRODES & HEATING ELEMENTS • WELDING CARBONS • VOLTAGE REGULATOR DISCS • "CERAMAGNET"® CERAMIC MAGNETS • ELECTRICAL CONTACTS • BRUSHES for all rotating electrical equipment • and many other carbon, graphite and electronic components.

ELIMINATE CONCRETE EROSION WITH ROWE'S EPOLOID MASTIC BASE 5-E-84

IT SPRAYS...IT TROWELS...IT CURES ROCK-HARD

"DOLLAR-SAVER" best describes Epoloid Mastic Base 5-E-84. Mixed with "flint-shot" silica sand, it protects new concrete—resurfaces eroded concrete—easily, quickly, at a welcome low cost—lower, we believe, than any other product on the market.

5-E-84 can be sprayed to trowel consistency 4 to 8 times faster than trowelling by hand. It can then be rolled speedily to a smooth finish.

Epoloid 5-E-84 gives long, long life to:

- concrete floors, walls, silos, holding tanks and cascade cooling tower pads.
- liners for salt brine tanks, waste trenches, sumps.
- bases for steel columns, pumps, motors.
- non-skid surfaces for ramps and industrial shower rooms.
- mortar for acid tile.

ROWE'S EPOLOID MASTIC BASE 5-E-84

...is a 100% solids blend of selected epoxy resins and plasticizers. It provides extreme hardness, yet retains maximum flexibility. It has excellent resistance to abrasion and to most chemicals. Requires no priming when sprayed, cures rapidly.

Continuous coating of 5-E-84 over juncture between steel columns or motors and concrete bases prevents seepage, rusting, erosion.

5-E-84 fills cracks, gives badly spalled, eroded floors a better-than-new surface.

WRITE FOR FREE BULLETIN

Get the facts on protecting new construction—on repairing existing trouble areas—at tremendous cost savings. Write for the "5-E-84" Technical Bulletin." It contains information on surface preparation, physical properties and resistance tables.

ROWE PRODUCTS INC.

COLLEGE AVENUE AND HYDE PARK BOULEVARD
NIAGARA FALLS, N. Y.—PHONE: BUTLER 5-9348

Specialists in protective coatings to the chemical process and allied industries since 1921.

Cut Maintenance Coating Costs In Half—or More With Rowe's Tough One-Coat Epoloid "K"

IT PRIMES...IT FINISHES—IN ONE COAT...IN ONE DAY

ONE product—Epoloid "K"—eliminates in ONE application ALL of these plant maintenance coating problems:

- Contamination between coats due to humidity and/or chemical environment
- Insufficient downtime hours to maintain structure and equipment in chemically active areas
- High cost of labor for paint application
- Large coating project with minimum man-hours available
- Economic imbalance between costs of coating materials and short-lived, ineffective protection
- Large crib stock that requires too much space, too large an investment and invites too much waste
- Delays in plant production due to in-progress painting

1—Get heavy mill build protection on sharp edges, nuts, bolts and other difficult contours.

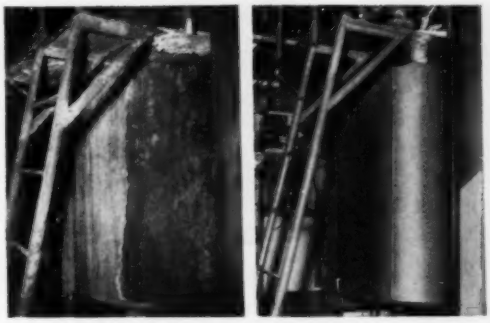

2—Get same-day preparation and coating.

ROWE'S ONE-COAT EPOLOID "K"

...is a catalyzed epoxy, scientifically formulated with a blend of epoxy resins and plasticizers, combined with chemically resistant pigments. It may be brushed or sprayed on any clean surface, free of rust and foreign matter, to provide 4-6 dry mil thickness for full, long-life protection of surfaces and equipment.

SAVE (50% of labor costs of a two-coat (prime-finish) procedure
(66% of labor costs of a three-coat (1 prime-2 finish) system

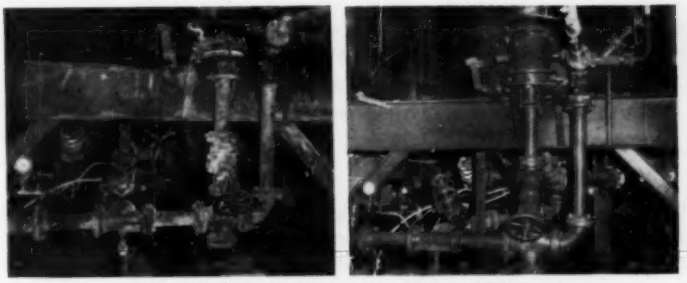

3—Get long-lasting, full protection without multiple coats.

ROWE PRODUCTS INC.

COLLEGE AVENUE AND HYDE PARK BOULEVARD
NIAGARA FALLS, N. Y.—PHONE: BUTLER 5-9348

Specialists in protective coatings to the chemical process and allied industries since 1921.

NEW from **SARGENT**

Model D

RECORDING TITRATOR

For Potentiometrically Indicated Reactions

- **DUAL MOTOR DRIVEN TITRATING ASSEMBLIES**
- **MULTIPLE DIRECT READING pH RANGES**
- **MUTIPLE DIRECT READING MILLIVOLT RANGES**
- **AUTOMATIC RATE CONTROL**
- **LOW COST**

A basic, universal recording titrator for any and all potentiometrically indicated reactions, using any form of electrode, either glass or metal, accommodating high or low resistance systems, aqueous or non-aqueous media, and all practical orders of constituent quantities whether in trace, micro or macro concentrations.

This titrator is at once a fast balancing, high precision, multi-range recording pH meter and millivolt meter and an efficient all-purpose titrating station with two independent working positions, each having full motorized titrant delivery systems with high speed filling and flushing, automatic safety switches and interchangeable small and large volume burette components. Consolidating these facilities to create an unprecedented work capacity are the synchronized burette and chart drive with direct volume reading on the chart axis and the new Sargent wide ratio automatic rate control.

For Complete Information Write For Bulletin D

Designed and Manufactured by **E. H. SARGENT & CO.**

SARGENT *SCIENTIFIC LABORATORY INSTRUMENTS • APPARATUS • SUPPLIES • CHEMICALS*

E. H. SARGENT & CO., 4647 W. FOSTER, CHICAGO 30, ILLINOIS

DETROIT 4, MICH. • DALLAS 35, TEXAS • BIRMINGHAM 4, ALA. • SPRINGFIELD, N.J.

High Energy:Weight Ratio, Nickel Cadmium Cells

J. C. Duddy and A. J. Salkind

The Carl F. Norberg Research Center, The Electric Storage Battery Company, Yardley, Pennsylvania

ABSTRACT

Conventional nickel cadmium cells contain the active materials in either porous sintered nickel plaques or in nickel or nickel-plated steel pockets or tubes. A new process, adaptable to continuous methods of production, has been developed in which the active and conductive materials are dispersed in a microporous plastic structure. Cells with the high energy to weight ratio of 40 whr/kg have been constructed. Cell volumes are equal to those of the sintered plate design for equivalent capacities.

In conventional nickel cadmium cells, the active materials are contained in the pores of sintered nickel plaques or in nickel or nickel-plated steel tubes or pockets. These cells have an energy to weight ratio of approximately 27 whr/kg for the sintered plate type, and 25 whr/kg for the pocket type. However, the active materials theoretically could deliver 250 whr/kg. The reduction in energy density is caused by the presence of electrolyte, separators, cell cases, hardware, and supporting structure for the active materials. A considerable portion of the weight of conventional nickel cadmium cells is alloted to this latter category, and the developments described in this paper were designed to produce a light-weight supporting structure for the active materials.

Experimental, Results, and Discussion

The supporting structures used in the fabrication of the nickel and cadmium electrodes described in this paper were microporous plastics. Plastic matrices, although not suitable for many electrode materials, are useful for nickel cadmium cells since the upper storage temperature imposed by the nickel electrodes is lower than the flow temperature of the matrix materials commonly available. Plastic electrodes were made by intimately mixing two incompatible polymers together on a rubber mill and loading the polymer blends with active materials. One of the two polymers was chosen so as to be soluble in some inexpensive solvent. The other was insoluble in the extraction solvent and served as a residual binding agent. When the extraction was to be done by water, the extractable polymer contained polar groups, usually hydroxyl groups, and did not have a very high degree of polymerization. Extraction of leachable polymers created capillary forces within the sheets of electrode material, and these forces were supplemented by the swelling of the polymer in the early stages of wetting by the solvent. Since the active material and residual plastic provided only nonrigid walls, the mix sheets therefore swelled 5-50% on wetting, resulting in electrodes with much greater porosity than the simple extraction of the soluble plastic could create. Electrodes produced by the above process had an average pore size of less than 1μ, but a total porosity between 10 and 50% of the volume of the electrode, depending on the ratios of active material and residual polymer to the leachable polymer, and the surface tension of the extraction solvent. These electrodes are hereafter referred to as the DP type electrodes.

Preparation of cadmium electrodes.—A typical formulation for the cadmium electrode was made by milling and sheeting a mixture of 3% polyethylene, 12% polyethylene oxide, and 85% cadmium oxide. Electrode materials prepared were given additional conductivity and strength by pressing the slabs of active material and plastic into nickel screen or wire or by extrusions on nickel screen or wire. With such formulations, the polyethylene oxide was extracted in water; a minimum of 24 hr usually was allowed for this extraction. The average pore size of electrodes was measured by making photomicrographs of thin horizontal slices of electrodes with an American Optical Model 2400 P metallograph. From photographs taken at 1500 magnifications with oil immersion lenses, the average pore size of standard production sintered plate type cadmium electrodes was found to be 2-10μ whereas the average pore size of DP electrodes after leaching of the polyethylene oxide and before formation was less than 1μ. The BET surface areas of sintered plate cadmium and plastic cadmium electrodes in the discharged condition after one charge-discharge cycle were determined and are

Table I. Surface areas obtained by BET method

Type	Sample wt, g	Areas in square meters/g: Electrode	Areas in square meters/g: Active material only
A. Cadmium Electrodes (In discharged state)			
Nickel plaque (unimpregnated)	12.08	0.2	—
Sintered cadmium	7.6	1.72	4.0*
DP (without grid) 121 A TYPE	5.40	3.9	4.1
B. Nickel Electrodes (In discharged state)			
Sintered nickel	8.05	21.9	50.0*
DP 125	2.6	35.1	—

* Calculated as 41% of electrode weight being active material.

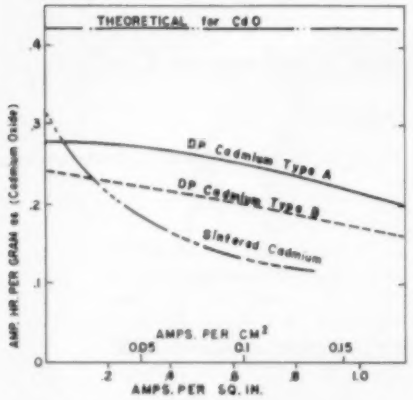

Fig. 1. Capacities of cadmium electrodes as a function of discharge rate.

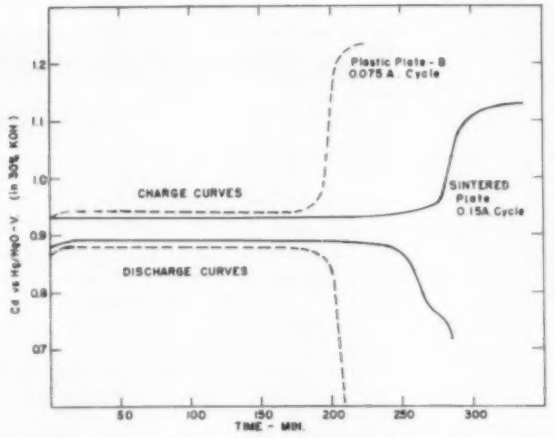

Fig. 2. Charge-discharge curves of cadmium electrodes

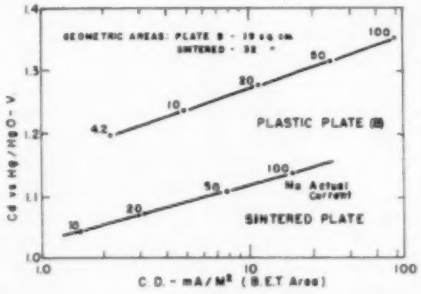

Fig. 3. Tafel curves for hydrogen evolution on cadmium electrodes. Numbers on the lines refer to the total current.

shown in Table I. Surface areas in square meters per gram are listed both in terms of total electrode weight and the weight of active material only. In the case of the sintered plates it was known that 41% of the total weight was active material. It can be seen that the raw nickel plaque contributes very little to the surface area of a plate and that the plastic cadmium electrodes have the same area per gram of active material as the sintered cadmium type.

Performance characteristics of cadmium electrodes.—The cadmium electrodes prepared by these techniques were capable of high-rate discharges without the addition of extra conductive powders. A comparison of discharge performance characteristics for 0.63 mm thick (0.025 in.) sintered plate and plastic cadmium electrodes is shown in Fig. 1. The A type in this figure is of the same type as the electrode used for the area determination given in Table I. The B type was obtained by a variation in the surface tension of the extraction solvent. Although the plastic electrodes did not perform as well as the sintered type at discharge rates below 0.03 amp/cm² (0.2 amp/in.²), at higher discharge rates they had better performance characteristics than the sintered type cadmium plates. As can be seen in the graph, at the extreme rate of 0.19 amp/cm² (equal to 1.25 amp/in.²), the electrochemical capacity of the cadmium electrode was 0.16 amp-hr/g of CdO for the plastic type electrode. This does not imply that the active material of the cadmium electrode is CdO, but efficiencies are reported in terms of CdO since this was the starting material. Typical charge and discharge curves for the plastic cadmium and sintered electrodes are shown in Fig. 2. The plastic plate was charged and discharged at 0.075 amp and the sintered plate at 0.15 amp; this gave the plates hourly capacities of the same order. It can be seen that the charge voltage of the plastic plate was slightly higher than that of the sintered plate and the discharge voltage was slightly lower. In Fig. 3 are given Tafel curves for hydrogen evolution on plastic and sintered plate cadmium electrodes. These electrodes were of the same composition as those used to obtain the data for the previous figure. The area involved in the abscissa was obtained from BET determinations of the surfaces of the electrodes in question. The numbers along the lines are the values for the currents used. Again, it was observed that the plastic electrode had a higher overvoltage at equivalent charge densities than the sintered plate, undoubtedly due to the absence of a substrate metal.

The capacity density of the cadmium plates described was 0.23 amp-hr/g of electrode without grids, compared to a value of 0.10 amp-hr/g for electrodes of the sintered type.

Preparation of nickel electrodes.—In the case of the nickel electrodes it was found necessary to incorporate graphite or nickel powder to improve the conductivity of the formulations. A typical formulation consisted of 6% polyethylene, 7% polyethylene oxide, 16% graphite, and 69% nickel hydroxide. As was shown in Table I, the surface area of the active material of the plastic electrodes was comparable to that of the sintered-type nickel electrodes.

Performance characteristics of nickel electrodes.—Plastic nickel electrodes were prepared which had a discharge capacity of 0.275 amp-hr/g of nickel hydroxide when discharged at low rates. This is equivalent to a faradaic efficiency of 95% based on a 1 valence change. In Fig. 4 are shown the performance characteristics for sintered plate and plastic nickel electrodes of 0.6 mm thickness. It is obvious that the efficiencies of the plastic elec-

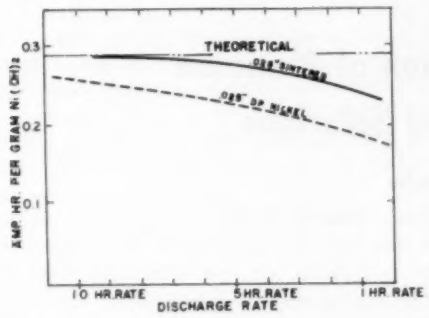

Fig. 4. Performance characteristics of nickel electrodes

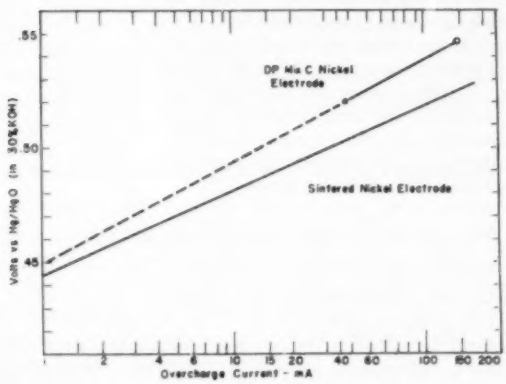

Fig. 5. Tafel curves for oxygen evolution on nickel electrodes. DP electrode: 2.7 g $Ni(OH)_2$, 40 cm^{-2} geometric area; sintered electrode: 0.7 g $Ni(OH)_2$, 12 cm^{-2} geometric area.

trodes made them suitable for discharges only up to the 4-hr rate, since at higher currents their efficiencies fell off rapidly. However, plates of the plastic type can be made thinner more easily than those of the sintered plate type, and effective current densities can be made much lower. The capacity density based on the total weight of material in the plastic plates was 0.208 amp-hr/g. This can be compared to a value of 0.1 amp-hr/g for a sintered nickel plate, 1/3 of the weight being active. Inclusion of metallic grids reduced the energy density of the plastic nickel plates to 0.15-0.17 amp-hr/g depending on the grid employed. Tafel curves for oxygen evolution on plastic and sintered plate nickel electrodes are shown in Fig. 5. The two electrodes were of different capacities and had different geometric and BET areas, but here again we see that the absence of substrate metal results in slightly higher overvoltages.

The nickel and cadmium electrodes previously described were assembled into cells ranging in capacities from 3 to 40 amp-hr. A number of cells were constructed with the following features of construction. They were made with 10 positive and 9 negative plates, each plate approximately 0.63 mm thick (0.025 in.). The weights of the compo-

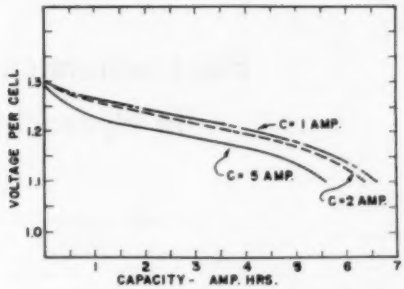

Fig. 6. Discharge characteristics of 10 cell DP nickel cadmium battery.

nents of the cells were approximately as follows: positive plates (10), 75 g; negative plates (9), 75 g; polystyrene case, 32 g; separators (woven nylon and sausage casing), electrolyte (30% KOH) and hardware, 53 g. The total cell weight was 235 g. These cells delivered 6.6 amp-hr at the ½ amp rate in their 154th cycle. The average voltage to a 0.6 v cutoff was 1.18 v. This is an energy output of 7.8 whr and an energy density of 33 whr/kg including excessive cell hardware. A multiple cell unit was fabricated with 10 cells in series in a monobloc assembly. This unit, made with an additional positive and negative plate in each cell, delivered 6.8 amp-hr at the ½ amp rate to a 1.05 v per cell cutoff and 7.5 amp-hr to a 0.6 v per cell cutoff. The latter corresponds to an energy density of 38 whr/kg. Typical discharge performance characteristics for this unit are shown in Fig. 6. Other cells have been constructed with similar electrodes in which the energy density of 40 whr/kg was achieved.

The fabrication process previously outlined is also very well suited to making electrodes in other than flat plate configurations as well as by extrusion. Positive and negative electrodes have been extruded in rod shapes with and without central wires. At our present electrode efficiency levels, we have approximately the same volumetric energy density as cells of the sintered plate type. We believe that our electrode efficiencies can be improved, and with but a moderate increase in electrode efficiency we could achieve an energy density of 50 whr/kg which would correspond to an energy volumetric density of 0.08 whr/cm^{-3}. In English units these values correspond to over 22 whr/lb and 1.3 whr/$in.^3$.

Acknowledgment

The authors wish to express their appreciation to The Electric Storage Battery Company for supporting this work and permitting its publication.

Manuscript received Dec. 7, 1960; revised manuscript received March 10, 1961. This paper was prepared for delivery before the Houston Meeting Oct. 9-13, 1960.

Any discussion of this paper will appear in a Discussion Section to be published in the June 1962 JOURNAL.

Electrochemical Corrosion of Platinum in Hydrochloric Acid Solutions

J. Llopis and A. Sancho

Instituto de Quimica Fisica "Rocasolano," Madrid, Spain

ABSTRACT

With solutions containing Cl^- ions Pt anodes dissolve as $PtCl_6^=$, this corrosion being quantitative for low current densities. It is known that attack by d.c. (i_c) is enhanced by increasing temperature, high Cl^- concentration, and high acidity. Some inhibitors, especially sulfur-containing compounds, almost inhibit anodic corrosion. Corrosion increases when a.c. (i_a) is superimposed. This effect increases with decreased frequency, being very important below 50 cps. With a 10 cps square wave, platinum corrosion is intense, and acidity and higher temperature enhance the attack. For i_c high enough to passivate the electrode, corrosion is nil until a "critical" value of the superimposed a.c. is reached. For a little higher i_a, corrosion increases, and with solutions of low acidity, it goes through a maximum with increasing i_a. The oscillographic anodic and cathodic charging curves have been studied and these are discussed.

Anodic corrosion of platinum requires a high overpotential. It can be studied in the presence of ions forming complexes; otherwise the electrode becomes passive, even at the lowest current densities.

In HCl, platinum dissolves at the anode as $PtCl_6^=$ (1, 2). Passivation is indicated under these conditions by a shift of the potential or a "knee" in the polarization curves. The first branch represents the corrosion process while, in the second branch, formation of Cl_2 on the passive electrode is the most important process (3). With increased concentration of HCl, higher current densities are required to achieve passivation (4).

On the other hand, at low current densities anodic corrosion of Pt in solutions of HCl shows a linear relation between log i and the potential, with a slope of the order of 0.1 v (5). This agrees with Ershler's findings (6) for platinized Pt electrodes in solutions of 15*N* H_2SO_4 containing HCl. A strong depolarization occurs when the temperature is increased, which leads to an increase in the current density required for passivation. The plot of log i as a function of $1/T$ for a given potential (0.860 v referred to s.c.s.) is linear, and $E_a = 20$ kcal/mole (5). The magnitude of this activation energy means that, under the conditions considered here, the anodic corrosion of Pt is a highly irreversible process.

The quantitative aspect of this anodic process was studied first under conditions of passivation (7-10) and, therefore, corrosion was nearly nil. Foerster *et al.* (11) were the first to observe that platinized Pt dissolves at the anode as Pt^{IV}. In the case of bright platinum Grube *et al.* (1, 2) showed the possibility of an anodic corrosion as $PtCl_6^=$ according to the Faraday law. These conclusions were confirmed later by Rius *et al.* (3, 12) who also showed the importance of the potential as a determining factor of the current efficiency, measured as Pt^{IV}, for a given value of the current density. These yields are about 100% if the potential is lower than that of passivation and nearly nil when the electrode becomes passive.

It is evident that the study of the passivation of a metal requires previous knowledge of the mechanism of its anodic corrosion. All factors increasing the overpotential of this process will enhance the passivation of the metal. Thus, some sulfur compounds exert a poisoning effect, increasing the overpotential for the anodic corrosion of Pt and therefore decreasing the current density required for its passivation. The most effective inhibitors are those containing the functional group SC (thiourea, xanthates, etc.) or SCN (thiocyanates), while the sulfinic and sulfonic compounds have very little effect (5).

Influence of Alternating Current

Generally speaking, the anodic corrosion of Pt is increased considerably by superimposing an alternating current. Using solutions of H_2SO_4 or NaOH, the electrolysis with superimposed currents produces on the anodes insoluble oxide films of no exactly defined composition. A review of this can be found in ref. (13), and the electrochemical behavior of these films was studied recently by Dietz and Nagel (14). With solutions of KCN, the attack on the anode is very intense and formation of $K_2Pt(CN)_4$ occurs (15, 16), while with solutions of HCl the product formed is H_2PtCl_6.

The depolarizing effect of a.c. on the anodic corrosion of Pt in solutions of Cl^- ions has been studied by Rius *et al.* (17) who found that the attack increases with higher a-c current density and lower frequency of the a.c. The d-c current density, i_c, required for passivation becomes larger as the frequency of the superimposed a.c. diminishes or its current density, i_a, increases. Also it was noticed that, for a given value of i_c high enough to passivate the electrode, corrosion begins only when i_a

reaches a "critical" value much greater than i_c, that is $i_a >> i_c$. The greater the i_c employed, the greater the critical value of i_a. For values of i_a a little higher than the corresponding critical value, the loss of weight per unit time Δ (mg hr^{-1} cm^{-2}) quickly reaches the theoretical value corresponding to the i_c applied, assuming the formation of $PtCl_6^{=}$ and considering the Faraday law.

In experiments carried out with only a-c current of frequencies lower than 100 cps and solutions of HCl as electrolyte, an intense corrosive action on the Pt electrodes also has been observed. The attack per unit time increases with i_a and is greater for lower frequencies. Brouillet and Epelboin (19), using 50 cps a.c. and concentrated solutions of $CaCl_2$, showed that Pt electrodes of small size can be electropolished. On the other hand, this kind of corrosion with dilute solutions of HCl can be useful for etching before metallographic observations of Pt (20).

Effect of Alternating Currents of Low Frequencies

Recently considerable interest has been given to the possible applications of alternating currents to all kinds of electrochemical processes, especially to electropolishing. On the other hand, as the results given above indicate that the effect of a.c. is greater for low frequencies, it seemed advisable to study the corrosion of Pt by a.c. at frequencies below 50 cps.

To carry out these experiments, two independent circuits, one for each type of current, were set up. Both circuits were distributed over a common section in which the electrolytic cell was placed (Fig. 1). The a-c current sources, sine waves (100 and 50 cps), and square waves (10 cps) consisted of electronic oscillators, and the current was introduced to the electrolysis circuit through a Roselson (ULT 34) transformer. To avoid interference, an inductance, H, (or a resistance for the lowest frequency) and a condenser, C, were inserted in the d-c and a-c circuits, respectively. Each circuit had the necessary measuring instruments; the a-c current was measured by a shunted "Cambridge" junction thermocell, combined with a galvanometer. Solutions of 4*N* HCl, 6*N* HCl, and 9.5*N* $CaCl_2$ + 10^{-3}*N* HCl were used as electrolytes. The experiments were carried out at 25° and 45°C.

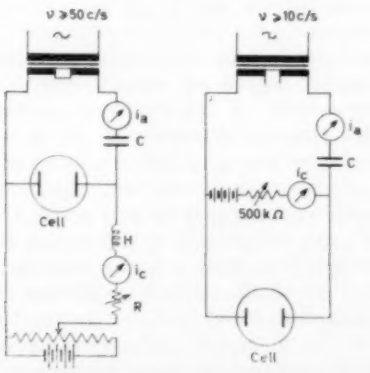

Fig. 1. Electrical circuits

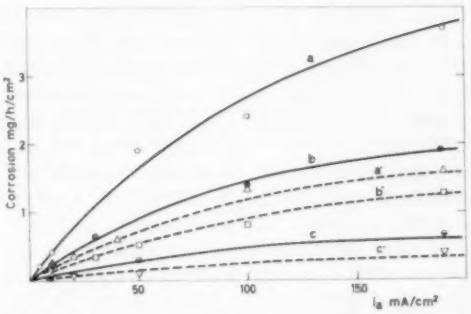

Fig. 2. Corrosion by square a.c., 10 cps: curve a, 6N HCl, 45°C; curve a', 6N HCl, 25°C; curve b, 4N HCl, 45°C; curve b', 4N HCl, 25°C; curve c, 10^{-3}N HCl + 9.5N $CaCl_2$, 45°C; curve c', 10^{-3}N HCl + 9.5N $CaCl_2$, 25°C.

The results obtained using only square a.c. (10 cps) are plotted in Fig. 2. The loss of weight Δ(mg hr^{-1} cm^{-2}) is represented as a function of the a-c current, i_a, for each of the above mentioned electrolytes and temperatures. These curves show how the acidity of the electrolyte and temperature enhance the attack of this metal.

The effect of superimposed currents has been studied in another series of experiments. Figure 3 shows the results of corrosion obtained with increasing i_a, superimposed in all cases on a given value of i_c (0.67 ma/cm^2). The solution used was that of $CaCl_2$, the temperature was 25°C. All the curves exhibit the same shape. Corrosion is nil until the a-c current reaches the critical value; for a little higher i_a a theoretical corrosion, calculated as above, is obtained. These results also show that the critical value of i_a decreases for lower frequency of the a.c. employed.

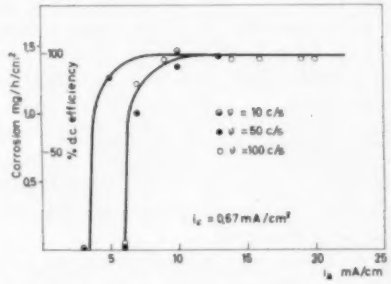

Fig. 3. Effect on corrosion of superimposed currents

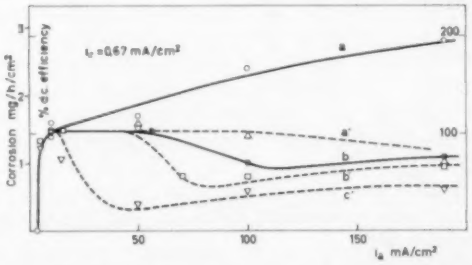

Fig. 4. Effect on corrosion of square a.c., 10 cps, superimposed to a given value of i_c = 0.67 ma/cm^2: curve a, 6N HCl, 45°C; curve a' 6N HCl, 25°C; curve b, 4N HCl, 45°C; curve b', 4N HCl, 25°C; curve c', 10^{-3}N $CaCl_2$ + 9.5N HCl, 25°C.

Finally, in a last series of experiments, the effect of i_a in the range 0-190 ma/cm² has been studied extensively. Figure 4 shows the results of corrosion obtained with 10 cps square a.c., superimposed on the given value of i_c (0.67 ma/cm²). It can be seen that, for values of i_a much higher than the critical value, the variation of corrosion depends on the temperature and composition of the electrolyte; thus with solutions of low acidity (solution of $CaCl_2$), the corrosion goes through a maximum with increasing i_a. In all cases, for high i_a the curves of corrosion tend toward those shown in Fig. 2, corresponding to experiments carried out with a-c current only. In extreme conditions of high acidity and temperature (6*N* HCl and 45°C), the addition of both effects, due to d-c and a-c currents, leads to an increasing corrosion of Pt as i_a increases.

Oscillographic Study of the Passivation of Pt

The oscillographic study of the cathodic and anodic charging curves may contribute to an explanation of the processes taking place on a corroding Pt anode. All these experiments were made in an all-glass, double-wall cell which allowed the electrolyte to be thermostated and permitted the bubbling of N_2 to keep an inert atmosphere inside the cell and to remove the gases evolved in the electrolysis. The oscillograms were obtained using a galvanostatic electrical circuit, which allows the recording of the variations of potentials with time on a Cossor oscillograph (model 1049), with extended time base ranges for low frequencies (up to 9 sec).

Anodic charging curves were obtained by switching on a constant anodic polarizing current after a cathodic prepolarization; the cathodic charging curves were obtained in the opposite way. Initial and final values of the potential were measured with a potentiometer in each experiment. These values have been used to draw the corresponding scales of potential for each time polarization curve.

In these series of experiments we have studied the effects of Cl^- and H^+ ions, temperature, and current densities, both anodic and cathodic. Now we shall describe only the most characteristic cases, although later in the discussion all the sets of results will be considered.

Study of the anodic charging curves.—Charging curves were obtained using a 4*N* HCl solution as electrolyte. In general, the procedure was to apply initially a cathodic current density i_- of 10 μa/cm² until the potential remained constant; then an anodic current i_+ was switched on suddenly and the variation of potential with time shown on the oscillograph was recorded by photography. Oscillograms for different values of the polarizing anodic current i_+ are shown in Fig. 5. In all of these experiments the flow of nitrogen through the electrolyte was maintained constant and the temperature was 45°C.

It was noted that all of these curves exhibit the characteristic inflection of passivation. These inflections appear, for the experiments considered here, between 300 and 400 mv.

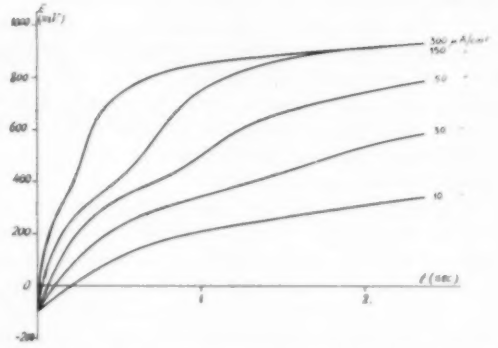

Fig. 5. Anodic charging curves, 4N HCl solution, different values of anodic polarizing current; cathodic prepolarizing current $i_- = 10$ μa/cm², constant flow of N_2, temperature 45°C.

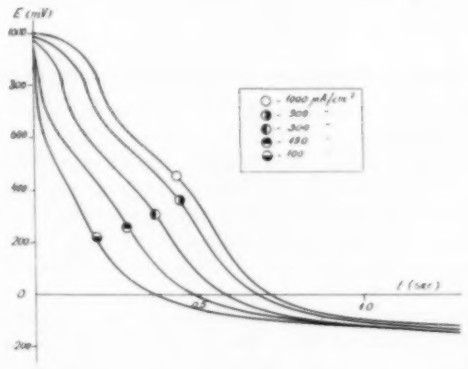

Fig. 6. Cathodic charging curves, 4N HCl solution, different values of anodic prepolarizing current; constant value of cathodic polarizing current $i_- = 400$ μa/cm², constant flow of N_2, temperature 45°C.

Study of cathodic charging curves.—These curves were obtained by starting from an anodic prepolarization with different values of i_+ until steady potential was reached, then suddenly switching on a cathodic current density $i_- = 400$ μa/cm², the same for all of the experiments. The experimental conditions were the same as above for the set of curves shown in Fig. 6. All of the curves show a potential arrest between 600 and 500 mv, which may be due to the process of depassivation.

If the flow of nitrogen is interrupted during both the anodic prepolarization and the recording of the charging curves, i.e., by working under conditions of natural convection, the curves obtained show a larger initial period of almost steady potential. This corresponds to the depletion of the Cl_2 accumulated close to the electrode, and it is followed by a rapid evolution of the potential to negative values. Under these conditions, the above mentioned step of depassivation is masked. Curves for a 6*N* HCl solution at 25°C are shown in Fig. 7.

If the transition time τ is the time between the switching on of the cathodic current (after the anodic prepolarization) and the onset of the steep decay of the potential (500 mv referred to the s.c.s.), it is seen that its value depends on the current density i_+ used in each case for the anodic

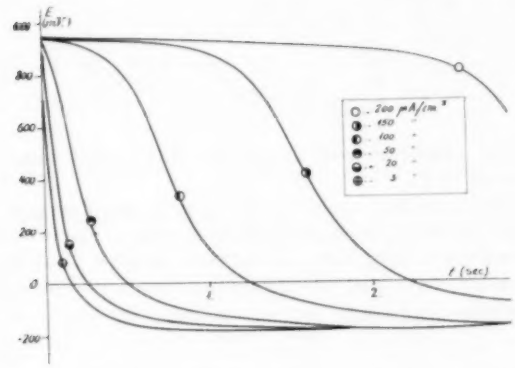

Fig. 7. Cathodic charging curves, conditions of natural convection, different values of anodic prepolarizing current; constant cathodic polarizing current $i_- = 400$ $\mu a/cm^2$, 6N HCl solution, temperature 25°C.

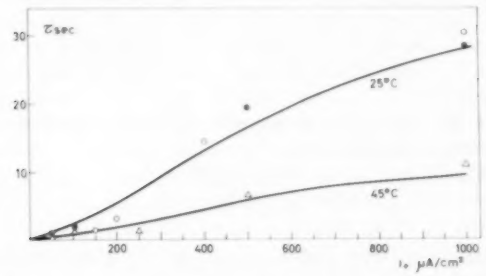

Fig. 8. Transition times for different values of anodic prepolarizing current i_+, conditions of natural convection; constant cathodic polarizing current $i_- = 400$ $\mu a/cm^2$. Open circle, 6N HCl, 25°C; circled x, 4N HCl, 25°C; open triangle, 4N HCl, 45°C.

prepolarization, the cathodic current i_- being the same for all of the experiments. Transition times thus obtained for a 6*N* HCl solution, 25°C, and for a 4*N* HCl solution, 25° and 45°C, are shown in Fig. 8.

Discussion

Interpretation of Anodic Charging Curves

As is known (21, 22), when an anodic current is switched suddenly on a Pt electrode and the electrolyte does not contain any oxidizable substance, the charging curves exhibit three regions: (*a*) charging of the hydrogen adsorbed; (*b*) charging of the double layer capacity at the metal solution interface; and (*c*) linear variation of the potential with time, tending then to reach a steady-state value. This last part corresponds to the "oxidation" of the electrode surface which was studied recently by Laitinen and Enke (23).

With acid solutions containing halides Hickling's results (24) showed that in the anodic charging curves the region (*c*) was not evident and the potential tends to reach a steady-state value less positive than in the absence of halides. However, these results were not sufficient to reach conclusions on the mechanism of these electrode processes; a more detailed study seems necessary. In the presence of Cl^- ions the anodic steady potential is high enough to make possible the surface oxidation of the Pt electrode. The anodic charging

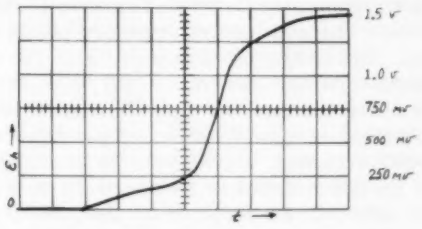

Fig. 9. Anodic charging curve for 1N H_2SO_4 + 10^{-3} N NaCl solution; polarizing current $i_+ = 1$ ma/cm²; potential referred to the H-electrode in the same solution (50 mv for each small division); time, 0.1 sec/small division; bubbling of N_2.

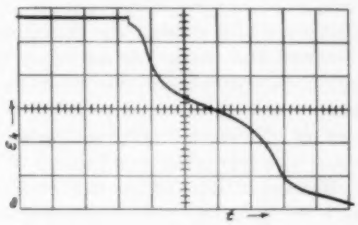

Fig. 10. Cathodic charging curve for the same solution used in Fig. 9; experimental conditions also the same as in Fig. 9. Anodic prepolarization $i_+ = 1$ ma/cm² during 30 sec; cathodic polarizing current $i_- = 1$ ma/cm².

curve for a solution of 1*N* H_2SO_4 + 10^{-3}*N* NaCl is shown in Fig. 9, and comparison with Fig. 1, 1*N* H_2SO_4 solution, of ref. (22) shows that the steady-state potential is less positive ($\cong$ 0.1 v) when Cl^- ions are present, but the linear section corresponding to the oxidation of the electrode is evident. Figure 10 reproduces the cathodic charging curve for the same solution and value of the polarizing current. This curve is the same shape as the one in Fig. 6; its interpretation will be given later.

When concentrated solutions of Cl^- ions are used, the possibility of corroding the Pt electrode must be considered. Thus it is interesting to observe the characteristic shape of the passivation curves plotted in Fig. 5. Using concentrations of HCl higher than 4*N* and sufficiently low current densities i_+, the potential stabilizes before passivation. Under these conditions all of the electricity is used to corrode the metal as $PtCl_6^=$. This process probably takes place on sites of the nonoxidized surface fraction where the demolition of lattice metal structure can occur most readily. Formation of chemisorbed Cl atoms may be an intermediate step. Formation of complex ions makes the process of dissolution easy. Some of these processes will act as a potential-determining step.

Electrode potentials will be higher at higher current densities, and blocking of the electrode surface by oxidation may take place. Until this happens the anodic corrosion will proceed at the uncovered surface fraction, although with increasing hindrance as the surface oxidation passivates the electrode. Formation of Cl_2 on the more or less passivated electrodes can account for both the inflection in the charging curves and the final values of the steady-state potentials. This mechanism is in accord with Schwabe's recent ideas (25).

Interpretation of Cathodic Charging Curves

Cathodic charging curves show two points of inflection. The shape of this curve and its strong dependence on the stirring of the electrolyte, as shown by comparing Fig. 6 and 7, suggest that the initial period of almost stationary potential, before its rapid dropping, corresponds to the ionization of the Cl_2 accumulated at the electrode interphase. This process will be governed by the laws of diffusion, and the boundary conditions will be those imposed by the type of experiments. When the concentration of Cl_2 close to the electrode tends toward zero the potential will drop rapidly toward negative values. Then reduction of the "oxidized surface" and the charging of the double layer must be taken into account to explain the second point of inflection and the shape exhibited by the cathodic charging curves before the hydrogen evolution region.

The laws of diffusion must be applied to the system under the following conditions. If x represents the dimension normal to the electrode surface, $C(x,t)$ will signify the concentration of Cl_2 at a distance x at time t. For the sake of simplicity, $x = \delta$ at the electrode surface and $x = 0$ at the limit of the diffusion layer. On the other hand, the experimental conditions permit one to assume that the concentration of Cl^- is constant both in x and t. Berzins and Delahay (26) have studied a similar problem by a rigorous treatment under conditions of semi-infinite linear diffusion.

The second law of diffusion

$$\frac{\partial C(x,t)}{\partial t} = D\frac{\partial^2 C(x,t)}{\partial x^2} \qquad [1]$$

must be solved under the boundary and initial conditions

$$\left.\begin{array}{lll} C = 0 & x = 0 & t \geq 0 \\ \dfrac{\partial C}{\partial x} = -\dfrac{i_-}{2DF} = k_- & x = \delta & t \geq 0 \\ C = \dfrac{i_+}{2DF}x = k_+ x & 0 \leq x \leq \delta & t = 0 \end{array}\right\} \qquad [2]$$

where i_- is the absolute value of the cathodic current, kept constant while the polarizing curves were taken.

A solution of this equation is

$$C = c + \chi \qquad [3]$$

where c and χ are the respective solutions of [1] under the following conditions

$$\left.\begin{array}{llll} c = 0 & \chi = 0 & x = 0 & t \geq 0 \\ \dfrac{\partial c}{\partial x} = k_- - k_+ & \dfrac{\partial \chi}{\partial x} = k_+ & x = \delta & t \geq 0 \\ c = 0 & \chi = k_+ x & 0 \leq x \leq \delta & t = 0 \end{array}\right\} \qquad [4]$$

Solution χ will be

$$\chi = k_+ x \qquad [5]$$

and solution c was obtained elsewhere (27, 28). Values of $C(x,t)$ at the electrode surface, $x = \delta$, are really the only interesting ones. In this case, the solution will be

$$C_\delta = \frac{\delta}{2FD}\left[-i_- + \frac{8(i_+ + i_-)}{\pi^2} \sum_0^\infty \frac{1}{(2n+1)^2} e^{-\frac{(2n+1)^2}{4}\pi^2 \frac{Dt}{\delta^2}} \right] \qquad [6]$$

after substitution of the values of k_+ and k_- introduced in [2].

If "transition time" is the time elapsed to reach the value $C_\delta = 0$ and large values of $D\tau/\delta^2$ are considered first, the exponentials will tend rapidly toward zero, and the following result can be obtained

$$\tau = \frac{4\delta^2}{\pi^2 D} \ln \frac{8(i_+ + i_-)}{\pi^2 i_-} \qquad [7]$$

For small values of τ, the series in [6] converges very slowly and a more convergent series expansion is convenient (25, 26). Thus, for $x = \delta$

$$C_\delta = \frac{1}{2FD}\left[i_+ \delta - (i_- + i_+) 2\sqrt{\frac{Dt}{\pi}} \right] \qquad [8]$$

and the transition time will be given by the following expression

$$\tau = \frac{\delta^2}{4}\frac{\pi}{D}\frac{i_+^2}{(i_- + i_+)^2} \qquad [9]$$

Expressions [7] and [9] permit one to calculate τ as a function of i_+ for a set of experimental conditions. In our case it is $i_- = 400$ μa/cm^2 and in Fig. 8 the theoretical curves for two values of the ratio $\delta/D^{1/2}$ are plotted. It is seen that experimental results at 25°C can be accounted for by the value $\delta/D^{1/2} = 8.21$ sec$^{1/2}$, while for those obtained at 45°C the value is $\delta/D^{1/2} = 4.74$ sec$^{1/2}$.

Now, taking as a representative datum $D = 1.41\ 10^{-5}$ cm^2 sec^{-1} (29), the following thicknesses for the diffusion layer are obtained: $\delta = 3.1\ 10^{-2}$ cm for the experiments at 25°C and $\delta = 1.8\ 10^{-2}$ cm for those at 45°C. In the first instance the value of δ agrees with that found in other cases of natural convection (30). The rather smaller value found at 45°C may be explained by a more intense convection and/or increase of diffusion coefficient under these conditions.

In experiments done with a continuous flow of nitrogen, the accumulation of chlorine at the electrode interphase is much smaller; therefore, the transition times will be shorter. Again, expressions [7] and [9] will give the dependence of τ on δ^2. In these cases, the singularities of the cathodic charging curves, such as the step due to depassivation, will be much more evident.

The arrest shown at 600 mv in the curves in Fig. 6 may be due to the reduction of the surface oxide formed during the passivation of the electrode. This step, which can be observed with 6*N* HCl solutions, is more evident with 4*N* HCl solutions and even more in experiments done with 4M KCl solution as electrolyte. Confirming this, it is interesting to note that, if the current density used for anodic prepolarization is much lower than that required for passivation, the above mentioned ar-

Fig. 11. Variation of potential during a cycle of the square a.c. (10 cps); electrolyte 6N HCl, temperature 25°C, current strength i_a = 50 ma/cm².

rest does not appear in the cathodic charging curves.

Variation of Potential during a Cycle of A.C.

An immediate conclusion which can be drawn from the above interpretation of the anodic and cathodic charging curves is that, during a cycle of a.c. superimposed on another polarizing d.c., the electrode potential may oscillate between that of formation of Cl_2 on a passive electrode (positive semicycle) and that of evolution of H_2 (negative semicycle). The following processes can be considered between both extreme values: (*a*) accumulation and depletion of Cl_2 at the electrode interphase; (*b*) changes in the oxidized fraction of the electrode surface; (*c*) corrosion of Pt as $PtCl_4^=$; (*d*) charging of the double layer; and (*e*) adsorption and ionization of H_2 at the electrode surface.

Each of these processes will occur in accordance with its own kinetics; therefore, when the frequency of the a.c. increases, only the most rapid will participate. The separate occurrence of these processes can be seen in the oscillograms obtained with a 10 cps square a.c. The oscillogram shown in Fig. 11 corresponds to the following conditions: electrolyte 6*N* HCl, temperature 25°C, i_c = 0, and i_a = 50 ma/cm². In this case the current density i_a is too high to see a step due to process (*c*) although this process occurs during a small fraction of the positive semicycle according to the corrosion results (Fig. 2). The potential oscillates between two extreme values and the amplitude of this oscillation depends not only on the a-c current density i_a but also on the remaining experimental conditions.

Study of the Corrosion of Pt by A.C.

For a given set of experimental conditions, the relative participation of process (*c*) will determine the intensity of the corrosion to be observed. The graphs showing corrosion as a function of i_a are given in Fig. 1-4.

In previous papers (13, 17, 31) it has been shown that the depolarizing effect of alternating current decreases notably with increasing frequency. Processes (*a*), (*b*), and (*c*) require time and cannot follow alternations of high frequency. In other words, it can be said that the faradaic impedance, acting in parallel with the double layer, does not fall off with increasing frequency as rapidly as does the impedance of the double layer; therefore at high frequencies most of the a.c. across the interface is used by process (*d*) of charging and discharging the double layer.

The study of the charging curves shows that the corrosion of Pt will be maximum while the potential is between 200 and 500 mv. From 500 to 900 mv the corrosion of this metal is still important, but the increasing participation of processes (*a*) and (*b*) must be considered. For potential values higher than 1.0 v the electrodes become passive and corrosion is nil. Finally, for negative values, only processes (*d*) and (*e*) take place and corrosion again is nil.

In this sense, the results obtained with only a.c. can be explained. It is observed that, as the concentration of H^+ ions in the electrolyte decreases, the electrode is at a passivation potential for a longer time during the cycle, and there is less corrosion. The effect of temperature can be explained in the same way.

When superimposed currents are used, these are defined by the a-c current i_a added to the polarizing d-c current i_c. If the latter is high enough to passivate the electrode, corrosion will not appear until a minimum value of i_a, at which the electrode can be depassivated during the negative semicycle. It has been seen that this minimum or critical value of i_a increases with increasing values of i_c; it depends also on the acidity of the electrolyte and on temperature.

Finally, it is interesting to observe that for a value of i_a a little higher than the critical, the corrosion corresponds quantitatively to the value of i_c. Now, for even higher values of a-c current, such that $i_a >> i_c$, the corrosion process will be controlled by a.c. Then, if solutions of low acidity are used, the electrode is at extreme values of potential for a longer time during a cycle and the corrosion will be smaller. Thus, the maxima of corrosion and results shown in Fig. 4 can be explained easily.

Manuscript received Dec. 19, 1960; revised manuscript received March 24, 1961.

Any discussion of this paper will appear in a Discussion Section to be published in the June 1962 JOURNAL.

REFERENCES

1. G. Grube, J. Helfer, and G. Luz, *Z. Elektrochem.*, **35**, 703 (1929).
2. G. Grube, F. Oettel, and H. Reinhardt, Gmelin's Handbuch der anorganischen Chemie, Pt(B) 298 (1942).
3. A. Rius and J. Calleja, *Anal. real soc. españ. fis. y quím.*, **41**, 961 (1945).
4. A. Rius, J. Llopis, and I. M. Tordesillas, *ibid.*, **48B**, 23 (1952).
5. A. Rius, J. Llopis, and I. M. Tordesillas, *ibid.*, **48B**, 639 (1952).
6. B. Ershler, *Acta Physicochim. USSR*, **9**, 139 (1944).
7. F. Haber and S. Grinberg, *Z. anorg. Chem.*, **16**, 198 (1898).
8. F. Haber, *ibid.*, **16**, 442 (1898).
9. P. Denso, *Z. Elektrochem.*, **8**, 147 (1902).
10. F. Bran, *ibid.*, **8**, 197 (1902).
11. F. Foerster, A. Nobis, and H.Stötzer, *ibid.*, **29**, 64 (1923).
12. A. Rius, J. Llopis, and I. M. Tordesillas, *Anal. real soc. españ. fis. y quím.*, **48B**, 35 (1952).
13. A. Rius, J. Llopis, and F. Colom, *ibid.*, **51B**, 11 (1955).

14. H. Dietz and K. Nagel, *Osterreich. Chemiker Zeit.*, **60**, 261 (1959).
15. A. Brochet and J. Petit, *Bull. Soc. Chim. France*, **31**, 359 (1904).
16. A. Brochet and J. Petit, *Ann. Chim. Phys.*, **3**(8), 433 (1904).
17. A. Rius, J. Llopis, and F. Colom, *Proc. CITCE*, **6**, 306 (1954).
18. J. Llopis and F. Colom, *Anal. real soc. españ. fis. y quím.*, **51B**, 379 (1955).
19. P. Brouillet and I. Epelboin, *Rev. met.*, **51**, 693 (1954).
20. E. Raub and G. Buss, *Z. Elektrochem.*, **46**, 195 (1940).
21. M. Breiter, G. A. Knorr, and W. Völkl, *ibid.*, **59**, 681 (1955).
22. J. Giner, *ibid.*, **63**, 386 (1959).
23. H. A. Laitinen and C. G. Enke, *This Journal*, **107**, 773 (1960).
24. A. Hickling, *Trans. Faraday Soc.*, **41**, 333 (1945).
25. K. Schwabe, *Electrochimica Acta*, **3**, 186 (1960).
26. P. Delahay, "New Instrumental Methods in Electrochemistry," p. 189, Interscience Publishers Inc., New York (1954).
27. A. Rius, J. Llopis, and S. Polo, *Anal. real soc. españ. fis. y quím.*, **45B**, 1013 (1949).
28. H. S. Carslaw and I. G. Jaeger, "Conduction of Heat in Solids," p. 104, Clarendon, Oxford (1947).
29. H. Euler, *Wien. Ann.*, **63**, 273 (1897).
30. J. N. Agar, *Discussions Faraday Soc.*, **1**, 26 (1947).
31. A. Rius, J. Llopis, and F. Colom, *Anal. real soc. españ. fis. y quím.*, **51B**, 1 (1955).

The Anodic Surface Oxidation of Gold

H. A. Laitinen and M. S. Chao[1]

Noyes Chemical Laboratory, University of Illinois, Urbana, Illinois

ABSTRACT

The surface oxidation of a smooth gold electrode in perchloric acid was studied by constant potential anodization and constant current cathodization under various conditions. The anodic reaction is explained as a mixed process of oxygen evolution and the formation of chemisorbed oxygen atoms which are presumed to take the configuration of auric oxide when more than one layer thick. The grain boundary diffusion of oxygen atoms may account for the residual current and the increase in the extent of oxidation at constant potential. Electron micrographs and double layer capacities are consistent with the other findings.

The surface oxidation of gold has been studied in parallel with that of platinum by means of chronopotentiometry (1-6), voltammetry (7), triangular voltage sweep (8), and chemical reaction (1, 9). As with the case of platinum, data and interpretations by various authors are not altogether consistent. For example, the presence (3) or absence (4, 9) of lower valent gold intermediates in the formation of gold(III) oxide has been postulated.

The present paper describes the results obtained with gold electrodes by techniques similar to those applied to platinum electrodes in this laboratory (10). Similarities and differences between these two noble metal electrodes are noted. Comparable results on gold electrodes by other authors are also presented and commented on. Besides, studies have been made on the surface structure of gold by electron microscopy. It is hoped that these additional findings will lead to a better understanding of the surface oxidation of gold and may also serve as a point of departure for new approaches.

Experimental

The arrangement of the electrolytic cell was essentially that reported before (10), except that a Dewar flask containing a dry ice-acetone mixture was added to cool the activated charcoal column.

The electrode was a 99.9+% gold foil 0.0125 cm in thickness and 1.0 cm^2 in apparent area, counting both sides. The foil was connected through a piece of gold wire to a piece of platinum wire, which was sealed in a soft glass tubing. Only the foil and the lower part of the gold wire were immersed in the solution during the experiments. The electrode was stored in 10*N* nitric acid when not in use. Occasional heating of the electrode at about 300° in air for 2-3 min helped to destroy the minute amount of organic substances that had been adsorbed on the surface during the experiments.

Perchloric acid was used exclusively as a noncomplexing, nonadsorbing, and effectively buffered medium. Unless otherwise specified, 1*N* was the concentration used. The solution was flushed continuously with purified nitrogen during the experiments, although it was found the results would not have been significantly different had oxygen been present (11).

Constant potential anodization was used to oxidize the electrode and constant current cathodization to measure the extent of oxidation throughout the present studies. The reasons for these choices as well the instrumentation required have been discussed (10). It may be mentioned here that while constant potential anodization has been used by several authors on platinum, its use on gold has not been found in literature.

The extent of surface oxidation measured is expressed as charge per unit area or Q/A for short. A charge of 0.45 millicoulombs/cm^2 may be visualized as corresponding to a single layer of oxygen atoms on the 111 plane, the prominent crystalline plane of a gold surface.

[1] Present address: The Dow Chemical Company, Midland, Michigan.

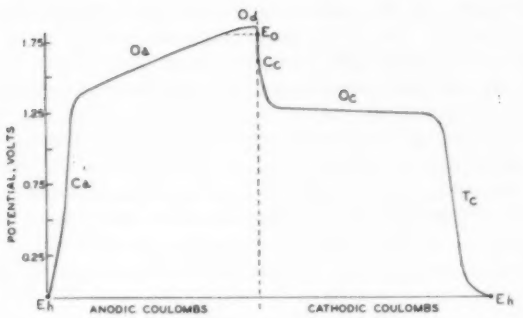

Fig. 1. Schematic chronopotentiograms

Results

Chronopotentiograms.—Schematic chronopotentiograms are shown as Fig. 1. Starting with the electrode at zero potential as referred to the standard hydrogen electrode (as are all potentials in this paper), the application of a constant anodic current brought about the following stages: the charging of the double layer (C_a), the surface oxidation (O_s), and the deep-seated oxidation (O_d) both O_s and O_d involving oxygen evolution also. Similarly, the application of a constant cathodic current to an oxidized electrode brought about the following stages: the charging of the double layer (C_c), the reduction (O_r, or cathodic arrest, as it is usually called), and the transition (T_c), involving mainly the charging of the double layer, into the hydrogen evolution potential. It is to be noted that the potential change in the oxidation stage (O_s) is much more conspicuous than that in the reduction stage (O_r). A stage preceding the charging of the double layer (C_a), usually present in the anodic chronopotentiogram of platinum, is missing, as hydrogen is neither adsorbed on nor dissolved in gold to any appreciable extent (3, 7).

Effect of strong anodization.—The effect of strong anodization on Q/A was observed by a 3-min anodization at each potential, followed by cathodization to determine Q/A (Fig. 2). At potentials larger than 1.95 v the rapid rise in Q/A indicates that the oxidation has gone below the surface and has become deep-seated. The oxides formed at these potentials were colored from black to orange and could be flaked away. The composition of the oxide layer was probably close to Au_2O_3 (12).

In contrast, platinum electrodes do not grow thick oxide layers even at high potentials, because platinum oxide, unlike gold oxide, does not behave as a good ionic conductor at high potentials.

As unduly strong anodization would drastically alter the surface of the electrode, care had been taken to keep the electrode away from this region. The highest potential applied in the following experiments was 1.75 v.

Effect of anodization potential.—Q/A as a function of anodization potential is shown as Fig. 3. When the electrode was kept at a reduced state of 0.65 v before the anodizations, the data obtained are plotted as the solid line. When the electrode was pre-anodized at a higher potential before being anodized at a lower potential, the data obtained

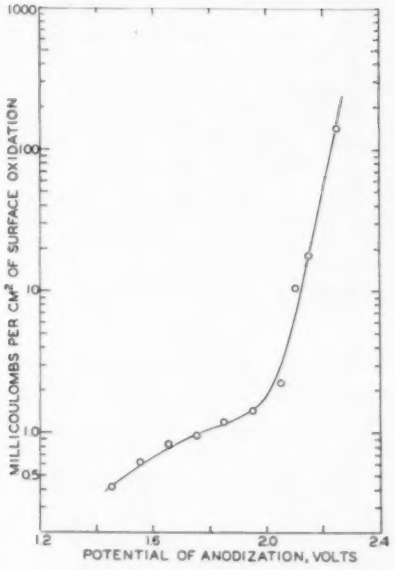

Fig. 2. Effect of strong anodization

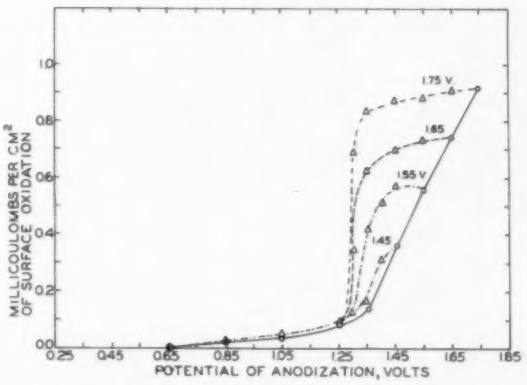

Fig. 3. Effect of anodization potential

are plotted as the broken lines. Both the anodization and the pre-anodization times were 1 min.

These hysteresis curves indicate that: (*A*) the surface oxidation reaction is highly irreversible; (*B*) the extent of oxidation is determined not only by the potential but also by the previous history of the electrode; (*C*) there is only one form of oxide as no potential has been found at which one oxide is stable but not another. The last point is also evident from the fact that only one cathodic arrest is observed in all cases. Similar conclusions have been arrived at in the case of platinum (10).

Hysteresis curves of gold electrodes, as observed by the voltage sweep method have been reported recently (8). The results for Q/A were some 50% larger than those in the present studies. The difference may be either due to the inherent nature of the two methods or due to the use of electrodes with rougher surface by Will and Knorr.

Open circuit drift of surface oxidation.—Q/A and the electrode potential at open circuit were studied as a function of time. The source of potential was turned off after a 1-min anodization. The electrode

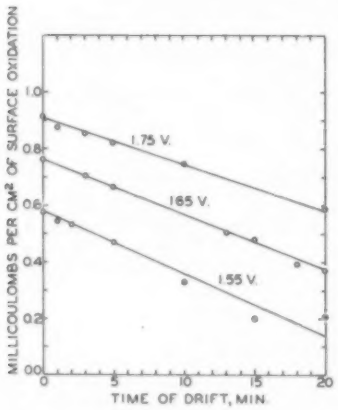

Fig. 4. Effect of open circuit drift

potential drift was recorded for different periods of time, at the end of which Q/A was determined. The potential dropped very rapidly at first but more slowly as time went on. For example, an electrode anodized at 1.75 v exhibited a potential drop of 205 mv during the first half minute, and 45 mv, 30 mv, and 20 mv during succeeding half-minute intervals. Similar behavior was observed with electrodes anodized at 1.65 v and 1.55 v. The potential of these electrodes all became 1.30 v after a drift of 15 min. On the other hand, Q/A decreased almost linearly with drifting time (Fig. 4).

These results confirm the conclusions of the last section, i.e., the extent of oxidation is not determined solely by the potential and that there is no evidence of mixed oxidation states.

If the decrease of Q/A is considered to be a zero order reaction, the rate constant will correspond to a current density of 0.28, 0.33, and 0.37 $\mu a/cm^2$ for electrodes anodized at 1.75 v, 1.65 v, and 1.55 v, respectively. This is in good agreement with Vetter and Berndt's value of 0.30 $\mu a/cm^2$ (5), which had been estimated as a correction to make the anodic Q/A independent of current density.

Effect of time of anodization.—Q/A was measured as a function of the time of anodization (Fig. 5). In each case the anodization of a reduced electrode (at 0.65 v) was discontinued after a definite period and the cathodic current was applied immediately. The first point on each curve corresponds to an anodization time of roughly 1 sec.

As was the case with platinum, each curve can be visualized as the composite of two reactions: a rapid initial reaction followed by a slow reaction. For example, at 1.75 v Q/A for 1-sec anodization amounted to some 75% of that for 15-min anodization. That the initial reaction takes only a short time is evident also in the data by the voltage sweep method (8). The slow reaction apparently represents a penetration of oxygen into the first atom layers of solid. The fact that even this slow oxidation is reduced on the cathodic cycle may be explained by the assumption that penetration by hydrogen ions rather than back-diffusion of oxygen is involved in the reduction. The nature of these two reactions can best be explained by the results in the next section.

Anodic current during oxidation.— When an anodic potential was applied to a reduced electrode (at 0.65 v), the anodic current rose instantaneously to the maximum output of the potentiostat of 50 ma and then rapidly died down to the order of 10 μa within the first 10 sec. For longer times, the current had a small but definite value (Fig. 6). Experiments in deaerated, quiescent solution gave the same set of curves with a lowering of current of 0.1 $\mu a/cm^2$ for each curve. Similar behavior has been observed on platinum (10). The results in oxygen-flushing and oxygen-saturated, quiescent solutions were practically identical with those in nitrogen-flushing and oxygen-free, quiescent solutions, respectively.

Each curve can be visualized as consisting of two portions: a rapidly decaying large current and a small residual current. While the large current can be identified with the Q/A at short time anodization and hence with the initial surface oxidation, the residual current can be explained by the grain boundary diffusion of oxygen atoms, as first proposed in the case of platinum electrodes (10). The possibility of the loss of oxygen atoms into the solution has been dismissed in the previous paper on the grounds that the disrupting of metal-oxygen bond should show a larger potential dependence

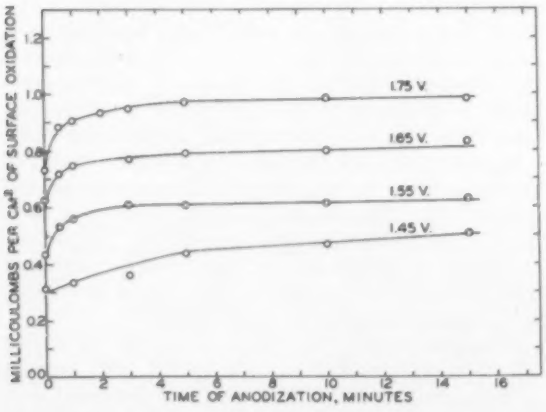

Fig. 5. Effect of time of anodization

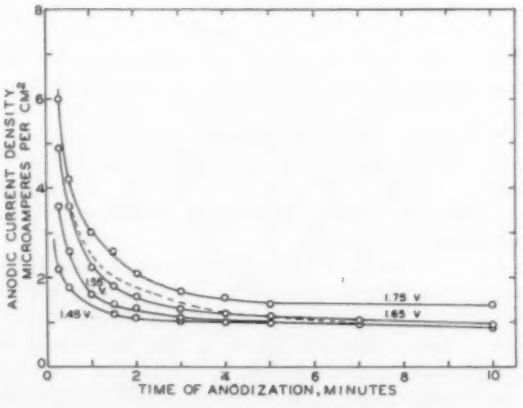

Fig. 6. Anodic current

and that microscopic examination of the electrode surface shows a more vigorous attack at the grain boundaries. It may be added here that: (*A*) the effect of stirring or the presence of oxygen gas is too small to be consistent with the loss of oxygen atoms as gas into the solution; (*B*) the recombination reaction through which the loss of oxygen into the solution could occur would not be expected to be a zero-order reaction as has been actually found. If one assumes a kinetically controlled (as opposed to mass-transfer controlled) surface reaction, the rate of which is independent of the potential and the amount of surface oxidation, then it would not be necessary to assume grain boundary diffusion. Such a surface reaction would not, however, account for the grain boundaries becoming visible upon oxidation of the surface (see below). That diffusion could account for the residual current is evident from the following argument.

The linear diffusion treatment calls for the current-time equation $i = n\mathbf{F}AC^{\circ}\ (D/\pi t)^{1/2}$. C° is 0.10 g at./cm³ if the concentration of oxygen atoms is assumed to be equal to that of gold atoms in the bulk. Taking i as 0.8 μa and A, the area of the diffusing surface, as 1 cm² from Fig. 6, the diffusion coefficient D is estimated to be 1.3×10^{-17} cm² sec⁻¹, the same order of magnitude as the corresponding value obtained for platinum. Using the values of D and C° above, the i at various times is calculated and plotted as the dotted line in Fig. 6. It can be said that the estimated values fairly parallel the experimental ones. The higher residual current at higher potentials can be attributed to the additional process of oxygen evolution.

By energy considerations the grain boundary diffusion coefficient can also be estimated from the relation $D = D^{\circ} \exp(-E/RT)$ (13). For the self-diffusion of gold, the activation energy E has been determined as 41.7 kcal/mole and the temperature-independent term D° as 0.091 cm² sec⁻¹ (13). With proper approximations E for the grain boundary diffusion of oxygen atoms in gold is estimated as 15 kcal/mole and D° as 0.01 cm² sec⁻¹ (14). The grain boundary diffusion coefficient D is calculated to be 10^{-10} cm² sec⁻¹.

The apparent discrepancy of the two grain boundary diffusion coefficients estimated above is to be expected. While the D estimated from the energy relation is the true coefficient, the D estimated from the anodic current is the "apparent" coefficient, obtained with the obviously impossible assumption that the total surface area is open to grain boundary diffusion. If the cross-sectional area of the grain boundaries is assumed to be 1% of the total surface area, a recalculation will bring D to the same order of magnitude as that from the energy relation.

Double layer capacity.—The equipment for the measurement of the double layer capacity by the current pulse method is shown in Fig. 7. A Tektronix Type 502 dual beam oscilloscope was used to display the trace of the electrode potential throughout the duration of the pulse, which was generated with a Tektronix Type 161 pulse generator. The traces were recorded photographically. The ratio of the current to the slope of the potential-time trace, $\Delta E/\Delta t$, gives the double layer capacity. Experimentally, the current was so adjusted that ΔE was 10-20 mv with a Δt of 200 μsec.

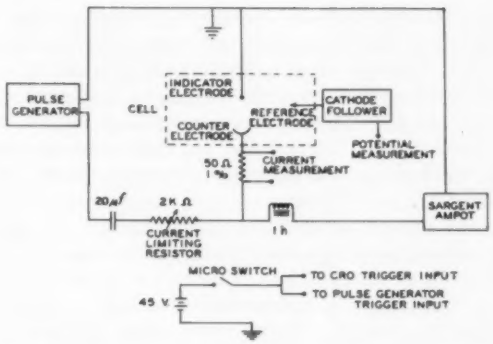

Fig. 7. Equipment for double layer capacity measurement

The principle of the current pulse method is well known (15). Its major advantages as noted in the present experiments are rapidity, visual indication as to whether a faradaic process is mixed with the charging process, and freedom from the effect of iR drop due to the Luggin capillary. Therefore, it is considered to be more convenient than the potential step method previously used (10, 11).

To diminish the lowering of the double layer capacity due to the traces of surface-active impurities adsorbed on the electrode, the electrode was first anodized at a high potential (1.65 v) to "kick off" the impurities. The relatively clean electrode was then reduced before being brought to any potential under study. With such treatment the precision was 3% or better.

The solid line in Fig. 8 represented the data obtained under the condition that the electrode had been kept at the potential under study for 1 min before the pulse was applied. The dotted line represented the condition that an additional preanodization of 1 min at 1.75 v was imposed.

The double layer capacity curve, like the Q/A curve (Fig. 3) exhibits hysteresis when plotted as a function of potential. The loop in the former curve is, however, barely noticeable because of the small change of capacity at more oxidizing potentials. The existence of hysteresis means that the surface oxidation and the double layer capacity are closely related.

The double layer capacity-potential curve of

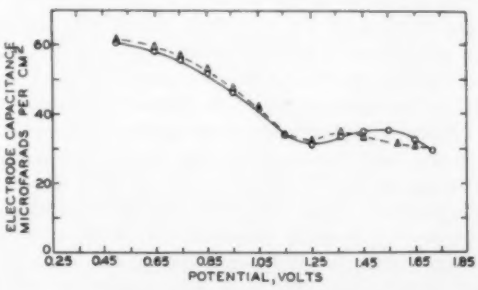

Fig. 8. Double layer capacity

gold electrodes may be divided roughly into two regions. Starting with a reducing potential of 0.45 v, the first region is characterized by a fall of double layer capacity with increasing potential until 1.25 v, at which surface oxidation begins. The second region covering the more oxidizing potential is marked by a relatively constant double layer capacity.

For many metals including platinum, the double layer capacity has been observed to increase with increasing anodization, with the rise beginning at the potential corresponding to surface oxidation. This apparently reverse trend observed with gold is reasonable, however, if the essentially constant region at highly anodic potentials is regarded as being brought about by a compensation of an increased double layer capacity due to oxidation superimposed on a decreasing double layer capacity due to electrostriction in the inner region of the double layer.

The double layer capacity of gold in acid solutions has been reported as 110 μf/cm^2 (1) and 150 μf/cm^2 (3) by chronopotentiometry and as 200 μf/cm^2 by voltage sweep method (8). The present data in the comparable potential region are 50-60 μf/cm^2. The discrepancy may be explained either by (*a*) different roughness factors of the electrodes, or (*b*) by the inclusion of faradaic charge transfer in the chronopotentiometric and voltage sweep methods to give an apparent double layer capacity which is too high. The larger potential change and the longer time involved in the two former methods would increase the tendency for an appreciable faradaic process.

Effect of acidity.—Perchloric acid of concentrations of 0.1, 0.01, and 0.001*N* was used in place of the usual 1*N* acid. For both the anodic and cathodic processes the potential shifted toward less positive potentials by about 2.3 $RT/\mathbf{F}$ v for a tenfold decrease in acid concentrations. The experimental values of the shift were 56 mv for the cathodic and 60 mv for the anodic process. This trend has been observed in gold as well as in platinum electrodes (5). $10^{-4}N$ acid did not follow this rule, presumably because of its insufficient buffer action.

With acid concentration up to about 6*N* the chronopotentiogram still followed the pH potential relation above. In 11.6*N* acid (undiluted 70% acid) Q/A was much smaller than expected. This may have resulted from a large decrease in the activity of water in such a concentrated solution. An additional cathodic arrest at 0.85 v was observed with some 11.6*N* acid samples. This arrest was presumably due to an impurity which may also have been responsible for the anomolous cathodic peak in the current-voltage curve of Bauman and Shain (7).

Double layer capacity measured in 0.1 and 0.01*N* acid was less reproducible than that in 1*N* acid, but allowing an experimental error of 10%, the capacity-potential curve exhibited the general shape of that in Fig. 8 with potential-pH shift mentioned above. The lack of dependence of the capacity on ionic strength means that the capacity is not primarily determined by the diffuse double layer.

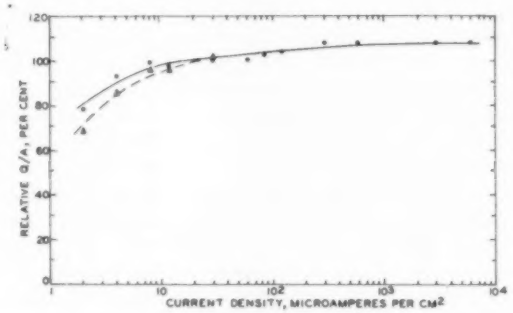

Fig. 9. Effect of current density

Effect of current density.—The effect of cathodic current density on Q/A was observed by applying current ranging from 2 μa to 6 ma/cm^2 to an electrode which had been anodized at 1.65 v for 1 min. As 30 μa/cm^2 was used throughout the present studies, the corresponding Q/A was considered as 100% as a basis for comparison (Fig. 9). On the higher current density side, increasing current density resulted in larger Q/A with a maximum increment of about 8%. This increment may be attributed to the nonequilibrium condition under which the electrode was reduced. On the lower current density side, Q/A dropped fairly rapidly with decreasing current density (dotted line). The deviation of Q/A from 100% in this region could be diminished but could not be completely eliminated if a correction of 0.3 μa/cm^2 due to the open circuit loss of oxidation was introduced (solid line). This deviation was also noted by Vetter and Berndt (5).

To test whether there was an alternate path that required less charge for reduction, the cathodic current was applied in pulses with equal resting times in between. At moderate current density (60 μa/cm^2), the sum of pulses of 2 sec each gave the same Q/A as that obtained in the normal, continuous way. At current densities below 12 μa/cm^2, the sum of pulses and the open circuit loss during resting times amounted to some 90% of the Q/A by the normal way at the same current densities. The difference between the 10-sec and the 30-sec pulses was small. These findings suggest an alternate path such as the decomposition of an active intermediate produced by partial reduction to give molecular oxygen, which escapes during the quiescent period. The data in Fig. 9 indicate that the alternate path is responsible for a fraction of the whole reduction process and becomes important only at very low current densities.

Anodic chronopotentiograms were run with the different current densities above. In the region of potential below 1.35 v, no arrest or abrupt change in slope was in evidence. This tends to discredit the intermediate formation of Au_2O and AuO, which have been inferred solely from the arrests observed (4, 9) and to support the view that these arrests are probably the effects of impurities (5, 6).

Electron microscopy studies.—Gold surfaces under different treatments were examined by means of RCA EMU-2 or -3 electron microscopes. The replica was made by shadow-casting the acetylated

cellulose replicating tape with palladium at an angle of 25° and then with carbon at 90° (11).

The surface of gold foil as received showed straight lines resulting from cool rolling. When the foil had been heated in an oxygen-natural gas flame to near white heat for a period of several minutes, these lines disappeared because of recrystallization and diffusion of the material of the elevated parts. All electrodes used in the present studies had undergone such fire polishing when first made. The fire polishing would be expected to cause the formation of small grains, the appearance of which is not apparent on the surface. Electrochemical reactions attack the grain boundaries more vigorously than the other parts so that the boundary lines become conspicuous on the surface of used electrodes. A reduced electrode which had been kept at 0.65 v and an oxidized electrode, kept at 1.65 v for 20 min before the replica was made, appeared quite similar. An electrode strongly oxidized at 2.15 v for 3 min had so thick a layer of oxide that the boundary lines were obscured.

Conclusion

In postulating a mechanism for the anodic process, hydroxyl radical is chosen among other one-electron oxidation products as the oxygen evolution intermediate because of its presence in the slow step of the oxygen evolution on platinum (16) and because of the similarity in the behavior of gold and platinum in hydrogen peroxide, which gives OH on decomposition (17).

$$Au + H_2O \rightleftharpoons Au\cdots OH + H^+ + e^- \qquad [1]$$

The chemisorbed OH readily undergoes the following reaction

$$Au\cdots OH \rightarrow AuO + H^+ + e^- \qquad [2A]$$

where AuO represents a chemisorbed oxygen atom layer rather than a definite oxide of divalent gold, or the following reaction in which oxygen is evolved through electrochemical attack

$$Au\cdots OH + H_2O \rightarrow Au\cdots OOH + 2H^+ + 2e^- \qquad [2B]$$

$$Au\cdots OOH \rightarrow Au + O_2 + H^+ + e^-$$

The clean surface regenerated in [2B] may undergo [1] again.

Further oxidation may take place on the AuO surface

$$AuO + H_2O \rightarrow AuO\cdots OH + H^+ + e^- \qquad [3]$$

$AuO\cdots OH$ has the same empirical formula as hydrated Au_2O_3 (12). That Au_2O_3 is the end product is supported by the finding that the potential of cathodic arrest and the electrode potential after open circuit drift suggest the existence of a potential-determining system in the neighborhood of 1.36 v, the experimental value of the standard potential of $Au(OH)_3/Au$ (18).

The gradually increasing anodic potential in the chronopotentiogram suggests that the anodic potential is a mixed potential for formation of an oxidized gold surface and for oxygen evolution.

Acknowledgment

One of the authors (M. S. C.) would like to acknowledge the financial assistance of the U.S. Air Force [Contract No. AF 33 (616)-5446] and the National Science Foundation [Research Grant NSF G-2420]. The assistance of Dr. R. A. Borasky in electron microscopy is gratefully acknowledged.

Manuscript received Jan. 16, 1961.

Any discussion of this paper will appear in a Discussion Section to be published in the June 1962 JOURNAL.

REFERENCES

1. G. Armstrong, F. R. Himsworth, and J. A. V. Butler, *Proc. Roy. Soc. (London)*, **A143**, 89 (1934).
2. G. Deborin and B. Ershler, *Acta Physicochim.*, **13**, 347 (1940).
3. A. Hickling, *Trans. Faraday Soc.*, **42**, 522 (1946).
4. S. E. S. El Wakkad and A. M. Shams El Din, *J. Chem. Soc.*, **1954**, 3098.
5. K. J. Vetter and D. Berndt, *Z. Elektrochem.*, **62**, 378 (1958).
6. D. Clark, T. Dickinson, and W. N. Mair, *Trans. Faraday Soc.*, **55**, 1937 (1959).
7. F. Bauman and I. Shain, *Anal. Chem.*, **29**, 303 (1957).
8. F. G. Will and C. A. Knorr, *Z. Elektrochem.*, **64**, 270 (1960).
9. J. K. Lee, R. N. Adams, and C. E. Bricker, *Anal. Chim. Acta*, **17**, 321 (1957).
10. H. A. Laitinen and C. G. Enke, *This Journal*, **107**, 773 (1960).
11. M. S. Chao, Ph.D. Thesis, University of Illinois (1961).
12. F. Jirsa and O. Buryanek, *Z. Elektrochem.*, **29**, 126 (1923).
13. S. Duchman and I. Langmuir, *Phys. Rev.*, **20**, 113 (1922).
14. D. Larazua, Private communication.
15. L. Gierst, *Proc. 7th Intern. Comm. Electrochem. Thermodynam. and Kinet, 1957*, 44.
16. J. O'M. Bockris and A. K. M. S. Huq, *Proc. Roy. Soc. (London)*, **A237**, 277 (1956).
17. J. O'M. Bockris and L. F. Oldfield, *Trans. Faraday Soc.*, **55**, 249 (1955).
18. R. H. Gerke and M. D. Rourke, *J. Am. Chem. Soc.*, **49**, 1855 (1927).

The Influence of Iodide Ions and Carbon Monoxide on the Anodic Dissolution of Active Iron

K. E. Heusler[1] and G. H. Cartledge

Chemistry Division, Oak Ridge National Laboratory,

Operated by Union Carbide Corporation for the U. S. Atomic Energy Commission, Oak Ridge, Tennessee

ABSTRACT

The kinetics of the dissolution of iron in sulfuric acid was investigated by polarizaton measurements in the presence of iodide ions or carbon monoxide as an inhibitor. The measurements included an oscillographic study of transient phenomena as well as steady states. The adsorption of iodide ions on iron was measured as a function of iodide concentration and anodic current density. The effects of iodide ions and carbon monoxide depend on the amount of inhibitor adsorbed on the iron surface. A possible mechanism for the dissolution of iron in the presence of iodide ions and carbon monoxide has been developed in analogy to the mechanism proposed earlier for the behavior in solutions not containing these inhibitors.

In solutions of sulfuric or perchloric acid the rate of dissolution of iron is a function of potential and pH (1), but does not depend on the concentration of the anions of these acids (2) or the concentration of cations of base metals or of organic cations (3). Walpert (4a) found the addition of halogenide ions to sulfuric acid solutions to lower the corrosion rate of iron. It was shown later by Iofa *et al.* (5) that iodide, which is the strongest inhibitor among the halogenide ions, decreases the rates of both the evolution of hydrogen and the dissolution of iron by being adsorbed on the iron surface. The inhibiting action increases with the concentration of the halogenide ion in the solution (4, 5).

A quantitative study of the influence of iodide ions on the dissolution of iron and the evolution of hydrogen is presented in this paper. Certain conclusions with respect to the change of the mechanism of dissolution due to the presence of iodide ions can be drawn by comparing the kinetics with and without additions of iodide to sulfate solutions of different pH values.

In attempting to obtain a more generalized picture of the inhibition of the dissolution of iron the effects of certain other additions were investigated. Formic and acetic acid inhibited the dissolution only to a small extent (2). Propionic and butyric acid (4a) and benzoic acid (6) apparently are stronger inhibitors. Carbon monoxide was found to inhibit very effectively by changing the kinetics in a way similar to that produced by iodide ions.

Since the inhibitor certainly acts by being adsorbed on the metal surface, some measurements of the amounts of adsorbed iodide ion as a function of concentration of iodide ion in the solution and of the rate of iron dissolution seemed to be necessary and have been made by determining the decrease of the iodide concentration in the solution after adsorption by use of tracer I^{131}.

[1] Present address: Max-Planck-Institut für Metallforschung, Stuttgart, Germany.

Experimental

Polarization measurements.—Electrolytic iron deposited according to Vetter (7) was used in all experiments. Platinum wires melted into glass at one end and connected to a copper lead were covered with a layer of iron approximately 0.2 mm thick. Two iron electrodes of this type were necessary for polarization measurements. The potential of one of them was measured against a saturated calomel electrode. This iron electrode and the reference electrode were connected by a Luggin capillary filled with the solution in which the iron was to be investigated. The other iron electrode in the second half cell, connected with the first half cell by a sintered glass disk, was used to pass a polarizing current through the cell. Sulfuric acid 0.5*f* prepared from triply distilled water and analytical grade concentrated sulfuric acid served as electrolyte. By adding solid analytical grade sodium hydroxide the pH was adjusted to the desired value. Freshly prepared concentrated solutions of potassium iodide in the sulfate solution were added to vary the iodide concentration in the cell. The solution in the closed cell was kept free from oxygen by passing a stream of pure helium through it. Measurements were made at the constant room temperature of 23°.

Polarization curves were obtained by passing a constant current through the electrode and recording the potential with a Brown recorder, using a vibrating reed electrometer as amplifier. Fast variations of potential after a change of the current were observed with a Tektronix 536 oscilloscope containing the plug-in units D and T.

Steady-state polarization.—The steady-state polarization curve of iron is shown by curve A in Fig. 1. In agreement with previous experiments (1), the Tafel line corresponding to the anodic dissolution of iron in pure sulfate solutions had a slope of about 30 mv (average from 12 polarizations was 31.4 mv), and the Tafel line corresponding to the cathodic

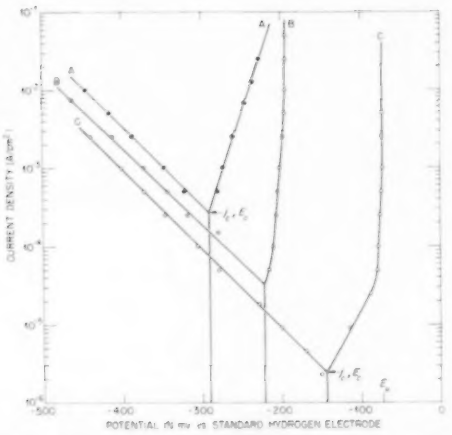

Fig. 1. Steady-state polarization curves for iron in 0.5f H_2SO_4 at 23°: A, in pure solution; B, with addition of $5.5 \cdot 10^{-4}$f KI; C, with addition of $5.5 \cdot 10^{-2}$f KI.

evolution of hydrogen had a slope of about 120 mv. The corrosion current density j_c determined from the intersection of anodic and cathodic Tafel lines at the corrosion potential E_c was somewhat higher than in the earlier experiments (1a), in which pure carbonyl iron was used, instead of electrolytic iron.

Additions of iodide yielding a concentration less than 10^{-4} *f* in the solution produced no measurable effect on the polarization curves. At higher concentrations of iodide the effects shown in Fig. 1, curves B, C, were obtained. The corrosion potential shifted to more noble values and the corrosion current density decreased, which indicates that the iron dissolution was inhibited to a greater extent than the hydrogen evolution. The addition of iodide shifted the Tafel line of cathodic hydrogen evolution to lower current densities or higher overvoltages, and the slope remained unchanged within the experimental error. The polarization curve of the anodic dissolution of iron was changed more drastically. Tafel lines were not observed. Anodic currents polarized the iron only to a certain potential, and a further increase of the current density by two or three decades did not change the potential significantly. This potential of unpolarizability, E_u, was found to be a function of iodide concentration and pH. A tenfold increase of the iodide concentration shifted E_u 53 (±6) mv toward more noble potentials, as Fig. 2 shows. Figure 3 shows the variation of E_u with pH, which is −59 (±6) mv per pH unit.

The steady-state corrosion potential deviated from E_u at high iodide concentrations more than at low concentrations. Steady states were reached after a few minutes at high anodic current densities. At low current densities of the order of the corrosion current density, up to 1 hr was necessary before the steady state was attained, especially after a preceding high anodic polarization.

To study the effect of carbon monoxide on the iron electrode, pure CO (C. P. grade, 99.5% CO, *ca.* 0.5% $N_2 + H_2$, no sulfur compounds) was passed through the solution instead of helium. After turning on the stream of CO the corrosion potential became more

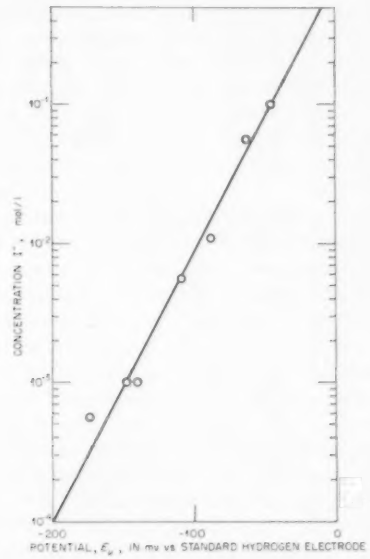

Fig. 2. Variation of the potential of unpolarizability, E_u, with iodide-ion concentration in 0.5f H_2SO_4.

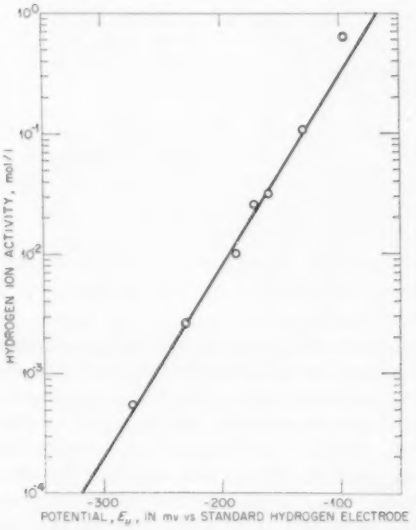

Fig. 3. Variation of the potential of unpolarizability, E_u, with pH at an iodide-ion concentration of 1×10^{-2}f in 0.5f sulfate solution.

noble, reached a maximum after about 10 min, then debased slowly and approached a steady state after 50–75 hr. (A similar behavior was observed after the solution had been made highly concentrated with iodide, but the whole process occurred about 100 times faster.) If the carbon monoxide was again replaced by helium, the corrosion potential ennobled in the first 30 min and debased afterwards toward the corrosion potential in the pure sulfate solution, which was reached within 2-3 hr. Any effects of CO on the polarization curve had disappeared after that time.

The steady-state polarization curve of the dissolution of iron in sulfate solutions saturated with CO of atmospheric pressure had the same shape as that

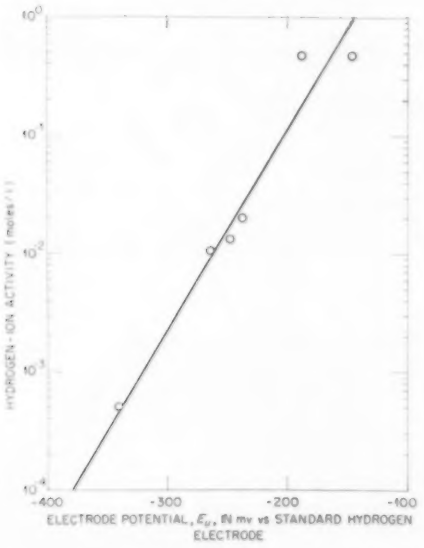

Fig. 4. Variation of the potential of unpolarizability, E_u, with pH in 0.5f sulfate solutions saturated with CO at atmospheric pressure and 23°.

obtained in the presence of iodide (Fig. 6). The potential of unpolarizability, E_u, again became more negative with increasing pH by about 59 mv/pH, as in the case of iodide (Fig. 4).

The experimental arrangement did not permit variation of the carbon monoxide pressure, but from the essentially similar behavior of the iron in presence of iodide, ennobling of E_u with increasing CO pressure has to be expected.

The Tafel line of cathodic hydrogen evolution was displaced to higher overvoltages after saturation of the solution with CO.

Transient effects in polarization.—Immediately after a stepwise increase of the anodic current density the potential rose to an overvoltage which was higher than that in the steady state at the higher current density. A maximum overvoltage was reached after a certain time necessary to charge the electrode capacity. If, starting from the same point on the steady-state polarization curve (*i.e.*, the same steady-state current density and potential), different additional currents were applied, a transient polarization curve was obtained by plotting current density *vs.* overvoltage taken after the electrode capacity had been charged. In pure sulfate solutions this transient polarization curve was a Tafel line with a slope of 63 mv (8). In the presence of iodide up to 0.2*f*, Tafel lines of approximately the same slope were found (Fig. 5). For a specified overvoltage with respect to the steady-state potential from which the transient polarization was started, the current densities in the transient polarization curves always were proportional to the current density of the initial steady state. A more complicated transient polarization curve was observed in solutions containing CO or high concentrations ($> 0.2f$) of iodide ion (Fig. 6). In solutions saturated with CO the maximum potential deviations from the steady-state potential were proportional to the additional anodic

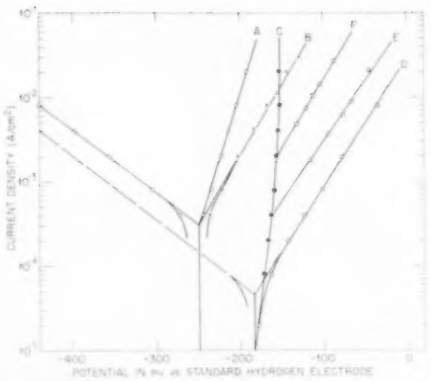

Fig. 5. Steady-state and transient polarization curves for iron in 0.5f H_2SO_4. Steady-state polarization curves: A, in pure acid, and C with addition of 10^{-5}f KI. Transient polarization curves: B, in pure acid without external prepolarizations; D, with addition of 10^{-5}f KI without external prepolarization; and with prepolarization of 0.4 ma/cm², E, and 2 ma/cm², F.

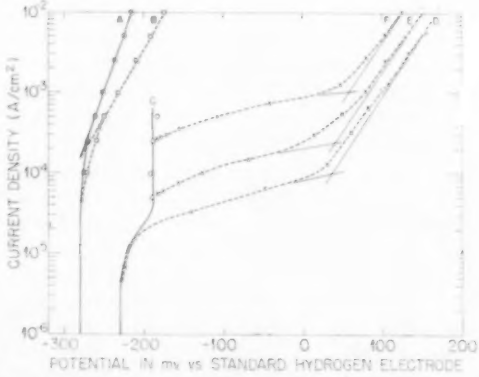

Fig. 6. Anodic steady-state and maximum overvoltage curves in 0.5f H_2SO_4 with or without saturation of the solution with carbon monoxide. Steady states: A, pure acid; C, acid saturated with CO. Maximum overvoltages: B, pure acid; acid saturated with CO, D without prepolarization; E and F, starting from the steady states corresponding to a prepolarization of 50 or 250 μa/cm² and measured by switching on additional currents.

current density: $\Delta E = R \cdot \Delta j$ in a range up to 200 mv. At higher overvoltages the usual Tafel line was observed, and measurements at different pH values showed first-order dependence on the hydroxide-ion concentration ($\delta \log j./\delta\ pH = 0.95$). The experimental data can be interpreted formally by two parallel processes, one yielding a Tafel line, the other having the effect of an ohmic resistance, R. The current densities j_{tr} in the transient polarization curves still are proportional to the steady-state current density j_{st}. This implies that the R is inversely proportional to the steady-state current density. Thus, the transient polarization curve can be described empirically by Eq. [1]

$$j_{tr} = j_{st}\left(1 + \frac{\Delta E}{A} + k \cdot \exp\frac{\Delta E}{\phi}\right) \qquad [1]$$

with ΔE = maximum deviation from the steady-state potential, $2.3\,\phi = 2.3\,\frac{RT}{2\alpha F} = 63$ mv, and $A = 87$ mv.[2]

[2] This value for A was obtained from CO-saturated solutions. It might be different in iodide solutions.

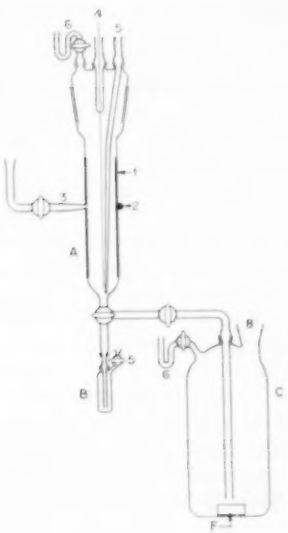

Fig. 7. Apparatus for adsorption measurements. A: Adsorption vessel with cylindrical iron electrode, 1, connected to the outside of the glass vessel by seal, 2; the capillary, 3, leads to the reference electrode; 4, platinum wire; 5, connections to helium supply or vacuum; 6, gas outlets. B: Counting vessel. C: Vessel for preparation and storage of solution, with magnetic stirrer, F. Connection to condenser and water boiler, 8. Distillation was conducted in a stream of helium. No grease was used on any joint.

The constant k is small for solutions saturated with CO ($k \approx 10^{-3}$), or containing high concentrations of KI ($k \approx 10^{-1}$ for 0.5f KI). At low concentrations of iodide k becomes large ($k >> 1$), and the influence of the part linear in ΔE disappears in Eq. [1].

Adsorption Measurements.—The adsorption of iodide on the surface of the iron electrode was determined by measuring the decrease of iodide concentration after the iron was brought in contact with the solution containing I^{131}. A similar method has been used by Kolotyrkin (9) and others (10) to study the adsorption of ions on metal surfaces. The apparatus used in our experiments is shown schematically in Fig. 7. A large ratio of surface area to volume is necessary. In order to satisfy this condition the inside of a glass cylinder (1.5 cm in diameter, 15 cm long) was platinized, covered electrolytically with a layer of copper about 0.5 mm thick and finally with a thin film of gold. For each of the experiments a new layer of iron about 0.2 mm thick was deposited electrolytically on the gold surface. The iron electrode was washed with hydrochloric acid and with oxygen-free, triply distilled water under a helium atmosphere until no reaction of the wash water with a silver nitrate solution was observed. A stream of helium was passed through the cylinder for several hours to dry the iron surface completely.

Solutions were prepared by distilling water onto a known amount of potassium iodide which was labeled with radioactive I^{131}. Concentrated sulfuric acid was added later through the counting vessel to render the solution 0.5f in H_2SO_4.

The activity of the I^{131} ions in the solution was determined by scintillation counting after filling the counting vessel with about 2.5 cm^3 of the solution to a certain mark which allowed duplication of the volume to about 1%. The height of the solution in the counting vessel was 7 cm, and the hole in the counter was only 5 cm deep. Therefore small changes of the volume of the solution did not affect the results of counting. The activity was adjusted to a counting rate of 150,000-500,000 counts/min to keep the statistical error small. Each sample was counted at least 4 min and at least 3 different samples were used to evaluate the initial activity accurately. Then, solution was forced into the cylinder containing the large cylindrical iron electrode and a platinum wire electrode in the center. The solution was filled to a certain mark and stirred with helium occasionally. Three or more samples of the solution from the adsorption cylinder were counted at each concentration.

From the decrease of activity, compared at a time $t = 0$ with the initial activity, the amount of adsorbed iodide was evaluated. Adsorption on glass surfaces was proved to be negligible; no correction was applied for adsorption on the platinum wire (0.8 mm diameter). Evaporation of water from the solution in the adsorption cylinder raised its concentration by measurable amounts after a few hours. Corrections of up to 0.004%/min had to be applied.

The potential of the iron was measured *vs.* a calomel electrode. Electrolytic contact was achieved by a hole in the iron cylinder and a capillary. The temperature in all experiments was the constant room temperature of 23°C.

Experimental results of adsorption measurements.—The adsorption of iodide at the corrosion potential was followed first as a function of time. An example is given in Table I for $1.5 \cdot 10^{-4}f$ KI in 0.5f H_2SO_4. The activities shown are corrected for decay and the volume of solution in the adsorption cell was 29 ml. Adsorption is thus constant after a few minutes.

The average values of the amounts of iodide ions adsorbed at the respective corrosion potentials are shown in Fig. 8. These potentials varied between −252 and −306 mv *vs.* the normal hydrogen electrode for the different concentrations; the corresponding values of E_a were approximately 100 mv more noble. In establishing the points for open circuit, between 8 x 10^5 and 5 x 10^6 counts were taken in order to give good statistics. The relative probable errors ranged between 0.75 and 2.6% for all concentrations except the highest, for which it was 4.6%. The figure shows the data in relation to a Langmuir isotherm of the form

Table I. Time dependence of the amount of iodide ion adsorbed on iron

Time, min, t	Initial counts per minute, A_0	Decrease of counts per minute, dA	Relative decrease of concentration, dA/A_0	Number of ads. ions on 1 cm^2 apparent surface area, N
5	182,763	3195	$1.75 \cdot 10^{-2}$	$0.77 \cdot 10^{15}$
16	182,763	3815	$2.09 \cdot 10^{-2}$	$0.91 \cdot 10^{15}$
48	182,763	3804	$2.08 \cdot 10^{-2}$	$0.91 \cdot 10^{15}$
111	182,763	3768	$2.06 \cdot 10^{-2}$	$0.90 \cdot 10^{15}$
1412	182,763	3845	$2.10 \cdot 10^{-2}$	$0.92 \cdot 10^{15}$

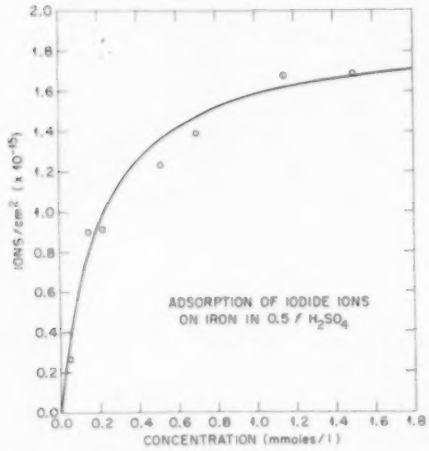

Fig. 8. Adsorption of iodide ions on iron. Experimental points and calculated Langmuir isotherm.

$$N = N_{max} \frac{c}{k + c} \qquad [2]$$

the calculated curve being a least-squares fit with $N_{max} = 1.91 \times 10^{15}$ ions/cm² and $k = 0.207$ mmoles/l. The deviations are slightly less if the data are compared with a Temkin isotherm (11) of the form

$$N = A \log a_o c \qquad [3]$$

with $A = 0.95 \times 10^{15}$ ions/cm² and $a_o = 40$ 1/mmole.

When current was being passed through the cell the measurement of adsorption presented several difficulties which made the data less precise than those on open circuit. The results of these measurements will be presented more fully in connection with the discussion of a proposed mechanism for the anodic process, but it may be indicated at this point that a marked decrease in adsorption was observed in those cases in which the current density sufficed to raise the potential close to the E_o value.

Discussion

The polarization measurements permit the following observations regarding the inhibitory action of the iodide ion at low concentrations. From Fig. 5, for KI $1 \times 10^{-5}f$ in $0.5f$ H_2SO_4, it is seen that the corrosion potential is ennobled by 64 mv and that the corrosion rates *at the respective corrosion potentials* differ by a factor of about 6. If the anodic currents are compared at the corrosion potential of the inhibited system, $10^{-5}f$ iodide decreases the corrosion rate by a factor of about 800. This inhibition is very dependent on the potential, however, and the figure indicates that it should disappear entirely at a potential about 50 mv more noble than E_o, owing to the unpolarizability induced by the inhibitor. At an inhibitor concentration of $1 \times 10^{-6}f$, transients are obtained that have slopes approximately the same as those observed in absence of inhibitor. In the experiments with carbon monoxide, it was shown that the adsorption and resulting inhibition are reversed by passage of helium through the inhibited system.

At higher concentrations of iodide ion and in solutions saturated with carbon monoxide, efficient inhibition is maintained at potentials considerably higher than the corrosion potential. In these cases transient maximum potentials differing from steady-state potentials are obtained only at potentials above E_o. The position of the Tafel lines ultimately observed from these transients (as in Fig. 6) indicates the persistence of much inhibition at these potentials. A complex of processes is indicated at intermediate potentials.

A mechanism for the dissolution of active iron in pure sulfate and perchlorate solutions has been proposed earlier by one of us (8). From the slopes of the Tafel lines in the steady state (30 mv) and in the transient polarization curves (63 mv), and from the reaction orders γ with respect to the hydroxyl ions, which are $\gamma = 2$ for the reaction in the steady state and $\gamma = 1$ for the reaction corresponding to the transient polarization curve, the following mechanism was derived: An iron atom on the surface and a hydroxyl ion react electrochemically to form a catalyzing surface compound (reaction [A]).

$$Fe + OH^- \rightleftarrows (Kat)_{ads} + e^- \qquad [A]$$

The catalyst reacts with a neighboring iron atom and a second hydroxyl ion to dissolve one ferrous ion and is regenerated during this process. To account for the observed reaction order in hydroxyl ions and the slope of the transient polarization curve the dissolution reaction must be such as to follow the kinetics indicated by Eq. [4]

$$j_o = k_o \cdot q \cdot a_{(OH^-)} \cdot \exp \frac{2\alpha FE}{RT} \qquad [4]$$

In this situation the concentration of catalyst, q, is momentarily constant when the current density or potential is changed and the 2α factor in the exponential term must equal 1. The over-all effect of the processes including the rate-determining step in the dissolution reaction was assumed to correspond to Eq. [B]

$$Fe + (Kat)_{ads} + OH^- \rightarrow (Kat)_{ads} + FeOH^+ + 2e \qquad [B]$$

In the steady state, reaction [A] is in equilibrium, hence q increases both with increase of $a_{(OH^-)}$ and with potential, according to the Nernst equation

$$q = k \cdot a_{(OH^-)} \exp \frac{FE}{RT} \qquad [5]$$

It follows from the applicability of this equation to the experimental data that the area covered by catalyst is small in comparison with the total surface area.

The adsorption of iodide ions or CO on the iron surface lowers the dissolution rate of iron. The measurements of the adsorption of iodide ion show this parallelism between adsorption and inhibition of the dissolution of iron. Thus, at a given potential, the anodic current density of iron dissolution decreases with increasing iodide concentration and increasing amount of adsorbed iodide. At the higher concentrations of iodide ions the amount of adsorbed iodide becomes smaller at higher anodic current densities, if the potential is close to the potential of unpolarizability.

The observed effects of iodide ions or carbon monoxide may arise from one or more of the following causes: (*a*) the activation energy of the dissolution reaction may be increased, (*b*) the concentration of adsorbed hydroxyl ions, and hence, of catalyst may be diminished, or (*c*) the frequency of finding an active metal atom contiguous to a catalyst site may be reduced. Since exactly similar effects arise from adsorption of either neutral carbon monoxide molecules or charged iodide ions, it appears unlikely that the effects may be ascribed to any significant changes in the potential in the diffuse side of the double layer. In a simplified picture the situation can be described as follows: in a relative area θ the adsorbed iodide increases the activation energy so sharply that dissolution cannot occur. The iron then dissolves from the remaining area $(1-\theta)$ only. The reaction rate (Eq. [4]) becomes proportional to $(1-\theta)$, and if it is assumed that the catalyst can be formed in the uncovered area only, in Eq. [5] q is also proportional to $(1-\theta)$.

Since at high current densities iodide is desorbed and since the desorption is observed at lower overvoltages the higher the pH is made (Fig. 3 and 4), one is led to the assumption that parallel to the process considered above iron can dissolve by a second process involving desorption of iodide. In analogy to the process described above, it will be assumed that in this second process an iron atom from an uncovered area $(1-\theta)$ reacts with a hydroxyl ion from the solution and an adsorbed iodide from the covered area θ to dissolve as ferrous ion. The adsorbed iodide is considered to leave the iron surface during the reaction, unlike the catalyst of the first process.[3]

The following expression for the total anodic current density is obtained from the preceding considerations

$$j_+ = k_+ \cdot q \cdot (1-\theta) \cdot a_{(OH^-)} \cdot \exp\left(\frac{2\alpha FE}{RT}\right) + k_+' \cdot \theta \cdot (1-\theta) \cdot a_{(OH^-)} \cdot \exp\left(\frac{2\beta FE}{RT}\right) \quad [6]$$

In the steady state the surface coverage of the catalyst is

$$q = k \cdot (1-\theta) \cdot a_{(OH^-)} \cdot \exp\left(\frac{FE}{RT}\right) \quad [7]$$

Substitution of [7] into [6] gives the total steady-state anodic current density

$$j_+ = k_+ k (1-\theta)^2 a^2_{(OH^-)} \exp\frac{(2\alpha+1)FE}{RT} + k_+' \theta (1-\theta)\, a_{(OH^-)} \exp\frac{2\beta FE}{RT} \quad [6a]$$

[3] The definition of θ is somewhat problematical. To apply the Nernst equation in the form $E = E^\circ + \frac{RT}{F} \ln \frac{q}{a_{(OH^-)}}$ in the absence of an inhibitor assumes the activity of iron to be constant and therefore the coverage corresponding to q to be small compared to the total surface available for reaction. In the presence of strongly adsorbed iodide ions or carbon monoxide, however, it is necessary to consider that the bare metal surface becomes restricted, or that θ represents, as a first approximation, the area covered by adsorbed I- or CO, whereas $(1-\theta)$ refers to the total bare area. At sufficiently high values of pH or of the potential it might be necessary to complicate the analysis by expressing the bare-metal area as $(1-\theta-f(q))$, in which $f(q)$ is some function of the area covered by adsorbed catalyst.

In this form the equation shows the differences between the two components of the anodic process with respect to the reaction orders in $a_{(OH^-)}$, θ, and $(1-\theta)$, and also the different dependencies on potential.

If the iron dissolution has reached a steady state, the adsorption of iodide also must have reached a steady state, or the rates of adsorption v_{ads} and of desorption v_{des} of iodide must be equal. The current density of the second anodic process is equivalent to a rate of desorption of iodide. But besides this process an additional normal desorption, in a first approximation independent of potential, certainly proceeds with a rate proportional to θ. One obtains

$$v_{des} = k_+' \cdot \theta \cdot (1-\theta) \cdot a_{(OH^-)} \cdot \exp\left(\frac{2\beta FE}{RT}\right) + k'_{des} \cdot \theta \quad [8]$$

The rate of adsorption is considered to be proportional to the area uncovered by iodide and the activity of iodide in the solution

$$v_{ads} = k_{ads} \cdot (1-\theta) \cdot a_{(I^-)} \quad [9]$$

(For dimensional consistency the v's are to be considered as current densities.)

The assumption that the adsorption of iodide or CO is independent of potential, if the corrosion of the iron is slow enough, has been made because adsorption of iodide was found to be independent of the potential at low current densities within the experimental error. The adsorbed iodide apparently forms a strong nonpolar bond with the iron surface, as is also expected for CO. In the case of hydroxyl ions reacting with the iron surface, the coverage, which is small compared to the maximum coverage under most experimental conditions, increases one decade if the potential becomes 60 mv nobler. This indicates a strong polarity of the bond. As is well known from the complex chemistry of the transition elements, the tendency to form nonpolar bonds increases in the direction $OH^- < I^- < CO$.

From $v_{ads} = v_{des}$ in the steady state an adsorption isotherm can be calculated which is quadratic in θ and is written conveniently in the form

$$E = \frac{R \cdot T}{2\beta F} \cdot \ln\left[\left(1 - \frac{k'_{des}}{k_{ads}} \cdot \frac{1}{a_{(I^-)}} \cdot \frac{\theta}{(1-\theta)}\right) \cdot \frac{k_{ads}}{k_+'} \cdot \frac{a_{(I^-)}}{a_{(OH^-)}} \cdot \frac{1}{\theta}\right] \quad [10]$$

Equation [10] contains two limiting cases, in both of which θ appears in the first degree only: If

$$k'_{des}\,\theta << k_+' \cdot \theta \cdot (1-\theta) \cdot a_{(OH^-)} \cdot \exp\left(\frac{2\beta FE}{RT}\right)$$

$$\theta = \frac{k_{ads}}{k_+'} \cdot \frac{a_{(I^-)}}{a_{(OH^-)}} \cdot \exp\left(-\frac{2\beta FE}{RT}\right) \quad [10a]$$

If, however, $k'_{des}\,\theta >> k_+' \cdot \theta \cdot (1-\theta) \cdot a_{(OH^-)} \cdot \exp\left(\frac{2\beta FE}{RT}\right)$

$$\theta = \frac{\frac{k_{ads}}{k'_{des}} \cdot a_{(I^-)}}{1 + \frac{k_{ads}}{k'_{des}} \cdot a_{(I^-)}} \quad [10b]$$

At base potentials and on open circuit, Eq. [10b] is valid and θ is independent of potential, as observed. Equation [10b] gives the maximum value of θ at a given activity of iodide ions in the solution. Since a potential of unpolarizability, E_u, is observed only if the "normal" anodic process has been largely inhibited, this implies a relatively high value of θ at potentials negative to E_u when the iodide-ion concentration is adequate for inhibition. The significance of E_u is that, at this potential, the value of θ begins to decrease rapidly, in accordance with Eq. [10a]. Thus, if the maximum value of θ is close to unity, the value of $(1-\theta)$ increases by a large factor in a narrow range of potentials at E_u, and at a potential only $\frac{2.3\,RT}{2\beta F}$ more positive than E_u the coverage has decreased to $\theta = 0.1$. The very rapid increase in current reflects the second-order dependence on $(1-\theta)$, the larger potential dependence and the much higher specific rate constant of the "normal" anodic process. It is seen that Eq. [10] and [10a] agree with the observations that E_u shifts to positive potentials with increase of iodide-ion activity or decrease of hydroxide-ion activity, the changes being 59 mv per decade of activity if $\beta \cong 0.5$ (Fig. 2, 3, and 4).

The relationship between potential and θ derived from Eq. [10] as a function of iodide-ion activity and pH can be used to calculate steady-state polarization curves from Eq. [6a]. Results in arbitrary units are represented in Fig. 9 for three values of the iodide-ion activity. The reference of the potentials to a hydrogen electrode in the same solution makes the curves applicable to any value of pH. For the calculation, k'_{4ss} was taken as 10^{-3}, $\alpha = \beta = 0.5$, and other constants were set equal to 1. Figure 10 shows the variation of θ with potential in accordance with Eq. [10] for the case where $a_{I^-} = 1$. The figure shows also the fraction of the total anodic current that is carried by the process involving electrochemical desorption of iodide ions. For the case considered, it may be seen that the total anodic current should increase by a factor of 10^8 in passing from $\theta = 0.99$ at $E = -2.4$ mv to $\theta = 0.01$ at $E = +120$ mv. Over the same range, the iodide current should increase only by a factor of 10^2.

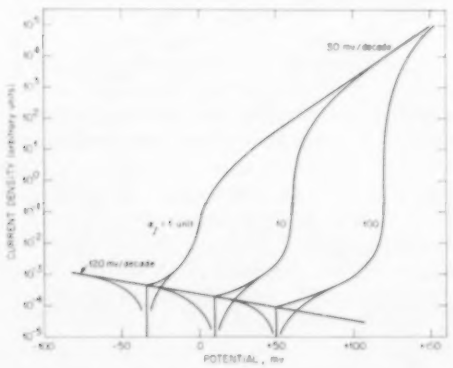

Fig. 9. Anodic polarization curves calculated from Eq. [6] and [10]. The cathodic polarization curve with a slope of 120 mv has been drawn arbitrarily. Current density in arbitrary units. Potentials are given vs. an arbitrary reference electrode having a certain potential difference vs. a hydrogen electrode in the same solution.

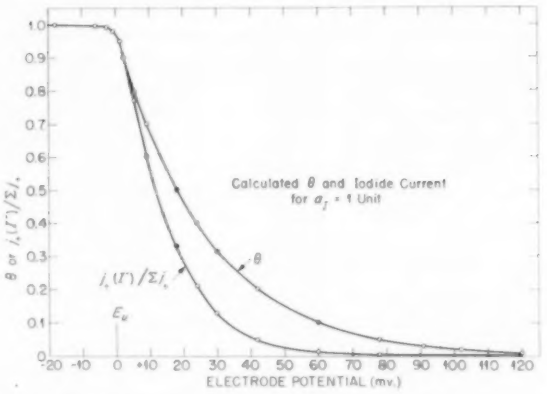

Fig. 10. Calculated values for the potential dependence of θ and also the fraction of the total anodic current carried by the iodide desorption reaction, $j_a(I^-)$. The conditions correspond to the case, $a_I = 1$, in Fig. 9.

The calculated curves are in reasonable agreement with the data obtained in the steady-state measurements. They not only reproduce the striking unpolarizability of the inhibited systems and the dependence of E_u on a_{I^-} and pH, but also show that the corrosion potential deviates from E_u the more, the higher the iodide-ion activity is made, even if no inhibition of the hydrogen evolution reaction is assumed. At the more negative potentials at which the iodide dissolution process dominates, the polarization curve is a Tafel with a slope of 59 mv/decade. At potentials about 59 mv positive to E_u, the "normal" dissolution process is dominant and the curve merges into the 30-mv Tafel which would be expected in the absence of iodide ions. It was not possible to measure the very high current densities at potentials corresponding to complete desorption because of excessive iR drops between the electrode and Luggin capillary, and also because the current densities at high iodide-ion activity approached those at which the first steps of passivation set in. Quantitative differences between the calculated and the measured curves occur at low anodic current densities. But neither is the reproducibility of the polarization curves at low current densities good enough, nor do the many simplifications[4] of the theory allow one to expect complete quantitative agreement.

As indicated previously, difficulty was encountered in the measurement of adsorption while passing current through the electrode. In order to have as large a ratio of iron surface to solution volume as possible, the volume of solution was limited to approximately 30 ml. Hence, passage of any consider-

[4] One of the simplifications comes from the fact that the same θ is used to represent areas covered with iodide, and areas from which adsorbed iodide is available for the dissolution of iron involving desorption of iodide ions. Or, the same $(1-\theta)$ is used to represent areas where hydroxyl ions may react according to reaction [A], where iodide ions can be adsorbed, and where reaction [B] can occur. The activation energy contours (i.e., the activation energy as a function of the sites of the surface) for those different reactions certainly are not the same. It is possible that sites belonging to θ in one reaction can belong to $(1-\theta)$ in another reaction. Thus, if always the same θ and $(1-\theta)$ are used in the preceding equations, the sum of θ and $(1-\theta)$ is not necessarily equal precisely to unity, but the approximation is necessary in absence of any known functional relation between the activation energy contours of the different reactions.

Table II. Change in adsorption close to E_u

Conc. I^-	$0.52 \cdot 10^{-3}$	$1.15 \cdot 10^{-3}$	$1.50 \cdot 10^{-3}$	$4.30 \cdot 10^{-3}$[a]
E_u (mv S.C.E.)	−418	−400	−394	~ −475
E's (mv S.C.E)	−514, −445	−525, ~E_u	−494, −407	−565, ~E_u
j's (ma/cm²)	0, 4.8	0, 8.3	0, 4.3	0, 8.3
N's·10^{15}	1.25, 0.85	1.61, 1.45	1.69, 0.15	0.38, 0.07
C.L.[b]	0.89	0.30	>0.99	>0.99
E's (mv S.C.E.)	−445, −	~E_u, −520	−407, −492	~E_u, −5.90
j's (ma/cm²)	4.8, 0	8.3, 0	4.3, 0	8.3, 0
N's·10^{15}	0.85, 1.19	1.45, 1.78	0.15, 2.22	0.07, 0.39
C.L.	0.87	0.50	>0.98	>0.96
E's (mv S.C.E.)	−445, −483	−457, ~E_u		
j's (ma/cm²)	4.8, 1.7	2.0, 8.3		
N's·10^{15}	0.85, 1.13	2.42, 1.45		
C.L.	0.79	0.95		

[a] 0.5f sulfate, pH initial, 1.60; final 2.27; other solutions were 0.5f H_2SO_4; [b] C.L. = confidence level.

able number of coulombs would inevitably cause a change in the pH value. Further, according to the model of the anodic processes proposed, the current would be expected to decrease the adsorption only when the potential approached the value of E_u. At lower potentials, the adsorption process is presumed to be essentially in equilibrium, without disturbances by the low current densities employed. To approach E_u, however, the currents had to be raised to as much as 1 amp and consequently could not be passed long enough in all cases to assure the attainment of a steady state. Also, according to the proposed model, passage of current should not be expected to change the adsorption significantly in solutions that were below the concentration required for extensive inhibition. In such cases, most of the current should be carried by the much faster "normal" anodic process. Finally, to avoid passage of excessive current, only one sample was taken for counting, so that the relative probable errors of the measurements with current passing ranged between 10 and 25%.

To the extent that the adsorption measured while current flowed may be considered to be valid, the data permit the following conclusions to be drawn. (i) With 0.05 and 0.15 x $10^{-3}f$ iodide solutions, no significant change in adsorption was observed. (ii) There was reasonably clear evidence that adsorption increased somewhat at the lower current densities (0.25 − 4 ma/cm²), the potentials, in these cases, being considerably negative to E_u. (iii) The potential of unpolarizability was reached or closely approached at 4.3 − 8.3 ma/cm² in iodide solutions that were 0.52, 1.15, 1.50, or 4.30 x $10^{-3}f$, respectively. In all ten of the comparisons of adsorption which the data permit, a lower adsorption was found at the higher current density, whether the current was being increased or decreased. A statistical examination of the counting data was made to determine the confidence level for each comparison. The results are given in Table II, from which it is seen that the confidence levels are 0.95->0.99 in five instances and 0.8-0.9 in three others, while the difference in adsorption is too small to be significant in two cases. The absence of an effect at the lowest, noninhibiting concentrations and the decrease in adsorption at potentials near E_u are what would be expected from the proposed mechanism. The increase of adsorption observed at low current densities also is to be expected on the basis of surface-charge considerations, and it is particularly significant that this initial increase is reversed at somewhat higher potentials.

In order to calculate polarization curves similar to the observed ones, values of θ have to be assumed that are higher than the coverages measured experimentally. This certainly is connected with the assumption of an adsorption energy uniform throughout the surface leading to the Langmuir isotherm Eq. [10b]. If the adsorption energy E^s of the iodide is different at different sites s of the surface, $k_{ads}/k'_{des} = f(E^s,s)$ has to be integrated over the total surface. A Temkin isotherm Eq. [3] is obtained under certain conditions by assuming a Langmuir isotherm for each of the sites with $E^s_s + dE^s \geq E^s_s \geq E^s_s - dE^s$ (11b). Sites with a high adsorption energy are covered almost completely at medium coverage with respect to the total surface. It is very probable that parts of the surface which have a small activation energy for the dissolution of iron, if they are not covered by iodide or CO, at the same time have a high adsorption energy for the inhibitor. θ in Eq. [10] should refer then to those "active sites" only, but the experimentally measured coverage refers to the total surface and therefore is certainly smaller.

Transient polarization curves such as those shown in Fig. 5 may be calculated by assuming that changes of the adsorption state of the iron surface are slow. If in Eq. [6] q and θ are considered to be constant, a transient polarization curve of the following form is obtained

$$j_{tr} = j_{st} \cdot \exp\left(\frac{2\alpha F \Delta E}{RT}\right) \qquad [11]$$

Equation [11] describes the experimental results for iodide concentrations between $c_{(I^-)} = 0$ and $c_{(I^-)} = 0.2f$ in 0.5f sulfate solutions.

At higher iodide concentrations as well as in solutions saturated with CO the more complex transient polarization curves as shown in Fig. 6 have been measured. Their theoretical explanation cannot be given without introducing additional assumptions.

Another effect which also occurs in the strongly inhibiting solutions certainly is related to the com-

plex transient behavior, namely, the characteristic reversals in the direction of shift of the open-circuit potential observed before steady states were attained after addition or removal of inhibitor. Thus, when carbon monoxide replaced helium, the potential ennobled rapidly and subsequently debased somewhat before becoming stable. When helium replaced carbon monoxide there was a slight ennobling before the potential fell to the value it previously had in the absence of inhibitor. The debasing of the corrosion potential after prolonged addition of carbon monoxide is connected with a slight increase of the corrosion rate, showing that the effect cannot be explained by a slowly increasing inhibition of the hydrogen evolution.

Both results, the reversal of shift of the open-circuit potential and the complex transient behavior, make it necessary to assume some specific effect at high coverages of the dissolving iron surface not represented merely by changes in the magnitudes of q and θ. A possible suggestion would be that the configuration of the surface components has to be considered in order to explain the experimental results in the transients. For the dissolution reaction to occur, the proximity of bare metal and adsorbed iodide ions or CO, or of bare metal and adsorbed hydroxide ions is required. It is quite possible that changes of the current density (considering the transient behavior) or of the inhibitor concentration (considering the shifts of the open-circuit potential) initially leave the surface with another configuration of the reactive surface components than is indicated by the numerical values of q and θ in the equations developed above. A new rate process would then come in, representing the redistribution of the components which enter into the dissolution reaction. If, for example, the current density is increased on a strongly inhibited iron surface, one expects a less favorable configuration to result initially, corresponding to higher overvoltages, since the most favorable proximities of bare metal and adsorbed iodide ions or CO disappear first because the dissolution is connected with desorption of iodide ions or CO. The process of redistribution of the reactive components later on creates new favorable proximities, and the overvoltage decreases with time. Further experimental investigation is required before a more detailed description of the mechanism of the processes responsible for the transient behavior at high inhibitor concentrations can be given.

To summarize the results, both iodide ions and carbon monoxide have been shown to adsorb reversibly on iron in sulfuric acid. The adsorption causes a slight increase in the overvoltage for evolution of hydrogen, but the chief effect is on the anodic polarization curve. The over-all effect is a considerable diminution of the corrosion rate.

It has been shown that the shape of the unusual polarization curves and their dependence on the pH value and the concentration of iodide ions may be accounted for by a kinetic analysis based on the combination of a previous treatment for the anodic dissolution of iron in absence of the inhibitors with an adsorption isotherm for iodide ions or CO containing a potential-dependent desorption term.

Acknowledgment

Stimulating discussions with the authors' colleagues, F. A. Posey and E. J. Kelly, are gladly acknowledged.

Manuscript received Nov. 15, 1960; revised manuscript received April 28, 1961. This paper was prepared for delivery before the Houston Meeting, Oct. 9-13, 1960.

Any discussion of this paper will appear in a Discussion Section to be published in the June 1962 JOURNAL.

REFERENCES

1. a. K. F. Bonhoeffer and K. E. Heusler, *Z. physik. Chem., N.F.*, **8**, 390 (1956); b. K. F. Bonhoeffer and K. E. Heusler, *Z. Elektrochem.*, **61**, 122 (1957); c. T. P. Hoar and T. Hurlen, "Proc. Meetings Intern. Comm. Electrochem. Thermodynam. and Kinetics, VIII, 1956," p. 445, Butterworths, London (1958); d. H. Kaesche, *Z. Elektrochem.*, **63**, 492 (1959); e. L. A. Larin and Z. A. Iofa, *Zhur. fiz. chim.*, **34**, 1470 (1960).
2. K. Heusler, Dissertation, Göttingen 1957.
3. a. Z. A. Iofa, E. I. Lyakhovetskaya, and K. Sharifov, *Doklady akad. nauk* (D.A.N.), **84**, 543 (1952); b. V. V. Losev, *ibid.*, **88**, 499 (1953).
4. a. G. Walpert, *Z. physik Chem.*, **A151**, 219 (1930); b. M. Tzentnershver and M. Straumanis, *ibid.*, **A162**, 94 (1932).
5. a. Z. A. Iofa and L. A. Medvedeva, *D.A.N.*, **69**, 213 (1949); b. Z. A. Iofa and G. B. Rozhdestvenskaya, *ibid.*, **91**, 1159 (1953).
6. E. J. Kelly and G. H. Cartledge, Chem. Div. Ann. Prog. Rep., ORNL-2782, p. 51, June 20, 1959.
7. K. J. Vetter, *Z. Elektrochem.*, **59**, 67 (1955).
8. K. E. Heusler, *ibid.*, **62**, 582 (1958).
9. a. L. A. Medvedeva and Ya. M. Kolotyrkin, *Zhur. fiz. chim.*, **31**, 2668 (1957); b. Ya. M. Kolotyrkin, *Trans. Faraday Soc.*, **55**, 455 (1959).
10. a. N. A. Balashova, *D.A.N.*, **103**, 639 (1955); b. N. A. Balashova, *Zhur. fiz. chim.*, **32**, 2266 (1958).
11. a. M. I. Temkin, *Zhur. fiz. chim.*, **15**, 296 (1941); b. S. Brunauer, K. S. Love, and R. G. Keenan, *J. Am. Chem. Soc.*, **64**, 751 (1942).
12. B. N. Kabanow, R. Burstein, and A. Frumkin, *Discussions Faraday Soc.*, **1**, 259 (1947).

Anodic Polarization of Stainless Steel in Chloride Solutions

G. M. Schmid and Norman Hackerman

Department of Chemistry, The University of Texas, Austin, Texas

ABSTRACT

Anodic polarization curves were measured on stainless steel electrodes in KCl solution up to 1.0N. The existence of maxima in the potential time curve was verified, and the time for the potential to decay to +0.5 v vs. SCE was measured. This depends on the time at open circuit just before measurement. For less than 3 min, it is a function of this time, for more, there is no effect, at least over one order of magnitude of the applied anodic current density. The data support the view that the effect of Cl^- can be due to sorption phenomena, without assuming an oxide film.

Recent experiments in this laboratory (1) showed that a maximum occurs in the potential-time curve during constant current anodic polarization of stainless steel in Cl^- solutions. There is also a minimum followed by a maximum in the electrode/electrolyte interface impedance.

Such a maximum in the potential-time curve for Fe first was reported by Haber and Goldschmidt (2). Evans (3) ascribed the effect to the ability of discharged chlorine to diffuse through a protective oxide film. Frumkin (4) thinks that Cl^- hinders the passivation of Fe by preventing "oxygen" from being desorbed. This point of view is supported by measurements of electrode capacities of Fe in Cl^- solutions (5) and by direct evidence that Cl^- retards adsorption and desorption of oxygen (6). Uhlig (7) explains the phenomena by preferential adsorption of Cl^-, or displacement of adsorbed oxygen by Cl^-, and subsequent attack on Fe due to the high rate of formation of the metal-halogen bond.

The effect of halide ions on stainless steel was studied by Morioka and Sakiyama (8). They conclude that the attack on the electrode depends not on penetrating but on oxidizing power (9). In alkaline solutions stainless steel is not corroded by Cl^-.

In a recent paper, Weil and Menzel (10) were able to show that preferential attack on Fe coincides with preferential adsorption of Br^-, independent of the availability of oxidizing conditions. They state that penetration of the passivating oxide film is facilitated by plastic deformation. The process of pitting is explained by assuming a higher mobility of Fe^{++} in the penetrated part of the oxide film. A more general statement to this effect was made by Maeda (11).

The present work was undertaken to elucidate further the effect of Cl^- on stainless steel during anodic constant current polarization.

Experimental

Measurements were made in a conventional type electrolytic cell. Good stirring was provided by a stirrer in a side compartment, open to air and connected to the cell proper by two arms. The solutions were kept air saturated by the pumping action of the stirrer, which blew a steady stream of air bubbles into the main compartment. A large area Pt wire gauze was the polarizing electrode and was used as a cathode only to avoid the possibility of anodic dissolution in acid, chloride-containing electrolytes (12).

The electrodes were taken from stock 18-8 stainless steel wire, type 302, 0.038 cm diameter, actual composition in per cent: C, 0.09; Mn, 1.42; Si, 0.33; P, 0.024; S, 0.017; Ni, 11.10; Cr, 18.40; Mo, 0.18; rest Fe. They were washed and degreased with acetone and benzene. No difference in behavior was found between samples treated 15 min at 1050°C and untreated electrodes. The solutions were made up with triple distilled water, of 10^{-6} ohm^{-1} cm^{-1} conductivity, and three times recrystallized salts. The concentration of KCl was 0.1-1.0*N*, the pH was adjusted by adding NaOH or H_2SO_4. The total concentration ordinarily was kept at 1.0*N* by adding the appropriate amount of Na_2SO_4. In the case of 1.0*N* KCl, pH 12 and 1.5, the total concentration was higher. Before adding KCl, the solutions were pre-electrolyzed for 48 hr at 10 ma with Pt electrodes.

The potentials were measured with respect to SCE with a Sensitive Research Instrument Corporation model PV potentiometer. A Hewlett-Packard Model 130B oscilloscope of input impedance 10^6 ohms was used instead, whenever the potential changed too fast with time to make balancing of the potentiometer possible. Direct current was supplied by a Lambda Model 32M power supply operated at 300 v and controlled by a set of resistors.

Results

If a stainless steel electrode in Na_2SO_4 is subjected to an anodic current density (C.D.) ranging from 10 $\mu a/cm^2$ to 20 ma/cm^2, it reaches and maintains a steady oxygen evolution potential as long as the current is applied (2 hr in this case). The same holds for solutions of pH 6 and 1.5, containing less than 0.3*N* KCl. According to Morioka and Sakiyama (8), this was true also for solutions up to 1.0*N* KCl at pH 12.

The electrodes behave quite differently in solutions of pH 6 and 1.5 with 0.3-1.0*N* KCl. At anodic C.D. greater than 10 $\mu a/cm^2$ a maximum appears in the potential-time curve (Fig. 1), the persistence

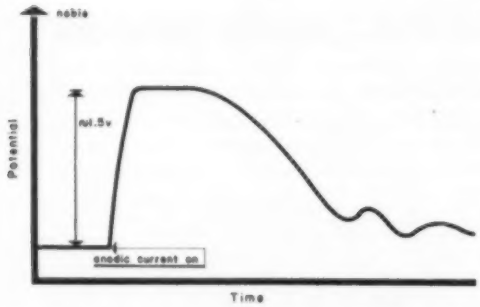

Fig. 1. Schematic potential vs. time curve. Stainless steel in chloride solutions.

of which depends on the Cl^- concentration. Despite continued flow of anodic current, the potential decays within 10 sec to more active values. With 0.6-1.0*N* KCl and high enough C.D. to give a potential maximum above +1.5 v, however, there is no decay. Here another electrode reaction seems to take over, presumably Cl_2 evolution.

Figure 2 shows anodic polarization curves obtained in solutions of three pH values, over a concentration range from chloride-free 1.0*N* Na_2SO_4 to 1.0 *N* KCl. Each point represents the maximum observed potential, regardless of whether it was steady or not.

The Tafel slope for the pH 12 solutions is 0.036 v (Fig. 2c); for pH 6, 0.110 v (Fig. 2b). The latter value is in good agreement with Uhlig and Woodside (13) for Cr-Fe alloys in chloride free 3% Na_2SO_4.

The behavior in acid solutions corresponds to an observation made by Heumann and Roesener (14) on Fe-25% Cr alloys in dilute HNO_3. They obtained an abrupt potential jump of about 0.2 v from +1.4 to +1.6 v at approximately 2 ma/cm² anodic. They state that this jump is more pronounced in dilute H_2SO_4 and this was found to be the case here (Fig. 2a). Presumably it is caused by transition from Cr dissolution at low C.D. to oxygen evolution at high C.D. In the present case, with 18-8 stainless steel, marked corrosion took place in the high C.D. region in solutions with 0.6*N* KCl or more. At such high potentials, Cl_2 evolution is possible thermodynamically and probably does occur simultaneously with O_2 evolution. Attack of the electrode by atomic chlorine would account for the marked corrosion. The shift in the jump toward higher C.D. seen in Fig. 2a can be attributed to the increasing acidity of the solutions. The Tafel slope for the flat portion is 0.048 v; for the steep portion, 0.140 v. Heumann and Roesener found hysteresis in their system and this was confirmed here. Figure 2a does not show this, however, since only curves for increasing C.D. were plotted.

In neutral and acid solutions, high Cl^- concentrations, and C.D. < 100 μa/cm², the time in which the potential rises and decays is about 1 sec. The process causing the potential to change from noble to more active values sets in early. The measured maximum in the potential-time curve is considerably lower than the values at higher C.D. and does

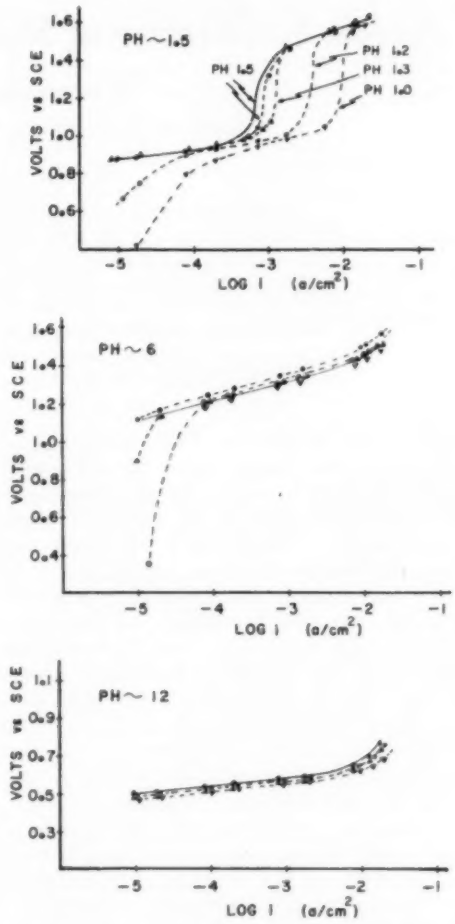

Fig. 2. Maximum observed potential vs. anodic current densities. Stainless steel in solutions containing: —, 1.0N Na_2SO_4; △, 0.3N KCl; ▽, 1.0N KCl; •, 0.1N KCl; o, 0.6N KCl. (a) (top) pH 1.5 to 1.0, (b) (center) pH 6, (c) (bottom) pH 12.

not fall on the Tafel line. Figure 2 shows, however, that in the Cl^- concentration and pH range investigated, the potential maxima give a Tafel slope which coincides with the one obtained with chloride-free Na_2SO_4. A possible exception is 1.0*N* KCl pH 1.0, where a different Tafel slope is obtained. Here the potential probably never reaches its full maximum value, due to the early decay.

Attempts to obtain a steady potential value after the potential maximum failed. The potential oscillates between −0.1 and +0.2 v. The frequency of the oscillation decreases rapidly at first, but does not damp out completely, even after 3 hr. The continued flow of anodic current causes the electrode to corrode.

No pitting was observed in solutions of pH 12, and the electrode was bright after the run, in agreement with Matthews and Uhlig (15). In neutral solutions the electrodes were heavily pitted and corroded uniformly in acid solutions, with an occasional pit at the water line.

In another set of experiments, the time between application of anodic current, reaching the poten-

Table I. Duration of maximum in potential-time curve in 0.3N KCl

Current density, ma/cm²	Time in pH 1.5, min	Maximum potential in pH 1.5, v vs. SCE	Time in pH 6, min	Maximum potential in pH 6, v vs. SCE
18.40	3.5	1.62	9.5	1.52
12.55	3.0	1.59	10.5	1.47
7.86	3.0	1.56	9.8	1.45
1.70	3.5	1.47	9.0	1.35
0.81	8.0	0.95	9.5	1.32
0.20	8.5	0.93	7.0	1.25

tial maximum and decaying back to +0.5 v (arbitrary) was measured. The reproducibility of measurements in chloride-containing solutions is poor, as reported by Weil and Menzel (10). Agreement on the same electrode is to within about 20%, but data taken on different electrodes vary 50% and more. The data reported here therefore are meant to give a picture of the general behavior and do not allow quantitative treatment.

Table I presents the data obtained on two electrodes in 0.3*N* KCl of pH 6 and 1.5 at different C.D. Five min at open circuit were allowed between measurements.

It is rather surprising that at pH 6 the measured times are essentially independent of C.D. over a log cycle. In pH 1.5 a break in the time values occurs at the jump in the polarization curve. A somewhat constant value for $>$ 1 ma/cm² differs from the value for two C.D. $<$ 1 ma/cm². In 0.3*N* KCl solutions potential maxima were observed in every experiment. In 0.6 and 1.0*N* KCl, the potential did not decay once it had reached +1.5 v. This is sufficient for Cl_2 evolution. Below that value the decay was very rapid ($<$ 5 sec).

In another set of experiments the anodic current was switched off the moment the decaying potential reached +0.5 v. After various lengths of time at open circuit, the same anodic current was switched on again. Results are shown in Table II. It can be seen that the time for the potential decay becomes larger with the time at open circuit. After about 3 min at open circuit, no change in the potential decay time was observed.

Discussion

The fact that the maximum potentials obtained on application of anodic current to 18-8 stainless steel electrodes, in the Cl^- concentration range investigated, have the same values as the steady-state potentials obtained with chloride-free Na_2SO_4 shows that the initial effect of the anodic current is the same in both cases. Frequently it has been found that adsorption of "oxygen" or some oxygen-containing species is a precursor to actual oxygen evolution (16). Therefore, it seems reasonable to assume that the initial effect of the anodic current is a conversion of adsorbed water dipoles into a layer of chemisorbed, oxygen-containing species. This assumption is supported by our observation that the charge involved in driving the electrode potential up to oxygen evolution is about 1 mcoulomb. Taking into account that a certain fraction of this amount will not cross the interface, but serves to charge the electrical double layer, not more than the equivalent of one or two monolayers are involved in this first step.

Table II. Duration of maximum in potential-time curve in 0.3N KCl pH 6, current density 0.7 ma/cm², anodic

Time at open circuit, sec	Duration of potential maximum, sec	Time at open circuit, sec	Duration of potential maximum, sec
2	2*	80	126
5	2*	100	145
10	22	120	190
20	12	180	300
40	59	240	275
60	97		

*Maximum potential <1 v vs. SCE.

In chloride-containing solutions a second electrode process is possible which tends to set the potential at more active values. This process is dependent on the Cl^- concentration and on the time during which the electrode has been at open circuit prior to anodic polarization. However, it is independent, to a first approximation, on the applied anodic C.D. We believe that during this stage a chemisorbed oxygen-containing layer is replaced by chemisorbed Cl^-. This is a time consuming process which is greatly facilitated by the large positive charge on the electrode and also by increased Cl^- concentration. In the potential region in question there is no great variation of potential with current, which explains the lack of dependence of this process on current. In acid solutions, which show two potential regions, the replacement time at higher potentials is shorter, due to the higher positive charge on the electrode. Both times are independent of the current in their respective potential range.

Chemisorption of Cl^- leads to removal of the protective passive layer at the electrode. This removal causes potential decay to more active values accompanied by corrosion of the electrode, except in cases where a high noble potential is sustained by Cl_2 evolution. With the Cl^- ions trying to maintain a chemisorbed Cl^- layer and the anodic current trying to restore passivity, the potential decay is rather irregular and potential oscillations are observed after the potential has reached active values. With the potential of the electrode at least 0.5 v below the reversible oxygen potential at this point and little adsorbed water dipoles present, passivity cannot be restored, and passage of anodic current leads to corrosion.

After the anodic current is switched off, the original conditions are established. This again is a time-consuming process as shown by the fact that the time during which O_2 evolution potentials are maintained with applied anodic current increases with increasing time at open circuit just before the experiment (Table II).

This model does not require the assumption of a passivating oxide film. The electrodes show pits in neutral solutions and corrode uniformly in acid solution. Both systems exhibit maxima in the potential-time curve showing that the process lead-

ing to potential decay is similar in both cases. Preferential chemisorption of Cl^- along cracks in the passivating oxide film, as suggested by Weil and Menzel (10), would require an occasional crack in neutral solution and innumerable cracks in acid solutions. This does not seem very likely. Some preferential chemisorption of Cl^- may very well occur at crystal faults of the metal, thus destroying passivity at that point and leading to pitting.

Summary

During anodic polarization, maxima in the potential-time curve have been observed at 0.3*N* Cl^- and above, except at pH 12. It is shown that the anodic Tafel slopes, obtained in 1.0*N* Na_2SO_4 and 0.1-1.0*N* KCl of pH 1.5, 6, and 12 coincide if the potential maxima are plotted. The time necessary for the potential to decay to an arbitrary value of +0.5 v *vs.* SCE has been measured and found to be independent over a log cycle of the applied C.D. However, this time is dependent on the time during which the system was at open circuit just before the measurement.

It is proposed that the first effect of the anodic current is the conversion of an adsorbed sheet of water dipoles into a protective, chemisorbed oxygen layer. With time, the chemisorbed oxygen is replaced by chemisorbed Cl^-, which causes a potential decay. It is pointed out that there is no binding reason to assume an oxide film to explain the pitting action of Cl^-.

Acknowledgment

The authors take this opportunity to express their appreciation for financial help to the Robert A. Welch Foundation of Houston, Texas, and to the Office of Naval Research under Contract Nonr 375(02).

Manuscript received Nov. 21, 1960.

Any discussion of this paper will appear in a Discussion Section to be published in the June 1962 JOURNAL.

REFERENCES

1. G. M. Schmid and Norman Hackerman, *This Journal*, **107**, 647 (1960).
2. F. Haber and F. Goldschmidt, *Z. Elektrochem.*, **12**, 49 (1906).
3. U. R. Evans, *J. Chem. Soc., London*, **1927**, 1020.
4. B. Kabanov, R. Burstein, and A. Frumkin, *Discussion Faraday Soc.*, **1**, 259 (1947).
5. L. W. Vanyukova and B. N. Kabanov, *Zhur. Fiz. Khim.*, **28**, 1025 (1954).
6. E. O. Ayazyan, *Doklady Akad. Nauk. S.S.S.R.*, **100**, 473 (1955).
7. H. H. Uhlig, *This Journal*, **97**, 215C (1950).
8. S. Morioka and K. Sakiyama, *Denki Kagaku*, **25**, 191 (1957).
9. Oxidizing agents are held responsible for the attack of halide ions on Fe by many authors. See for example U. F. Franck, *Korrosion u. Metallschutz*, **8**, 504 (1958).
10. K. G. Weil and D. Menzel, *Z. Elektrochem.*, **63**, 669 (1959).
11. M. Maeda, *Naturwissenschaften*, **44**, 557 (1957).
12. A. Slygin and A. Frumkin, *Acta Physicochim. U.R.S.S.*, **3**, 796 (1935).
13. H. H. Uhlig and G. E. Woodside, *J. Phys. Chem.*, **57**, 280 (1953).
14. Th. Heumann and W. Roesener, *Z. Elektrochem.*, **57**, 17 (1953).
15. J. W. Matthews and H. H. Uhlig, *Corrosion*, **7**, 419 (1951).
16. F. G. Will and C. A. Knorr, *Z. Elektrochem.*, **64**, 270 (1960).

Thermodynamics of the Interaction of Niobium and Tantalum with Oxygen and Nitrogen at Temperatures near the Melting Point

J. Paul Pemsler

Nuclear Metals, Inc., Concord, Massachusetts

ABSTRACT

The concentration of nitrogen and oxygen present in niobium and tantalum in equilibrium with the pure gas has been determined as a function of pressure at each of three temperatures near the melting point, and in the liquid phase at the melting point. A curious solubility inversion was noted in the tantalum-oxygen system where the oxygen concentration in equilibrium with a specified pressure of oxygen is lower at 2850° than at 2960°C. Data were used to calculate the partial molar and integral values of the free energy, enthalpy, and entropy of dissociation of solutions of nitrogen in niobium and tantalum, and partial molar free energy and enthalpy of dissociation of solutions of oxygen in niobium and tantalum.

Niobium and tantalum are becoming increasingly important as structural materials for use at high temperatures. The mechanical properties on which such use is based are known to be affected greatly by the presence of small amounts of impurity atoms in the lattice. These properties are particularly sensitive to the presence of the gaseous elements oxygen, nitrogen, and hydrogen. It is important therefore to evaluate quantitatively the affinity of the metal for these gases. Thermodynamic data concerning the solution of gases at very high temperatures up to the melting point and in the liquid phase would

Table I. Chemical analysis of niobium and tantalum

Element	Niobium ppm	Element	Tantalum ppm
O	150	C	<10
N	45	O	10
H	<5	H	—
C	<30	N	10
Al	<20	Fe	<20
B	<1	Cr	<10
Cd	<1	Ni	<10
Cr	<20	Si	<30
Cu	<40	Nb	<25
Fe	<100	Al	<50
Mg	<20	Cu	<50
Mn	<20	Ti	<10
Mo	<20	Mo	150
Ni	<20		
Pb	<20		
Si	<100		
Sn	<20		
Ta	520		
Ti	<150		
V	<20		
W	<150		
Zn	<20		

help define the conditions both wherein the metals absorb gases and wherein the gaseous impurities can be removed.

The present work seeks to provide such data by studying the equilibrium reactions of niobium and tantalum with oxygen and nitrogen at very high temperatures.

Experimental

Materials.—A double electron-beam vacuum-melted niobium rod 1 in. in diameter and 21 in. long was obtained from the Wah Chang Corporation of Albany, Oregon, and a 3.4 lb electron-beam vacuum-melted tantalum ingot was obtained from the National Research Corporation of Cambridge, Massachusetts. The analyses reported by the suppliers are given in Table I.

The gases used were purified according to the following schemes:

Oxygen

Tank oxygen → Anhydrone → platinum asbestos at 300°C → Anhydrone → Ascarite → liquid nitrogen trap → system.

Nitrogen

Tank dry nitrogen → copper turnings at 600°C → Anhydrone → Ascarite → liquid nitrogen trap → system.

Analytical procedure.—Nitrogen was determined by means of the micro-Kjeldahl method (1). Samples were dissolved in platinum dishes with concentrated hydrofluoric acid and hydrogen peroxide.

Oxygen was determined with the aid of a National Research Corporation vacuum fusion unit. Samples were melted in a graphite crucible and the carbon monoxide evolved converted to CO_2. The difference in pressure before and after freezing out the CO_2 was used as a measure of the oxygen content.

Apparatus.—Thermodynamic data were obtained by equilibration of the gas at various pressures with metal at elevated temperature. The apparatus used for the equilibration is shown schematically in Fig.

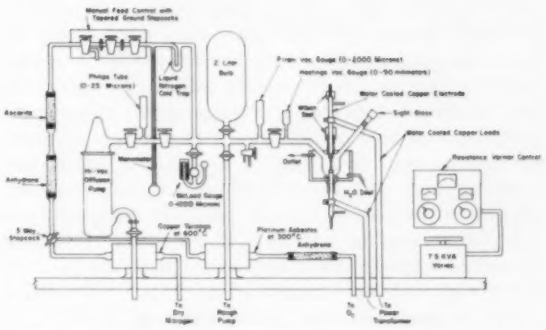

Fig. 1. Apparatus for equilibrium of gas with solid metal

1. The sample consisting of a rectangular parallelepiped about 2 x 3 x 40 mm long was resistance heated to the test temperature between water-cooled copper electrodes. Samples were given a preliminary outgassing at 10^{-6} mm Hg for 5 min at a temperature near the melting point. The temperature of the sample then was adjusted to the value required and purified gas admitted to the system.

Pressure measurement and control.—A temperature gradient existed in the sample, since it was heated between water-cooled electrodes, the ends being much cooler than the uniform central zone. Portions of the sample near the ends were often in a temperature range where nitriding or oxidation converted that area to the nitride or oxide while the center zone, at a uniform higher temperature, may have been dissolving gas to form a solid solution. Thus, even after equilibrium was established in the uniform temperature zone, areas forming nitride or oxide continually absorbed gas so that a slow bleed of gas into the system was needed to maintain constant pressure. This was achieved by the use of tapered stopcocks equipped with a fine control adjustment.

Data were obtained by approaching the composition in equilibrium with gas at a given pressure from compositions both above and below the equilibrium composition. In some experiments gas was bled in until the pressure reached the desired value and then was held constant for the duration of the run. In other experiments the gas pressure was brought to a value considerably above (often a factor of 10 above) the final equilibrium pressure. The high pressure was maintained for a sufficient period of time to reach a steady state. Gas then was removed from the system, lowering the pressure to the equilibrium value being investigated. This latter pressure was maintained for an additional period of time in order to establish the final equilibrium. Chemical analysis indicated that the final concentration of gas in the metal was identical whether approached from above or below, and hence a true equilibrium was attained.

Pressure was measured by means of a Pirani vacuum gauge with 0 to 2 mm-Hg range, a McLeod gauge with a 0 to 5 mm-Hg range, a Hastings vacuum gauge with a 0 to 30 mm-Hg range, or a mercury manometer with a 0 to 760 mm-Hg range, depending on the pressure.

Temperature measurement.—The temperature of the sample was maintained constant during the experiment by adjusting a vernier attached to a vari-

able transformer which controlled the current through the sample. Temperatures were measured with an optical pyrometer calibrated at a wavelength of 0.65 μ. An emissivity calibration correction was made by observing the temperature of a sample with a small hole drilled into it to a depth sufficient to approximate black-body conditions (depth-to-breadth ratio of eight). The emissivity value of 0.362 calculated for niobium is substantially different from the older value of 0.49 (2). The value of 0.352 for tantalum is in excellent agreement with the value of 0.350 reported by Glazier *et al.* (3). The melting point of niobium was determined as 2740°K, in agreement with a value of 2740°K reported by Schofield (4) and higher than the value of 2690°K reported by Wilhelm *et al.* (5). The melting point of tantalum observed here was 3290°K, in agreement within experimental error of the value 3270°K reported by Langmuir and Malter (6). During equilibration no attempt was made to correct emissivity values for changes due to the dissolution of nitrogen or oxygen in the metal or the appearance of a shiny subnitride layer on the surface. All samples were shiny upon examination after the conclusion of an experiment, and it is believed that emissivity changes occurring during the course of equilibration, corresponding to temperature errors, were fairly small.

Liquid drop.—Equilibrium of the liquid phase was accomplished by suspending a liquid drop vertically in the center of the metal sample attached to the electrodes. Specimens were similar to those used in the solid phase studies but portions of the center were ground away so that the sample had the appearance of a flat tensile specimen. The tension between the electrodes had to be controlled carefully to offset the thermal expansion of the sample. This control was accomplished by a series of reduction gears attached to the electrode and to a coarse and fine adjustment dial. In this way very small vertical adjustments of the top electrode relative to the fixed bottom electrode could be made. It also was found possible, by adjusting the interelectrode distance, to achieve fine adjustment of the temperature and to control instabilities developing in the drop due to vibration. Forcing the electrodes together would increase the drop diameter and decrease its length. The corresponding reduction in electrical resistivity of the compressed sample would decrease the overall size of the drop. The temperature of the drop was taken as the melting point. This value may be slightly in error due to superheating of the drop and to the change in melting point of the metal with dissolved nitrogen or oxygen. However, the thermodynamic data obtained from the solid phase experiments extrapolate smoothly to the liquid region, indicating that the temperature of the drop probably was not very different from the melting point of the pure metal.

Examination of samples.—Samples were examined metallographically after each experiment, and microhardness traverses were made on selected samples to insure the absence of a concentration gradient within the metal.

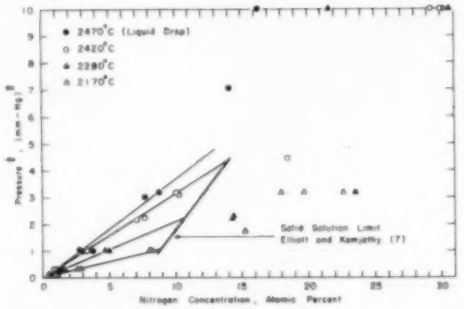

Fig. 2. Sievert's law plot of solubility of nitrogen in niobium

Results

Equilibrium data.—Nitrogen.—Sievert's law (which is a modification of Henry's law) states that at constant temperature the solubility of a diatomic gas in a metal is proportional to the square root of the pressure

$$S = kP^{1/2}$$

This law should hold at low concentrations of gas in the metal, where an ideal solid solution may exist. A Sievert's law plot for niobium-nitrogen is shown in Fig. 2. The nitrogen solubility is a linear function of the square root of the pressure within the solubility range. There is a slight curvature of the line depicting the liquid drop data. The terminal solubility of nitrogen in niobium in equilibrium with Nb_2N as determined by Elliott and Komjathy (7) is shown on the graph. Points to the right of this line are not equilibrium values, but represent partially nitrided samples as discussed below. Terminal solubilities in the liquid phase have not been determined.

Metallographic examination was made on all alloys in the as-quenched state. Quenching was achieved by interrupting the resistance heating; samples cooled from the experimental temperature to below red heat in about 10 sec. It is not known whether this cooling rate was sufficient to retain the high temperature structures. Niobium samples containing up to about 0.5 a/o nitrogen were homogeneous throughout with no evidence of a second-phase precipitate. Albrecht and Goode (8) report the terminal solubility of nitrogen in niobium as 1.2 a/o at 1100°C and 0.28 a/o at 800°C.

Samples containing between about 0.5 a/o nitrogen and the saturation values reported by Elliott and Komjathy (7) and indicated in Fig. 2 consist of a dispersion of second-phase particles in the niobium matrix. The second phase is presumed to be Nb_2N (7). Since isothermal diffusion in binary alloys cannot produce such a dispersed two-phase structure, the Nb_2N must have precipitated on quenching. Thus, all the nitrogen was present in solution at the elevated temperatures.

Samples containing more than the solution limit of nitrogen were observed to consist of a scale of varying thickness surrounding a zone containing a dispersion of Nb_2N in a matrix of niobium saturated with nitrogen. The scale was identified by x-ray diffraction as Nb_2N. The extent of nitriding probably

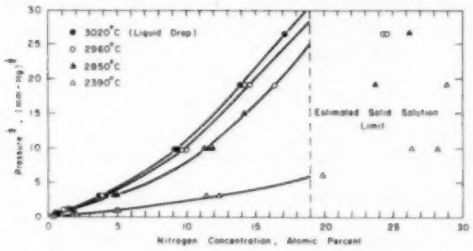

Fig. 3. Sievert's law plot of solubility of nitrogen in tantalum

is controlled by the rate of diffusion of nitrogen ions, niobium ions, or both through the Nb_2N layer. Thus, the extent of conversion of the sample to Nb_2N depends on the dimensions of the sample, the temperature, and the time of the reaction. Nitriding for long times completely converts the niobium to Nb_2N. The pressure of nitrogen necessary to form an Nb_2N scale varies from about 1 mm at 2170°C to about 20 mm at 2420°C.

A Sievert's law plot for tantalum-nitrogen is shown in Fig. 3. No high-temperature solubility values of nitrogen in tantalum are available in the literature. On the basis of metallographic examination of the alloys, an approximate terminal solubility line is sketched in Fig. 3. At the lowest temperature, 2390°C, the concentration varies linearly with the square root of pressure. At higher temperatures there is appreciable curvature beyond 6 a/o. Above the solid-solubility limit the data scatter widely, reflecting the extent to which Ta_2N was formed on a particular sample.

Samples quenched from high temperature and containing up to about 11 a/o nitrogen exhibited no second-phase precipitate when examined metallographically. The room temperature solubility of nitrogen in tantalum may, therefore, be as high as 11 a/o, or tantalum may be capable of retaining large amounts of nitrogen in supersaturated solution when quenched from high temperature. Gebhardt *et al.* (9) fix the room temperature solubility as less than 5 a/o. In the composition range of about 11 a/o nitrogen to the solid solution limit, a dispersion of second-phase particles in the tantalum matrix is observed at room temperature. Beyond the solid-solution limit a nitride layer is present. Quenched alloys containing from 25 to 28 a/o nitrogen exhibit complete nitriding of the tantalum. Brauer and Zapp (10) report a structure, referred to as Ta_2N, with a homogeneity range of 29-33 a/o nitrogen, while Schönberg (11) reports the homogeneity range from 28 to 31 a/o nitrogen. Thus, Ta_2N is nonstoichiometric, and its composition depends on the temperature and external nitrogen pressure.

Oxygen.—Data for the niobium-oxygen and tantalum-oxygen systems are summarized in the Sievert's law plots shown in Fig. 4 and 5. The scatter of data in the oxygen-metal systems is much larger than that obtained in the nitrogen-metal systems. This may be due in part to the necessity of working at low pressures in the oxygen systems, where the error in reading the pressure may be appreciable. The temperatures used in this investigation are

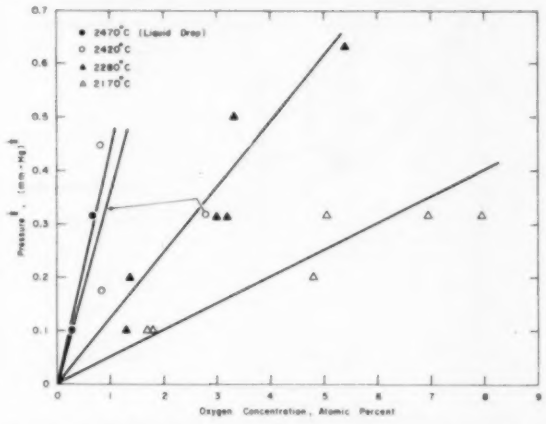

Fig. 4. Sievert's law plot of solubility of oxygen in niobium

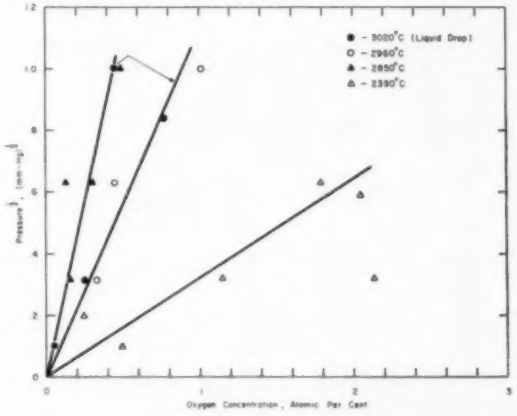

Fig. 5. Sievert's law plot of solubility of oxygen in tantalum

above the melting points of the metal oxides, so no oxide scale can form on the sample. The maximum concentration of oxygen which can be obtained in a metal-oxygen alloy at a particular temperature is limited to a value corresponding to the composition of the solidus point at that temperature.

The niobium-oxygen data, as shown in Fig. 4, resemble the niobium-nitrogen data as shown in Fig. 2, but a curious solubility inversion exists in the tantalum-oxygen system. Tantalum-oxygen solutions are less stable at 2850°C than they are at 2960°C, or in the liquid; a given pressure of oxygen will result in a more concentrated solution at 2960°C than at 2850°C. If these data can be extrapolated to lower pressures, it would suggest that vacuum degassing at high temperatures in the solid phase can result in a lower ultimate oxygen concentration than can be obtained by electron-beam vacuum-melting. The rate of oxygen removal of the liquid undoubtedly will be more rapid than in the solid, but the ultimate attainable oxygen concentration is lowest at some temperature below the melting point. Additional work is needed in this area to confirm these results and to establish the optimum temperature for gas removal.

Metallographic examination at room temperature revealed that niobium alloys containing more than

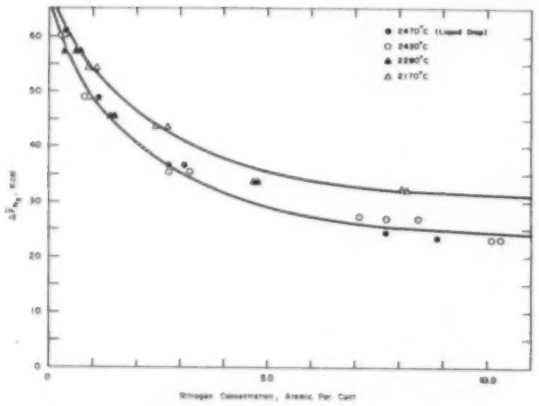

Fig. 6. Partial molar free energy of dissociation of niobium-nitrogen solid solution.

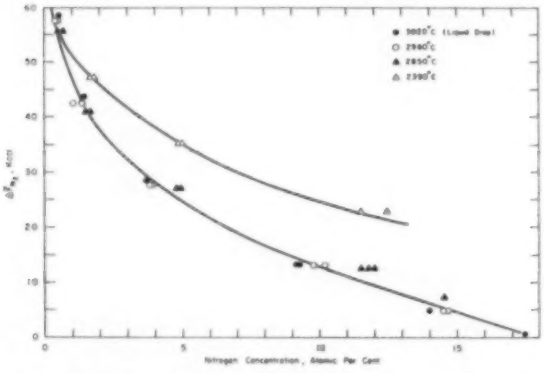

Fig. 7. Partial molar free energy of dissociation of tantalum-nitrogen solid solution.

about 7 a/o oxygen exhibited a second-phase precipitate, probably NbO. All tantalum alloys examined were uniform.

Thermodynamic data.—The partial molar free energy ($\Delta\overline{F}$) of dissociation of a solid solution of a gas in a metal is given by the expression

$$-\Delta\overline{F} = RT \ln P$$

where R is the gas constant, T is the absolute temperature, and P is the equilibrium pressure.

The variation of the partial molar free energy of dissociation of solid solutions of nitrogen in niobium and tantalum with concentration are depicted in Fig. 6 and 7. Values of $\Delta\overline{F}$ are for one mole of nitrogen, i.e., for the reaction $y\text{NbN}_{\frac{2}{y}} = y\text{Nb} + \text{N}_2$. According to the fundamental nature of the free energy of solution, the affinity of the metal for nitrogen increases with decreasing concentration. Partial molar free energies are observed to increase with decreasing temperature, indicating the increased stability of the solid solution at lower temperature. Throughout the region beyond the solution limit where the reaction (Nb or Ta)N_{sat} + N_2 → (Nb or Ta)$_2$N is occurring, the partial molar free energy becomes invariant and would be represented by a horizontal line out to the lower limit of composition of (Nb or Ta)$_2$N.

The relation between the partial molar and integral values of the free energy of dissociation is given by the equation

$$\Delta F = N\int_0^x \Delta\overline{F}\, dx$$

where N is the atom fraction of niobium or tantalum and x is the ratio of the atom fractions, $x = \frac{N_{N_2}}{N_{metal}}$. ΔF is expressed as the integral free energy of dissociation per gram atom, *i.e.*, for the reaction $\frac{1}{2+y}$ ($y\text{NbN}_{\frac{2}{y}} = y\text{Nb} + \text{N}_2$). Thus, the integral free energy of dissociation may be evaluated by measuring the area under the curves in Fig. 6 and 7 with the abscissa expressed as atomic fraction, x (12). Values of partial and integral free energies of dissociation near the melting points are given in columns 2 and 3 of Tables II and III. The values of 33 a/o nitrogen represent the free energies of dissociation of Nb_2N and Ta_2N near the respective melting points of the metal.

The partial molar enthalpy ($\Delta\overline{H}$) and entropy ($\Delta\overline{S}$) for the reaction $y\text{NbN}_{\frac{2}{y}} = y\text{Nb} + \text{N}_2$ are related to the partial molar free energy by the equation

$$\Delta\overline{F} = \Delta\overline{H} - T\,\Delta\overline{S}$$

Combining with the expression for $-\Delta\overline{F}$ given above

$$2.303 \log P = \frac{-\Delta\overline{H}}{RT} + \frac{\Delta\overline{S}}{R}$$

Therefore, at constant composition, if $\Delta\overline{H}$ is temperature independent, a plot of log P vs. $1/T$ will be linear. The slope of the line will be equal to $\frac{-\Delta\overline{H}}{2.303\,R}$ and the intercept at $T = \infty$ will be equal to $\frac{\Delta\overline{S}}{2.303\,R}$.

Plots of log P *vs.* $1/T$ for the compositions indicated are shown in Fig. 8 and 9. For niobium, the

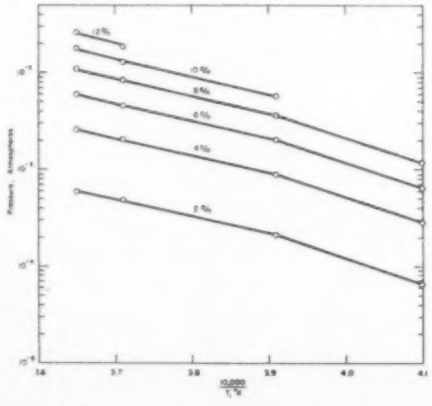

Fig. 8. Equilibrium pressure of nitrogen over niobium containing various amounts of nitrogen.

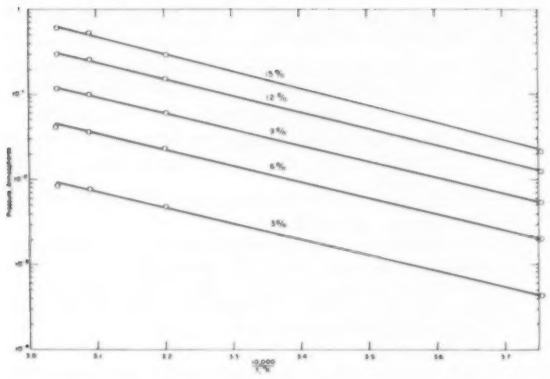

Fig. 9. Equilibrium pressure of nitrogen over tantalum containing various amounts of nitrogen.

data can be represented as falling on two straight lines. The partial molar enthalpy of dissociation thus can be considered constant in each of the two temperature ranges studied, and has values of ΔH = 84 kcal/mole N_2 in the range 2280°-2470°C, and ΔH = 121 kcal/mole N_2 in the range 2170°-2280°C. Values of the integral enthalpy of dissociation and the partial molar and integral entropies of dissociation of niobium-nitrogen at the melting point are given in columns 4 to 7 of Table II.

In the tantalum-nitrogen system, the plot of log P *vs.* $1/T$ can be considered linear throughout the temperature range studied. The partial molar enthalpy of dissociation is therefore a constant and has the value ΔH = 88 kcal/mole N_2. Values of the integral enthalpy of dissociation and the partial molar and integral entropies of dissociation of tantalum-nitrogen at the melting point are given in columns 4 to 7 of Table III.

The partial molar free energies of dissociation of niobium- and tantalum-oxygen alloys are tabulated

Table II. Thermodynamic properties of niobium-nitrogen at the melting point

Nitrogen, a/o	$\Delta\bar{F}$, kcal/mole N_2	ΔF, kcal/g-atom	$\Delta\bar{H}$, kcal/mole N_2	ΔH, kcal/g-atom	$\Delta\bar{S}$, cal/degree/mole	ΔS, cal/degree/g-atom
2	40	1.0	81	1.6	−15.5	−0.18
4	32	1.7	83	3.3	−18.5	−0.53
6	27	2.3	84	5.0	−20.4	−0.89
8	25	2.9	85	6.8	−21.6	−1.35
10	24	3.2	87	8.7	−22.9	−1.82
33	24	8.3		27.7	−22.9	−7.35

Table III. Thermodynamic properties of tantalum-nitrogen at the melting point

Nitrogen, a/o	$\Delta\bar{F}$, kcal/mole N_2	ΔF, kcal/g-atom	$\Delta\bar{H}$, kcal/mole N_2	ΔH, kcal/g-atom	ΔS, cal/degree/mole	ΔS, cal/degree/g-atom
3	32	0.9	86	2.6	−17.5	−0.35
6	22	1.2	86	5.2	−20.6	−0.76
9	14	2.4	86	7.7	−22.5	−1.42
12	9	2.7	90	10.8	−24.4	−2.23
15	5	2.8	93	14.0	−25.8	−2.92
33	0	2.4		29.3	−27	−8.0

Table IV. Partial, molar free energy of dissociation of niobium-oxygen solid solutions

Temp, °C	Oxygen concentration, a/o	$\Delta\bar{F}$, kcal/mole O_2
2470	0.2	61
	0.7	49
2420	0.5	54
	0.8	44
	2.8	48
2280	1.3	57
	1.3	50
	2.8	41
	3.0	45
	3.2	45
2170	1.7	54
	1.8	54
	4.8	47
	5.1	43
	6.9	43
	7.9	43

Table V. Partial molar free energy of dissociation of tantalum-oxygen solid solutions

Temp, °C	Oxygen concentration, a/o	$\Delta\bar{F}$, kcal/mole O_2
3020	0.05	74
	0.25	58
	0.45	43
2960	0.33	57
	0.45	48
	1.00	42
2850	0.13	46
	0.14	55
	0.32	46
	0.50	41
2390	0.30	52
	0.50	59
	1.25	47
	1.80	40
	2.05	40
	2.12	47

in Tables IV and V. Data for the tantalum-oxygen system indicate the anomalous behavior of the tantalum-oxygen system at 2850°C where alloys are less stable than at the melting points.

Plots of log P *vs.* $1/T$ are shown in Fig. 10 and 11. The partial molar enthalpy of dissociation of nio-

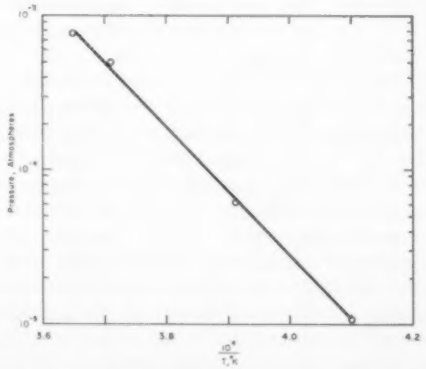

Fig. 10. Equilibrium pressure of oxygen over niobium containing 1.75 a/o oxygen.

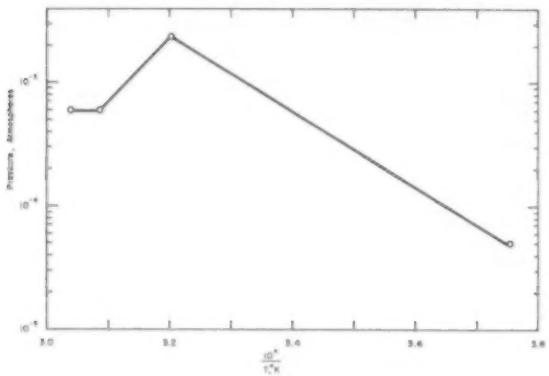

Fig. 11. Equilibrium pressure of oxygen over tantalum containing 0.3 a/o oxygen.

bium-oxygen alloys, ΔH, is constant in the temperature range investigated and has the value 198 kcal/mole. The solubility inversion in the tantalum-oxygen system is reflected by a change in the sign of the slope of the log P *vs.* $1/T$ curve (and hence a change in the sign of $\Delta \overline{H}$).

Acknowledgment

This work was performed under USAF Contract No. AF33(616)-6627.

Manuscript received Nov. 28, 1960; revised manuscript received March 24, 1961.

Any discussion of this paper will appear in a Discussion Section to be published in the June 1962 JOURNAL.

REFERENCES

1. E. B. Read and H. M. Read, The Chemical Analysis of Zirconium and Zircaloy Metals, Report NMI-1171 (1957).
2. G. K. Burgess and R. G. Waltenberg, *Bull. U. S. Bur. Standards*, **11**, 591 (1915).
3. L. F. Glazier, Jr., R. D. Allen, and I. L. Saldinger, Mechanical and Physical Properties of the Refractory Metals, Tungsten, Tantalum and Molybdenum, Above 4000°F, Report No. M1826, Aerojet-General Corporation, Azusa, Calif.
4. T. H. Schofield, *J. Inst. Metals*, **85**, 372 (1957).
5. H. A. Wilhelm, O. N. Carlson, and J. M. Dickinson, *J. Metals*, **6**, 915 (1954).
6. D. B. Langmuir and L. Malter, *Phys. Rev.*, **55**, 743 (1949).
7. R. P. Elliott and S. Komjathy, Columbium-Nitrogen System. Paper presented at Columbium Metallurgy Symposium, Lake George, New York, June 9-10, 1960.
8. W. M. Albrecht and W. D. Goode, Jr., Reactions of Nitrogen with Niobium, Report BMI-1360 (1959).
9. E. Gebhardt, H. D. Seghezzi, and W. Dürrschnabel, *Z. Metallkunde*, **49**, 577 (1958).
10. G. Brauer and K. H. Zapp, *Z. anorg. Chem.*, **277**, 129 (1954).
11. N. Schönberg, *Acta Chem. Scand.*, **8**, 199 (1954).
12. O. Kubaschewski and E. LL. Evans, "Metallurgical Thermochemistry," John Wiley & Sons, Inc., New York (1956).

Niobium Solid Electrolytic Capacitors

N. Schwartz, M. Gresh, and S. Karlik[1]

Bell Telephone Laboratories, Incorporated, Murray Hill, New Jersey

ABSTRACT

The suitability of niobium as the anode for solid electrolytic capacitors has been investigated. Field crystallization of the amorphous niobium oxide film has been found to be a determining factor for the properties of these capacitors. Purity of the porous anodes as dependent on the sintering conditions, formation temperature and voltage, and formation electrolytes, parameters all known to control the initiation of crystallization, have been correlated with the initial and life test properties of these capacitors. The initial properties of niobium solid electrolytic capacitors prepared under optimum conditions compare favorably with equivalent tantalum components. However, with the current purity of niobium powder, only units with operating voltages up to 20 v survive a life test at 85°C, with the failures of capacitors rated at higher voltages attributed to the partial crystallization of the amorphous film during formation.

The tantalum solid electrolytic capacitor (1, 2) has provided a component for the electronic industry comparable to the conventional wet electrolytic type for use where large values of capacitance are required, since an anodically grown oxide film is utilized as the dielectric in both structures. However, the substitution of a high conductivity solid semiconductor, manganese dioxide, for the usual aqueous electrolyte has provided improved shelf aging, high retention of electrical characteristics to low temperatures, and lower dependence of capacitance and loss upon frequency. While widely accepted for low voltage circuitry, the solid electrolytic capacitor has a maximum voltage (35-60 v) and temperature (85°-110°C) operating range which curtails the general use of these components. Moreover, the cost of tantalum metal is high, its bulk density is high, and it is a strategic material since significant sources of good quality ores are foreign.

Many metals and their oxide films (3) have been investigated as a substitute for tantalum. The chemistry of niobium is similar to that of tantalum, and commercially available forms of the metal with purity comparable to tantalum have become available in the last few years. The kinetics and mechanism of formation of the anodic oxide films (4) appear to be similar to tantalum. Niobium has half

[1] Present address: Aerovox Corp., New Bedford, Mass.

the bulk density of tantalum, an important factor when either economic or weight advantages must be considered. It has also been reported that niobium ores are more plentiful than tantalum ores (5).

In considering any metal for the anode in the solid electrolytic capacitor, many of its properties must be evaluated due to the operation involved in the fabrication of the component. The preparation of the porous anode, by pressing of the powder and subsequent vacuum sintering at temperatures above 1600°C, is a major item. The sintering, besides providing strong mechanical bonds between powder particles, allows an extensive purification of the metal due to direct volatilization of impurities or their oxides. The importance of this process for tantalum capacitors has been evaluated recently (6) with the conclusion that the kinetics and thermodynamics of diffusion and solid-gas equilibrium require temperatures of the order of 2000°C to have this important process parameter operate efficiently. Studies in the vacuum sintering of niobium for consolidation to bulk densities (7, 8) suggest a similar conclusion for the fabrication of porous niobium anodes. A temperature of 2000°C is only 400°C below the melting point of niobium, however, and some difficulty may be anticipated in obtaining maximum purification without excessive loss of porosity due to shrinkage.

Vermilyea (9) has demonstrated for tantalum that the anodic film growth consists of a two-stage process. One of these is the formation of the amorphous oxide film with desirable dielectric properties, while the other is a subsequent field induced transformation to a crystalline film with poor dielectric properties. For tantalum, at the current state of the technology, these processes are easily separable, while the present work on niobium will demonstrate a high degree of complexity due to the almost concurrent occurrence of these two mechanisms of growth. This complicating feature is not inherent to the high field formation of niobium oxide films, but rather appears to depend to a major extent on the available purity of the metal.

This work is concerned with the fundamental features of the processing of niobium for solid electrolytic capacitors and the relationship of these features to the electrical characteristics of the finished component.

Experimental

Anodes consisting of niobium foil or porous pellets were used. Semiquantitative analysis of metallic impurities in the anodes was performed by spectrographic techniques, carbon by a combustion method employing a Leeco apparatus, and interstitial gas impurities by vacuum fusion. In the latter analysis, the nitrogen evolution is never complete, and therefore the reported values may have only relative significance. The surface areas of the powder and pellets were determined by B.E.T. methods using krypton gas as the adsorbant (10).

Porous anodes were formed by pressing 0.3 g of powder, with a temporary binder, in a double action press. The unsintered pellets were cylindrical with a diameter of 0.187 in. and a height ranging from 0.125 to 0.145 in. depending on the desired density. An axial integral lead of niobium wire was inserted during the pressing operation, and the pellets were sintered in a tantalum support within a modified NRC Vacuum Furnace, Type 2904B, utilizing tantalum resistance heaters and radiation shields. The temperature rise of the furnace was adjusted to maintain the pressure below 20 μ, and during 1 hr at the specified temperature the pressure would decrease typically to 0.3μ. After sintering, the pellets were allowed to cool at room temperature under vacuum.

The sintered pellets were anodized, using a tantalum cathode, in groups of 3 to 5 at a current density of 50 ma/g of niobium until the desired voltage was reached. This voltage was then maintained for 3.5 hr. After formation of the anodic film, five layers of manganese dioxide were applied by successive decompositions of manganous nitrate solutions at 400°C in a muffle furnace. To repair damage to the oxide film, the anodes were reformed in the forming electrolyte at a maximum current density of 10 ma/g to 75% of the original formation voltage. The manganese dioxide deposition and reforming processes were then repeated. The external cathode was applied utilizing the usual carbon coat and sprayed solder. Before determining the initial electrical properties, the capacitors were aged for 17-24 hr at room temperature and 150% of the working voltage. The d-c leakage was determined after 15-30 sec at the rated voltage, and the capacitance and dissipation factor determined on a series capacitance Wheatstone Bridge using an a-c signal of less than 0.5 v. The dissipation factor, tan δ, is given by $2\pi f C_s R_s$, where C_s and R_s are the measured equivalent series capacitance and resistance, and f is the frequency.

Foil anodes, 0.5 x 1 in., were either degreased in trichlorethylene, or vacuum annealed in the same sintering furnace used for the pellets, and then formed without any further treatment. The capacitance and dissipation factor were measured in a separate cell in 8N H_2SO_4 using a platinized-platinum cathode of equal area about 0.5 cm from the anode.

Results and Discussion

Dielectric properties of niobium oxide films.—In order to delineate the differences between tantalum and niobium oxide films, some comparisons were made of their dielectric properties. Tantalum and niobium foils were vacuum annealed at 2050°C and anodized in 60% acetic acid at 30°C at 10 ma/cm^2 to different formation voltages. The capacitance comparison in Fig. 1 demonstrates a linear relationship with essentially zero intercept between the inverse capacitance per unit area and formation voltage over the entire range of voltage investigated. The niobium oxide films yield a 20% larger capacitance per unit area than tantalum, which is in agreement with the results of Young (11). His values for anodic niobium and tantalum oxides, respectively, are 41 and 27.6 for the dielectric constant and 20.2 and 16.6Å/v for the inverse field strength. The 20% increase in capacitance for niobium apparently results

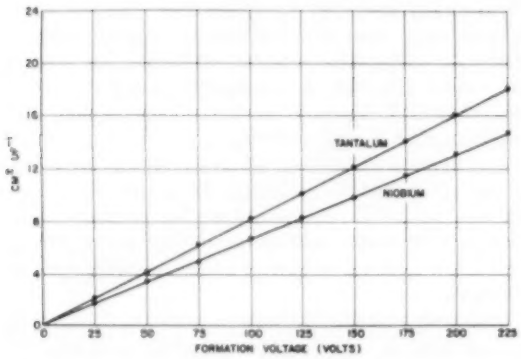

Fig. 1. Comparison of inverse capacitance per unit area as a function of formation voltage for tantalum and niobium oxide films (measurements on foil anodes at 1 kc in 8N H_2SO_4).

from the large difference in the dielectric constants being largely canceled by the increase of film thickness for a given formation voltage.

The dielectric loss of the oxide has been estimated by utilizing measurements on the same foils over a frequency range of 0.05-20 kc. The analysis is based (12) on the relation

$$\tan \delta = \tan \delta' + 2\pi f C_1 R_2 \qquad [1]$$

where tan δ is the measured dissipation factor of the capacitor; tan δ' is the dielectric loss of the oxide film and is assumed to be relatively independent of frequency (13); C_1 is the measured capacitance; R_2 is the frequency independent resistance of the electrolyte; and f is the frequency. The comparison for tantalum and niobium oxide films in Fig. 2 demonstrates that the latter has a slightly lower dielectric loss for all formation voltages. In most capacitors this minimum dielectric loss cannot be realized. Either the geometry of a porous or rolled foil anode introduces a large resistance for the last term of Eq. [1], or degradation of the dielectric occurs during processing steps such as the pyrolysis of manganous nitrate solutions at 300°-500°C to form the semiconductor cathode.

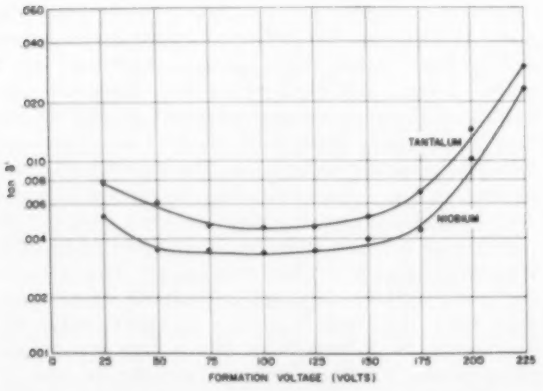

Fig. 2. Comparison of the dielectric loss as a function of formation voltage for tantalum and niobium oxide films (measurements on foil anodes at 1 kc in 8N H_2SO_4).

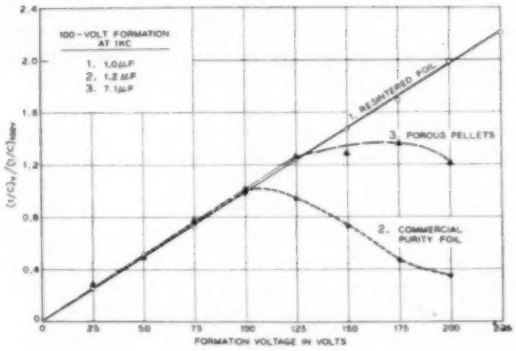

Fig. 3. Comparison of normalized inverse capacitance as a function of formation voltage for three types of niobium anodes (measurements at 1 kc in 8N H_2SO_4).

Anodization characteristics for niobium oxide films.— This study was concerned with the type and quality of the oxide film formed by anodization at room temperature in 60% acetic acid. The primary criterion was the variation of capacitance with formation voltage,[2] shown for three different types of anodes in Fig. 3. Curve 2 illustrates the relationship for commercial purity foil, probably having a purity similar to that of the niobium powder shown in Table I. Above 100 v there is a marked increase in capacitance with increasing voltage instead of the expected linear decrease. Moreover, at these voltages the oxide film does not show the clear interference colors exhibited below 100 v, and by 150 v has a gray matte-like appearance, which can be associated with crystallization of the amorphous oxide film. On these foils, however, crystallization at isolated areas could be observed with a microscope even at 100 v, although under polarized light they do not have the characteristic sector configuration described by Vermilyea for field crystallized tantalum oxide (9, 19).

The characteristics of similar foil annealed at 2050°C under vacuum for 1 hr before anodization is shown in curve 1 of Fig. 3. For these samples, clear colored films were observed up to 225 v, the highest voltage used, and an exact linear relationship exists for the inverse capacitance as a function of formation voltage. The possible changes caused by the heat treatment are: (*a*) recrystallization of in diameter; and (*b*) a chemical purification due to the metal with grain growth to the order of 0.1-1 mm direct volatilization of impurities or their oxides. At present, there is no direct evidence to support either process as being the determining factor in the change in anodization properties. Analytical data (Table I) indicate that the purification of niobium powder during sintering is strongly dependent on temperature in the range of 1850°-2100°C, with the capacitor properties also showing a strong dependence on sintering temperature. Literature results however, indicate that grain growth is substantially complete by 1800°C, with no strong tem-

[2] For purposes of visual comparison, the reciprocal capacitance at any voltage relative to its value for a 100 v formation is plotted as a function of the formation voltage. This use of a normalized reciprocal capacitance avoids the necessity of comparing surface areas and roughness factors, assuming that these do not change in each case as a function of the formation voltage.

Table I. Purity of niobium powder and sintered porous pellets

Material	Sintering temp, °C	Metallic impurities, ppm				Interstitial impurities, ppm				Per cent purity[b] (by Diff)
		<10	10-50	50-300	100-3000	C	O	H	N[a]	
Powder		Ag, Ca, Mg, Mn	Ni, Si, Zr	Cu, Ti	Fe	1900	2600	85	500	99.29
Pellet	1850	Ni, Si, Ag, Mg, Zr	Ca, Cr, Mn	Fe, Ti		30	208	6	170	99.91
Pellet	2100	Ag, Fe, Si, Mg, Mn, Zr	Ca, Cr, Ti			10	300	7	200	99.94

[a] Vacuum fusion analysis for nitrogen is in general irreproducible, and the values listed are approximate.
[b] Purity exclusive of tantalum, and calculated by taking the midpoint of each range as the impurity level.

perature dependence between 1800°-2000°C (8). We tentatively assume that the improved characteristics after vacuum annealing are essentially due to increased purity, with more work required to exclude the structure of the metal surface as a determining factor. These results tend to suggest that for sufficiently pure anode material, amorphous niobium oxide films can be formed to at least 225 v.

For porous pellets (curve 3, Fig. 3) sintered at the same temperature as the foil, marked deviations from linearity occur above 125 v, and obvious visual crystallization by 175 v. The difference in properties between the vacuum treated foil and porous pellets can be ascribed to the complex internal structure of the latter. This structure may introduce a steric factor caused by strain between the oxide and the complicated surface. Perhaps a factor of more importance is that purification during vacuum sintering is hindered by the tortuous paths by which impurities must diffuse for removal at the surface. The important aspect of these data is that a 35-v operating niobium solid electrolytic capacitor requires a formation voltage of 100-130 v, the range in which crystallization is initiated. At the present stage of development 20-v and lower rated niobium porous anode capacitors, where the formation voltages are below 100 v, compare favorably with equivalent tantalum units. However, despite satisfactory initial d-c leakages of samples rated at 35 v, their life at 85°C and 35 v is less than two weeks. These failures are attributed to the presence of crystallized areas in the oxide film, and the process variable investigation has concentrated on those factors known to control the rate of crystallization.

An evaluation of these factors has been guided by the results of Vermilyea (9) who has made a detailed investigation of the field crystallization of tantalum oxide. His proposed mechanism is that crystallization nucleates at impurity or heterogeneous sites after the amorphous film has grown, with this process cracking and pushing aside the original amorphous film and terminating in a crystalline oxide film with twice the thickness of the original one. This mechanism implies that as crystallization proceeds the capacitance should be less than expected, rather than greater as indicated in Fig. 3 above 100 v. This apparent contradiction has been resolved by experiments on tantalum foil, and the difference appears to be a function of the rate and extent of crystallization. With the high rates used by Vermilyea, resulting in complete crystallization of the surface, the final capacitance is exactly half that of the original amorphous film; under low rates of crystallization, as used here, the capacitance is higher than that of the amorphous film, and the entire surface is not crystallized. A possible explanation for the latter effect is that at an intermediate growth stage where the crystallites have pushed aside the amorphous layer, but not joined together, the boundary between the crystalline and amorphous regions is penetrated with microfissures. The multiplicity of defects produced in this manner would result in a high capacitance, similar to the results reported for zirconium and tantalum (14) where microfissures have been postulated. As was found in these latter studies the capacitance of a partially crystallized niobium oxide film exhibits a very high-frequency dependence (Fig. 4).

The capacitance-frequency results in Fig. 4 were obtained on the same resintered foil during anodization at 120 v and 90°C. The current-time relationship for anodization at constant voltage at these conditions, where crystallization is greatly accelerated, is shown in Fig. 5. The general shape of the curve, with a maximum in current, is typical of the crystallization of an amorphous film (9). The numbers associated with each point are the capacitance values for the foil at 1 kc in 8N H_2SO_4. Crystallization of the amorphous niobium oxide film which proceeds at a reasonable rate between 5-60 min is associated with a large increase in capacitance. After 105 min, when the crystallization process is essentially complete, the capacitance starts to decrease again. The final capaci-

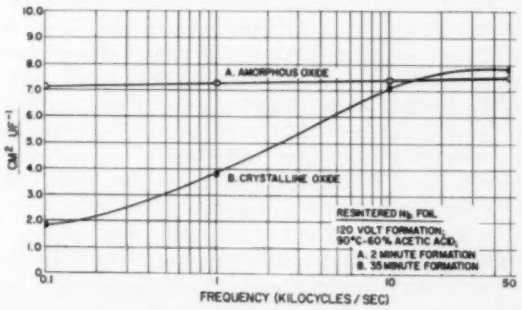

Fig. 4. Capacitance-frequency dependence for amorphous and crystallized oxide films. Formation conditions for vacuum annealed niobium foil anodes: (a) amorphous film—90°C, 120 v, 4 min after reaching constant voltage; (b) crystallized film— 90°C, 120 v, 120 min after reaching constant voltage.

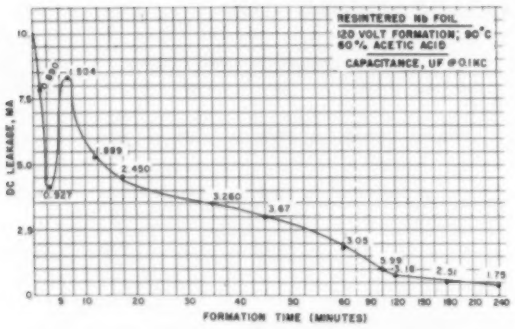

Fig. 5. Current-time relation for resintered niobium foil anodized at constant voltage at 120 v and 90°C in 60% acetic acid. Capacitance values at each point were measured at 25°C in 8N H_2SO_4 at 1 kc. Note the change in time scale between 60 and 90 min.

tance after long anodization periods approaches that of an amorphous film, indicating that the ratio of dielectric constant to thickness at a given formation voltage is approximately the same for either a crystalline or an amorphous film or else that the microfissures are never completely healed.

In this discussion an attempt has been made to demonstrate that, despite qualitative differences, a similar mechanism exists for the crystallization of tantalum and niobium oxide films. The conclusions drawn by Vermilyea concerning the factors determining crystallization should then be equally applicable to the niobium system.

Process parameter investigation for solid electrolytic capacitors.—The important factors (9) which contribute to crystallization are: (*a*) *electrolytes for formation*, where an unexplained dependence exists on the type and concentration of solution; (*b*) *temperature of anodization*, where a normal activation energy dependence exists; (*c*) *formation voltage*, where higher voltages increase the rate of nucleation; and (*d*) *purity of the anode*, where impurities on the surface may serve as nucleation sites. For the first factor, the mechanism of formation of the crystalline film must differ considerably from the amorphous film formation where the rate-determining barrier does not occur at the oxide-electrolyte interface (15). Many electrolytes, both aqueous and nonaqueous, have been investigated for niobium including 40-80% acetic acid, 0.1-2% acetic acid, boric acid, borate buffer, nitric acid, sulfuric acid, sodium phenoxide-phenol in acetone, and ammonium pentaborate in ethylene glycol. Of these only 60% acetic acid has proved useful in suppressing crystallization, and all studies reported here utilized this system for the oxide film formation. Solutions of lower conductivity tend to suppress crystallization, but even this generalization is not completely valid. A solution of 0.1% acetic acid has a conductivity approximately equal to 60% acetic acid ($\sim 3 \times 10^{-4}$ mho-cm^{-1}), but the latter is considerably more efficient in yielding uncrystallized films. It would appear that the particular anions and their local concentration are the more important parameters involved in the electrochemical reaction at the oxide-electrolyte interface.

Table II. Effect of formation temperature and voltage on properties of niobium solid electrolytic capacitors, formation electrolyte, 60% acetic acid

Formation conditions °C	Voltage	Film thickness,* Å	Cap., μf	Initial leakage UA/(UF-v), 20 v, 25°C	85°C	Fraction failed at 20 v, 85°C, 2000 hr
4	80	1300	12.6	0.025	0.54	0
30	60	1300	14.1	0.055	1.13	0.33
50	60	1300	15.0	0.077	1.50	0.33
4	130	2380	7.93	0.21	2.2	0
30	110	2380	8.47	0.31	4.7	1.0
50†	110†	2380	6.91	0.28	3.9	0.33

* Calculated from Young's (11) value of 21.6 Å/v at room temperature and the fact that the film interference color was the same within each set.
† These samples visually crystallized.

The effects of formation voltage and temperature during formation have been investigated simultaneously. Since the thickness of the oxide film at any voltage depends on the temperature of formation, empirical adjustments of the formation voltage at each temperature were made to arrive at the same film color (*i.e.*, film thickness). In terms of capacitance values, these adjustments were only partially successful since they have an average deviation of ±7%. Samples with film thicknesses equivalent to a 60 v and 30°C formation (1300Å) and 110 v and 30°C (2380Å) formation were prepared at three different temperatures, and both sets were arbitrarily rated at 20 v in a life test at 85°C. The important results (Table II) are: first, at each formation temperature the initial leakages at both 25° and 85°C are lower for a 60-v formation than a 110-v formation; and second, at each film thickness both the initial leakage and failure on life are minimized at the lowest formation temperature. Both of these results agree with the predicted dependence of factors (*b*) and (*c*) above and tend to confirm that the leakage and instability on life are related to the extent of crystallization of the oxide film during formation. In seeking the optimum level for factor (*b*) attempts to use a temperature of −10°C for the formation did not result in a significant improvement of properties. The temperature dependence in the range of 4°-50°C is not strong enough to allow samples formed at 130 v and 4°C to survive a life test at 35 v and 85°C. For units rated at 20 v or lower all formations are performed at 4°C due to the improved properties indicated in Table II.

In this work the effect of purity of the anode has been investigated directly by varying parameters of the sintering process, where thermal purification occurs.[8] In the sintering studies, the temperature was varied from 1850° to 2100°C and the time at heat from 0.5 to 2 hr. The impurities both for the initial powder and for pellets sintered for 1 hr at the appropriate temperature are shown in Table I. The reduction in carbon and oxygen results from the formation of carbon monoxide (18). It is apparent that considerably more purification is accomplished at 2100° than 1850°C. Physical properties of the anodes and electrical characteristics of solid electrolytic

[8] A chemical purification process involving selective electrochemical etching of the oxide film on the formed anode has also been investigated and has provided improved performance (16).

Table III. Effect of sintering conditions on the properties of 35 v niobium solid electrolytic capacitors*

(A) Sintering conditions and physical characteristics of anodes				
Sintering temp, °C	1850	2000	2100	2100
Sintering time, hr	1	1	1	2
Rel. density, initial	0.53	0.54	0.53	0.53
Rel. density, final	0.58	0.59	0.61	0.63
Per cent volume shrinkage	9.2	9.7	13.7	20.0
Surface area, cm^2/g	325		207	
(B) Electrical properties of capacitors formed to 110 v				
Capacitance, $\mu f/g$ anode	39	33	28	25
Dissipation factor, 1 kc	0.92	0.067	0.055	0.076
D-C leakage, 35 v, $\mu a/(\mu F\text{-}v)$	13.4	0.12	0.058	1.93
Fraction of surface area used	0.63		0.55	

* The powder had a particle size distribution of 30%, 150-75μ; 40%, 75-30μ; and 30%, less than 30μ. The surface area of the powder was 1,243 cm^2/g.

capacitors made from them are summarized in Table III. The thousandfold decrease in leakage as the sintering temperature is raised is associated with a loss of impurities, which at 2100°C results in a purity of 99.94%. The higher purity results in an improved dielectric oxide film which is reflected in the improved dissipation factor as the sintering temperature is increased to 2100°C The loss of capacitance by going from 1850° to 2100°C is fairly large and is closely related to the degree of sintering indicated by the greater volume shrinkage and decrease in total surface area. This shrinkage is at least three times larger than for tantalum pellets made from powder of similar particle characteristics and is to be expected since the sintering is performed within 300°C of the niobium melting point. The increase in leakage and dissipation factor when the sintering time at 2100°C is increased to 2 hr may be due to a large shrinkage, resulting in narrow pores and a complex internal surface which cannot be anodized and reformed efficiently.

The surface area measurements on powder and pellets have been used previously for tantalum (10) where it has been shown that a fourfold decrease in surface area occurs during sintering at 2000°C for "low capacitance" powder, and that the deposition of manganese dioxide is at least 70% efficient in covering the available surface area. For an 1850°C sintered niobium pellet, the loss of surface area is also a factor of four, but rises to a sixfold decrease at 2100°C, the temperature most appropriate for impurity removal. The fraction of the surface area used is calculated by comparing the area determined by capacitance measurements to the B.E.T. surface area measurement. This factor is not as large as for the tantalum system, and the reasons for this are obscure. The discrepancy may be related to an inexact knowledge of the capacitance per unit area value. More fundamental reasons may be the initiation of crystallization or the closing of pores due to the large shrinkage values. The latter explanation appears quite plausible since the surface utilization efficiency decreases with increasing sintering temperature.

Since the sintering process is a function both of powder particle size distribution and unsintered pellet density, an investigation similar to that outlined in Table III was performed with a coarse powder (150-75μ) and with both the coarse and distributed powders at a relative green density of 0.64. The results are that at any given density the coarse powder has less shrinkage, about 25% less capacitance due to a smaller initial surface area, and equivalent leakages; for any given powder size, the higher density results in equivalent leakage with about 7% less capacitance.

The results of the sintering investigation have confirmed that higher purity anodes yield capacitors with improved electrical properties. It is presumed that a decreased crystallinity of the oxide film results from the improvement in purity. However, the purification is not sufficient in terms of life test stability, since despite the favorable low leakages, all 35-v rated capacitors, independent of particle size, density, or sintering condition, have failed during a life test at 85°C. The purification accomplished by sintering has been pushed to the limit in the present study, since the use of a higher temperature would result in excessive shrinkage probably causing results similar to the 2-hr process at 2100°C. Similar studies have been performed with several other major suppliers of niobium powder, and although some differences exist, the conclusions presented above are equally applicable to these powders.

Comparison of tantalum and niobium solid electrolytic capacitors.—A quantitative comparison of 20-v rated capacitors is shown in Table IV. In general, the yield of capacitance per unit volume (calculated on the basis of anode volume) is comparable, but due to the difference in density, the yield per unit weight is twice as large for niobium. The average temperature dependence for niobium capacitors is +885 ppm/°C compared to +775 ppm/°C for tantalum. The dissipation factor-temperature dependence for niobium capacitors as shown in Fig. 6 is much larger than for tantalum capacitors. The unusual increase in dissipation factor at low temperatures is really dependent on the choice of 1 kc as the measurement frequency. Figure 7 illustrates the dissipation factor as a function of frequency for various temperature conditions for the 20-v rated samples.

Table IV. Comparison of 20-v rated solid electrolytic capacitors

Type	Capacitance		Dissipation factor, 1 kc	Leakage, $\mu a/(UF\text{-}v)$
	Unit vol, UF/cc	Unit weight, UF/g		
Tantalum	180	20	0.05	0.005
Niobium	200	38	0.06	0.022

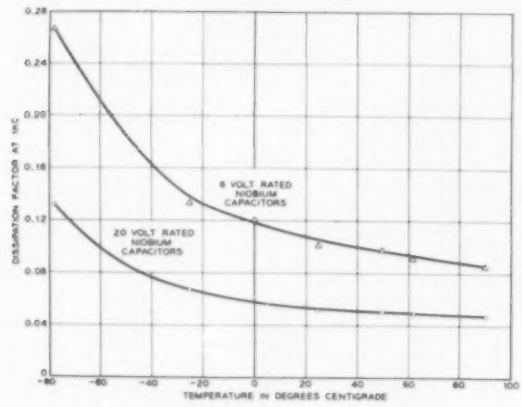

Fig. 6. Dissipation factors as a function of temperature of niobium solid electrolytic capacitors.

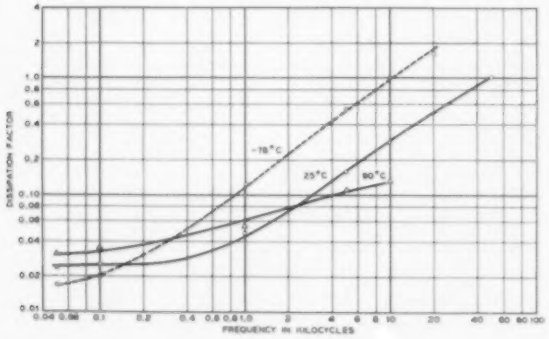

Fig. 7. Dissipation factor as a function of frequency at three different temperatures for 20-v niobium solid electrolytic capacitors.

The dissipation factor at 10 kc is determined mainly by the resistance of the semiconductor cathode, which increases with decreasing temperature; at 0.05 kc, the dissipation factor is controlled by the oxide dielectric, and here the dissipation factor decreases as expected with decreasing temperature (12). The resultant at 1 kc is a combination of the two trends, with the series resistance effect predominating at low temperatures.

Activation energy plots for d-c leakage at 50, 100, and 150% of the rated voltage are shown in Fig. 8. It is only above room temperature that a linear dependence occurs with an activation energy of 9.9 ± 0.1 kcal, independent of test voltage. The marked deviations from linearity below room temperature depend on the test voltage, and at the present time no firm explanation exists for the shape of these curves. It is possible that the marked curvature at low temperatures is due to a slow capacitive current decay, although the measurement procedure was designed to minimize such an effect. Extended time measurements would have to be performed to establish this point. For comparable tantalum solid electrolytic capacitors, the linear relationship extends over the entire temperature range studied, with an activation energy of approximately 13 kcal.

The d-c leakage-voltage characteristics of these capacitors are very asymmetric, with the dependence

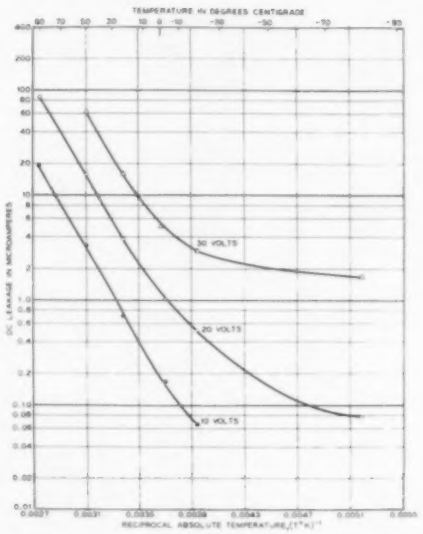

Fig. 8. Leakage as a function of temperature for 20-v niobium solid electrolytic capacitors.

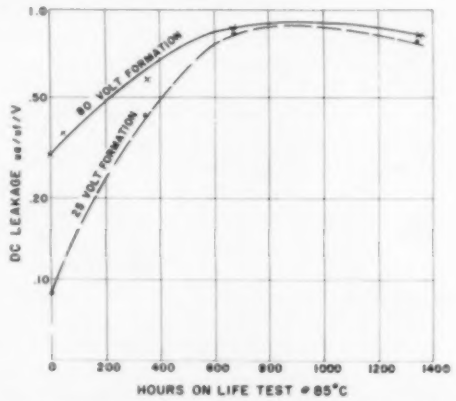

Fig. 9. Leakage during life test at 85°C and rated voltage for 6- and 20-v niobium solid electrolytic capacitors.

in either direction being approximately exponential. The asymmetry can be expressed by the ratio of positive *rated voltage* to the negative voltage where equal currents flow; this ratio is 22 for 20-v rated niobium capacitors and is approximately the same for equivalent tantalum capacitors.

The life test leakage data for capacitors formed at 25 and 80 v and rated at 6 and 20 v, respectively, are given in Fig. 9, where the rise in leakage during the early stages of the test is similar to that of higher voltage rated tantalum solid capacitors. In general, 6-v capacitors survive a 3000-hr life test at 85°C and 8 v; 20-v capacitors survive from 1000-3000 hr depending on the powder lot and processing conditions; and 35-v capacitors all fail within 300 hr. Improvements for the 20-v capacitors can probably be achieved readily by the use of a quality control program for the powder purity and more rigorous control of the over-all processing.

Conclusions

This work has shown that, with the current purity of niobium powder, capacitors comparable to tanta-

lum in almost all initial properties can be prepared. In general for niobium the leakage is higher, the low-frequency dissipation factor lower, and the yield of capacitance per unit weight higher than for tantalum. A severe limitation exists that ratings above 20 v cannot survive a life test at 85°C.

The predicted dependence of the d-c properties of the finished capacitors on purity, formation temperature, and formation voltage tends to confirm that these failures are related to partial crystallization of the oxide film during formation. The solution of this problem in the immediate future can proceed in two directions. One of these is an investigation of the role the electrolyte plays in the formation of the crystalline films. Our qualitative observations and those of Vermilyea indicate that the electrolyte is intimately involved in the mechanism of formation, and a detailed investigation is required to elucidate this fundamental feature. Without this detailed information, the selection of an electrolyte for formation will remain the art that it is today. The other approach is the commercial development of powders with a purity of a higher order than is available now. Actually, the niobium powders have a purity comparable to current tantalum powders (6). However, there is a marked difference in the purification accomplished during sintering under identical conditions. A tantalum pellet sintered at 2000°C and 1 hr has an impurity level reduced to where each metallic component, exclusive of niobium, is below 10 ppm, with the over-all purity approaching 99.99%. Data in Table I show that there is more difficulty in reaching these levels for niobium. This difference can easily be due to differences of thermodynamics and diffusion in the two host metals, but at present no evidence is available to suport this contention. The extensive shrinkage of niobium during sintering as compared to tantalum (14% at 2000°C, compared to a value of 2% for tantalum) as noted previously is related to their difference in melting points. This extensive shrinkage could easily narrow pores, and in the extreme actually close them, so that the diffusion of impurities out of the pellet would be considerably hindered. The surface utilization efficiency decreases with increasing temperature, and this tends to suggest the presence of such closed or narrowed pores within the pellet. The optimum sintering conditions must therefore always represent a balance between those conditions leading to adequate purification and those resulting in excessive shrinkage. In this study, this balance appears to occur for sintering conditions of 2100°C for 1 hr, and no further improvement can be expected by using higher temperatures or longer times. These conclusions suggest that niobium capacitors would always require a higher purity powder than tantalum to achieve equivalent properties in finished components.

The exact mechanism by which crystallization of the oxide film contributes to failure has not been ascertained. The general experience that crystallized films exhibit higher leakage in solution indicates that they are inferior to amorphous films as a dielectric material. The interpretation of the high capacitance of partially crystallized films as being associated with microfissures at the periphery of the crystalline area offers some explanation for the mechanism of failure. A recent mechanism proposed for tantalum capacitor failure (17) is not inconsistent with the site of failure occurring at a crystalline area with its associated microfissures. An alternate explanation is that the microfissures may be blocked initially with gaseous oxygen (14), thus providing low initial leakage, but at elevated temperatures may be released by expansion, resulting in contraction of the film and failure.

Summary

Niobium solid electrolytic capacitors can be prepared up to 20-v ratings with properties comparable to equivalent tantalum components. A severe limitation exists for capacitors rated above 20 v since, despite favorable initial leakages at room temperature, very early failures occur at 85°C. These failures are associated with partial crystallization of the amorphous oxide film during formation at higher voltages. The process parameter investigation has confirmed this conclusion, and optimum conditions for porous pellet fabrication and oxidation have been obtained. The current available purity of niobium, despite extensive purification during sintering, is not sufficient to prevent crystallization of the oxide films.

Acknowledgments

The authors wish to express their appreciation to D. A. McLean and C. C. Houtz for many stimulating suggestions, and to E. K. Jaycox for the spectrographic analysis, R. W. Ryan for the carbon determination, R. Brown for the vacuum fusion analysis, and W. G. Guldner for the surface area measurements.

This work with D. A. McLean as project leader, was sponsored in part by Contract DA-36-039-sc-74996 administered by the U.S. Army Signal Research and Development Laboratories, Fort Monmouth, New Jersey.

Manuscript received Jan. 30, 1961. This paper was prepared for delivery before the Chicago Meeting, May 1-5, 1960.

Any discussion of this paper will appear in a Discussion Section to be published in the June 1962 JOURNAL.

REFERENCES

1. R. L. Taylor and H. E. Haring, *This Journal*, **103**, 611 (1956).
2. D. A. McLean and F. S. Power, *Proc. IRE*, **44**, 872 (1956).
3. D. A. McLean, N. Schwartz, J. K. Werner, and M. Gresh, "Improved Electrolytic Capacitors," Jan. 15, 1960, Final Report, Contract DA-36-039-sc-74996.
4. L. Young, *Trans. Faraday Soc.*, **52**, 52 (1956).
5. A. Lunchick and C. Peabody, *Proc. Elec. Comp. Conf.*, **1960**, 87.
6. C. C. Houtz and S. Karlik, *ibid.*, **1959**, 116.
7. L. R. Williams and T. J. Heal, Plansee Proceedings, p. 350, 1958.
8. R. T. Begley and L. L. France, "Reactive Metals," Met. Soc. Conf. Vol. 2, p. 183 (1958).
9. D. A. Vermilyea, *This Journal*, **102**, 207 (1955); *ibid.*, **104**, 542 (1957).
10. W. G. Guldner and C. C. Houtz, *ibid.*, To be submitted.

11. L. Young, *Can. J. Chem.*, **38**, 1141 (1960).
12. D. A. McLean, *This Journal*, **108**, 48 (1961).
13. P. Wirbel and D. G. deGroot, *Phillips Res. Repts.*, **13**, 489 (1958).
14. L. Young, *Trans. Faraday Soc.*, **55**, 842 (1959).
15. D. A. Vermilyea, *This Journal*, **103**, 690 (1956).
16. R. W. Berry, N. Schwartz, M. Gresh, and M. Urban, *ibid.*, To be submitted.
17. A. V. Fraoli, *IRE Trans.*, **CP-5**, 72 (1958).
18. W. D. Klopp, C. T. Sims, and R. I. Jaffee, in "Technology of Columbium (Niobium)," p. 106, J. Wiley & Sons, Inc., New York (1958).
19. R. Bakish, *This Journal*, **107**, 653 (1960).

Mechanism of Addition Agent Reaction in Bright and Leveling Nickel Deposition

I. Studies with Radioactive Sodium Allyl Sulfonate

Seward E. Beacom and Bernard J. Riley

Research Laboratories, General Motors Corporation, Warren, Michigan

ABSTRACT

Organic addition agents synthesized with C-14 as well as S-35 have been used in a continuing study of the leveling phenomenon associated with the deposition of bright nickel. Analysis of deposits and the gaseous products of deposition have given information concerning the breakdown of addition agents and have led to a model which may account for the synergistic effect on leveling brought about by combinations of addition agents.

Radiotracer techniques have shown (1, 2) that sodium allyl sulfonate, which imparts some leveling characteristics to a bright nickel plating solution, is preferentially adsorbed onto the high points of an irregular surface. This was considered as verification of a part of the leveling theory which assumes that the leveling process is initiated by this preferential adsorption on peaks.

The plating system used was a Watts-type nickel solution with the addition agents being sodium allyl sulfonate (SAS) and N-allyl quinaldinium bromide (NAQ). The former was tagged with S-35. To obtain a more complete picture it is clear that both compounds ought to be tagged.

Inasmuch as it is known that the radioactive addition agents are included in the nickel deposits, it is important to consider in what form they are included. It has been suggested (3-6) that sulfur-containing additives are reduced to sulfide and included in that form. Unfortunately, few experimental details are given to support this view. Evidence has been presented (7, 8) to show that the sulfonate group of sodium allyl sulfonate is reduced to and included as sulfide in nickel deposits. Thus it is necessary to consider how the allyl sulfonate molecule is broken down or cleaved to permit such a reduction. This points up the necessity of tagging both ends of the molecule and determining the ratio of sulfur to nickel and carbon to nickel included in deposits.

Reduction of sulfonate to sulfide has been examined polarographically, and identification of sulfide in the nickel deposits has been made by a qualitative test. Cleavage of the addition agent has been studied by examination of the gaseous products obtained during the electrodeposition of nickel.

It is recognized that two addition agents are usually required to produce full brightness in nickel plating, and that a synergistic effect takes place. Thomas (9) has shown that a synergism also occurs in leveling, at least for the addition agent system reported in this paper. These deposits had a nominal thickness of 0.0025 cm, having been plated for 128.4 amp-min/dm^2 at a current density of 3.2 amp/dm^2. Thomas' data are given in Table I where the Δ columns show the decrease in surface roughness brought about by the addition agents singly and in combination. Note that a greater degree of synergism occurs on the roughest surface examined.

In explanation of the concept of preferential adsorption to initiate leveling, it appears that a "blocking action" occurs on the peaks thereby diverting current to the valleys. If synergism in the leveling action occurs, then perhaps an interaction of some type takes place between the addition agent molecules. Possibly a new molecular species is produced, or one of the addition agents influences markedly the degree of adsorption of the other addition agent.

It is the purpose of this and succeeding papers to report on an investigation of the cleavage of the addition agents and their eventual inclusion in deposits, as well as on an examination of the possible interactions between the compounds, and to present some speculations as to the adsorption and syner-

Table I. Effect of two addition agents on roughness

Original roughness, μin.	First additive,[1] μin.	Δ_1, μin.	Second additive,[2] μin.	Δ_2, μin.	$\Delta_1 + \Delta_2$, μin.	Both additives,[3] μin.	Δ_3, μin.
17	11	6	7	10	16	4	13
50	49	1	32	18	19	18	32
120	110	10	100	20	30	55	65
350	325	25	310	40	65	150	200

[1] Sodium allyl sulfonate only.
[2] N-allyl quinaldinium bromide only.
[3] Sodium allyl sulfonate plus N-allyl quinaldinium bromide.

gistic effects brought about by coulombic attraction, pi-bonding, and ion-association.

Experimental and Results

Synthesis of C-14 tagged sodium allyl sulfonate.—To gain information about the possible breakdown of sodium allyl sulfonate it seemed necessary to tag the allyl group as well as the sulfonate group. The metathesis reaction was carried out between 1 millimole of allyl bromide containing C-14 as the labeled atom, and a slight excess of sodium sulfite, by a procedure described previously (1). The product was positively identified by infrared analysis. Since there is no indication of cleavage of a carbon-carbon bond, the position(s) of the tag is irrelevant. When the compound was used as an addition agent in a Watts-type bath to deposit bright nickel on a surface consisting of peaks and valley, both autoradiographic and slit-counting procedures (1, 2) indicated preferential adsorption of the sodium allyl sulfonate on peak areas.

Breakdown of addition agents.—Polarographic examination of solutions containing sodium allyl sulfonate, using the rotating nickel micro-electrode, gave no reduction wave indicative of reduction of sulfonate to sulfide.

A simple qualitative spot test to demonstrate the presence of sulfide sulfur is available (10). The reaction between sodium azide and iodine to produce nitrogen gas is catalyzed by the presence of sulfide sulfur. The nickel deposits obtained in this study produced nitrogen gas, thus demonstrating the presence of sulfide sulfur. Known sulfides, pure nickel, and other metals were used as controls.

The experimental procedure developed to identify the gaseous products resulting from the deposition of nickel consisted of electrolyzing 500 milliliters of solution using nickel electrodes. A special electrolysis cell was constructed to collect about 140 ml of the gaseous products and transfer them to a 140-ml gas sample bottle. Separate nickel solutions containing sodium allyl sulfonate, N-allyl quinaldinium bromide, and both of the addition agents, respectively, were electrolyzed for about 3 hr under normal plating conditions. Approximately 75 ml of the gas was introduced into the gas sample bottle which had been evacuated to 10μ.

The gases were analyzed by using a Perkin-Elmer, Model 154-C, Vapor Fractometer. Both a Perkin-Elmer "A" column (di-normal decylphthalate) and a column of dimethyl sulfolane were used for identification and quantitative estimation of the gaseous products. The "A" column operated at 50°C, the flow rate of the helium carrier gas was 60 ml/min, and the 5-ml samples varied in pressure from 200-500 mm. The dimethyl sulfolane column operated at 25°C, the flow rate of the helium carrier gas was 50 ml/min, and the 5-ml samples were run at a pressure of about 200 mm. A sample of pure propylene gas was used for calibration purposes.

Propylene was identified in the gaseous products (mainly hydrogen) obtained when nickel was deposited from solutions containing the addition agents under investigation. An average of several samples from solutions containing both of the addition agents shows a propylene content of 0.02 v/o; 0.016 v/o was obtained from the bath containing sodium allyl sulfonate only, and 0.004 v/o from the bath containing N-allyl quinaldinium bromide only.

Inclusion of S-35 and C-14 in deposits.—If breakdown of the allyl sulfonate occurs during electrodeposition, then studies of the addition agent, tagged in one case with S-35 and in the other with C-14, should yield values for the amounts of sulfur and carbon retained in the deposit different from the one sulfur to three carbon atoms found in the allyl sulfonate group.

Sulfamate-nickel plated flat steel panels 6.5 cm^2 in area were plated for 25 min at 4.3 amp/dm^2 in a bath containing S-35 tagged allyl sulfonate. A repeat set was plated under identical conditions in a bath containing the C-14 tagged allyl sulfonate. The radioactivity was determined by proportional counting of a 1 cm^2 area in the center of the foil, after removal. In addition, they were cross-sectioned and their thicknesses determined microscopically. These data were then used to calculate the number of sulfur atoms and carbon atoms per million atoms of nickel. Details of the calculations are given in the Appendix.

In addition to the flat steel samples, this study also included the use of the 350 μin. precision roughness specimens (2). Runs were made both with and without the second addition agent, N-allyl quinaldinium bromide. Figure 1 summarizes the results as a series of bar graphs showing atoms of sulfur and carbon per million atoms of nickel. Each bar represents the average of three determinations. The reliability of these averages is estimated to be 1%.

The open bars indicate those samples plated from baths containing allyl sulfonate only, while the cross-hatched ones represent data obtained from baths containing both allyl sulfonate and N-allyl quinaldinium bromide. A comparison of any two corresponding bars for sulfur and carbon, i.e., 1 and 5, 2 and 6, etc., shows that 1S:3C ratio is not obtained. Since the departure of the ratio from 3:1 exceeds 2.5% in all cases, it must be considered meaningful and some cleavage must have occurred.

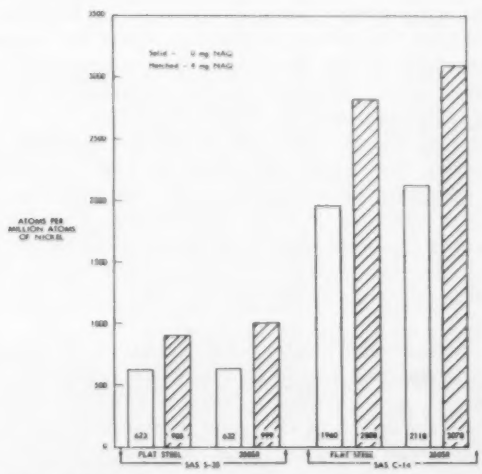

Fig. 1. Sulfur and carbon retained in the plate from SAS

Examination of addition agent interaction.—With the particular addition agent system being studied, synergism occurs in the leveling process. In an attempt to explain this synergism, it has seemed necessary to investigate the interactions which may occur between the two addition agents.

One approach was to examine any possible interactions by means of spectrophotometric analysis. Dilute aqueous solutions of sodium allyl sulfonate and N-allyl quinaldine bromide were prepared and their absorption characteristics determined over the range 2050-4000Å by means of a Cary recording spectrophotometer. Runs were made on a sodium allyl sulfonate solution, an N-allyl quinaldinium bromide solution, a mixture of the two solutions in the same ratio as that used in the plating bath, and the mixture after it had been allowed to stand for 1 and 2 hr. Other runs were made with the mixed addition agents under electrolytic conditions using sulfuric acid at pH 3.0, a current density of 4.32 amp/dm^2 for 15 min at room temperature, with platinum electrodes and with nickel electrodes. The spectra showed no evidence of interaction between the two addition agents to form any new species identifiable by absorption of ultraviolet radiation.

A second approach to a possible explanation of the synergism which occurs in leveling is to examine the influence of the concentration of the N-allyl quinaldinium bromide on the amount of the allyl sulfonate or its reduction product included in the nickel deposit. If these molecules interact in any way at the cathode surface, then conceivably they may bring about an increased "blocking effect" on the peaks. Also, as Thomas (9) has shown, the synergistic effect increases with increase in roughness. Therefore, it seemed necessary to determine the steady-state isotherm of the sodium allyl sulfonate considering both the S-35 and C-14 tagged groups, and to examine the influence of the N-allyl quinaldinium bromide on this sorption. Also, it appeared necessary to investigate the possible interaction of the two addition agents on both flat and rough surfaces.

The steady-state isotherms were obtained by using 6.5 cm^2 sulfamate-nickel-plated flat steel panels which were then plated in bright nickel baths for 25 min at 4.3 amp/dm^2. In the first series, the isotherm was obtained for the S-35 tagged sodium allyl sulfonate alone, and then in the presence of N-allyl quinaldinium bromide. The inclusion of the S-35 on the panels was measured by the proportional flow counter. The results, shown in Fig. 2, indicate typical steady-state isotherms and show conclusively that the presence of N-allyl quinaldinium bromide increases the sorption of sodium allyl sulfonate. The second series, using the C-14 tagged sodium allyl sulfonate, gave similar results. These are shown in Fig. 3.

Further experiments were carried out to measure the interaction of the two addition agents on both flat and rough surfaces. Beginning with a solution which contained S-35 tagged sodium allyl sulfonate as the only addition agent, increasing amounts of N-allyl quinaldinium bromide were added. The experimental procedure using first the flat panels and

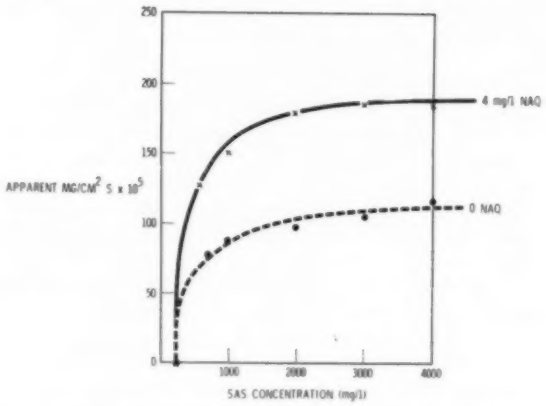

Fig. 2. SAS (S-35) inclusion vs. SAS concentration

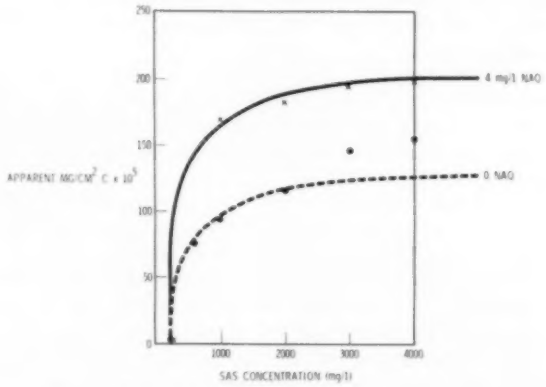

Fig. 3. SAS (C-14) inclusion vs. SAS concentration

then the 350 μin. precision roughness specimens was the same as that employed above.

Figure 4 shows that the amount of N-allyl quinaldinium bromide present in the bath very definitely influences the amount of included S-35. Furthermore, the amount of included S-35 is greater on the rough surface than on the flat panel.

The word "apparent" has been used in the ordinate units of these figures to indicate that no correction has been applied to account for the absorption of radioactivity due to the thickness of the sample. This was not considered necessary since all samples were plated under identical conditions of time and current density. These conditions gave samples which were infinitely thick with respect to the beta radiations of S-35 and C-14.

Discussion

Organic addition agents probably undergo a stepwise sequence of adsorption, cleavage, and reduction. The results obtained for the inclusion of the sodium allyl sulfonate as a function of its own concentration in the absence and presence of N-allyl quinaldinium bromide, Fig. 2 and 3, indicate quite clearly, by the similarity of the curves, that adsorption must have been the first step of the mechanism. If cleavage and reduction had taken place prior to adsorption, then the curves should be dissimilar due to the different electronic character of the observed cleavage products.

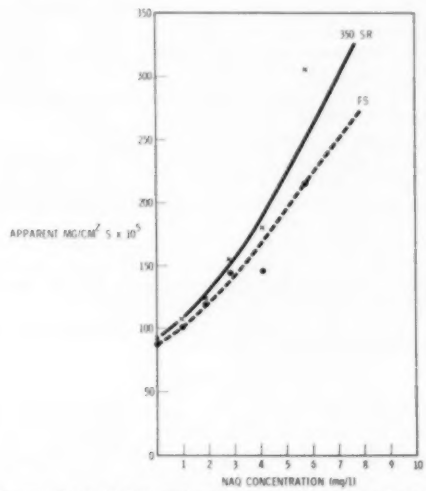

Fig. 4. SAS (S-35) inclusion vs. NAQ concentration

The experimental evidence indicates that both propylene and sulfide ion are considered to be breakdown products. In considering the allyl sulfonate, it seems reasonable to expect that cleavage of the carbon-sulfur bond is required prior to the reduction of the allyl group to propylene and the sulfonate group to sulfide ion. The reducing conditions existing at the electrode, namely hydrogen gas and fresh nickel surface, are certainly conducive to the reduction of the allyl group to propylene. While some of the gaseous product would escape, the larger portion might be expected to adsorb onto the electrode because of the well-known tendency of double-bonded hydrocarbon gases to adsorb onto fresh nickel surfaces.

Further support for the concept of cleavage is found in the ability to measure quantitatively the amount of propylene obtained from the addition agents singly and in combination. The results indicate cleavage of the carbon-sulfur bond in the allyl sulfonate group and the carbon-nitrogen bond in the N-allyl quinaldinium group. No great amount of information has been obtained about the cleavage of the N-allyl quinaldinium group except to note that propylene is produced during electrolysis. Work is now in progress to tag both the allyl group and the quinaldine ring to acquire a more complete picture of the cleavage of this addition agent.

Numerous investigators have measured the sulfur content of bright nickel deposits, and several have reported that they consider the sulfur coming from sulfonated addition agents to be present in the sulfide form. While experimental verification of the presence of sulfide is limited, it seems to be completely lacking as far as substantiation of a mechanism of sulfide formation is concerned. Saubestre (11), for example, considers that the reduction takes place through an intermediate mercaptan formation. Irrespective of mechanism, it appears that, following cleavage of the carbon-sulfur bond, the sulfonate group is reduced at least in part to sulfide at the electrode surface and included as such in the deposits.

Some very interesting results have been obtained by attacking this problem via the use of the tagged allyl sulfonate. As the calculations of sulfur to nickel atoms and carbon to nickel atoms have shown, the exact ratio of three carbon atoms to one sulfur atom is not obtained in the deposits. This further illustrates that cleavage has occurred. While it has been shown that the allyl group is reduced and, in part, escapes as propylene gas, apparently the larger part of the propylene is adsorbed onto the cathode and eventually included in the deposit. Any proposed ratio of carbon to sulfur of 3 to 1, or less than 3 to 1, assumes that all of the sulfide formed is in the deposit. However, apparently not all of the allyl sulfonate is cleaved and reduced, or at least not all of the sulfide is included in the deposit. This may account for the greater than 3-to-1 ratio obtained. Any uncleaved allyl sulfonate ions included in the deposits, or for that matter, any ion or compound originating from allyl sulfonate and containing three carbon atoms and one sulfur atom, would not alter these results since they would be included in exactly the 3-to-1 ratio of carbon to sulfur.

In attempting to arrive at a satisfactory explanation for the mechanism by which these addition agents can bring about leveling, the following is proposed.

The allyl sulfonate group, although it is negative, is impelled to the cathode under diffusion-controlled conditions and adsorbed onto the cathode by adsorption forces which overcome repulsive coulombic forces. In fact, the pi-bonding situation which exists around the double bond of the allyl group dictates firm adsorption on the cathode. The negative end of the molecule would tend to be oriented away from the cathode and would present a repulsive force for other incoming allyl sulfonate groups. Consequently, limited coverage or blockage of the surface would result and leveling action would also be limited.

In the case of the positive N-allyl quinaldinium group, coulombic attraction would bring this ion to the electrode surface and tend to keep it there. In addition, strong pi-bonding forces are present to enhance adsorption. Support for this concept is provided by the recent work of Volkova (12) who found that cationic pyridine derivatives were adsorbed onto the dropping mercury electrode, thereby permitting the close approach of anions of dissociated substances.

As shown in Fig. 1 through 4, N-allyl quinaldinium bromide in the solution increases the inclusion of both carbon and sulfur from the allyl sulfonate. It is suggested that in the presence of both of these addition agents the charged groups would be arranged alternately on the surface. Perhaps these groups lie flat and thus cover more of the surface of a peak. This would lead to more effective blocking and thereby to enhanced leveling. It is apparent from the similarity of adsorption shown in Fig. 2 and 3 that this action of the alternate adsorbed ions precedes any cleavage and reduction steps.

This arrangement of alternate negative and positive ions might be thought of as an "ion-pair" or, preferably, "ion-association." According to Kraus (13) and Hamer (14), ion-pairs can exist in a medium of low dielectric constant. Supposedly, such a

situation exists near the surface of a working cathode. Thus, this concept of ion-association suggests, in effect, a neutralization of repulsive forces and an enhancement of attractive forces which may contribute to a greater blockage of the surface and attendant leveling. Perhaps this is the cause of the observed synergism obtained both in brightness and in leveling.

This idea might be extended to speculate on the cause of the synergism apparent on rough surfaces. As indicated in Fig. 4, the addition of N-allyl quinaldinium bromide brings about a greater inclusion of both carbon and sulfur from the allyl sulfonate. This is particularly noticeable on the 350 μin. precision roughness specimen. Let us consider this in terms of the effect of the diffusion layer thickness.

A thinner diffusion layer should exist on the peaks than in the valleys of an irregular surface (15-17). The diffusion of organic molecules to a peak would be facilitated and would be retarded to a valley. In a previous publication (18) it was shown that there is indeed a greater diffusion layer thickness in the valleys than there is on the flat surrounding areas.

In the present work concerning the inclusion of S-35 from tagged allyl sulfonate in terms of N-allyl quinaldinium bromide concentration, the greater pick-up on a rough surface than on a flat surface has been demonstrated. Thus it seems that the differences in diffusion layer thickness existing on peaks and in valleys may account for differences in organic addition agent diffusion. This presumably leads to a difference in blockage of the surface and a difference in the degree of leveling obtained.

Acknowledgment

The authors gratefully acknowledge the assistance of Warren Florance and Roger Gatrell of the Chemistry Department who carried out infrared and vapor phase chromatographic analyses, respectively.

Manuscript received Feb. 6, 1961; revised manuscript received April 18, 1961. This paper was prepared for delivery before the Houston Meeting, Oct. 9-13, 1960.

Any discussion of this paper will appear in a Discussion Section to be published in the June 1962 JOURNAL.

REFERENCES

1. S. E. Beacom and B. J. Riley, *This Journal*, **106**, 309 (1959).
2. S. E. Beacom and B. J. Riley, *ibid.*, **107**, 785 (1960).
3. E. Raub and M. Wittum, *Met. Indust. and Met. Finishing*, **38**, 206, 315, 429 (1940).
4. V. Zentner, A. Brenner, and C. W. Jennings, *Plating*, **39**, 865 (1952).
5. A. V. Pamfilov and R. M. Morgart, *Ukrain. Khim. Zhur.*, **23**, 684 (1957).
6. R. M. Morgart and O. E. Panchuk, *Zhur. Priklad. Khim.*, **32**, 833 (1959).
7. J. J. Hoekstra, Doctoral Dissertation, Wayne State University, 1957.
8. H. Gotthard, Diplomarbeit, Karlsruhe, 1959.
9. J. D. Thomas, Private communication.
10. F. Feigl, "Spot Tests in Inorganic Analysis," p. 303 ff. 5th ed., Elsevier, Amsterdam (1958).
11. E. B. Saubestre, *Plating*, **45**, 1219 (1958).
12. V. Volkova, *Nature*, 185, 743 (1960)
13. C. A. Kraus, *J. Phys. Chem.*, **60**, 129 (1956).
14. W. J. Hamer, Editor, "The Structure of Electrolytic Solutions," John Wiley & Sons, Inc., New York (1959).
15. D. G. Foulke and O. Kardos, *Proc. Am. Electroplaters' Soc.*, **43**, 172 (1956).
16. S. A. Watson and J. Edwards, *Trans. Inst. Met. Finishing*, **34**, 167 (1957).
17. E. Bertorelle, I. R. Bellobono, and C. Bordonali, *ibid.*, **35**, 231 (1958).
18. S. E. Beacom, *Plating*, **46**, 814 (1959).
19. G. T. Rogers, M. J. Ware, and R. V. Fellows, *This Journal*, **107**, 677 (1960).
20. G. Gleason, J. Taylor, and D. Tabern, *Nucleonics*, **8**, No. 5, 12 (1951).
21. A. Kulishenko, *Zhur. Fiz. Khim.*, **28**, 1186 (1954).
22. E. Broda and T. Schoenfeld, "Handbuch den Mikrochemischen Methoden," F. Hecht and M. Zacherls, Editors, Vol. 2, p. 16, Vienna (1955).
23. M. Curtis and J. Heyd, AEC Document, MLM 842, April (1953).

APPENDIX

To compute the number of sulfur and carbon atoms per atom of nickel, the following equation from the recent article by Rogers, Ware, and Fellows (19) was utilized.

$$P = \frac{W \mu C}{k S \rho (1 - e^{-\mu t})}$$

where P is the number of atoms of sulfur or carbon per atom of nickel; W the weight of nickel in grams per gram atom (g/g at.); k the efficiency factor of the counting system expressed as counts per minute per millicurie (cpm/mc); S the specific activity of sulfur or carbon in the plating bath expressed as millicuries per gram atom (mc/g at.); μ the linear absorption coefficient of sulfur or carbon expressed as centimeters^{-1} (cm^{-1}); ρ the density of nickel in grams per cubic centimeter (g/cm^3); C the net counts per minute per square centimeter of the sample (cpm/cm^2); and t the thickness of the sample in centimeters (cm).

An independent value of μ/ρ, the mass absorption coefficient, was determined from an aluminum absorption curve, *i.e.*, $\log_{10}$ of the count rate against absorber thickness (mg/cm^2). Table II shows a comparison of the values for S-35 and C-14 obtained in this study with others appearing in the literature. The values from this study agree quite closely with most others, and they were used in the calculations. Since the value of the mass absorption coefficient is essentially independent of the absorbing medium, its value can be used to obtain μ, the linear absorption coefficient for S-35 and C-14 in nickel. Such a step gives a μ for S-35 of 1.97×10^3 cm^{-1} and a μ for C-14 of 2.14×10^3 cm^{-1}.

The value for k, the efficiency factor, was likewise determined experimentally and found to be 1.45×10^9 cpm/mc for the gas proportional counting system used. The specific activity of sulfur was determined as 0.80

Table II. Mass absorption coefficient, μ/ρ (cm^2/mg) for S-35 and C-14

	S-35	C-14
Gleason *et al.* (20)	0.21	0.26
Rogers *et al.* (19)	0.30	
Kulishenko (21)	0.23	
Broda and Schoenfeld (22)	0.22	0.25
Curtis and Heyd (23)	0.22	
Riley and Beacom	0.22	0.24

Table III. Representative data for atom ratio calculations

Cathode	Net, cpm/cm^2	NAQ concentration, mg/liter	Thickness, cm $\times 10^3$	S/10^3 Ni	Average
FS	47	0	1.3	570	
FS	52	0	1.3	630	
FS	56	0	1.4	669	623
FS	76	4	1.4	908	
FS	77	4	1.3	934	
FS	73	4	1.4	873	905

mc/g at. and that of carbon as 0.29 mc/g at. All counting was done in the center of the area plated by placing a lead foil with a 1 cm^2 opening in it over the plated foil. Thickness measurements were made microscopically on the cross sections of the foils using the same areas as were counted.

Table III gives representative data for sulfur from which the averages of the first two bars in Fig. 1 were obtained. The sample calculation for sulfur below indicates how the data were handled.

$$P = \frac{(58.7\ \text{g/g at.})\ (1.97 \times 10^3\ \text{cm}^{-1})\ (47\ \text{cpm/cm}^2)}{(1.45 \times 10^5\ \text{cpm/mc})\ (0.80\ \text{mc/g at.})\ (8.9\ \text{g/cm}^3)\ [1 - e^{-(1.97 \times 10^3\ \text{cm}^{-1})(1.3 \times 10^{-3}\ \text{cm})}]}$$

$P = 5.7 \times 10^{-4}$ at. of sulfur per atom of nickel or 570 at. of sulfur per 10^6 at. of nickel.

The same equation, using the appropriate values, was used to calculate the carbon results.

The Electrophoretic Deposition and Recrystallization of Synthetic Fluorphlogopite Mica

W. McNeill, J. E. Chrostowski, and T. J. Mackus

Research and Development Group, U. S. Army Ordnance Arsenal, Frankford, Philadelphia, Pennsylvania

ABSTRACT

The reconstitution of synthetic fluorphlogopite mica powder into larger sheets by electrophoretic deposition and hot-pressing was investigated. Lamellar polycrystalline sheets were formed by electrophoretic deposition from suspensions of 5-20μ mica particles in n-amyl alcohol at a current density of 0.5 ma/in.^{2} and at 100-300 v d.c. The effects of concentration of the suspension particle size of the mica and size distribution, deposit thickness, suspension flow, and current density on deposit density, and structure were studied.

Recrystallization of the electrophoretic mica deposits was obtained by pressing them between molybdenum sheets at 2000 psi and 1300°C. A number of transparent and slightly flexible recrystallized samples were obtained, but their mechanical properties did not equal those of natural mica.

High-quality natural mica, which must be imported by this country, is expensive and many attempts have been made to synthesize it. An electric furnace synthesis of fluorphlogopite mica was developed by the Bureau of Mines (1), but the yield of usable large crystals was quite low, creating a need for a reconstitution process to upgrade the synthetic product.

This investigation[1] was undertaken to determine whether polycrystalline mica sheets composed of small particles and exhibiting lamellar particle orientation could be obtained by electrophoretic deposition. Presumably, these features would make subsequent high-temperature recrystallization proceed more readily.

Electrophoretic deposition requires that the material to be deposited first be suspended in finely divided form in a fluid medium. In the present case, it was necessary to avoid aqueous media to minimize contamination of the mica particle surfaces and also to prevent gas evolution at the deposit electrode. Many organic liquids have been used in electrophoretic deposition and, in general, the most stable[2] suspensions are those formed in polar liquids (1-3), particularly where an OH group is present (4). It has also been noted that the density of sediments is greater for stable suspensions than for flocculating suspensions (5), and that flat particles, such as mica and kaolin, tend to orient and settle faster. Schofield and Sampson (6) found that face to face orientation of suspended kaolin particles (which could be achieved by varying the ionic constituents in the suspension) resulted in denser sedimentation deposits.

Experimental

Suspension preparation.—A series of experiments was carried out to screen ethers, alcohols, ketones, and hydrocarbons, both aromatic and aliphatic. The most stable suspensions of fluorphlogopite mica were obtained with the aliphatic alcohols C_4 to C_{10}, and n-amyl alcohol was selected for further study. This choice was based mainly on the physical properties of this alcohol which made it convenient to use.

The requirements for the grinding process to be used in suspension preparation were that it produce mica particles of micron size with as large area-to-thickness ratio as possible, smooth edges and faces, and minimum contamination. Wet grinding techniques were studied because freshly exposed mica surfaces are subject to contamination by adsorption of oxygen or moisture from the air. Dry redistilled n-amyl alcohol was used as the liquid medium.

The test procedure was to place a drop of suspension representing each grinding technique on a microscope slide and allow it to air-dry prior to examination. A petrographic microscope was used to observe orientation and mean diameters of par-

[1] This work was done at Frankford Arsenal and supported by the General Services Administration under Contract No. GS-OOP-(D)-18145.

[2] The terms "stable" and "flocculating" are used to define suspension properties. "Stable" suspensions are those in which the particles remain separate until the moment of deposition or sedimentation. In "flocculating" suspensions, the particles combine with others to form aggregates or floccules prior to deposition.

ticles, the condition of edges and surfaces, and the presence or absence of ultrafine particles. The adhesion of the latter to larger particles might make it impossible to obtain a flat oriented deposit. The condition of crystal edges and particle orientation was studied by placing the samples between the Nicol prisms of the microscope, crossing them, and observing the extent to which the field was darkened. Particle thickness was determined by microscopic measurement of the clear border along the edges of particles on slides which had been "shadowed" with silver by vacuum deposition at a known angle. Ball milling, cone milling, mechanical mortar and pestle grinding, ultrasonic disintegration, and Waring Blendor grinding were investigated. The latter gave the largest yield of smooth, thin, particles in the subsieve range and was used for subsequent preparation of suspensions.

Grinding times of several hours were used, and in the final stages of the grinding process the steel grinding blade was replaced by a perforated Teflon disk. The suspension preparation procedure developed in this study was as follows: 800 g of flake synthetic mica and 2 liters of dried n-amyl alcohol were ground 3 hr in a 1 gal Waring Blendor using a steel blade. The mica was first heated for 2 hr at 500°C to remove any moisture adsorbed on it. The n-amyl alcohol was dried over anhydrous sodium sulfate, decanted, distilled, and the fraction collected between 136° and 137.5°C was added. After grinding, the mixture was diluted to 4250 ml with dried n-amyl alcohol and allowed to stand overnight. Three layers appeared on standing and from these the middle layer, which was a concentrated liquid suspension, was separated. This was diluted approximately 2:1 to 2700 ml with dried n-amyl alcohol, and again allowed to stand overnight. Three layers appeared, and from these the middle layer was separated. The volume of this suspension was about 800 ml and the concentration, determined gravimetrically, was 187 g/l. The suspension was ground for 1 hr in a Waring Blendor equipped with a perforated 3 in. Teflon disk, and was then ready to be used for electrophoretic deposition. The particle size range for suspensions prepared in this way was approximately 5-25 μ, and the diameter to thickness ratio was about 10. Different particle size ranges were obtained by varying the dilution volumes and sedimentation times.

Survey of deposition variables.—A number of deposition variables that were likely to be important also were indicated in the literature. Hamaker (3) obtained electrophoretic deposits from unstabilized suspensions and reported that the density of the deposits increased with deposit thickness, suspension concentration, and rate of deposition. Benjamin and Osborn (2) obtained electrophoretic deposits of Al_2O_3 and $BaSr(Co_3)_2$ with particles ranging in size from 0.5 to 150 μ. They did not, however, report the effects of particle size on the properties of the deposit.

The shape and motion of the suspended particle might be expected to affect the structure of the electrophoretic deposit, but no direct information on this was found. Marshall (7) quotes von Busagh (8) and Bradfield and Zocher (9) who showed that suspended flat particles orient during flow between flat surfaces or in round tubes. The particles tend to orient parallel to one another and are inclined downstream with respect to the walls of the channel. Orientation of flat particles in electric fields has also been observed by Procopiu (10) and Marshall (11). These observations indicated that the flow of a mica suspension over an electrode during electrophoretic deposition might affect the structure of the deposit since flat particles oriented parallel to the electrode surface just prior to deposition would be expected to retain that orientation during deposition. The movement of the suspension might also dislodge deposited particles that were loosely held or at an angle to the electrode surface and leave only the particles which were securely bonded. The effects of the particle size, suspension concentration, current density (deposition rate), suspension flow, and coating thickness on the density of electrophoretic mica deposits were studied by means of a factorial design experiment. A single replication was used, and the density of the electrophoretic deposit was measured with each set of conditions. It had been observed in preliminary experiments that there was a tendency for the mica particles to deposit with a long axis parallel to the electrode surface. Departures from this type of particle orientation would be reflected as a decrease in the density of the dried mica deposits. X-ray back reflection photographs can also show preferred orientation in a polycrystalline mass, but would be a much less sensitive technique with particles of the geometry used in this investigation. Two particle size ranges were studied. These were 5-25 μ and 44-105 μ. Suspensions of 50-190 g/l of mica were prepared for each particle size range.

The electrophoretic deposition cell was a straight-walled round glass dish which was approximately 4 in. in diameter. The deposit formed on the cathode, which was placed vertically in the suspension, midway between two anode plates which were 0.5 in. apart. The cathodes were nickel, 0.5 x 1.0 x 0.021 in., and the anodes were platinum, 0.5 x 1.0 x 0.010 in. Current densities of 0.5 to 2 ma/in.^{2} were used. Rotary flow of the suspension during deposition was provided with a magnetic stirring device which spun a plastic coated bar magnet, placed in the suspension container. Flow rates of approximately 1 ft/sec and zero were used.

The deposition voltage was not studied as an independent variable, but was adjusted to yield the desired current density. The voltage required for the formation of the deposits varied from about 65 to 1200, with the highest voltages being required for the higher current density and the dilute suspensions. The voltage required to yield a particular current density generally increased as the deposit grew in thickness and therefore had to be adjusted manually during deposition.

Deposit thickness depended on the current density and the length of time deposition was continued. The "thinner" deposits were approximately

Table I. Densities of electrophoretic mica deposits

			Susp. conc. 190 g/l Deposit thickness, 0.03 in.	Susp. conc. 190 g/l Deposit thickness, 0.005 in.	Susp. conc. 50 g/l Deposit thickness, 0.03 in.	Susp. conc. 50 g/l Deposit thickness, 0.005 in.
			g/cm³			
Current density 2 ma/in.²	Flow rate 1 ft/sec	Particle size 44-105μ	0.80	0.81	0.78	0.81
		Particle size 5-25μ	0.97	1.05	0.90	0.83
	Zero flow	Particle size 44-105μ	0.93	0.84	0.82	0.80
		Particle size 5-25μ	0.99	0.97	0.93	0.91
Current density 0.5 ma/in.²	Flow rate 1 ft/sec	Particle size 44-105μ	0.91	0.88	0.90	0.85
		Particle size 5-25μ	1.10	1.35	1.04	1.02
	Zero flow	Particle size 44-105μ	0.86	0.93	0.79	0.97
		Particle size 5-25μ	1.08	1.15	0.93	1.04

0.005 in. thick, and the "thicker" deposits were approximately 0.30 in. thick. Densities were measured by the buoyancy method using mercury as the liquid for immersion of samples. Weighted electrodes were used which could be coated with mica and also suspended from a sensitive balance for weighing. Each density determination required the weighing of the electrode in air and in mercury both before and after deposit formation. The volume of the electrode before and after deposit formation was calculated from these values, and their difference was the volume of the deposit. Dividing deposit weight by volume yielded a value for the bulk density of the mica deposit. The experimental data are shown in Table I, with the levels of each of the variables indicated in the margins at the top and on the left. The number in each square is the measured density of the deposit obtained using the indicated conditions.

An inspection of the density values in Table I shows that for every set of conditions the fine particle suspension yielded a denser deposit than the coarse particle suspension, and it was therefore obvious that particle size was highly significant.

An analysis of variance was performed on the density data for the 16 specimens coated in the fine particle suspensions. The highest order interaction was used to calculate the test variance. It was found that suspension concentration and deposition rate had significant effects on deposit density, but that this was not significantly affected by either flow of the suspension during deposition or the final thickness of the deposit. Finally, there were no significant interactions between any of the four main effects.

The flatness or surface uniformity of the electrophoretic deposits varied greatly. Those obtained with suspensions of the larger particles (44-105 μ) were quite rough, lacked mechanical strength, and frequently covered the electrode surface incompletely. With the fine particle suspensions, the deposits were generally quite smooth and always covered the electrodes completely.

Further experiments on the effects of particle size, suspension concentration, and rate of deposition were conducted. It was observed that maximum density of the electrophoretic deposits was obtained with a narrow range of particle size (5-25 μ) and was decreased when smaller mica particles were present in the suspension. The most probable explanation is that the small particles tend to adhere to the flat surfaces of the large particles preventing them from packing tightly in the electrophoretic deposit.

It was also shown that there was no difference in the rate of deposition of small and large particles in the range 1-44 μ. Samples of a suspension of this composition were studied at intervals as the suspension was depleted by electrophoretic deposition. No change in particle size distribution was observed.

Increasing the suspension concentration and decreasing the rate of deposition were both found to produce very small increases in deposit density.

Orientation of Mica Particles in Electrophoretic Deposits

In the previous experiments, flow of the suspension over the electrodes did not affect the density of the deposits significantly. The study of deposition variables had been carried out using flowing suspensions because this had been found to yield smoother deposit surfaces and also minimized depletion of the suspension in the vicinity of the electrode. The question next considered was the degree of orientation of the mica particles in electrophoretic deposits.

A larger cell was built in which suspension flow was obtained by means of a centrifugal pump that cycled the suspension through a steel pipe inserted in the suspension container. A diagram of the apparatus is shown in Fig. 1. With this apparatus it was possible to obtain a fairly rapid viscous flow of suspension over the electrodes during deposition. Deposits up to 3 x 3 in. in size could be obtained.

The deposition was carried out using a suspension containing 187 g/l of 5-20 μ mica particles. At

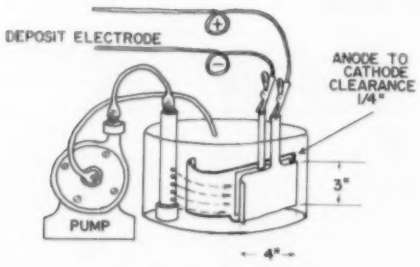

Fig. 1. Electrophoresis cell

Fig. 2. Delamination of mica deposit in n-amyl alcohol

0.5 ma/in.^{2}, a deposition time of about 2 min was required to form deposits 20 mils thick. The voltage during deposition rose from about 100 to 300.

Evidence of lamellar orientation of the particles in electrophoretic depositions of mica was obtained by delamination in liquids and x-ray back reflection.

The large deposits made in the deposition cell shown in Fig. 1 were found to have a very marked flat orientation which could be observed directly by delaminating the deposit in liquid. A mica deposit was allowed to dry in air and then immersed in fresh n-amyl alcohol. It swelled and delaminated into a series of very well-defined thin layers. Figure 2 is a photograph of a 2 x 2 in. deposit in the process of delaminating. The streaks in the liquid are due to bubbles and particles moving during the 2-sec exposure which was used.

Flat mica particles lying parallel in a laminated electrophoretic deposit might also be ordered with respect to the crystal axes in the cleavage planes. This plane in mica exhibits hexagonal symmetry and thus has six equivalent positions when rotated through 360° around the hexagonal axis. X-ray measurements were made to determine whether any such ordering was present. A 1½ x 2 in., air-dried, electrophoretic deposit of mica was used. Unfiltered radiation from a copper target was allowed to impinge on the center of the mica deposit at an angle of 90°. The back reflection pattern (Fig. 3) showed a series of concentric circles and each circle was of uniform intensity around its circumference. This showed the mica particles to be randomly oriented within laminae.

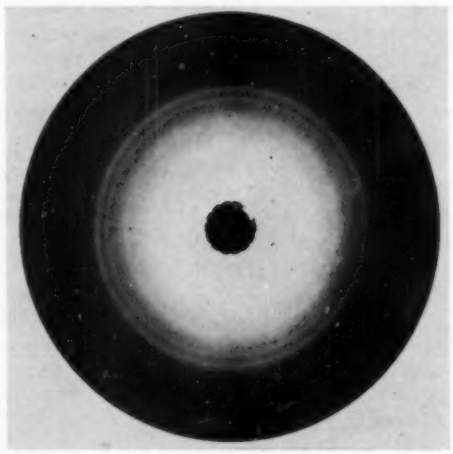

Fig. 3. Back reflection x-ray pattern from electrophoretic deposit of synthetic mica.

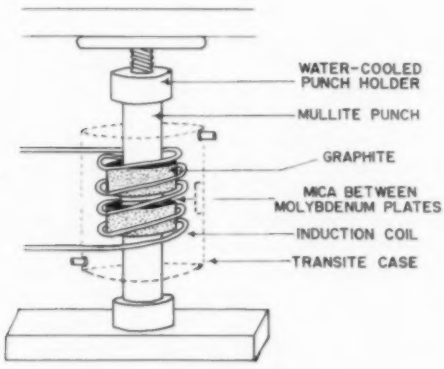

Fig. 4. Hot pressing apparatus

Recrystallization

The electrophoretically deposited mica sheets are quite brittle and chalky when dry and possess insufficient mechanical strength to be of practical value. If handled carefully, they can be removed from the electrodes and subjected to recrystallization treatments. The crystallization and thermal stability of synthetic fluorphlogopite mica had been studied by Van Valkenberg and Pike who observed cloudiness in samples heated at 1000°C for 3 days (12). Hatch *et al.* (13) measured weight losses for similar crystals heated above 900°C and attributed these to loss of fluorine and potassium fluoride. The electrophoretic deposits we prepared showed no evidence of crystal growth at temperatures low enough to avoid volatilization losses, and thus it was necessary to enclose samples by pressing them between molybdenum plates during heating. The apparatus used for this is shown in Fig. 4. The transite case was equipped with ports to provide for a dry nitrogen atmosphere during heating and had a window for observation of samples. Experiments were carried out using 2 x 2 in. sheets of

mica which had been formed on flat nickel cathodes by electrophoretic deposition at 0.5 ma/in.^{2} from a suspension containing 187 g/l of 5-25 μ particles. These were stripped from the cathodes by heating at 290°C. Recrystallization was observed with pressures ranging from 500 to 2000 psi and temperatures ranging from 1100° to 1350°C. Results were somewhat erratic due to the difficulty of controlling temperatures and thermal gradients, and in most cases only part of the sample showed significant crystal growth. Most extensive recrystallization was observed at a pressure of about 2000 psi and a temperature of about 1300°C. Several of the electrophoretic deposits were converted to transparent, slightly flexible sheets by hot-pressing under these conditions. The change occurs very rapidly; 1-10 min at the maximum temperature was sufficient to produce 200-fold increases in crystal size. None of the recrystallized samples were as transparent or flexible as single crystals of natural mica, but were shown to be fluorphlogopite mica by x-ray diffraction. When heating times were extended beyond 30 min, the recrystallized mica sheets gave evidence of decomposition, being rough and no longer transparent.

Conclusions

Lamellar polycrystalline sheets of fluorphlogopite mica can be formed by electrophoretic deposition of particles suspended in n-amyl alcohol. The lamellar electrophoretic deposits can be converted to transparent and slightly flexible sheets of mica by pressing between molybdenum plates at 2000 psi and 1300°C in a dry N_2 atmosphere.

Acknowledgments

The authors wish to express their appreciation to A. Gallaccio and L. Teitell of this laboratory, to S. Di Vita of the Signal Corps Laboratories, Fort Monmouth, New Jersey, and to the members of the Interdepartmental Committee on Mica of the General Services Administration, Washington, D. C., for helpful suggestions and interest in this work. Thanks are also due to Dr. A. Van Valkenberg of the National Bureau of Standards and R. Feder of this laboratory for x-ray measurements.

Manuscript received Sept. 8, 1960; revised manuscript received April 24, 1961.

Any discussion of this paper will appear in a Discussion Section to be published in the June 1962 JOURNAL.

REFERENCES

1. H. Koelmans and J. T. G. Ovebeek, *Discussions Faraday Soc.*, **18**, 52 (1954).
2. M. Benjamin and A. B. Osborn, *Trans. Faraday Soc.*, **36**, 287 (1940).
3. H. C. Hamaker, *ibid.*, **36**, 279 (1940).
4. J. C. Dunbar and T. J. Mitchell, *J. Sci., Food and Agriculture*, **4**, 190 (1953).
5. E. J. W. Mardles, *Trans. Faraday Soc.*, **37**, 321 (1941).
6. R. K. Schofield and H. R. Sampson, *Discussions Faraday Soc.*, **18**, 135 (1954).
7. C. E. Marshall, "The Colloid Chemistry of the Silicate Minerals," Academic Press, Inc., New York (1949).
8. A. Von Buzach, *Kolloid Z.*, **47**, 233 (1929).
9. R. Bradfield and H. Zocher, *ibid.*, **47**, 233 (1929).
10. S. Procopiu, *Ann. Phys.* **1**, 213 (1924).
11. C. E. Marshall, *Trans. Faraday Soc.*, **26**, 173 (1930).
12. A. Van Valkenburg and R. G. Pike, *J. Research NBS*, **48**, 367, R-P2323 (1952).
13. R. A. Hatch, R. A. Humphrey, and E. C. Worden, Bureau of Mines, *Rept. Investigations F283* (1956).

Electroless Deposition of Gold from Aqueous Solution on Base Metals of Nickel and Iron-Nickel-Cobalt Alloys

Robert F. Walton

Hermetic Seals Department, Transistor Products Division, Texas Instruments Incorporated, Dallas, Texas

ABSTRACT

A new solution formulation for the chemical (electroless) deposition of gold is proposed. The main constituents of this solution are potassium gold cyanide, citric acid or tartaric acid, tungstic acid, and N,N-diethylglycine sodium salt. Optimum concentrations of these constituents were determined by a statistical evaluation of the solution at four concentration levels. Investigation of such variables as immersion time, solution temperature, and pH, which affect the chemical deposition of gold from solution, enabled determination of optimum operating conditions.

The solution described in this paper as an electroless gold plating solution was initially formulated during the development of an "acid" gold electroplating solution. Investigation of organic brighteners for use in the acid gold solution eventually resulted in experimentation with N,N-diethylglycine sodium salt. It was this organic salt which we now believe acted as a reducing agent in the chemical deposition of gold.

Organic brighteners for the gold solution were evaluated by performing Hull cell tests on the acid gold solution containing the brightening agent. During the Hull cell evaluation tests of the brighteners, a steel Hull cell panel was left immersed for 4 to 5 min in an acid gold solution containing N,N-diethylglycine sodium salt. Upon returning to the Hull cell tests it was noted that gold had deposited on the steel panel although no current had been applied to

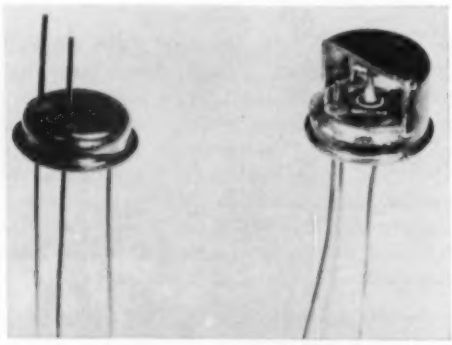

Fig. 1. (a) (left) Glass-to-metal sealed "header" to which germanium or silicon semiconductor is mounted; (b) (right) cut away view of finished transistor.

the cathode. Further investigation revealed that the gold deposit was adherent and had to be an immersion type or electroless type of deposit.

One of the long range projects of the author's company has been automation of gold plating processes. We found that automation of our operation for gold plating semiconductor components parts was feasible with the electroless gold plating process. Figure 1a shows a view of the component part of interest in electroless gold plating. This part, referred to as a header, is shown in a cut-away view of the finished transistor in Fig. 1b. At present, these parts are barrel electroplated from either a cyanide or "acid" gold solution in lot sizes of 2,000 units. The barrel used in plating headers is 8 in. in diameter by 18 in. long, ID. The four metal parts of each header, the three lead wires, and the eyelet or platform are insulated from each other by a glass multiform. Therefore, electrical contact must be made to each of the four metal parts in order to insure gold plating the header. A gold thickness of 12.64 mg/in.^{2} (40 μin.) is required on each header to protect the unit from strong acid etchants such as the CP-4 etch used to etch the germanium or silicon semiconductor. The semiconductor is subjected to this CP-4 etch for 30 sec. Gold plating the headers in an electroless gold solution enables us to load the units automatically on a conveyor belt passing through the solution. Thickness of the gold deposit is controlled by the length of time the units are immersed in solution. With the preceding objective in mind, experiments were designed which enabled us to make a detailed investigation of the electroless gold solution.

Experimental

The optimum concentration of constituents and optimum operating conditions for the electroless gold plating solution were determined from a series of statistically designed tests. A total of 96 different types of solutions were evaluated to determine optimum concentration of constituents in the solution. Four panels were plated in each solution for varying lengths of time. The total number of individual tests, therefore, was 384.

Two basic types of solutions were evaluated in this series of tests. The first was a solution in which potassium gold cyanide was acidified with citric acid. The second was a solution in which tartaric acid was used to acidify the potassium gold cyanide.[1] Table I specifies the levels of the variables tested in the citric acid base electroless gold solution. Table II specifies the level of the variables tested in the tartaric acid base solution.

Table I. Variables evaluated to determine optimum concentration and operating conditions of citric acid base electroless gold solution

Potassium gold cyanide concentration, g/l	7, 14, 28
Citric acid concentration, g/l	0, 15, 30, 60
Tungstic acid concentration, g/l	0, 22.5, 45, 90
Sodium hydroxide concentration, g/l	35.6 wt % tungstic acid concentration
N, N-diethylglycine sodium salt† concentration, g/l	3.75 for all solutions
Phthalic acid monopotassium salt‡ concentration, g/l	25.0 for all solutions
Time of immersion of base metal in solution, min	30, 60, 90, 180
Temperature of solution, °F	185°-200° for all solutions
Agitation	Mechanical

† Obtainable from Eastman Organic Chemicals Dept., Eastman Kodak Co., Rochester, N. Y.
‡ Obtainable from Eastman Organic Chemicals Dept., Eastman Kodak Co., Rochester, N. Y.

Table II. Variables evaluated to determine optimum concentration and operating conditions of tartaric acid base electroless gold solution

Potassium gold cyanide concentration, g/l	7, 14, 28
Tartartic acid concentration, g/l	0, 15, 30, 60
Tungstic acid concentration, g/l	0, 22.5, 45, 90
Sodium hydroxide concentration, g/l	35.6 wt % tungstic acid concentration
N, N-diethylglycine sodium salt concentration, g/l	3.75 for all solutions
Phthalic acid monopotassium salt concentration, g/l	25.0 for all solutions
Time of immersion of base metal in solution, min	30, 60, 90, 180
Temperature of solution, °F	185°-200° for all solutions
Agitation	Mechanical

The solutions were evaluated on the basis that an electroless plating process should continue to deposit metal at a constant rate until the solution was depleted of metal content. We sought a linear relationship between the weight of the gold deposit in mg/in.^{2} and the time the panel was immersed in solution. The slope of the straight line resulting from a graph of weight of metal deposited in mg/in.^{2} *vs.* immersion time of the panel in minutes represents the plating rate of the electroless solution in mg/in.^{2}/min. One of our objectives was to maximize the electroless solution plating rate.

Each of the 96 solutions was evaluated by making a graph showing the weight of gold deposited per unit

[1] The potassium gold cyanide solution is to be acidified in tanks provided with local exhaust hoods or under laboratory type fume hoods. The liberation of poisonous gases upon adding acid and cyanide material necessitates that proper ventilation procedure be followed.

area for each panel *vs.* the length of time the panel was immersed in solution. The best straight line was fitted to the experimental data by the method of least squares. Correlation coefficients were calculated for each solution to determine the significance of an apparently linear relationship between the weight of gold deposited per unit area and the time of immersion of the panel in solution. The assumption was made that a possible linear relationship existed between the weight of gold per unit area and immersion time only when the correlation coefficient equalled or exceeded 0.950 for two degrees of freedom.

Five solutions from each group, citric acid and tartaric acid, were further tested to determine an apparent linear relationship between the weight of gold per unit area and immersion time. The choice of the five solutions from each group was based on three factors: (*a*) the existence of a correlation coefficient of 0.950 or better; (*b*) the deposit of gold on the base material had to be relatively smooth (*i.e.*, very few nodules after a 3-hr plating period), adherent, and show no evidence of black spots or pitting of the base metal; (*c*) the plating rate in mg of gold/in^2/min had to be as large as possible.

The five solutions from each group were evaluated on both Kovar base material and pure nickel base material for immersion times of 5, 10, 15, 30, 60, 120, 240, and 360 min. Kovar[3] material is an alloy of 53.24% Fe, 29.00% Ni, 17.00% Co, 0.5% Mn, 0.2% Si, and 0.06% C.

As before, the best regression line was fitted to the experimental data for each of the ten solutions tested. Correlation coefficients were calculated in order to determine the significance of a linear relationship between the weight of gold deposited per unit area and immersion time. The regression line having the fastest plating rate was considered to represent the most desirable solution. Table III specifies the optimum chemical composition of the two best electroless gold solutions of the five solutions chosen from the citric acid group and the two best solutions of the five tartaric acid base solutions.

The electroless gold solutions were prepared in the following manner:

1. A solution of acidified potassium gold cyanide is prepared by dissolving potassium gold cyanide in deionized water, dissolving the acid in deionized water, and combining the two solutions. The combined solutions are mixed thoroughly, heated to about 140°F, and allowed to cool to room temperature. The end product will be called solution "A." Adequate exhaust ventilation is required when mixing potassium gold cyanide and acid solutions.

2. The tungsten solution is prepared by dissolving sodium hydroxide in deionized water, then cooling the solution to room temperature. Tungstic acid is dissolved in the sodium hydroxide solution. This solution will be called solution "B."

3. Solution "C," a buffer solution of potassium acid phthalate and sodium hydroxide, is prepared. The sodium hydroxide is dissolved in deionized water after which the potassium acid phthalate is dissolved in the sodium hydroxide solution.

4. The N,N-diethylglycine sodium salt is dissolved in deionized water. This solution will be referred to as solution "D."

5. Solutions "A" and "B" are combined together. The pH of the resulting solution is adjusted to a pH value of 5.0-6.0 with the acid or base previously used. Solutions "A" and "B" should be combined as soon as possible in order to prevent the decomposition of gold salt in solution "A."

6. Solution "C," the buffer solution, is added to the adjusted mixture of solutions "A" and "B."

7. Finally, solution "D" is added to the buffered mixture of solutions "A," "B," and "C." The electroless solution is heated to a temperature of 185° to 200°F and the metal panel inserted into solution.

The electroless gold solution utilized the N,N-diethylglycine sodium salt as the reducing agent and the tungstic acid as a grain refiner. Finally the potassium acid phthalate-sodium hydroxide (3) is used to buffer the solution at a pH of 5.0-6.0.

Results

Results of electroless gold plating tests performed on Kovar, nickel, and copper base material are shown in Tables IV and V. The results shown are for the two optimum citric acid type of solutions and the two optimum tartaric acid type of solutions. Also indicated in Table IV and V are the correlation coefficient of the regression line and the plating rate. Again, the optimum electroless gold plating solutions were classified as those having the largest correlation coefficient (1.000 representing perfect linear correlation) for weight of deposit/unit area versus immersion time, and fastest deposition rate. The ap-

Table III. Optimum concentration of chemical constituents of both citric acid base and tartaric acid base electroless gold solutions

	Citric acid electroless gold		Tartaric acid electroless gold	
Solution No.	60	6	72	64
Potassium gold cyanide concentration, g/l	28.0	14.0	28.0	7.0
Citric acid concentration, g/l	60.0	15.00	None	None
Tartaric acid concentration, g/l	None	None	60.0	60.0
Tungstic acid concentration, g/l	45.0	None	45.0	45.0
N, N-diethylglycine sodium salt concentration, g/l	3.75	3.75	3.75	3.75
Phthalic acid monopotassium salt concentration, g/l	25.0	25.0	25.0	25.0
pH (adjusted with citric acid, tartaric acid, or sodium hydroxide), g/l	5.0 to 6.0	5.0 to 6.0	5.0 to 6.0	5.0 to 6.0
Agitation, mechanical				

Table IV. Test results from citric acid base electroless gold solution

Immersion time, min	Weight of gold deposit, mg/in.² Sol. No. 60	Weight of gold deposit, mg/in.² Sol. No. 6	Base material	Regression coefficient	Metal deposition rate, mg/in.²/min
5	1.250	1.138	Kovar		
10	1.486	1.362	Kovar		
15	2.541	1.289	Kovar		
30	2.700	2.038	Kovar	0.997 (sol No. 60)	0.05306 (sol No. 60)
60	5.599	3.188	Kovar	0.997 (sol No. 6)	0.02654 (sol No. 6)
120	8.099	4.541	Kovar		
240	14.315	7.071	Kovar		
360	20.273	10.867	Kovar		
5	0.553	0.709	Nickel		
10	1.600	1.989	Nickel		
15	1.685	2.425	Nickel	0.981 (sol No. 60)	0.04404 (sol No. 60)
30	2.978	3.247	Nickel	0.953 (sol No. 6)	0.01835 (sol No. 6)
60	5.838	4.022	Nickel		
120	6.983	5.051	Nickel		
240	10.073	6.521	Nickel		
360	17.993	8.300	Nickel		
5	0.267		Copper		
10	0.581		Copper		
15	0.638		Copper	0.916 (sol No. 60)	0.00339 (sol No. 60)
30	0.561		Copper		
60	0.929		Copper		
120	1.014		Copper		
240	1.623		Copper		
360	1.527		Copper		

Table V. Test results from tartaric acid base electroless gold solutions

Immersion time, min	Weight of gold deposit, mg/in.² Sol. No. 72	Weight of gold deposit, mg/in.² Sol. No. 64	Base material	Regression coefficient	Metal deposition rate, mg/in.²/min
5	0.965	2.388	Kovar		
10	1.304	3.729	Kovar		
15	2.043	5.442	Kovar		
30	3.150	7.011	Kovar	0.912 (sol No. 72)	0.05553 (sol No. 72)
60	3.964	8.894	Kovar	0.959 (sol No. 64)	0.04415 (sol No. 64)
120	11.998	6.800	Kovar		
240	21.015	15.818	Kovar		
360	17.131	19.576	Kovar		
5	0.928	1.382	Nickel		
10	1.243	0.982	Nickel		
15	1.503	1.847	Nickel		
30	3.115	3.036	Nickel	0.984 (sol No. 72)	0.3946 (sol No. 72)
60	5.169	3.565	Nickel		
120	7.328	4.216	Nickel	0.965 (sol No 64)	0.03185 (sol No. 64)
240	11.863	6.622	Nickel		
360	14.775	14.099	Nickel		
5	0.518		Copper		
10	0.625		Copper		
15	0.847		Copper		
30	0.754		Copper	0.956 (sol No. 72)	0.00302 (sol No. 72)
60	1.063		Copper		
120	1.110		Copper		
240	1.442		Copper		
360	1.714		Copper		

pearance and adhesion of the gold deposit were also evaluated in determining the optimum solutions.

The data in Tables IV and V are represented graphically in Fig. 2 and 3. Figure 2 indicates the relationship between immersion time in solution and weight of gold deposited per unit area for panels of Kovar, nickel, and copper in citric acid-type electroless gold solutions No. 60 and 6. Figure 3 indicates the relationship between immersion time in solution and weight of gold deposited per unit area for panels of Kovar, nickel, and copper in tartaric acid-type solutions No. 72 and 64.

The electroless gold deposit was evaluated for both appearance and adherence of the deposit to Kovar and nickel base materials. Results of this evaluation indicated that the most adherent and best appearing gold deposit on ferrous alloy base materials, *e.g.*, Kovar, was obtained from the citric acid base solution No. 60. The tartaric acid base solution, No. 72, resulted in the most adherent and best appearing gold deposit on nickel base material. Electroless gold deposited on copper base material had about equal appearance and adherence whether deposited from the citric acid or tartaric acid type of solution.

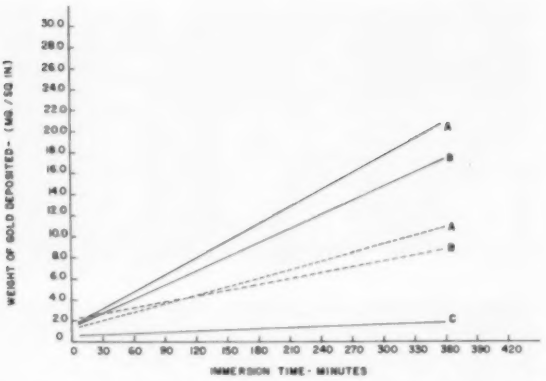

Fig. 2. Relationship between immersion time and weight of gold deposited from citric acid base electroless gold solution. A, Kovar alloy (iron-nickel-cobalt) base metal; B, nickel base metal; C, copper base metal; solid line, solution No. 60 curve; broken line, solution No. 6 curve.

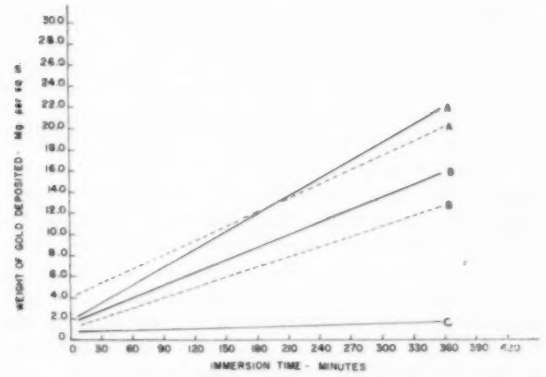

Fig. 3. Relationship between immersion time and weight of gold deposited from tartaric acid base electroless gold solution. A, Kovar alloy (iron-nickel-cobalt) base metal; B, nickel base metal; C, copper base metal; solid line, solution No. 72 curve; broken line, solution No. 64 curve.

The extremely slow rate of metal deposition of electroless gold on copper base material renders the process of depositing gold from electroless solutions on copper impractical.

A series of tests were performed to determine the relationship between the deposition rate of gold from the electroless plating solutions and various operating variables. Variables evaluated were: (*a*) the concentration of N,N-diethylglycine sodium salt in the electroless gold plating solution; (*b*) solution temperature; and (*c*) types and degrees of solution agitation. Electroless gold plating tests on Kovar base material were performed with the citric acid-type solution. Nickel base material was gold plated from the tartaric acid-type solution. All tests were performed in citric acid electroless gold solution No. 60 and tartaric acid electroless gold solution No. 72. Both solutions 60 and 72 were at the same concentration as given in Table III and the same operating conditions as given in Table I or II unless otherwise specified. The concentration of N,N-diethylglycine sodium salt was varied over a concentration range of 0-15 g/l. Solution 60 was evaluated at seven levels of N,N-diethylglycine sodium salt concentration and solution 72 was evaluated at four levels of concentration. The rate of deposition of gold from solutions 60 and 72 was evaluated at three levels of temperature, 150°, 180°, and 212°F. Finally, the metal deposition rate was also evaluated under conditions of no solution agitation, mechanical agitation with a magnetic stirrer, and finally, ultrasonic agitation.

Table VI. Test results from variation of N,N-diethylglycine sodium salt

Concentration of N, N-diethylglycine sodium salt, g/l	Metal deposition rate, mg/in.²/min	Base material	Regression coefficient	Avg wt of gold deposit, mg/in.²
Solution No. 60				
0	0.02575	Kovar	0.892	7.398
1.875	0.02687	Kovar	0.932	6.235
3.750	0.05306	Kovar	0.997	7.033
5.625	0.03594	Kovar	0.958	6.825
7.500	0.02665	Kovar	0.914	7.165
11.250	0.05586	Kovar	0.995	8.258
15.000	0.05152	Kovar	0.979	8.498
Solution No. 72				
0	0.01924	Nickel	0.939	3.201
3.75	0.03946	Nickel	0.984	5.740
7.50	0.02074	Nickel	0.904	3.941
15.00	0.01781	Nickel	0.956	3.670

Number of panels for each test solution: 8
Immersion time: 5, 10, 15, 30, 60, 120, 240, and 360 min
pH: 5.0-5.3
Solution temperature: 180°-190°F
Type of agitation: mechanical

Results of the variation of N,N-diethylglycine sodium salt concentration on the deposition rate of gold from the electroless gold plating solutions are given in Table VI. These results are shown in graphical form in Fig. 4.

The effect of solution temperature variation on the deposition rate of gold from the electroless gold plating solutions is given in Table VII.

Results of the effect of various types of agitation on the deposition rate of gold from the electroless gold plating solutions are shown in Table VIII.

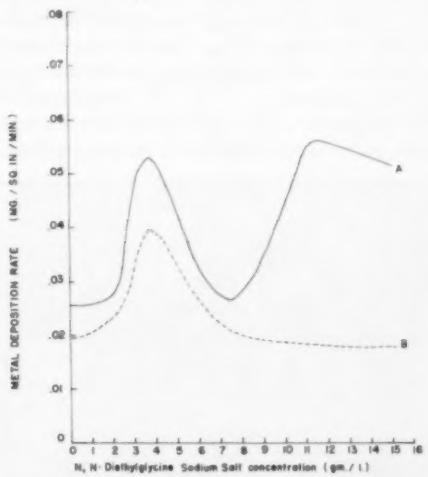

Fig. 4. Relationship between the concentration of N,N-diethylglycine sodium salt and the rate of gold deposition from electroless gold solutions. A, Kovar alloy (iron-nickel-cobalt) base metal; B, nickel base metal; solid line, solution No. 60 curve; broken line, solution No. 72 curve.

Table VII. Test results from variation of solution temperature

Operating temperature of electroless gold solution, °F	Metal deposition rate, mg/in.²/min	Base material	Regression coefficient	Avg wt of gold deposit, mg/in.²
Solution No. 60				
150	0.03072	Kovar	0.958	5.399
180	0.05306	Kovar	0.997	7.033
212 (bp)	0.04625	Kovar	0.971	7.731
Solution No. 72				
150	0.01126	Nickel	0.894	2.036
180	0.03946	Nickel	0.984	5.740
212 (bp)	0.05230	Nickel	0.987	6.879

Number of panels for each test solution: 8
Immersion time: 5, 10, 15, 30, 60, 120, 240, and 360 min
pH: 5.0-5.3
Concentration of N, N-diethylglycine sodium salt: 3.75 g/l
Type of agitation: mechanical

Table VIII. Test results from variation of solution agitation

Type of solution agitation	Metal deposition rate, mg/in.²/min	Base material	Regression coefficient	Avg wt of gold deposit, mg/in.²
Solution No. 60				
None	0.05463	Kovar	0.975	6.090
Mechanical, magnetic stirrer	0.05306	Kovar	0.997	7.033
Ultrasonic	0.04274	Kovar	0.986	5.918
Solution No. 72				
None	0.02896	Nickel	0.976	4.464
Mechanical, magnetic stirrer	0.03946	Nickel	0.984	5.740
Ultrasonic	0.02032	Nickel	0.969	2.698

Number of panels for each test solution: 8
Immersion time: 5, 10, 15, 30, 60, 120, 240, and 360 min
pH: 5.0-5.3
Concentration of N, N-diethylglycine sodium salt: 3.75 g/l
Solution temperature. 180°-190°F

The appearance of the deposit from the electroless gold solution is shown in Fig. 5 and 6. Figure 5 is a photograph of the gold deposited from the citric acid type of solution (*i.e.*, No. 60) on Kovar panels. Reading from left to right the immersion time of the panels in solution is 5, 10, 15, 30, 60, 120, and 240 min. Figure 6 shows nickel panels plated with gold deposited from the tartaric acid type of solution (*i.e.*, No. 72). Again, reading from left to right the immersion time of the panels in solution is 5, 10, 15, 30, 60, 120, and 240 min. Inspection of the panels plated for 240 min reveals a rough texture to the gold deposit. Evidence of gold nodules can also be identified on the panels plated for 240 min in the citric acid type of solution.

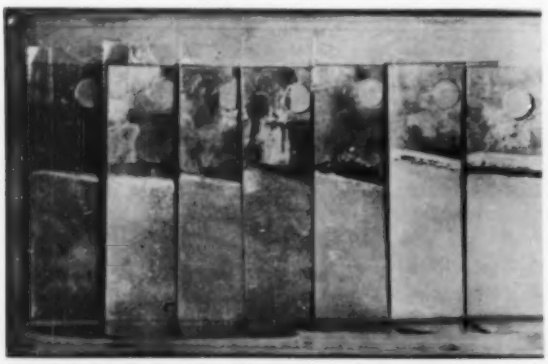

Fig. 5. Surface characteristics of electroless gold deposited on Kovar panels from citric acid type solution No. 60.

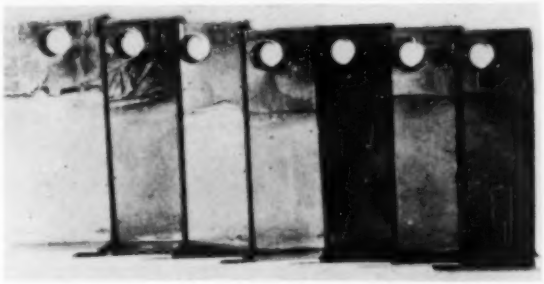

Fig. 6. Surface characteristics of electroless gold deposited on nickel panels from tartaric acid type solution No. 72.

Figures 7, 8, 9, and 10 are useful photomicrographs for comparison of cross sections of both Kovar and nickel panels electroless gold plated from critic acid-type solution No. 60. All photomicrographs are at a magnification of 1540 power. Figure 7 shows the thickness of gold electroless plated in 10 min immersion time on Kovar base material. In Fig. 8 the gold was electroless plated in 240 min time on Kovar material. The increase in gold thickness with the increase in immersion time is quite evident by comparison of Fig. 7 and 8. Figure 9 shows the thickness of gold deposited on nickel base material in 5 min immersion time from citric acid-type solution 60. Finally, Fig. 10 indicates the thickness of gold deposited on nickel in 240 min immersion time. Comparison of Fig. 9 and 10 shows an increase in gold

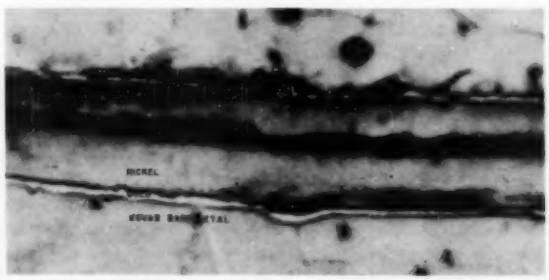

Fig. 7. Photomicrographic cross section of electroless gold deposited in 10 min on Kovar base material from citric acid type solution number 60. Magnification 1540X before reduction for publication.

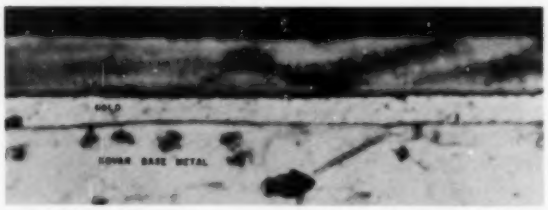

Fig. 8. Photomicrographic cross section of electroless gold deposited in 240 min on Kovar base material from citric acid type solution No. 60. Magnification 1540X before reduction for publication.

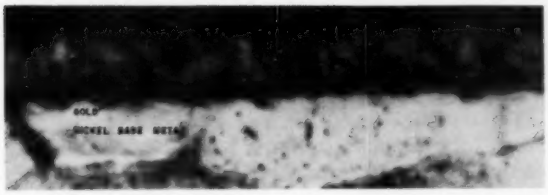

Fig. 9. Photomicrographic cross section of electroless gold deposited in 5 min on nickel base material from citric acid type solution No. 60. Magnification 1540X before reduction for publication.

Fig. 10. Photomicrographic cross section of electroless gold deposited in 240 min on nickel base material from citric acid type solution No. 60. Magnification 1540X before reduction for publication.

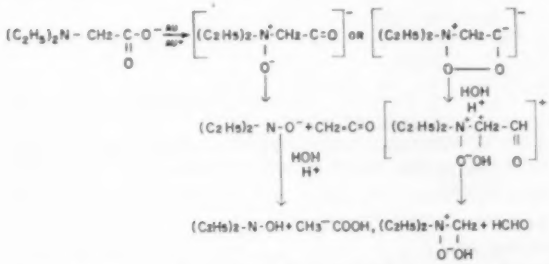

Fig. 11. Proposed mechanism for N,N-diethylglycine sodium salt acting as a reducing agent.

thickness with an increase in immersion time. This increase of metal deposited with increasing time indicates that the metal is deposited by an electroless type of mechanism.

Discussion

Evaluation of both the citric acid and tartaric acid types of electroless gold plating solutions indicated that the citric acid-type solution deposited the most adherent and best appearing gold deposit on ferrous alloy base material, *e.g.*, Kovar. The tartaric acid-type solution deposited the most adherent and best appearing electroless gold deposit on nonferrous base material, *e.g.*, nickel. Both the citric acid type and tartaric acid-type solutions were equally good in depositing electroless gold on copper.

The tartaric acid type of electroless plating solution had a faster rate of deposition of gold on Kovar and nickel base material as compared to the citric acid type of solution. The tartaric and citric acid types of electroless gold plating solutions had about the same rate of deposition of gold on copper. As shown in Fig. 3 and 4 the rate of gold deposition on copper is so slow as to render this electroless method of gold plating copper impractical.

The concentration of the constituents in both the citric acid-type solution and the tartaric acid-type solution which exhibited the optimum electroless gold plating characteristics is:

Type of solution	Citric acid base	Tartaric acid base
Potassium gold cyanide (67% gold)	28.0 g/l	28.0 g/l
Citric acid	60.0 g/l	None
Tartaric acid	None	60.0 g/l
Tungstic acid	45.0 g/l	45.0 g/l
Sodium hydroxide	16.0 g/l	16.0 g/l
N,N-diethylglycine sodium salt	3.75 g/l	3.75 g/l
Phthalic acid monopotassium salt	25.0 g/l	25.0 g/l
pH (adjusted with citric acid, tartaric acid, or sodium hydroxide)	5.0-5.5	5.0-5.5

Conclusions

Experimental evidence indicated that the rate of deposition of gold varied in a cyclic fashion with increasing N,N-diethylglycine sodium salt concentration. The same cyclic variation of rate of metal deposition was noted for both the citric acid type and tartaric acid type of electroless gold solutions. Increasing the N,N-diethylglycine sodium salt concentration in the citric acid-type solution resulted in the rate of metal deposition increasing until the first maximum deposition rate was achieved at a N,N-diethylglycine sodium salt concentration of 3.75 g/l. Further increase in N,N-diethylglycine sodium salt concentration resulted in the plating rate decreasing and then commencing to increase until a second maximum deposition rate was achieved at 11.25 g/l N,N-diethylglycine sodium salt concentration. An increase of N,N-diethylglycine sodium salt concentration in the tartaric acid-type solution resulted in the rate of metal deposition increasing until a maximum deposition rate was obtained at a N,N-diethylglycine sodium salt concentration of 3.75 g/l. Further increases in the concentration of N,N-diethylglycine sodium salt resulted in a decrease in metal deposition rate.

Examination of experimental results indicates that solution temperature is the major factor in obtaining a fast rate of metal deposition. The rate of metal deposition increases on both Kovar and nickel base materials plated from either type of solution when the solution temperature is increased. Boiling of the solution should be avoided since this decreases the rate of metal deposition, possibly by partial decomposition of the organic constituents of the solution.

Finally, experimental evidence indicates that ultrasonic agitation of the solution decreases the rate of metal deposition. Mechanical agitation of the solution results in a slight increase in the rate of metal deposition as compared to an unagitated solution. Mechanical agitation is preferable to no agitation of the solution.

In summary, the operating conditions for the optimum rate of gold deposition from the electroless gold solution are:

Solution temperature: 190°-200°F
Agitation: mechanical, rapid
pH: 5.0-5.3

Concentration of N,N-diethylglycine sodium salt: 3.75 g/l for citric acid or tartaric acid types of solution, 11.25 g/l for citric acid type of solution

Mechanism

We believe that the N,N-diethylglycine sodium salt acts as the reducing agent in the electroless plating of gold from both the citric acid and tartaric acid solutions. The minimum or near minimum metal deposition rate for each solution as shown in Table VII and Fig. 4 occurs when there is no N,N-diethylglycine sodium salt in the electroless gold solution. Minimum deposition rates occurring at increased N,N-diethylglycine sodium salt concentration are explained by undesirable organic side reactions.

Experimental evidence indicates that the mechanism of electroless gold plating begins as an immersion gold deposit on the base material. Extrapolation of all curves of Immersion Time *vs.* Weight of Gold Deposited shown in Fig. 2 and 3 indicates the presence of a gold deposit at zero immersion time. The weight of the gold deposited at zero immersion time varies between 0.5 and 4.0 mg/in.^{2} of plating area. We believe that the gold deposit is immersion plated in the first few seconds that the base material is in solution. This initial gold deposit acts as a catalyst for the N,N-diethylglycine sodium salt. The N,N-diethylglycine sodium salt undergoes a reaction in which one of the products of the reaction acts as a reducing agent, supplying electrons to reduce the gold ions very similar to the Wolff (4) rearrangement. The Wolff rearrangement of a diazo ketone results in a product of a carboxylic acid or a derivative of such an acid. In this rearrangement a catalyst of silver or a silver ion results in an intermediate product of a ketene.

The chemical equation in Fig. 11 we believe expresses the reducing action which occurs with N,N-diethylglycine sodium salt.

Acknowledgment

The author acknowledges the assistance of Mr. D. S. Pokras for his development of analytical methods for these solutions as well as for many helpful suggestions. He also wishes to acknowledge the help of Mr. T. L. Sullens and Mrs. Nancy D. Allan in performing the experimental work and Mr. Heinz Heise for his assistance in the metallurgical phase of this project.

Manuscript received Feb. 17, 1961. This paper was prepared for delivery before the Houston Meeting, Oct. 9-13, 1960.

Any discussion of this paper will appear in a Discussion Section to be published in the June 1962 JOURNAL.

REFERENCES

1. R. O. Hull, *26th Annual Proc, Am. Electroplaters' Soc.*, 52 (1939).
2. "Kovar Alloy," p. 4, The Carborundum Co., Latrobe, Pa. (1958).
3. "Handbook of Chemistry and Physics," 40th ed., p. 1722, Chemical Rubber Publishing Co., Cleveland, Ohio (1958-1959).
4. G. W. Wheland, "Advanced Organic Chemistry," 2nd ed., p. 461, John Wiley & Sons, Inc., New York (1949).

Porosity Measurements on Gold Plated Copper

Martin S. Frant

Research Division, AMP Incorporated, Harrisburg, Pennsylvania

ABSTRACT

Using a chemical porosity test (in which the specimen is exposed to an ammonia-ammonium persulfate solution whch attacks copper but not gold, so that the amount of copper dissolved is a measure of the porosity of the coating), deposits from the conventional cyanide gold bath and 6 proprietary baths were compared for porosity. The relationship between porosity and thickness was found to be $P = at^{-n}$, where P is chemical porosity, a varies for each bath, t is gold thickness, and n generally varies between 1.3 and 2. A linear relationship, with a slope close to 1, was found for the variation of porosity with current density in 2 baths. The pattern of the other four does not show a systematic relationship.

Fundamentally, electroplate porosity can be defined either in terms of the relative amount of "empty" volume in the deposit, resulting in various impregnation tests (1), or in terms of the relative amount of exposed base area. The latter have resulted in electrographic (2) and other anodic tests (3), measurement of gas flow rates through stripped metal films (4), and sundry chemical exposure techniques. A literature search in 1947 (5) uncovered well over two hundred references. Of these however, most were concerned with counting individual pores, and only a few with quantitative measurements.

From a practical viewpoint, the role of the electrodeposit is usually to protect the underlying surface from environmental attack, and we have therefore chosen to define porosity according to the latter definition above, and to use a technique which measures porosity in terms of exposure of basis metal to environmental attack. This quantitative technique is based on a qualitative test first described in the literature in 1927 (6), in which a dilute ammonia-ammonium persulfate solution (which attacks copper but not tin) was used as a porosity test for the tin plated copper. Zürcher and Lüder (7) have since studied the test in consider-

able detail and have found that the amount of copper dissolved by the reagent was directly proportional to the exposed copper surface area and to contact time, strongly affected by agitation rate, not affected by ammonia concentration, but dependent on the concentration of persulfate.

The ammonia-ammonium persulfate test solution described herein cannot be used to measure the exposed copper area directly, because the limitation on the rate of attack is probably the transport of reagent into, and the transport of oxidation products out of the pores. This rate will fall off as the fourth power of the pore size (8) and is a theoretical limitation on the method as an absolute measurement. However, because any corrosion process would suffer the same limitation, this measure of "porosity" is felt to be a better indication of corrosion resistance than an absolute value for the total exposed area.

In the specific case of gold plating on copper, the variety of test techniques has led to conflicting results on the porosity of gold deposits reported for the same bath (9), and at a recent national meeting several speakers pointed to the lack of information on the relationship between porosity and thickness (10).

The purpose of this paper is to show a test procedure which measures the porosity of gold plated specimens, to compare the porosity of gold plating from different baths, to see what the relationships are between porosity and thickness, and then to show how the test procedure will measure the effect on porosity of changing one of the plating bath variables.

Experimental

Specimens were stamped from Electrolytic Tough Pitch grade copper and were 0.6 in. long with a tongue and barrel section (11), with a 0.18 in. hole in the tongue.

Samples were plated in a number of different commercially available baths. In each case cleaning was carried out by conventional procedures, generally by etching in a nitric-phosphoric acid solution (12). Each load consisted of 250 pieces, and the instructions were that each lot was to be plated in a small revolving barrel, the so-called "jeweler's" barrel. Wherever possible, the evaluation of plating baths was done on samples which had been plated by the bath manufacturer himself, presumably under optimum conditions. The platers were asked to prepare 10 lots, of which the first lot was to be 10 millionths of an inch and each succeeding lot was to be 10 millionths thicker, up to 100 millionths.

Plating thickness measurements were made by x-ray fluorescence measurements using the technique developed by Zimmerman (13); results were plotted on arithmetic normal probability paper (14). The porosity tests were run by placing ten specimens each in a 125-ml Erlenmeyer flask, and adding 25 ml concentrated ammonium hydroxide and 25 ml 1M ammonium persulfate from separate burets. The flasks were then placed on a low-speed reciprocating shaker and agitated for exactly 30 min. The shaker was adjusted so that the solution was rocked gently in order to minimize abrasion of the specimens. At the end of the 30-min period the solutions were decanted and stored in an ice-bath until analysis. The amount of copper in the solution was determined using a Beckman Model DU Spectrophotometer at 580 mμ (15), and the porosity is described as ppm of copper in the solution. Ten lots of ten each were run for each thickness, and the porosity values were plotted on probability paper. The order of running was randomized to avoid systematic variations. Thickness values and porosity values used in this report are the 50% intercepts. For normally distributed lots this value is both the median and the mean (16).

Results

Relationship between porosity and thickness.— Figure 1 shows the results of thickness determinations on samples prepared in a conventional hot cyanide bath (17). This bath, the oldest commercial gold plating bath, contains no alloying metals other than impurities. It can be seen that in general the slopes in Fig. 1 are quite gentle. This indicates that the bath has good throwing power. The lines are not evenly spaced, and there is some actual overlap of thicknesses. This suggests that the plater was not able to control accurately all of the variables in his plating bath.

Figure 2 shows the porosity *vs.* thickness results obtained on the samples plated in the conventional hot cyanide bath. From Fig. 2, the following conclusions can be made: (*A*) The data seem to fall essentially on a straight line when plotted on log-log paper. This means the results fit an equation of the type

$$P = \frac{a}{(\text{thickness})^n}$$

The value of n in this case is just under 2. (*B*) In this group, and in several others, when overlaps in thickness distributions occur, the corresponding porosity values are found to deviate from the best straight line. See, for example, the 35 millionths thick samples in Fig. 2.

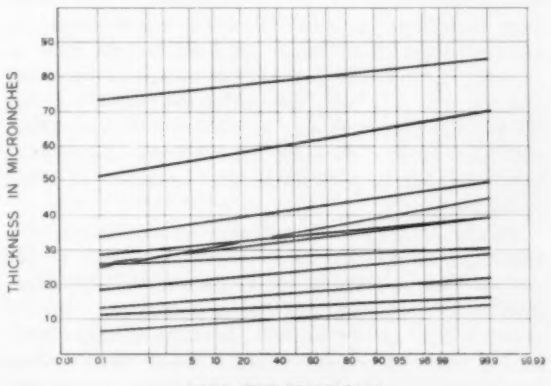

Fig. 1. Thickness distributions as measured by x-ray fluorescence; conventional hot cyanide gold plating bath; samples plated by bath manufacturer. Results are plotted on arithmetic normal probability paper.

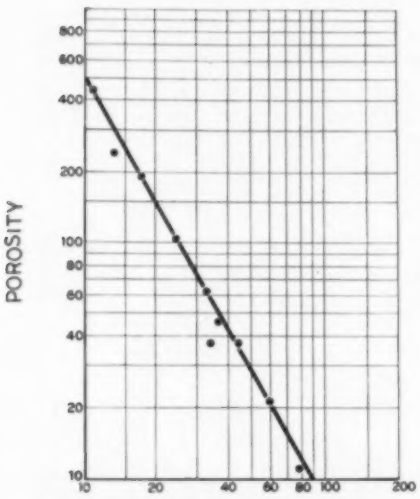

Fig. 2. Log-log plot of gold plate porosity vs. thickness for conventional hot cyanide gold plating bath, as prepared by bath supplier.

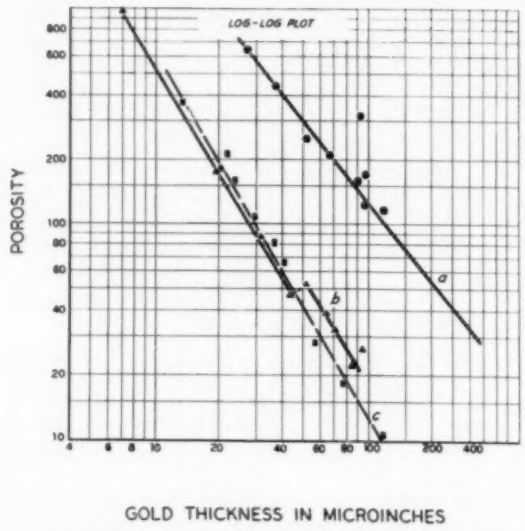

Fig. 3. Porosity vs. thickness results for commercial bath A (alkaline cyanide, with silver as a brightener): (a) plated at a commercial facility, location I; (b) plated in the laboratory, location II; (c) plated by bath manufacturer, location III.

The first commercial bath tried is labelled Bath A; it was prepared in a production facility. The bath was found to be an alkaline cyanide type containing 1% silver as a brightening agent. The slopes of the thickness distributions were quite gentle, indicating that this is a bath with good throwing power. For some unknown reason, one lot of specimens, the fifth thickest, was not distributed normally. The result of this can be seen in Fig. 3a which is a plot of the log porosity against the log of the average thickness. The one lot which was not normally distributed varies considerably from the porosity results obtained on the other eight lots. As in Fig. 2, the porosity becomes smaller with increasing thickness. For Fig. 3a n has a value of about 1.3. If this line is compared with Fig. 2 it will be seen that the conventional hot cyanide bath produced much less porous deposits than this particular bath, as operated at this particular location.

Samples were then prepared in the same type of commercial bath but in the laboratory. The thickness distributions were found to have somewhat steeper slopes than those obtained for the bath at location I, indicating that the chemical composition of the bath was not quite the same, or that the plating geometry was somewhat different. There was also more difference between the slopes from batch to batch, indicating the presence of some variation.

Figure 3b shows the porosity *vs.* thickness relationships found for this commercial bath at the second location. The slope is parallel to the slopes previously observed and has a numerical value of about 1.5. A rather unusual feature of these samples is that the porosity values appeared to fall on two parallel lines, indicating the presence of some uncontrolled variable in the plating.

The porosity values obtained in this commercial bath A at location II were considerably lower than those obtained in the same bath at location I, and indicate that the location of the bath may be a factor in the porosity value obtained. The term "location" includes bath composition, bath geometry, and all the other variables which change from one situation to another.

The manufacturer of the commercial bath was then asked to prepare samples under as closely identical conditions as possible to the previous runs at locations I and II. Figure 3c shows the porosity *vs.* thickness results. The two lines are virtually identical, although the samples prepared by the manufacturer show less variability.

Other commercial baths were then tried. The thickness distributions found from a mildly acid cyanide bath (containing a citrate buffer and having nickel as the alloying element) showed slopes which became steeper as the thickness increased. This is not unusual in barrelplating, although it was not as marked in the thickness results on bath A. Figure 4 shows the porosity *vs.* thickness results obtained from bath B. Here, too, a similar slope (somewhat less than two) was found, and the porosity values, in fact, are almost exactly the same as those found for commercial bath A.

The thickness distributions on another proprietary bath, bath C (a neutral cyanide gold bath containing silver as the alloying element, and organic brightening agents), were found to have quite gentle and uniformly spaced slopes, but all of the thicknesses were approximately twice that requested. These samples included some of the thickest gold samples run in this series. Apparently the manufacture had difficulty in predicting the thickness of his gold plate or else a miscalculation was made.

The porosity results from this neutral gold bath are shown in Fig. 4. A rather interesting result is observed. The points start out having a slope similar to that observed previously, but at thicknesses

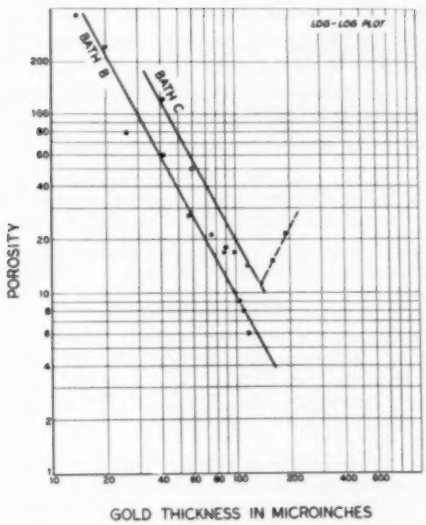

Fig. 4. Porosity vs. thickness results for two other cyanide-containing gold plating baths. Bath B had a citrate buffer and contained nickel as the brightener; Bath C contained silver and organic brightening agents.

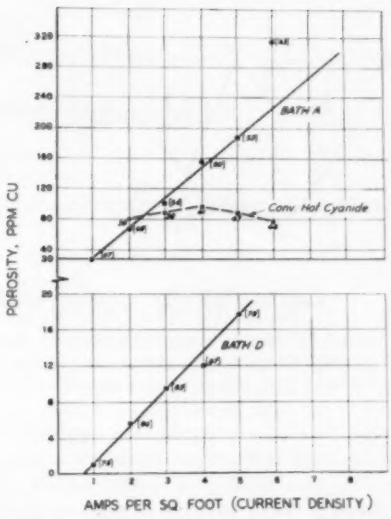

Fig. 6. Linear plot of porosity vs. current density for three gold plating baths. Numbers show the actual average thickness for each lot. Samples for all three were taken from lots prepared by the bath manufacturer.

greater than 150 millionths of an inch the porosity begins to increase again. It is not known whether this effect would hold for other baths, since these were the thickest samples under test. It is postulated that, due to stress or some similar factor, cracking and an increase in porosity occur as the thickness begins to build up.

In Fig. 5 are shown the porosity results from two acid gold baths having very low porosities. Bath D, which uses an ethylenediamine tetraacetic acid complex and contains small amounts of cobalt, has a low efficiency, and as a result it is somewhat difficult to control for accurate thicknesses. There were a number of overlaps in the thickness distributions, and some of these straddle the line in Fig. 5. Bath E is an acid citrate gold bath, containing nickel as a brightener, and trace amounts of cobalt (probably as an impurity).

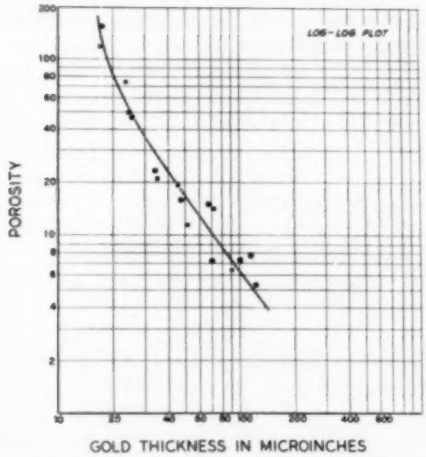

Fig. 5. Porosity vs. thickness results for two acid gold baths. Bath D, indicated by the closed circles, had an ethylenediamine tetraacetic acid gold complex, and contained cobalt. Bath E, indicated by the closed squares, was an acid citrate bath, and contained nickel and cobalt.

For both baths there was a considerable amount of scatter in the porosity values. Since the values were the lowest observed in the series, it is not known whether the variability is inherent, or whether the porosity is approaching the limits of detection with this technique.

Relationship between porosity and current density.—The results above indicated that there is not only the difference in porosity to be expected from different baths, but under some conditions large differences in porosity may be observed between the same gold plating bath in different locations. As part of an effort to determine some possible causes for this difference, the relationship between the porosity and current density has been studied.

Figure 6 shows the results obtained on 6 lots that were plated in the alkaline cyanide bath which has previously been designated by the letter A, to approximately the same thickness. It is, of course, difficult to obtain exactly duplicated thicknesses, even when the number of coulombs is held constant, because of variations in bath efficiency at different current densities. The actual thicknesses of each lot are shown on the graph. As can be seen, there is a direct linear relationship between porosity and current density. Above 5 amp/ft^2 the efficiency appears to fall off. For this bath, the faster one attempts to plate, the greater the porosity.

Figure 6 also shows the results of the same kind of test on one of the commercial baths which showed an inherently low porosity. Here too, the same linear relation holds, and here too, the faster the bath is operated the greater the porosity.

In addition, the porosity *vs.* current density relationship for a conventional hot cyanide bath is shown. Unlike the other two baths above, there is no direct linear relationship; instead the variation

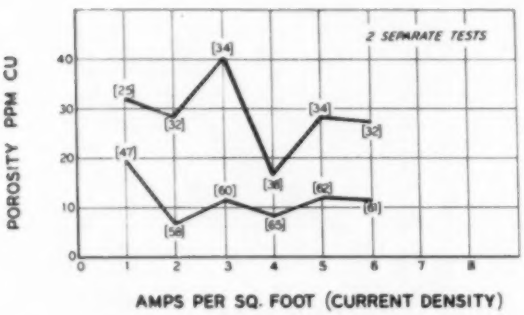

Fig. 7. Effect of current density on porosity. Commercial bath E as prepared by bath manufacturer in two separate lots. Bracketed numbers show the actual average thicknesses.

in porosity is not very great, but appears to reach a maximum and then taper off.

While the two acid gold baths which gave the lowest porosity seem to have a similar composition and porosity *vs.* thickness behavior, the effects of current density on porosity are quite different. Figure 7 shows the results obtained on the acid gold bath which had both cobalt and nickel. The first curve obtained was the upper one, with thicknesses averaging about 35 millionths of an inch. There seems to be no systematic relationship between the current density and the porosity. After these results were obtained, a request was made for a second set of samples at a different thickness. Approximately two months had elapsed. The results of the second set are shown in the lower line. The lines appear to follow the same trend, so that the effect is not due to accidental variations during plating. No theoretical explanation can be advanced at this time for the unusual shape of this porosity *vs.* current density curve.

Conclusions

In summary, there is a very definite relationship between the porosity and thickness of gold plate for most of the gold plating baths which have been examined. The relationship can be expressed by an equation of the form $P = at^{-n}$ where n generally varies between 1.3 and 2. The porosity measuring technique described also has been used to study the effect of current density, and it is found that for some baths there is a direct linear relationship, but that this is by no means true for all gold plating baths. Extension of the technique for the determination of the effect of other variables on gold-plate porosity should be straightforward.

Manuscript received Dec. 19, 1960; revised manuscript received April 7, 1961. This paper was prepared for delivery before the Houston Meeting, Oct. 9-13, 1960.

Any discussion of this paper will appear in a Discussion Section to be published in the June 1962 JOURNAL.

REFERENCES

1. H. Reichert, German Pat. 643,031, March 22, 1937; E. C. Rollason, *Metallurgia*, **16**, 125 (1937); V. Duffek, *Z. Metallkunde*, **30**, 265 (1938); T. DeForrest, *Trans. Am. Soc. Metals*, **31**, 739 (1943); R. W. Pilcher, Private communication quoted in Thon, *op. cit.*
2. H. R. Miller and E. B. Friedl, *Plating*, **47**, 520 (1960).
3. (*a*) M. Clarke and S. C. Britton, *Trans. Inst. Metal Fin.*, **36**, 58 (1958); (*b*) R. A. Ehrhardt, *Tech. Proc. A. E. S.*, **47**, 78 (1960).
4. N. Thon, *A. E. S. Research Rept. No.* **28**, pp. 24, A. E. S., Newark, N. J. (1954).
5. N. Thon, and E. T. Addison, Jr., *Monthly Review of the A. E. S.*, **34**, 445 (1947).
6. E. Schürmann and H. Blumenthal, *Elektrotechn. Zeit.*, **36**, 1925 (1927).
7. V. Zürcher and J. Lüder, *Bull. schweiz. elektrotezhn. Ver.*, **42**, 271 (1951).
8. This assumes a simple capillary-tube model for the pores, and the applicability of the Poiseuille-Hagan Law. Cf., G. W. Scott Blair, "A Survey of General and Applied Rheology," 2nd ed., pp. 135-41, Pitman and Sons, Ltd., London (1949).
9. Compare, for example, R. Seegmiller, *Tech. Proc. A. E. S.*, **47**, 74 (1960), with ref. 3b above.
10. Cf. discussion by N. Hall, R. Seegmiller, Q. Dietz, and others, *ibid.*, pp. 236-8.
11. For a drawing of the specimen, see M. S. Frant, *Plating*, **45**, 157 (1958).
12. S. Spring, "Metal Finishing Guidebook," 28th ed., p. 269, Metals and Plastics Publications, Westwood, N. J. (1960).
13. R. Zimmerman, *Iron Age*, **186**, 84 (1960).
14. D. Peckner, *Mat. in Design Eng.*, **52**, 138 (1960).
15. O. Milner, *Ind. and Eng. Chem., Anal. Ed.*, **18**, 94 (1946).
16. R. S. Burington and D. C. May, "Handbook of Probability and Statistics," pp. 83-4, Handbook Publishers, Inc., Sandusky, Ohio (1953).
17. A. Korbelak, "Gold Plating" in "Metal Finishing Guidebook," p. 332.

Influence of Thiourea on the Deposition Reactions of Iron and Nickel

Richard D. DeMars

Research Center, International Business Machines Corporation, Yorktown Heights, New York

ABSTRACT

The deposition reactions of iron and nickel were studied polarographically in solutions containing the metal ion and potassium chloride and the metal ion, potassium chloride, and thiourea. Analysis of the polarographic waves using Koutecky's method yielded values for the kinetic parameters, αn_a and $k^\circ_{f,h}$, for the reduction reactions. The effect of temperature and thiourea concentration on these parameters was studied. These results can lead to qualitative predictions about the composition of films plated from similar solutions. The value of such predictions for the case of the plating solutions studied is illustrated by a series of plated iron-nickel films.

The addition of thiourea to plating baths in order to alter the physical properties (i.e., brightness, strain, crystal size, etc.) of the plated films is a technique that is well established. Qualitative observations of the effect of thiourea on nickel deposition have been reported (1, 2). Tsu (3) has reported the extreme variations in magnetic properties and crystal parameters of plated iron-nickel films caused by the addition of thiourea to the plating solution.

In this work, quantitative results were obtained on the kinetic parameters for the reduction of iron and nickel from chloride base solutions. The effect of the addition of thiourea to these solutions on these kinetic parameters also was investigated. The results of such a study make it possible to speculate, at least qualitatively, on the composition behavior of alloys plated from similar solutions. It is not possible to make quantitative predictions on this behavior because of the extreme differences which exist between those experimental conditions utilized to obtain the kinetic data and those used to obtain the plated films. The speculations in this case have some chance for success because of the simplicity of the plating solution. The complexity of many plating solutions would prohibit any speculation about its deposition behavior even if the basic deposition reactions of the metal ions present were well known.

A series of iron-nickel films plated from solutions similar to those studied appears to substantiate the qualitative predictions made from knowledge of the basic reduction reactions of iron and nickel.

Theory

A variety of electrochemical techniques are available (4) which can be used to investigate the influence of thiourea on the deposition processes of nickel and iron. The polarographic method was used in this study because of its ease of application and rigorous theoretical basis (5-7).

Koutecky's (5) treatment for the interpretation of polarographic waves controlled by diffusion and reaction rate is very rigorous and will be used in this work. This treatment has been applied to a study of the iodate reduction by Delahay and Mattax (11). For totally irreversible waves, this method yields values of the ratio of the instantaneous currents i/i_d as a function of the parameter λ, where i is the current flowing at potential E, i_d is the current which would flow if the reaction were reversible, and

$$\lambda = k_{f,h}\, t_d^{1/3}/D_o^{1/3}$$

where $k_{f,h}$ is the heterogeneous rate constant, t_d is the drop time, and D_o is the diffusion coefficient.

A plot of i/i_d vs. λ along with a table of values used to construct the curve have been given by Delahay (8). From these data and the experimental polarogram it is possible to determine values of $k_{f,h}$ as a function of E for a given reduction process. If the kinetics of the electrode process is controlled by a single rate-determining step, the dependence of $k_{f,h}$ on E is given by

$$k_{f,h} = k^\circ_{f,h} \exp\left(-\alpha n_a E\mathbf{F}/RT\right) \qquad [4]$$

where $k^\circ_{f,h}$ is the value of $k_{f,h}$ at $E = 0$ (*vs.* Normal Hydrogen Electrode); α is the transfer coefficient, n_a is the number of electrons transferred in the rate-determining step, R is the gas constant, $\mathbf{F}$ is the faraday, and T is the absolute temperature. This relation indicates that a plot of log $k_{f,h}$ against E should give a straight line with a slope equal to $-\alpha n_a \mathbf{F}/RT$. The intercept of this line at $E = 0$ (*vs.* N.H.E.) gives the value of $k^\circ_{f,h}$.

Using the results and procedures outlined above it is possible to obtain values of αn_a and $k^\circ_{f,h}$ for an electrochemical reduction system. These quantities are the fundamental constants of an electrode process (9).

This method was used to obtain the fundamental constants for the nickel and iron reduction reactions studied in this work.

Experimental

Apparatus.—All polarograms were recorded on a Sargent Model XV recording polarograph which

was modified by taking the output current from the cell and feeding it directly into the amplifier of a Sargent Recorder (1.25 mv full scale, 1 sec response). This arrangement made it possible to record the maximum (instantaneous) currents during drop life required for a theoretical interpretation of the waves.

The cell, a conventional H-type, was regulated at the desired temperature for all work by means of a constant temperature water bath.

Potentials for the polarograms were measured with a Rubicon precision potentiometer.

The iron-nickel films were plated at a controlled cathode potential using a power supply similar to that reported by Greenough, *et al.* (10). The other plating parameters such as temperature, agitation, electrode spacing, etc., were controlled very carefully during film deposition. The substrates used for the plated films were glass made conducting with evaporated nickel and were similar to those described by Tsu (3).

Materials.—All chemicals were reagent grade and were used without further purification. Solutions were prepared with doubly distilled water. Linde high purity nitrogen was used without further purification to remove oxygen from the solutions.

Plating solution composition.—Bath 1. $FeCl_2 \cdot 4H_2O$, 300 g/l; $NiCl_2 \cdot 6H_2O$, 40 g/l; $CaCl_2$ 180 g/l.

Bath 2. $FeCl_2 \cdot 4H_2O$, 300 g/l; $NiCl_2 \cdot 6H_2O$, 40 g/l; $CaCl_2$, 180 g/l; $(NH_2)_2CS$, 0.2 g/l.

Bath 3. $FeCl_2 \cdot 4H_2O$, 300 g/l; $NiCl_2 \cdot 6H_2O$, 40 g/l; $CaCl_2$, 180 g/l; $(NH_2)_2CS$, 31 g/l.

All solutions were adjusted to a pH of 1.0 with HCl and maintained at 65° ± 1°C for all plating.

Results

Reduction of nickel and iron.—The kinetic parameters, an_a and $k^\circ_{f,h}$, for the reductions of nickel and iron were obtained in solutions containing only the metal ion and potassium chloride in one case and the metal ion, potassium chloride, and thiourea in the other case.[1]

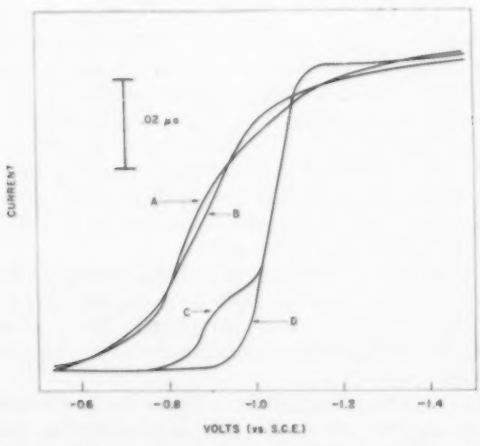

Fig. 1. Effect of thiourea on the polarographic reduction of nickel. A, 4.00 x 10^{-4}M $NiCl_2 \cdot 6H_2O$, 7.00 x 10^{-3}M thiourea; B, 4.00 x 10^{-4}M $NiCl_2 \cdot 6H_2O$, 4.00 x 10^{-3}M thiourea; C, 4.00 x 10^{-4}M $NiCl_2 \cdot 6H_2O$, 1.00 x 10^{-2}M thiourea; D, 4.00 x 10^{-4}M $NiCl_2 \cdot 6H_2O$. All solutions contained enough KCl to make the ionic strength 0.200.

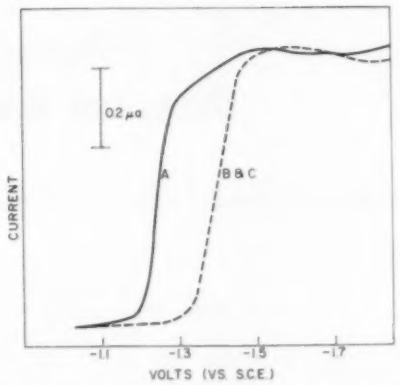

Fig. 2. Effect of thiourea on the polarographic reduction of iron. A, 4.00 x 10^{-4}M $FeCl_2 \cdot 4H_2O$, 4.00 x 10^{-3}M thiourea; B, 4.00 x 10^{-4}M $FeCl_2 \cdot 4H_2O$, 1.00 x 10^{-2}M thiourea; C, 4.00 x 10^{-4}M $FeCl_2 \cdot 4H_2O$. All solutions contained enough KCl to make the ionic strength 0.200.

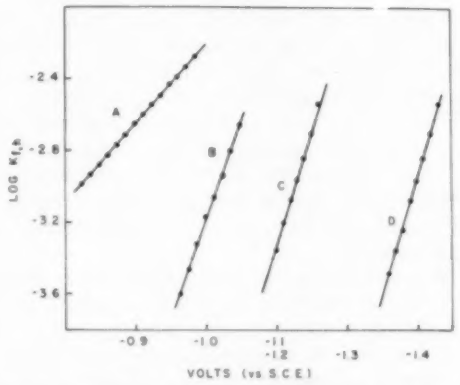

Fig. 3. Logarithm of the heterogeneous rate constant as a function of potential. A, 4.00 x 10^{-4}M $NiCl_2 \cdot 6H_2O$, 4.00 x 10^{-3}M thiourea; B, 4.00 x 10^{-4}M $NiCl_2 \cdot 6H_2O$; C, 4.00 x 10^{-4}M $FeCl_2 \cdot 4H_2O$, 4.00 x 10^{-3}M thiourea; D, 4.00 x 10^{-4}M $FeCl_2 \cdot 4H_2O$. All solutions contained enough KCl to make the ionic strength 0.200.

The reductions of nickel and iron from aqueous solution are well known to be irreversible. A number of criteria were applied to ensure that the reduction waves of the two metal ions in the presence of thiourea also were irreversible.

The current was found to be independent of the height of mercury, H, at the foot of the wave but proportional to $H^{1/2}$ in the diffusion current region. Plots of log $(i_d - i)/i$ *vs.* E were nonlinear. Furthermore, it was shown that $E_{1/2}$ depends on the drop time, t_d (12). The polarographic waves obtained for the reduction reactions in these solutions are illustrated in Fig. 1 and 2, where only the maximum currents during drop life are plotted against applied voltage. The analysis of these polarograms using Koutecky's (1) method leads to values of $k_{f,h}$ as a function of potential. Typical plots of log $k_{f,h}$ *vs.* potential are illustrated in Fig.

[1] Previous results on the nickel reduction in potassium chloride (11) and potassium nitrate (12) cannot be applied in this study because of the difference in solution parameters.

Table I. Values of kinetic parameters

Solution	αn_a	$k^\circ_{f,h}$
Ni, KCl	0.35	6.3×10^{-13}
Ni, KCl, thiourea 0.1M	0.16	3.2×10^{-12}
Ni, KCl, thiourea 0.2M	0.15	3.1×10^{-12}
Ni, KCl, thiourea 0.4M	0.16	3.0×10^{-12}
Ni, KCl, thiourea 0.7M	0.16	3.2×10^{-12}
Fe, KCl	0.36	2.5×10^{-22}
Fe, KCl, thiourea 0.1M	0.38	1.3×10^{-20}
Fe, KCl, thiourea 0.2M	0.37	1.2×10^{-20}
Fe, KCl, thiourea 0.4M	0.38	1.3×10^{-20}

Table II. Data for plated films

Bath[a]	Current density[b]	Voltage[c]	Fe/Ni + [d] Fe
1	26	−0.94	0.91
	41	−1.02	0.90
	75	−1.26	0.93
2	26	−0.86	0.43
	41	−0.96	0.60
	75	−1.26	0.81
3	26	−0.96	0.30
	41	−1.05	0.50

[a] Bath composition given in materials section.
[b] milliamperes 1 cm^2.
[c] Volts *vs.* S.C.E.
[d] Analyzed spectrophotometrically in the analytical service laboratory of the Magnetics Department.

3. The values of the kinetic parameters obtained for the reductions studied are given in Table I.

The temperature dependence of αn_a and $k^\circ_{f,h}$ was determined as a function of thiourea concentration. The behavior was uniform at all concentrations of thiourea investigated, and the abnormal dependence encountered by Delahay and Mattax (11) for the reduction of nickel in chloride was not encountered in the reduction of the nickel-thiourea complex.

In order to be sure that the results obtained were not influenced by the cation used, solutions containing sodium chloride and calcium chloride as the indifferent electrolyte were investigated. The data showed that the cation used did not alter the results.

The value of $m^{2/3}\,t^{1/6}$ at $E = -1.20$ v (*vs.* S.C.E.) was 2.12.

Plated iron-nickel films.—A series of films was plated as a function of various plating parameters. The data for the plated films are summarized in Table II.

Discussion

The data given in Table I show that the thiourea has a pronounced effect on the value of αn_a in the case of the nickel reduction. They also show that both reduction waves are shifted to more anodic potentials as a result of thiourea addition.

The alteration of the deposition reactions as a result of thiourea addition can occur for a number of reasons. The two most likely processes will be considered. The first process involves an interaction of the metal species with thiourea to form a complex which is reduced more easily than the metal species. Such an interaction might be expected to produce a change in the value of αn_a since it could cause a significant change in the rate-determining step.

The second process involves the adsorption of thiourea at the electrode-solution interface which leads to enhanced deposition of the metals species. In this process the thiourea is adsorbed on the electrode surface and acts as a bridge for electron transfer to the metal species. Such bridge mechanisms have been proposed for some oxidation-reduction reactions in solution (13). This type of reaction is quite likely, since thiourea is known to be adsorbed at mercury-electrolyte interfaces (2, 14). In such a reaction, the value of αn_a might or might not be altered depending on whether or not the energy barrier for the rate-determining step was altered.

The experimental evidence does not make it possible to state which of the many possible mechanisms is rate controlling in the reactions studied. The alteration of the deposition reaction in the case of nickel-thiourea reduction is probably caused by complex formation. The existence of such a complex has been advanced previously (2) and appears to be substantiated by the double wave obtained for the nickel reduction at low thiourea concentrations.

The values of αn_a obtained in this study indicate that the number of electrons involved in the rate-determining step for the reductions of both nickel and iron is one. The mechanism of reduction for these two ions therefore would be one in which the rate-determining step involves the addition of the first electron to the reducible species.

Using the data from the log $k_{f,h}$ *vs.* potential plots for the various solutions, it is possible to predict, at least qualitatively, the composition of films plated from similar solutions. Since the slopes of the plots for the reductions of iron and nickel in thiourea-free solutions are equal, the composition would be expected to be very insensitive to changes in applied voltage. That this is actually the case is illustrated by the data in Table II. The data on bath 1 show that the weight ratio of iron to nickel remains essentially constant at 0.90 over a given potential range.

The log plots for the reductions in solutions containing thiourea have slopes which are quite different from one another. In this case, the film composition would be expected to be very sensitive to changes in applied voltage. Also, the plots cross at a given point so that it should be possible to get films which are both iron rich and nickel rich by plating at the proper applied voltage. These trends are both substantiated by the data in Table II listed for bath 2.

The plots for solutions with high thiourea concentrations indicate that the trends noted at low concentrations should carry over to these solutions. The results for bath 3 are consistent with this prediction. The lower Fe/Ni ratios in these solutions are caused by a higher concentration of the more easily reduced nickel-thiourea complex which results in a higher nickel content in the plated film.

It is not possible to make quantitative calculations on film composition from a consideration of the polarographic rate constants because of the extreme differences in conditions utilized to obtain the data from the two systems. The study does illustrate, however, the value of using basic electrode reaction parameters to predict the reduction behavior of metal ions in plating solutions.

Conclusion

The effect of thiourea on the relative rates of a cathodic deposition of iron and nickel from mixed chloride solutions is paralleled by the effects of thiourea on the polarographic waves in separate solutions of the ferrous and nickelous chlorides. Quantitative evaluation of the polarographic waves yields values for the basic deposition reactions of iron and nickel in such solutions and makes it possible to speculate on the composition behavior of iron-nickel films plated from similar solutions. The speculations for the particular solutions studied appear to be substantiated by a series of plated iron-nickel films.

The application of similar techniques may be of extreme value in the future where prior knowledge of deposition behavior might make it possible to produce films with particularly desirable magnetic properties.

Acknowledgment

The author would like to acknowledge the assistance given by Dr. R. S. Smith, Dr. L. E. Godycki, Ignatius Tsu, and J. Charles Lloyd. The technical assistance of R. C. DiBenedetto is also gratefully acknowledged.

Manuscript received Jan. 6, 1961; revision received, April 13, 1961. This paper was prepared for delivery before the Houston Meeting, Oct. 9-13, 1960.

Any discussion of this paper will appear in a Discussion Section to be published in the June 1962 JOURNAL.

REFERENCES

1. See for example, L. I. Antropov and S. Ya. Popov, *J. Appl. Chem. U.S.S.R.*, **27**, 191 (1954).
2. J. S. Sallo and R. D. Fisher, *This Journal*, **107**, 277 (1960).
3. I. Tsu, *Plating*, **47**, 632 (1960).
4. These techniques have been reviewed by P. Delahay, "New Instrumental Methods in Electrochemistry," Interscience Publishers, Inc., New York (1955).
5. J. Koutecky, *Chem. Listy.*, **47**, 323 (1953); also *Collection Czechoslov, Chem. Communs.*, **18**, 597 (1953).
6. P. Delahay, *J. Am. Chem. Soc.*, **73**, 4944 (1951); also P. Delahay and J. E. Strassner, *ibid.*, **75**, 1430 (1953).
7. M. G. Evans and N. S. Hush, *J. Chem. Phys.*, **49**, C159 (1952).
8. P. Delahay, "New Instrumental Methods in Electrochemistry," pp. 77-79, Interscience Publishers, Inc., New York (1955).
9. S. Glasstone, K. Laidler, and H. Eyring, "Theory of Rate Processes," pp. 575-587, McGraw-Hill Book Co., New York (1941).
10. M. L. Greenough, W. E. Williams, Jr., and J. K. Taylor, *Rev. Sci. Ins.*, **22**, 484 (1951).
11. P. Delahay and C. C. Mattax, *J. Am. Chem. Soc.*, **76**, 5314 (1954).
12. P. Kivalo, K. L. Oldham, and H. A. Laitinen, *ibid.*, **75**, 4148 (1953).
13. See for example H. Taube, *ibid.*, **77**, 4481 (1955).
14. F. W. Shapink, M. Oudeman, K. W. Leu, and J. N. Helle, *Trans. Faraday Soc.*, **56**, 415 (1960).

Some Factors Affecting the Surface Chromium Content of Electrochemically Treated Tin Plate

P. R. Carter

Applied Research Laboratory, United States Steel Corporation, Monroeville, Pennsylvania

ABSTRACT

The effect of variations in treating conditions on the surface chromium content of cathodic-dichromate treated tin plate was studied. Bench-scale and pilot-line studies and a mill trial showed that increasing the coulomb level of the cathodic-dichromate treatment resulted in an increase in the level of chromium compounds (hereafter referred to as chromium level or content) in the treatment film; however, at a constant coulomb level, decreased chromium contents were obtained with increasing cathodic current density. Increased chromium levels were obtained from either high-temperature or low-pH solutions. Also, it appears that treatment films having higher chromium contents usually exhibit superior resistance to oxide film growth. Analysis of the data shows that only 10% of the theoretical amount of chromium(III) is deposited during treating, the rest of the electricity presumably being dissipated in the evolution of hydrogen. A mechanism for the formation of the treatment film is suggested that appears to be consistent with the observed facts.

Many passivating treatments for tin-plate surfaces have been suggested over the years to inhibit the oxidation of tin. Thick tin-oxide films formed during warehouse storage, in addition to being aesthetically objectionable, can cause difficulties in lacquering, lithographing, and soldering.

In a recent paper, Neish and Donelson (1) discussed the development of the cathodic-dichromate treatment, which is now being used on much of the electrolytic tin plate produced in the United States and throughout the world. They also reviewed previous and contemporary research in this

area. Although differences in the effectiveness of various treatments have been apparent, attempts to associate these differences with structural differences in the treatment film by using electron-diffraction techniques have been unsuccessful (1, 2).

Accordingly, a comprehensive study of the effect of variations in treating conditions on the surface chromium content of cathodic-dichromate treated tin plate was undertaken. This paper comprises the results of this study and the interpretation of the data to yield a mechanism for treatment-film formation.

Materials and Experimental Work

The program consisted of the following three experiments: (*a*) pilot-line trial, (*b*) bench-scale experiments, and (*c*) commercial trial. In all experiments, unless otherwise specified, the treating conditions consisted of making the tin plate the cathode in a sodium dichromate electrolyte (20-30 g/l) maintained at 46°-52°C and treating with 32.3 millicoulombs/cm² of electricity. In the pilot-line trial cathodically-anodically treated lots were produced in the same manner as noted above with an added anodic treatment consisting of 2.7 millicoulombs/cm². Mild steel anodes slightly wider than the panel or strip were used in all experiments.

Table I-A. Pilot-line trial

Lot No.	Order of production	Cathodic treating current, millicoulombs/cm²	Current density, ma/cm²	Treatment polarity*
1	1	10.8	5.4	C
2	2	10.8	5.4	CA
3	3	21.5	10.8	C
4	7	21.5	10.8	CA
5	8	32.3	16.2	C
6	9	32.3	16.2	CA
7	10	43.1	21.5	C
8	11	43.1	21.5	CA
9	15	53.8	26.9	C
10	16	53.8	26.9	CA
11	17	64.6	32.3	C
12	4	64.6	32.3	CA
13	5	75.4	37.7	C
14	6	75.4	37.7	CA
15	12	43.1	10.8	C
16	13	43.1	37.7	C
17	14	43.1	37.7	CA

* Anodic treatment = 2.7 millicoulombs/cm².

Table I-B. Pilot-line trial

Lot No.	Surface chromium, μg/cm² of surface	Process enamel adhesion performance (Scotch-tape adherence)*	Reducible oxide,** millicoulombs/cm²
1	0.43	0.2	3.10
2	0.45	2.4	0.93
3	0.59	0.7	1.69
4	0.53	1.2	0.68
5	0.57	0.3	1.30
6	0.71	1.4	0.70
7	0.70	0.2	1.44
8	0.69	3.0	0.78
9	0.89	0.7	1.63
10	1.02	3.6	0.78
11	0.80	0.3	1.57
12	1.06	3.1	0.74
13	1.13	0.4	1.74
14	1.01	3.9	0.84
15	0.79	0.5	0.99
16	0.55	0.1	2.45
17	0.53	0.4	0.99

* 0 = perfect, 10 = very poor.
** After 12 weeks storage.

Table II. Bench-scale experiments

Lot No.	Cathodic treating current, millicoulombs/cm²	Current density, ma/cm²	Surface chromium, μg/cm² of surface	Reducible oxide,* millicoulombs/cm²
1	26.9	26.9	0.73	1.83
2	53.8	26.9	1.01	1.70
3	80.8	26.9	1.12	1.36
4	107.7	26.9	1.57	0.71
5A	32.3	21.5	0.75	2.26
5B	32.3	21.5	0.78	1.95
6	53.8	26.9	0.97	1.98
7	53.8	53.8	0.78	1.95
8	53.8	80.8	0.58	3.13
9	32.3	32.3	0.73	2.76
10	43.1	43.1	0.75	2.54
11	64.6	64.6	0.67	2.71
12A	32.3	21.5	0.73	2.31
12B	32.3	21.5	0.73	2.76
13A	32.3	16.2	0.75	2.53
13B	32.3	16.2	0.73	1.86
14	64.6	32.3	0.84	2.32
15	43.1	21.5	0.97	2.02
16	3.2	32.3	0.34	3.69
17	6.5	64.6	0.34	4.00

* After 4 weeks storage.

The lots produced in the pilot-line trial are identified in Table I-A. These lots were tin-coated at a line speed of 46 m/min and were electrostatically oiled. An electrode 152.5 cm long was used for the cathodic portion of the treatment for all lots with the exception of lot No. 15, for which two 152.5-cm electrodes were used, and lots No. 16 and 17, for which a single 86.3-cm electrode was used. Lot No. 15 was treated in both the down pass and in the up pass; all other lots were cathodically treated in the down pass only.

The lots produced in the bench-scale experiments, identified in Table II, consisted of 10.2- by 15.2-cm panels of nonchemically treated tin plate, which were cathodically treated in a beaker following a cathodic cleaning (2-5 amp for 30 sec) in a 0.25% sodium carbonate solution.

The lots produced in this mill trial are identified in Table III. These lots were tin-coated at a line speed of 259 m/min and were electrostatically oiled with cottonseed oil. The variations in current density at a given coulomb level (total current constant) were obtained by varying the number of passes used; each pass was 152.5 cm long. A 2-tank system was used with a down pass and an up pass in each tank. If the down pass and the up pass in the first tank are called pass 1 and pass 2, respectively, and pass 3 and pass 4 are similarly defined as the down pass and the up pass in the second tank, then a one-pass treatment was obtained by using pass 3 only, a two-pass treatment

Table III. Mill trial

Lot No.	Order of production	Cathodic treating current, millicoulombs/cm²	Average current density, ma/cm²	No. passes	Current amperes, Generator No. 1	Current amperes, Generator No. 2	Surface chromium, μg/cm² of surface	Reducible oxide,* millicoulombs/cm²
1	3	13.0	9.3	4	490	490	0.48	2.54
2	9	13.0	18.4	2	980	—	0.55	1.91
3	15	12.6	35.8	1	—	950	0.39	2.99
4	13	19.5	18.4	3	975	490	0.48	2.14
5	10	19.4	27.5	2	1460	—	0.60	1.29
6	17	19.4	55.0	1	—	1460	0.58	2.42
7	2	23.9	16.9	4	900	900	0.67	1.30
8	6	26.0	36.7	2	1950	—	0.59	0.84
9	16	26.0	73.4	1	—	1950	0.64	2.23
10	5	38.5	27.3	4	1450	1440	0.73	1.10
11	14	39.1	37.0	3	1980	960	0.70	1.30
12	7	39.0	55.2	2	2930	—	0.67	0.82
13	4	51.9	36.7	4	1950	1950	0.82	1.01
14	11	49.9	70.6	2	3750	—	0.71	1.05
15	1	58.6	41.5	4	2200	2200	0.79	0.93
16	12	58.6	55.4	3	2950	1460	0.74	1.70
17	8	49.9	70.6	2	3750	—	0.71	0.84

* After 12 weeks storage.

with passes 1 and 2, a three-pass treatment with passes 1, 2, and 3, and a four-pass treatment with all four passes.

Tests used.—The treated tin plate was tested for the concentration of chromium in the surface film, hereafter referred to as surface chromium [a modification of Hill's method (3) was used], process enamel adhesion performance,[1] and resistance to oxide film growth (humid-storage pack test at 37.8°C and 85% relative humidity). A coulometric method (4) was used to measure the amount of oxide on tin plate by electrolytic reduction in 0.0017M hydrobromic acid at a constant current density of 51.2 μa/cm².

Results and Discussion

Pilot-line trial.—The test results, given in Table I-B, show that the cathodic treatment at the lowest coulomb level (lot 1, 10.8 millicoulombs/cm²) gave poor resistance to oxide film growth in humid storage.

The chromium content of lots 1 through 14 is plotted *vs.* millicoulombs/cm² in Fig. 1, where it is apparent that there is a linear increase of chromium level with increasing coulomb level. A surprising fact is that at any given level of cathodic treatment the surface-chromium level of cathodically-anodically treated plate is the same as that of plate given only the cathodic treatment. This point is discussed in more detail later. Although increasing the cathodic treating current for cathodically treated plate from 10.8 to 21.5 millicoulombs/cm² greatly improved the resistance to oxide film growth, further increases in the coulomb level with its associated increase in surface chromium did not improve the resistance to oxide film growth of the plate; however, it should be noted that the general resistance to oxide growth was very good even at relatively low surface-chromium levels. In addition, the cathodic-anodic treatment, as anticipated, was observed to provide resistance to oxide film growth superior to that obtained with the cathodic treatment.

A plot, Fig. 2, of process enamel adhesion performance *vs.* millicoulombs/cm² indicates that the process enamel adhesion performance of the cathodically-anodically treated plate is affected adversely by increasing the coulomb level. It may be that a similar relationship would have been ob-

[1] This test provides a measure of the relative adhesion of a lacquer to a tin plate surface after the lacquered surface has been exposed to food processing conditions.

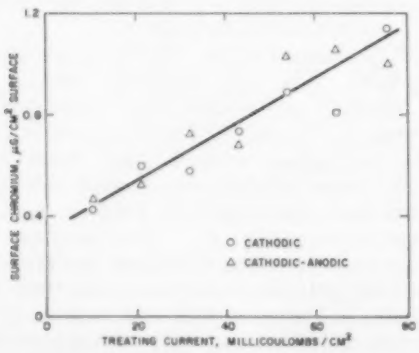

Fig. 1. Effect of cathodic current density on chromium content of tin-plate treatment films (pilot-line lots).

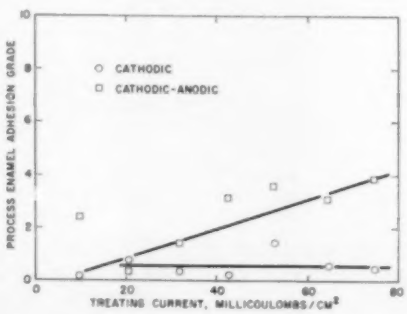

Fig. 2. Effect of cathodic current density on process enamel adhesion performance of electrochemically treated tin plate (pilot-line lots).

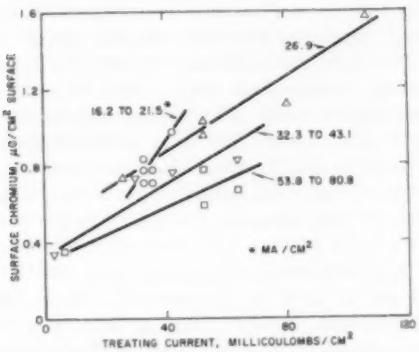

Fig. 3. Effect of cathodic coulombs at constant current density on the chromium content of tin-plate treatment films (bench-scale lots).

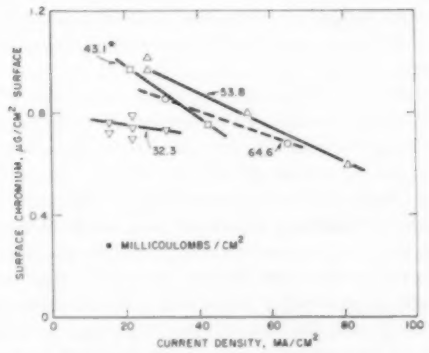

Fig. 4. Effect of cathodic current density at constant coulombs on the chromium content of tin-plate treatment films (bench-scale lots).

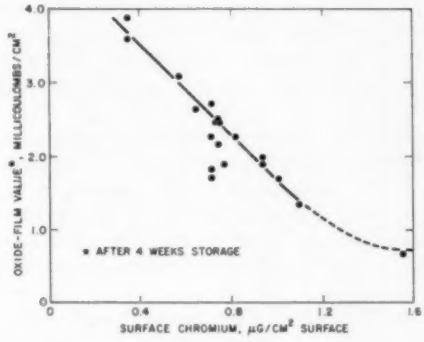

Fig. 5. Effect of surface chromium on reducible oxide (bench-scale lots).

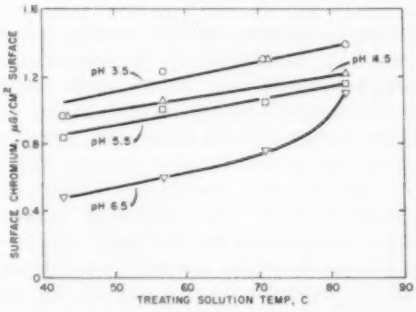

Fig. 6. Surface chromium as a function of treating solution pH and temperature.

served with the cathodically treated plate if the over-all process enamel adhesion performance of the cathodically treated plate had been poorer.

Inasmuch as a constant line speed and the same anode were used in the production of lots 1 through 14, no distinction can be made between the independent effect of current density and millicoulombs/cm². (In other words, current density and millicoulombs/cm² were linearly related.) However, lots 15, 7, and 16 were all produced at 43.1 millicoulombs/cm² with respective current densities of 10.8, 21.5, and 37.7 ma/cm². The corresponding surface-chromium levels were observed to decrease from 0.79 to 0.70 to 0.55 μg Cr/cm² of surface with accompanying reducible oxide values after storage of 0.99, 1.44, and 2.45 millicoulombs/cm². Thus, it appears that, at a constant coulomb level, increasing the current density results in decreased surface-chromium levels and decreased resistance to oxide film growth.

Bench-scale experiments.—To distinguish more explicitly between the aforementioned effects of current density and coulomb level, the lots listed in Table II were prepared. The chromium content of the surface film is plotted as a function of cathodic coulomb level (at constant current density) in Fig. 3 and as a function of cathodic current density (at constant millicoulombs/cm²) in Fig. 4. Although there is scatter in the data and some of the lines are determined by only two points, it is apparent that the increase in surface chromium is dependent on the number of millicoulombs/cm² used and that at a constant coulomb level increasing the current density decreases the chromium level. Thus, the effect of coulomb level and current density on surface chromium is consistent with that noted above for the pilot-line results. There is a suggestion, Fig. 4, that at 32.3 millicoulombs/cm² increasing the current density in a low current density range (16.2 to 32.3 ma/cm²) has little effect on the surface-chromium level.

A plot of the reducible oxide *vs.* the surface-chromium level for these lots, Fig. 5, reveals that a good relationship exists between these two variables, increasing surface chromium providing increasingly superior resistance to oxide-film growth.

The results of an investigation of the effect of treating-solution temperature and pH (NaOH was used to adjust the pH) are plotted in Fig. 6. In the ranges studied the surface chromium increases with decreasing pH and increasing temperature. The effect of extremely long treating times was studied at two pH levels, 4.3 and 10.8, Fig. 7, to determine whether the relationship shown in Fig. 1 is true for very large cathodic treating currents. The data in Fig. 7 show that in this extremely large range of cathodic treating current (0.1-10,000 sec, 32.3 ma/cm²), the relationship is no longer a linear one as suggested in Fig. 1 and 3. The surface-chromium levels for films produced in the acid-treating solution follow a square-root-of-time dependence, whereas the surface-chromium levels obtained for

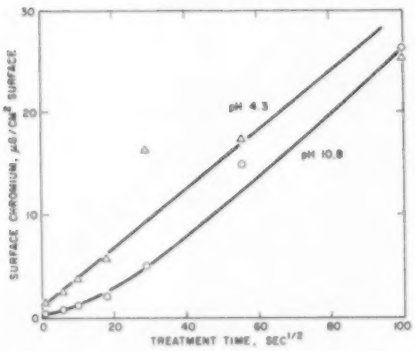

Fig. 7. Surface chromium as a function of cathodic treatment time and pH.

films produced in the alkaline treating solution do not appear to have a simple functional time dependence throughout the entire range studied. In agreement with the data presented in Fig. 6, more chromium is deposited at equivalent treating currents from the acid solution. The convergence of the two curves at long times might have been anticipated; however, the prediction would have been for a leveling off of the "acid" curve caused by the increase in pH at the cathode. Although the two treating solutions had equal Cr(VI) concentrations, the sodium ion concentration and the conductivities of the two solutions were different. Therefore, no attempt will be made to interpret these data further. One additional point of interest is that electron diffraction studies of the treatment showed that the film produced in the acid bath was amorphous, whereas a definite pattern was obtained for the "alkaline" film. The pattern did not correspond to any known oxide of Fe, Sn, or Cr.

Commercial trial.—Results of the evaluation of the commercially prepared lots, Table III, generally confirm the observations made in the pilot-line trials and bench-scale experiments. The highest surface-chromium values obtained in this trial (0.79 and 0.82 μg Cr/cm^2 of surface) are appreciably lower than the maximum values obtained on the pilot line and in the bench-scale experiments ($>$ 1.10 μg Cr/cm^2 of surface). This difference was probably caused by the relatively high current densities used at the mill at comparable coulomb levels. Another point to be noted is that the effect of current density (at constant coulomb level) was obtained only at the higher coulomb levels; the relation between chromium content and current density at coulomb levels below 39 millicoulombs/cm^2 appears to be random.

In this connection it should be emphasized that different current densities were obtained by using different chemical treatment steps. For example, the highest current density was obtained by passing the strip through the solution in the first tank with the current turned off and then treating the strip in the down pass only of the second tank, whereas the lowest current density was obtained by having the current on in all four passes. The latter treatment did not have the nonelectrochemical dips before and after the chemical treatment. It is not suggested that any specific effects can be attributed to these differences; however, it is important to realize that the current density effects are confounded with unavoidable treatment variations. In this connection it is interesting to note that lots 3, 6, and 9, which had the poorest resistance to oxide film growth in their respective treating-current groups (although the chromium level was not always the lowest), were the only single-pass lots produced in this trial. On the other hand, lots 2, 5, 8, 12, 14, and 17, which had the best resistance to oxide film growth in their respective groups (lots 13 and 14 had equivalent resistance to oxide film growth), were all prepared with two electrochemical passes in the first tank followed by a chemical dip in the second tank.

Lacquer evaluation showed that process enamel adhesion, spray, and drop-wetting test performances were uniformly good over the entire range of test variables.

Processing differences in trials.—The results obtained from the three experiments are generally in agreement. For example, higher chromium contents were associated with increasing coulomb levels. However, a more detailed analysis of the data reveals certain discrepancies, such as the relatively poor resistance to oxide film growth for the bench-scale samples compared with that of the commercial and the pilot-line lots at comparable surface-chromium levels. In this regard it should be noted that the tin-plate samples were processed differently in the three trials. One difference was that in the bench-scale experiments the current was not applied to the panel until it was completely immersed in the electrolyte; this procedure was necessary to avoid the application of extremely high current density to the bottom of the panel as it entered the electrolyte. It is true that three of the commercial lots (lots 3, 6, and 9) were also immersed in the electrolyte prior to electrochemical treating and exhibited relatively poor resistance to oxide film growth. Another difference was that, with the exception of these three lots, which were treated in one pass only, all commercial lots were given chemical treatments in two, three, or four equal doses that were divided by short intervals of time in which practically no current flowed. The last and perhaps most important difference was the fact that the material used in the bench-scale experiments was cathodically cleaned prior to chemical treatment to reduce the oxide on the plate. However, whether it had been cleaned or not, the plate used in these trials would be different from that used in the pilot-line and commercial trials; uncleaned plate would have a heavier oxide than the pilot-line or commercial material. No further reference will be made to these differences other than to state that their effects are indeterminate at the present time.

Mechanism of Treatment-Film Formation

If the theoretical amount of Cr (III) deposited from the Cr (VI) electrolyte when 32.3 millicou-

lombs of electricity per cm^2 are passed through the solution is calculated (by Faraday's law), a value of 5.8 μg Cr/cm^2 of surface is obtained. This is approximately 10 times more Cr than is actually observed. A similar calculation shows that 3.1 millicoulombs of electricity per cm^2 of surface are needed to reduce the oxide on the plate after melting and quenching. These calculations are quite straightforward and do not require the adoption of any specific mechanism.

Any mechanism must explain the following facts: (*A*) ten times more coulombs than are necessary to reduce the existing oxide are passed through the solution; (*B*) cathodically cleaned samples having much lower initial oxides prior to electrochemical treatment had Cr contents at least as high as the commercial and pilot-line samples under comparable treating conditions; (*C*) the chromium content of the surface film is proportional to the number of coulombs used.

A tentative mechanism that appears to explain some of the facts is suggested as follows: The existing oxide is cathodically reduced, very likely by reaction with hydrogen atoms, and the freshly reduced tin then reacts instantaneously with the dichromate during the early part of the electrochemical treatment (while the current is still on) to form mixed Sn and Cr oxides, with the Cr in the trivalent state and the Sn probably present mainly in the tetravalent state. The Cr content of the film is then built up with increasing coulombs by simply adding Cr (III) to the existing lattice composed of the mixed Sn and Cr oxides. Upon removal of the panel from the treating solution, a thin film of hexavalent chromium is chemisorbed on the surface of the treatment film to form a mixed Cr oxide, such as $Cr_2O_3 \cdot CrO_3$; oxides having ratios other than 1:1 and having various waters of hydration are also possible. Many mixed Cr oxides of the above form and of lower valence and hydration states exist (5, 6).

Although the suggested mechanism is highly speculative, it does seem to explain many of the observed facts.

1. The increasing Cr content of the treatment film with increasing coulombs is due to an increasing deposition of Cr (III).

2. The cathodic-anodic treatment film has the same Cr content as the cathodic film having the same level of cathodic treatment because the anodic current is used to oxidize some of the Cr (III) in the existing film to form additional mixed Cr oxides.

3. The relatively thick layer of mixed oxides on the cathodic-anodic treatment film affords relatively better resistance to oxide film growth to the tin plate and at the same time makes this treatment somewhat more sensitive to certain critical lacquers.

4. At constant cathodic coulombs, the decreasing Cr content of the film with increasing current densities is explained by concentration polarization with respect to Cr (VI). If it is assumed that the reduction of Cr (VI) takes place by reaction with hydrogen atoms, then the hydrogen atoms can be removed by

$$H + H \rightarrow H_2 \qquad [1]$$

or

$$H + Cr\ (VI) \rightarrow Cr\ (\text{lower valence state}) + H^+ \qquad [2]$$

Under all conditions reaction [1] is dominant because, as previously noted, only 10% of the current is used to reduce Cr (VI), with the other 90% presumably used in evolving hydrogen. At high current densities reaction [2] becomes relatively less important and hence less Cr (III) is deposited. This explanation is consistent with the fact that the relation between current density and Cr was not apparent with the commercial lots until the high coulomb, high current density lots were produced.

The observed temperature effect, Fig. 6, is in accordance with the above observations.

The mechanism offered above is consistent with the existing experimental data and offers an explanation for previously unexplained, isolated phenomena. This mechanism can be used as a working hypothesis in planning experiments to test the validity of implications drawn from it.

Manuscript received Dec. 15, 1960; revised manuscript received April 28, 1961. This paper was prepared for delivery before the Houston Meeting, Oct. 9-13, 1960.

Any discussion of this paper will appear in a Discussion Section to be published in the June 1962 JOURNAL.

REFERENCES

1. R. A. Neish and J. G. Donelson, *Food Technol.*, **14**, 37 (1960).
2. S. C. Britton and K. Bright, *Metallurgia*, **56**, 163 (1957).
3. U. T. Hill, "Determination of Chromate Residue on Tin Plate and Chromium in Steel," paper given at the Pittsburgh Conference on Analytical Chemistry and Applied Spectroscopy, 1953. Unpublished.
4. R. P. Frankenthal, T. J. Butler, and R. T. Davis, Jr., *Anal. Chem.*, **30**, 441 (1958).
5. M. J. Udy, Chromium, Vol. I, Chemistry of Chromium and Its Compounds, pp. 113-130, Reinhold Publishing Corp., New York (1956).
6. R. S. Schwartz, I. Fankuchen, and R. Ward, *J. Am. Chem. Soc.*, **74**, 1676 (1952).

Crystal Growth and Structural Study of the Barium-Titanium-Phosphate Phosphor

D. E. Harrison and G. Shirane

Research Laboratories, Westinghouse Electric Corporation, Pittsburgh, Pennsylvania

ABSTRACT

Examination of single crystals and powder samples of the compound $2BaO:TiO_2:P_2O_5$ revealed a reversible crystallographic inversion at 1040° ± 5°C. Both modifications have monoclinic symmetry. The high-temperature form can be quenched and at room temperature the lattice constants are $a_o = 16.578Å$, $b_o = 5.437Å$, $c_o = 4.756Å$, and $\beta = 94°0'$. The low-temperature phase can be indexed with very similar "basic" lattice constants, and yet, for corresponding reflections the x-ray line intensities are quite different from those of the high-temperature form. However, doubling of the a_o and c_o parameters is required to account for weak extra spots which appear in single crystal photographs of the low-temperature phase. Powder patterns of both phases have been indexed to 40° 2θ. Crystals grown from the melt were always twinned with two types of twinning being distinguished. In one case the b-c plane and in the other case the a-b plane is the twin or composition plane. Fluorescent emission spectra of the phases are identical in shape, and they are characterized by a double peak. The spectrum of the high-temperature form lies about 0.02 ev toward longer wavelengths than does the low-temperature form.

In a previous paper Harrison (1) reported on the phase relations in the system $BaO-TiO_2-P_2O_5$. The compound $2BaO:TiO_2:P_2O_5$ was isolated and shown to be responsible for the luminescence which was first reported by Henderson and Ranby (2).

The results of an x-ray study on single crystals of $2BaO:TiO_2:P_2O_5$ (2:1:1) and fluorescent emission curves of 2:1:1 are presented in the present paper.

Experimental Procedure

Single crystals of 2:1:1 were grown from the melt by either of two methods. In the first method, compositions near the 2:1:1 ratio were supercooled about 10°C and nucleated by seeding with crystal fragments of 2:1:1 (mp 1197° ± 3°C). Upon re-heating the solidified mass, single crystals were freed from one another by melting of the eutectic material at grain boundaries. Crystals were removed from the melt by adhesion to a cold probe which was hoisted from the bath and allowed to cool. Compositions near the 2:1:1 ratio on the join $2BaO:P_2O_5$-$2BaO:TiO_2:P_2O_5$ yielded clear, transparent crystals which could be cleaved readily to a tabular form. The largest crystals recovered were 4 mm on an edge and approximately 0.5 mm thick. There was complete agreement between x-ray powder patterns obtained from ground-up single crystals and powder prepared by solid-state calcination of stoichiometric 2:1:1.

The second method of growing single crystals simply involved fusion of stoichiometric 2:1:1 composition followed by slow cooling in a furnace. Single crystals prepared in this manner were only fractions of millimeters in dimension, but satisfactory for x-ray study.

Differential thermal analysis (DTA) data were obtained with automatically recording apparatus similar to that described by Gruver (3).

The immersion technique was used to determine refractive indices of crystals. Indices were measured to an accuracy of ± 0.001.

Fluorescent emission spectra were obtained with a Beckman spectrometer using a 2537Å light source. Individual readings were made at 100Å intervals except when the values changed abruptly, in which case readings were made at 50Å intervals.

Results and Discussion

Single crystal studies have revealed two polymorphs of $2BaO:TiO_2:P_2O_5$. Both phases are monoclinic. A very small reversible thermal effect was observed by DTA at 1040° ± 5°C. X-ray examination of samples prepared by firing at temperatures near 1040°C established that a crystallographic phase change does occur in the vicinity of this temperature. The high-temperature phase can be quenched, and it inverts rapidly to the low-temperature form when reheated to 1000°C.

Twinning habits.—Six crystals were examined; three each of a high-temperature phase designated α and of a low-temperature phase designated β. Weissenberg pictures revealed two twin habits which are pictured in Fig. 1. Type (100) twin, Fig. 1(a), has the b-c plane as the twin or composition plane. Type (001) twin, Fig. 1(b), has the a-b plane as the twin or composition plane.

The two types of twinning can be distinguished optically by a characteristic laminar structure on the type (001) twin. However, extinction banding sim-

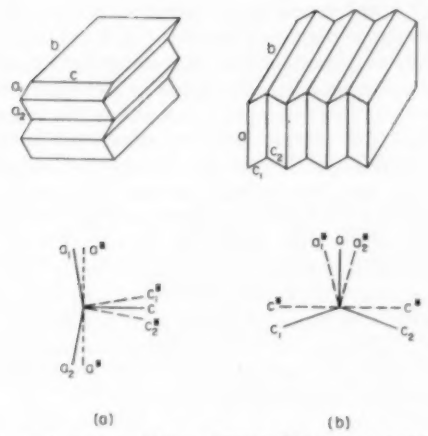

(a) (b)

Fig. 1. Twinning habits of $2BaO:TiO_2:P_2O_5$. (a) (100) type twin with b-c plane as twin or composition plane; (b) (001) type twin with a-b plane as twin or composition plane. a* and c* denote the reciprocal lattice.

ilar to that found in the mineral orthoclase was not observed.

All of the x-ray pictures of both the α and β phases showed almost identical intensities for corresponding reflections of two twin components. This implies that the twin lamellae have about the same volume and are quite small. A rough estimate of the maximum twin component thickness can be made from the linear x-ray absorption coefficient, which is 860 cm^{-1} for CuKα, and the relative intensities of x-ray spots. Calculations indicate a maximum lamella thickness of about 0.5 μ. However, the actual thickness may be much smaller than this value.

The first method described for crystal growth always gave type (100) twins whereas the second method yielded a mixture of the two twin types. Both α and β phases exhibited either type of twinning.

Refractive index.—Microscopic examination revealed no differences between the α and β forms. Since the crystallographic "b" axis is the fast ray direction, the b direction corresponds to optic n_α of the biaxial indicatrix, i.e., $n_\alpha < n_\beta < n_\gamma$. The index n_α equals 1.671 ± 0.001 for both the α and β forms. Neither interference figures nor untwinned crystals were found. Consequently, measurement of n_β and n_γ was not possible.

Lattice parameters and space groups.—Twin components can be separated unambiguously on the Weissenberg pictures. Examination of the (hkO), (Okl), (hOl) and a few higher layer photographs established the following results for the two forms of 2:1:1.

The high-temperature form, α, has the parameters $a_o = 16.66$, $b_o = 5.45$, $c_o = 4.77$ and $\beta = 94°0'$, and an extinction rule of $h + k + 1 = 2n$.[1] Assuming two molecules per unit cell, the theoretical x-ray density is 4.05 g/cc. The measured density was 3.97 g/cc. Lattice parameters which best fit the powder data are listed in Table I. X-ray powder data are indexed up to 40° 2θ (CuKα) and are tabulated in Table II.

[1] According to the convention of the International Tables, it is necessary to take a new a_o axis as follows: $\vec{a}' = \vec{a}_o + \vec{c}_o$. The extinction rule now becomes $h + k = 2n$ for (hkl), and the space group is either C_{2h}^3(C2/m), C_2^3(C2), or C_s^3(Cm).

Table I. Lattice parameters of α- and β-$2BaO:TiO_2:P_2O_5$

α-$2BaO:TiO_2:P_2O_5$	β-$2BaO:TiO_2:P_2O_5$
$a_o = 16.578$Å	$a' = 16.591 \times 2$Å
$b_o = 5.437$Å	$b' = 5.435$Å
$c_o = 4.756$Å	$c' = 4.758 \times 2$Å
$\beta = 94°0'$	$\beta = 94°0'$

Table II. Indexed powder patterns of α- and β-$2BaO:TiO_2:P_2O_5$

	α-$2BaO:TiO_2:P_2O_5$				β-$2BaO:TiO_2:P_2O_5$		
hkl	d_{calc}	d_{meas}	I/I_o meas	hkl	d_{calc}	d_{meas}	I/I_o meas
200	8.310	8.300	19	200	8.316	8.307	14
110	5.167	—	—	110	5.166	—	—
10$\bar{1}$	4.671	4.667	4	10$\bar{1}$	4.672	4.686	14
101	4.501	4.503	6	101	4.502	4.514	15
400	4.155	4.158	54	400	4.158	4.158	30
310	3.881	3.883	43	310	3.881	3.882	75
30$\bar{1}$	3.746	3.751	4	30$\bar{1}$	3.747	3.748	8
011	3.585	3.590	25	011	3.585	3.587	100
301	3.496	3.497	4	301	3.497	3.490	7
21$\bar{1}$	3.231	3.231	9	21$\bar{1}$	3.233	3.231	24
211	3.356	3.354	9	211	3.357	3.357	22
510	2.836	2.833	13	510	2.837	2.829	24
50$\bar{1}$	2.821	—	—	50$\bar{1}$	2.823	—	—
41$\bar{1}$	2.788	2.794	12	41$\bar{1}$	2.789	2.794	32
600	2.770	2.771	100	600	2.772	2.778	51
020	2.718	2.718	13	020	2.718	2.718	39
411	2.647	2.646	12	411	2.647	2.647	32
501	2.642	—	—	501	2.643	—	—
220	2.584	—	—	220	2.584	—	—
002	2.384	2.384	7	002	2.385	2.385	32
12$\bar{1}$	2.350	2.349	4	12$\bar{1}$	2.349	2.349	8
20$\bar{2}$	2.335	2.335	4	20$\bar{2}$	2.336	2.339	10
121	2.327	2.328	6	121	2.327	2.329	14
420	2.275	2.277	7	420	2.275	2.274	14
202	2.251	—	—	202	2.251	—	—
61$\bar{1}$	2.250	2.251	9	61$\bar{1}$	2.251	2.249	14

The principle reflections of the low-temperature form can be indexed with nearly the same lattice constants that fit the high-temperature phase.

In addition to the spots which can be indexed on the "basic" unit cell, there are weak extra spots which can be indexed by doubling the a_o and c_o spacings, i.e., $a' = 2a_o$, $b' = b_o$, and $c' = 2c_o$. The extinction rules which apply are as follows: (khl), $h + l = 2n$; (hOl), $h = 2n$, $l = 2n$; and, (OkO), $k = 2n$.[2] Lattice constants are listed in Table I and x-ray powder data indexed to 40°2θ (CuKα) are tabulated in Table II.

X-ray line intensities of the dimorphs.—The small thermal effect and the similarity in lattice constants suggests that the low-temperature form is derived by an ionic displacement of the high-temperature phase. However, it is unusual to have such a dramatic change in line intensity, see Table II. Since barium ions have a very high scattering factor, small displacements may be sufficient to produce such an effect. The weak additional spots are probably a result of shifts in the positions of the lighter ions.

Hoffman (4) speculated that the change in line intensity is the result of preferred orientation due to crystal growth at temperatures greater than about

[2] Again using the convention of the International Tables and taking a new a_o axis, the space group is C_{2h}^5(P^{21}/c).

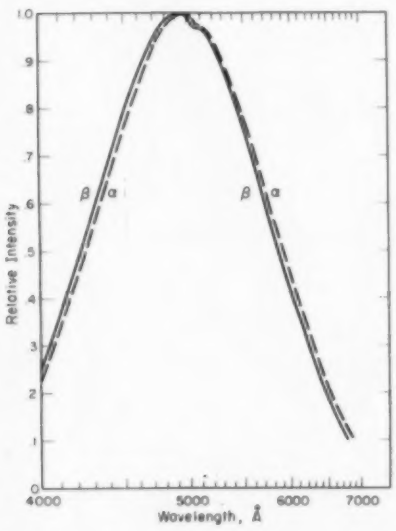

Fig. 2. Fluorescent emission curves of α- and β-2BaO:TiO_2:-P_2O_5 (2537Å excitation): curve (β) β-2BaO:TiO_2:P_2O_5; curve (α) α-2BaO:TiO_2:P_2O_5.

1090°C. However, it has been demonstrated that the change is due entirely to a crystallographic phase change and not to preferred orientation even after prolonged sintering at 1150°C.

Fluorescent emission.—Fluorescent emission curves (2537Å excitation) of α- and β-2:1:1 are shown in Fig. 2. They were obtained from powder samples which were prepared by solid-state calcination. The shape of both curves is the same with the α-2:1:1 emission curve displaced from the β-2:1:1 curve by about 0.02 ev toward longer wavelength. The curves shown have been normalized, but in fact the relative intensities of the two phases are about the same. In particular, the double peak is preserved in both curves. This suggests that the fluorescent center or centers are the same in both phases. The small shift in spectral position presumably caused by minor perturbation of the light center is consistent with the minor crystallographic differences between the two modifications. Visual examination of the two twin types with a microscope using uv illumination revealed no apparent differences in fluorescence. Thus, the type of twinning appears to have no significant influence on the fluorescence process.

Acknowledgment

The authors thank E. C. Subbarao for obtaining the D.T.A. data and N. T. Melamed for determining fluorescent emission spectra and for their stimulating discussions

Manuscript received March 3, 1961. This paper was prepared for delivery before the Indianapolis Meeting, April 30-May 3, 1961.

Any discussion of this paper will appear in a Discussion Section to be published in the June 1962 JOURNAL.

REFERENCES

1. D. E. Harrison, *This Journal*, **107**, 217 (1960).
2. S. T. Henderson and P. W. Ranby, *ibid.*, **98**, 479 (1951).
3. R. M. Gruver, *J. Am. Ceram. Soc.*, **31**, 323 (1948).
4. M. V. Hoffman, *This Journal*, **107**, 1024 (1960).

Photoetching and Plating of Gallium Arsenide

R. W. Haisty

Texas Instruments Incorporated, Dallas, Texas

ABSTRACT

The effects of light in the gold chemiplating and the etching of gallium arsenide have been investigated by partially illuminating samples submerged in various solutions. The plating occurs at the nonilluminated and etching at the illuminated region on n-type material, whereas the reverse is true for p-type. Etching can be accomplished in very dilute electrolytes, such as 0.1M KCl, by the action of light. A qualitative explanation for the experimental results is given, based on the photoeffects made possible by the bending of the energy bands in the space charge region of the semiconductor when it is placed in electrolytes.

In attempting to delineate n-n$^+$ junctions in a gallium arsenide bar by a gold chemiplating technique similar to that described by Silverman and Benn (1) for silicon, it was found that, when the face was illuminated, the gold tended to plate only on the sides and bottom of the bar. To ascertain that the gold plates preferentially on the dark region, a 1-mm diameter light spot was projected onto a small, lapped bar of n-type GaAs (n_e = 1.3×10^{17} cm^{-3}) submerged in the gold plating solution, using the set-up pictured in Fig. 1. The plating solution used was that given by Pudvin

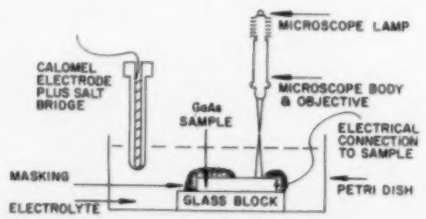

Fig. 1. Set-up for projecting a small light spot on samples submerged in etching or plating solution. Provisions are also made for measuring the potential of the sample against a calomel electrode.

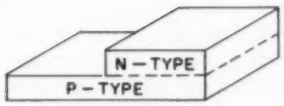

Fig. 2. Arrangement of junction for studying preferential gold plating with various conditions of illumination.

and McNamara (2), consisting of 10 g of potassium gold cyanide and 200 g of potassium hydroxide per liter of solution. The gold plated rapidly everywhere except under the lighted spot.

The experiment was repeated using p-type GaAs ($n_h = 2.1 \times 10^{16}$ cm^{-3}). A lapped or sandblasted bar would not plate at all, even after several hours; however, on an etched surface a thin gold plate appeared on the lighted spot almost immediately, but, of course, plating action stopped as soon as the plate was thick enough to block the light from the GaAs surface. The recombination velocity is possibly so high on the abraded surfaces that the excess electrons generated by the light are not available to the solution for reducing the gold.

To further clarify the delineation of junctions in GaAs by gold chemiplating, a sample with a junction was arranged as shown in Fig. 2, so that the light spot could be projected onto either the n- or p-type region with the entire sample submerged in the plating solution. It was found that either type plated in the same way in the p-n bar as it did separately. The platings obtained with the various combinations of illumination and surface treatment are summarized in Table I.

Photoetching

In the plating experiments it was found that n-type GaAs under the light spot was etched appreciably. This was investigated further by attempting to etch in several electrolytes with the light spot. Etching of n-type material at the lighted spot proceeded at about the same rate in 0.1 and 1.0M KCl, KNO_3, NH_4Cl, or 1.0*N* HCl or KOH. It was considerably faster in the alkaline gold cyanide solution. In potassium acetate the lighted spot was covered by a brown film and no etching occurred. This was the expected result because, as will be explained later, the other solutions are either sufficiently strong acids or bases to keep the oxidation products in solution or, in the case of the salts, the solution becomes acidic in the anode region as the electrochemical etching process proceeds. This acidic region does not form in potassium acetate solution, so the GaAs is protected by the oxide film which soon covers the lighted region.

When p-type GaAs in dilute KCl solution was illuminated with the light spot, the GaAs was oxidized at the dark region. A wafer left in the solution overnight turned dark blue everywhere except at the light spot. Electron diffraction showed β-Ga_2O_3 on the blue surface. A piece of the same p-type crystal left in the solution in the dark for the same length of time showed no visible evidence of oxidation.

This result is consistent with the gold plating results, where the gold plated at the lighted spot, showing that it is more cathodic than the dark area in p-type material. In the plating experiments it was necessary to have an etched surface before the reaction would go, whereas the oxidation in KCl solution was done on a lapped surface. This suggests that the driving potential is less in the plating solution than in the KCl solution. The open-circuit photovoltages measured in the plating solution and

Table I. Plating obtained with various combinations of illumination and surface treatment

Sample	Lighting	Results
n-type, lapped or sandblasted	Dark	No plate
	1 mm diam. spot	Heavy plate everywhere except lighted spot
	Entire top surface	Heavy plate on side, none on top surface
n-type, etched	Dark	No plate
	1 mm diam. spot	Plate everywhere except lighted spot, but nonadherent
	Entire top surface	Heavy plate on sides, nonadherent
p-type, lapped or sandblasted	Dark	No plate
	1 mm diam. spot	No plate
	Top surface	No plate
p-type, etched	Dark	No plate
	1 mm diam. spot	Thin plate on lighted surface
	Top surface	Thin plate on lighted surface
p-n junction, sandblasted	Dark	No plate
	Light spot on p-type	No plate
	Light spot on n-type	Entire n-type plated except 1 mm diam. illuminated spot
	Top surface, both p & n, lighted	Plate on n-type edges only
p-n junction, etched	Dark	Same as sandblasted
	Light spot on p-type	Thin plate under light spot only
	Light spot on n-type	Same as sandblasted
	Top surface, both p & n, lighted	Same as sandblasted

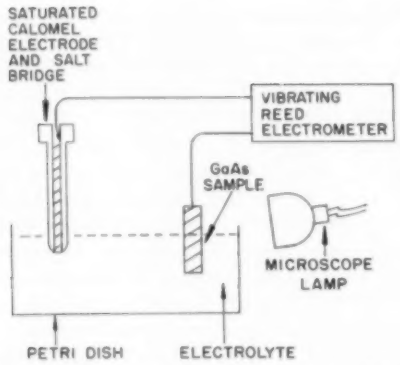

Fig. 3. Arrangement for measuring photovoltages

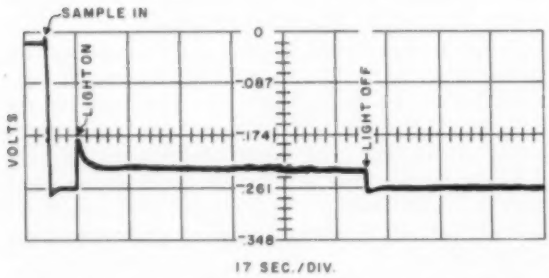

Fig. 4. Copy of oscilloscope trace showing drift in photovoltage of p-type GaAs in 1.0M KCl. Input impedance of amplifier was 10^9 ohms.

KCl solution also indicate that this is so; however, the results are not conclusive because of both long and short time drifting in the potentials of p-type GaAs in these solutions. The photovoltages of both types in these solutions, and also in 1*N* KOH and HCl, were measured against a saturated calomel electrode with a Carey Vibrating Reed Electrometer, using the experimental set-up shown in Fig. 3. The results are given in Table II. The voltages of the other combinations, except for n-type in HCl, were quite steady and reproducible. The waveform of the photovoltage of p-type GaAs in KCl solution showing the short-time changes is shown in Figure 4. It is not yet clear to what extent the fast and slow changes we observed here can be interpreted as the instantaneous and slow photoeffects which have been described by Dewald (3). The rate of the slow drift was affected considerably by stirring, for example, but it could not be eliminated completely.

Discussion

The etching process in germanium and silicon has been pictured by Turner (6) as being electrochemical in nature, with local cell currents flowing between anode and cathode sites on the semiconductor surface, and the material going into solution at the anode sites. The etchant must contain both an oxidizing agent and an agent to dissolve the oxidation products so that fresh semiconductor surface is continuously presented to the etchant at the anode sites. Since it does not seem immediately obvious that these criteria are met in the photoetching of GaAs in 0.1M KCl, this system will be discussed, and the principles outlined to explain this etching in terms of Turner's electrochemical model will be applied to the other etchants and to the plating experiments.

As shown by both Gerischer and Beck (5) and Dewald (3), when a semiconductor electrode is placed in an oxidizing electrolyte, one expects electrons to be transferred from the valence band of the semiconductor to the solution, which amounts to hole injection into the semiconductor. With n-type GaAs in an oxidizing solution, the bands will be bent up in the space charge region and the solution will see p-type material. This is the situation illustrated in Fig. 5 (a). If the semiconductor in contact with the solution is now illuminated, the electron-hole pairs produced tend to separate in the electrostatic field, holes going to the p-side and electrons to the n-side. Under open-circuit conditions and if there were no diffusion of carriers due to thermal agitation, the situation approaches that illustrated in Fig. 5 (b) and a relatively large photovoltage can be measured. In practice there is some current flow, and the intermediate case pictured in Fig. 5 (c) exists. As Dewald (3) and Gerischer (4) have shown, one expects a large photovoltage when the bands are bent up in n-type material and a small photoeffect in p-type material. The reverse is true with the bands bent down.

If only a portion of the n-type GaAs in contact with the solution is illuminated, it becomes more anodic than the dark portion and local cell currents will flow, via the solution, between the illuminated and dark portions. To confirm the electrochemical nature of this process, and trace the circuit involved, the following experiment was done: an n-type sample of GaAs with an insulated lead attached was carefully masked with shellac except for a small area on one face which could be flooded with uniform illumination. Any local cell action due to the photovoltage was thus prevented since no nonilluminated portion of the sample made electrical contact with the solution. The sample, masked in this way, was first submerged in KCl solution and illuminated overnight without the insulated lead making contact to the solution. A

Table II. Open-circuit photovoltages of GaAs in various solutions

Potentials measured against a saturated calomel electrode. The sign of the emf is the sign acquired by the GaAs.

	Gold plating solution		1*N* KOH		1M KCl		1*N* HCl	
	Dark	Light	Dark	Light	Dark	Light	Dark	Light
p-type	−0.57	−0.55 to −0.60 (drifting)	−0.72	−0.73	−0.24	−0.16 (drifting)	+0.015	+0.100
n-type	−0.72	−1.15	−0.72	−1.20	−0.24	−0.56	+0.005	−0.35 (drifting)

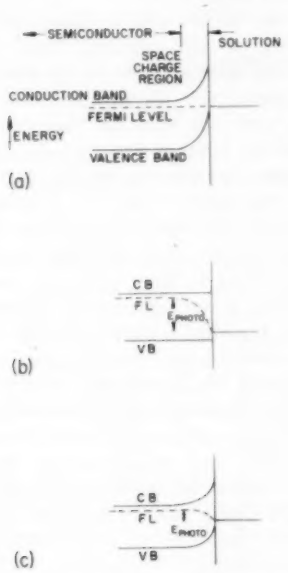

Fig. 5. Energy level diagram for n-type semiconductor in oxidizing solution: (a) Semiconductor not illuminated; (b) Semiconductor strongly illuminated, no current flow; (c) Semiconductor strongly illuminated, actual case where there is some current flow.

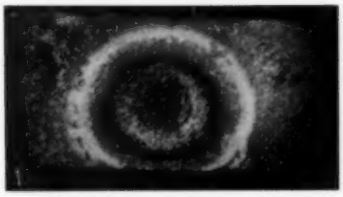

Fig. 6. Gallium arsenide (n-type) photoetched at a small light spot in KCl solution for 17 hr, showing ring formation. Magnification 20X before reduction for publication.

microscopic examination afterwards showed no evidence of etching or oxidation. When the experiment was repeated either with the insulated lead connected to a platinum wire dipping into the solution or with the masking removed from a small area of the nonilluminated region of the sample, the GaAs was etched at the lighted spot and the oxide powder collected on the shellac around it. Evidently, then, the etching is due to electrochemical action in which the illuminated region becomes positive with respect to the rest of the sample and oxidation occurs there if, and only if, the circuit is completed by allowing the more negative, or nonilluminated, part to make electrical contact with the solution.

In his work on the photovoltaic effect in binary compounds, Williams (7) reported that there was no evidence of extensive chemical reaction of n-type GaAs illuminated in 0.1M KCl even after prolonged current flow. It may be that the entire sample in contact with the solution was strongly illuminated and the oxidation products diffused completely away from it, fell to the bottom of the container, and so were not detected (in his experiment, the electrical contact between the negative side of the GaAs and solution would have been provided by the calomel electrode). Also, in our experiment the etching rate was probably much faster. The nonmasked area was about 4 x 10^{-2} cm^2 and the light intensity was adjusted to give a current of 20 μa. This current density of 5 x 10^{-4} amp/cm^2 is several times greater than indicated by William's data for his experiment.

All of the experiments reported here were done in air, so the oxidizing agent was probably oxygen. The KCl supplies ions for charge transfer in the solution. As the oxidation proceeds, OH^- ions are consumed, and the solution becomes acidic in the anode region. This was actually observed by adding a few drops of BDH Universal Indicator to the solution. The entire solution was pale yellow at first (pH = 6), and after about an hour the region around the lighted spot turned pink (pH < 4). If a little hydrogen peroxide is added to speed up the oxidation, the lighted region turns pink very rapidly. The oxidation products stay in solution in this region and precipitate when they diffuse out of it. If the solution is not disturbed, this action can cause the formation of rings on the surface around the lighted spot. Figure 6 shows this effect on a GaAs bar which was photo-etched in 0.1M KCl for 17 hr.

The center, spongy appearing area where etching occurred is about 1/3 the diameter of the light spot. It is surrounded by a narrow gray ring which looks like the normal sandblasted surface. The next ring outward has a shiny silver appearance, and its outer edge coincides with the edge of the light spot. The next ring is gold-colored and shades into a dark blue ring, both looking like typical thin oxide films. The blue ring is not evident on the photograph as it is covered by the white powder which began to precipitate just past its inner edge and continued outward.

In fairly concentrated HCl or KOH the oxidation products are soluble and the ring formation was not observed. When potassium acetate solution is used, the region around the anode does not become sufficiently acidic to dissolve the oxides, and the reaction proceeds only until the lighted spot is covered by an oxide film.

The etching proceeds much faster in the alkaline gold cyanide solution, probably because the $Au(CN)_2^-$ provides an easily reduced species for the cathode reaction (6). It was also found that triangular etch pits were formed on the A side (gallium side) of a (111) oriented slice in the region between the deeply etched lighted spot and the start of the gold plate; this region was illuminated faintly by scattered light. Figure 7 shows the triangular etch pits formed on the A side. The very dark region is the edge of the hole where gross material removal occurred. The etch pits are large near the hole and decrease in size rapidly going out from it, presumably as the light intensity falls off. No etch pits were found on the B side; the bottom of the hole was covered with hillocks. Richards and Crocker (8) found that acidic oxidizing etches attack the B face more rapidly than the A face, and that etch pits are normally formed

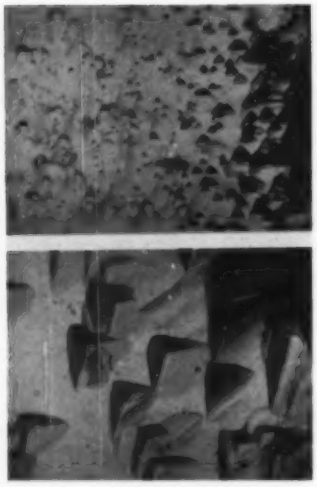

Fig. 7. Etch pits formed near the lighted spot on n-type GaAs in alkaline gold cyanide plating solution. The A face of a (111) oriented slice is shown. Regular shaped pits were not found on the B face. (a) (top) Magnification 125X before reduction for publication. (b) bottom) Magnification 500X before reduction for publication.

only on the A face. They added Ag ions to slow down the rate of attack and were thus able to produce etch pits on the B face. In our photoetching, the B face does not seem to etch faster than the A face, but so far, it has not been possible to produce etch pits on the B face. This suggests that perhaps something more than the rate is involved in getting pits on the B face.

Conclusions

The effects of light in the chemigold plating and etching of GaAs have been investigated and the open-circuit photovoltages measured for both n- and p-type in various electrolytes. The photovoltages measured were consistent with the theories of Gerischer and Beck (5) and Dewald (3), i.e., n-type material in oxidizing solution had a large photovoltage and p-type essentially none. The explanation proposed for the fact that n-type material submerged in the plating solution is etched at an illuminated spot while the gold plates at the dark region, pictures an electrochemical process being driven by the photovoltaic cell produced by the bending of the energy bands in the space charge region of the GaAs in an electrolyte. In the above example, the illuminated part of the GaAs in contact with the solution becomes positive with respect to the rest of the sample, as holes from electron-hole pairs produced by the light tend to diffuse to the p-region at the semiconductor-solution interface and electrons diffuse to the n-type bulk of the sample. The diffusion length for excess carriers in GaAs is very short, so just outside the lighted region a net current of electrons will flow from the n-type bulk back into the p-type surface layer. The surface will thus be less positive in the nonilluminated area, and the conditions for local cell corrosion currents exist. If the entire surface in contact with the solution is illuminated uniformly, the local cell action cannot occur, and no etching is observed unless an electrical connection is made between the GaAs sample and the solution so that electrons can leave the n-type GaAs bulk and return to the solution.

Acknowledgments

The author wishes to thank R. E. Johnson and C. G. Peattie for very helpful discussions and suggestions; G. R. Cronin and E. W. Mehal for supplying the gallium arsenide; and D. P. Miller for the electron diffraction work.

Manuscript received Feb. 27, 1961.

Any discussion of this paper will appear in a Discussion Section to be published in the June 1962 JOURNAL.

REFERENCES

1. S. J. Silverman and D. R. Benn, *This Journal*, **105**, 170 (1958).
2. J. F. Pudvin and J. E. McNamara, Semiconductor Symposium, Electrochemical Society, Pittsburgh, October 1955.
3. J. F. Dewald, in "The Surface Chemistry of Metals and Semiconductors," H. C. Gatos, Editor, p. 205, John Wiley & Sons, Inc., New York (1960).
4. H. Gerischer, *ibid.*, p. 177.
5. F. Beck and H. Gerischer, *Z. Elektrochem.*, **63**, 943 (1959).
6. D. R. Turner, *This Journal*, **107**, 810 (1960).
7. R. Williams, *J. Chem. Phys.*, **32**, 1505 (1960).
8. J. L. Richards and A. J. Crocker, *J. Appl. Phys.*, **31**, 611 (1960).

Boron Diffusion in Silicon

E. L. Williams[1]

Semiconductor Division, Sylvania Electric Products Incorporated, Northlake, Illinois

ABSTRACT

The diffusion of boron in silicon has been investigated by a p-n junction method over the temperature range of 1050°-1350°C and in silicon material where the n-type impurity density varied over a range 2 x 10^{15} to 8 x 10^{19} at./cm^3. The diffusion coefficient was found to decrease gradually as the purity of the n-type silicon increased. For silicon on the order of 0.1 ohm-cm resistivity $D = 16 \exp(-85 \pm 5 \text{ kcal}/RT)$ cm^2 sec^{-1}. The effect on the diffusion coefficient of both the bulk impurity density and the boron density in the surface region is discussed.

Kurtz and Yee (1) recently reported on their investigation of boron diffusion in silicon over the temperature range of 1050°-1350°C. They reported lower diffusivities and a slightly lower activation energy than that reported by Fuller and Ditzenberger (2), who had measured the diffusion of boron in silicon over the temperature range of 950°-1275°C. The experimental conditions of both investigations were nearly the same except that the surface concentration of boron in Kurtz and Yee's work was reported to be 10^{17}-10^{18} at./cm^3 in comparison to Fuller and Ditzenberger, who reported 10^{21}-10^{22} at./cm^3. Kurtz and Yee attributed the variation of diffusivity of the two investigations to this difference in the surface concentration based on a field-aided diffusion theory. According to Reiss, Fuller, and Morin (3), electric fields arise in an extrinsic semiconductor with a nonuniform impurity concentration due to the rapidly diffusing electrons and holes in comparison to the diffusing impurity atoms. In the case of boron diffusion in extrinsic silicon, the holes have a tendency to diffuse faster than the ionized boron atoms, thus creating a space charge. To prevent this, an electric field is set up to keep the two distributions equal. Such "built-in" electric fields could enhance the diffusivity in an extrinsic semiconductor by a factor as much as two (1, 4) over the diffusivity in an intrinsic semiconductor. At diffusion temperatures around 1000°C the density of the intrinsic carriers (5) is of the order of 10^{19}/cm^3 so that the density of the diffusing boron atoms would have to approach or exceed this intrinsic carrier density before a "built-in" field would be expected to influence the diffusivity. Because Kurtz and Yee worked with boron densities of approximately 5 x 10^{18} at./cm^3, they did not expect any field-aided diffusion to be observed, but they did in Fuller and Ditzenberger's work where the surface concentration was from 10^{21} to 10^{22} at./cm^3, which exceeded the density of the intrinsic carriers.

Another factor which may affect the diffusion of boron in silicon is the bulk impurity density. Millea (6) measured the diffusivities of phosphorus, antimony, tin, and indium in intrinsic, heavily doped n-type and heavily doped p-type silicon and found that the diffusivities were affected by the bulk impurity density. He observed that the diffusivities of phosphorus and antimony in the n-type were twice their corresponding values in the intrinsic material, while their diffusivities in the p-type were only one-half their corresponding values in the intrinsic material. For tin, the diffusivity in the n-type increased only about one-half its value in the intrinsic silicon, whereas in the p-type it was nearly equal to its value in the intrinsic. The opposite changes were found for indium; the diffusivity was six times greater in the p-type and about one-half less in the n-type than in the intrinsic silicon. This effect of the bulk impurity density on the impurity diffusion in silicon is similar to that observed in germanium (7). In germanium it was found also that the bulk impurity density affects the self-diffusion coefficient (8), the self-diffusion coefficient being greater in heavily doped n-type than in intrinsic and being greater in the intrinsic than the heavily doped p-type. It was concluded in these investigations that these effects of bulk impurity density on the diffusion coefficient are indicative of diffusion by means of a vacancy mechanism.

In this investigation the diffusion of boron in silicon was studied in one material over a temperature range of 1050°-1350°C and at one temperature in a material where the n-type impurity concentration varied from 10^{15} to 10^{20} at./cm^3. The diffusion was allowed to take place from a constant concentration source so that under these boundary conditions the solution of the differential diffusion equation gives the results (9)

$$C = C_s \operatorname{erfc}\left(\frac{X}{2(Dt)^{1/2}}\right) \qquad [1]$$

where C is the concentration of the diffusing impurity after time t at distance X from the surface, C_s is the surface concentration of the impurity, and D is the diffusion coefficient. The temperature dependence of the diffusion constant may be described by an Arrhenius-type equation

$$D = D_o \exp - E_a/RT \qquad [2]$$

where E_a is the activation energy, R is the gas constant, and T is the absolute temperature. From measurements of D as a function of temperature, one is

[1] Present address: Owens-Illinois Technical Center, Toledo, Ohio.

able to evaluate E_a and D_o. The diffusion coefficient was evaluated from Eq. [1] by using the p-n junction method with t and C being constant throughout the temperature range. The surface concentration, C_s, was obtained from measurements of the sheet resistivity of the diffused layer and the functional relationship of $1/(\rho_s X)$ to C_s given by Backenstoss (10).

Experimental Procedure

Each diffusion experiment was for 16 hr in air in a furnace automatically controlled to ±2°C. The boron diffused into the silicon from a layer of B_2O_3 on the surface of phosphorus-doped silicon slices which had been cut parallel to the (111) direction, mechanically lapped, and then chemically polished for 1 min in an agitated solution of concentrated HNO_3 and HF acids ($15HNO_3$ to 2HF). The B_2O_3 layer was applied by placing several drops of methyl alcohol, saturated with B_2O_3, on one side of the silicon slice and allowing the alcohol to evaporate. The amount of boron in this oxide layer always was kept much greater than the amount which diffused into the silicon so that it could be assumed that the diffusion was essentially from a constant source and Eq. [1] would apply. Solving Eq. [1] for D gives the result

$$D = \frac{1}{4t}\left\{\frac{X}{\text{argerf}\,(1 - C/C_s)}\right\}^2 \qquad [3]$$

In calculating D from Eq. [3] by the p-n junction method, X is considered to be the distance from the surface to the junction where the concentration of the boron impurity is equal to the concentration of the n-type impurity present in the silicon. For depths greater than 25μ a "focusing" technique was employed for measuring the depth of the junction, and for depths less than 25μ the "interference" technique described by Bond and Smits (11) was employed. The p-n junctions were delineated by staining with a $AgNO_3$ staining solution (12). In the focusing method a small groove at a 3° angle to the surface was lapped carefully in the specimen, which was held in a special jig, so that after staining it was possible to focus with the fine focus of a metallurgical microscope both on the original surface of the slice and on the junction with a minimum of movement of the specimen. The depths measured by this method were accurate to ±1μ.

The concentration of the n-type impurity in each slice was determined from a resistivity measurement made by a four-point probe (13) after the slice had been lapped and polished, and from the resistivity *vs.* n-type impurity relationships given by Prince (14) and by Backenstoss (15). This impurity concentration is C of Eq. [3] at distance X, the depth of the p-n junction.

The surface concentrations, C_s, were determined from the $1/(\rho_s X)$ *vs.* C_s curves given by Backenstoss (11) where ρ_s is the four point probe sheet resistivity of the diffused silicon slice and X is the p-n junction depth. The value of C_s was found to be approximately 3×10^{20} at./cm³, which is lower than one would expect in comparison to the C_s values of 10^{21}-10^{22} at./cm³ obtained by Fuller and Ditzenberger (2), since they allowed the diffusion to take place from B_2O_3 vapor whereas here the diffusion was from a B_2O_3 layer placed on the silicon surface. A recalculation (16) of Backenstoss' values for the determination of the $1/(\rho_s X)$ *vs.* C_s curve resulted in a little higher value for C_s of the order of 10^{21} at./cm³.

Table I. Diffusion coefficients for boron in silicon over the temperature range 1050°-1350°C

Temp, °C	$X \cdot 10^4$ p-n Junction depth, cm	Diffusion coefficient, cm²/sec	
		$C_s = 3 \times 10^{20}$	$C_s = 2 \times 10^{21}$
1050	5.0	1.7×10^{-13}	1.3×10^{-13}
1090	7.7	4.0×10^{-13}	3.1×10^{-13}
1150	14.8	1.5×10^{-12}	1.2×10^{-12}
1200	25	4.2×10^{-12}	3.3×10^{-12}
1250	40	1.2×10^{-11}	8.5×10^{-12}
1300	64	2.8×10^{-11}	2.2×10^{-11}
1350	105	7.4×10^{-11}	5.8×10^{-11}

In the experiments to determine the temperature coefficient of the diffusion coefficient of boron in silicon special precautions were taken to insure that the surface concentrations and the bulk impurity concentrations were the same from specimen to specimen. In order to accomplish this, "floating zone" silicon (Merck) on the order of 0.1 ohm-cm resistivity was used, and some of the samples were cut from the same silicon slice after the B_2O_3 layer had been applied and the slice had a heat treatment at 1300°C for a few seconds to melt the B_2O_3 layer. Also the junction depths for these samples were measured at a location on each sample which was the same distance from the center of the original silicon slice. These extra precautions did not yield results which differed appreciably from diffusion measurements made with adjacent slices cut from the silicon ingot, but it did indicate that the surface concentration was the same for all the samples.

Results and Discussion

The p-n junction depths of one series of measurements made over the temperature range of 1050°-1350°C are given in Table I. The specimens for these measurements were all cut from the same silicon slice after the B_2O_3 layer had been applied and are typical of other runs made over the same temperature range. In this investigation the diffusion time as well as the n-type impurity concentration was the same, respectively, at each temperature so that the only variable which changes with temperature was X, the p-n junction depth. Therefore, the activity energy E_a of Eq. [2] can just as well be evaluated from measurements of X as a function of temperature as from measurements of D as a function of temperature. In Fig. 1 is shown the log X *vs.* $1/T$ curve for the values given in Table I. The slope of this curve corresponds to an activation energy of 85 ± 5 kcal/mole which is in good agreement with previous investigations (1, 2, 17).

Since there is some question as to the exact value of the surface concentration obtained in this investigation, it is a little harder to evaluate D_o of Eq. [2]. For this reason, the diffusion coefficients were calculated from Eq. [3] for both a C_s value of 3×10^{20} and 2×10^{21} at./cm³. The results of these calculations are included in Table I along with

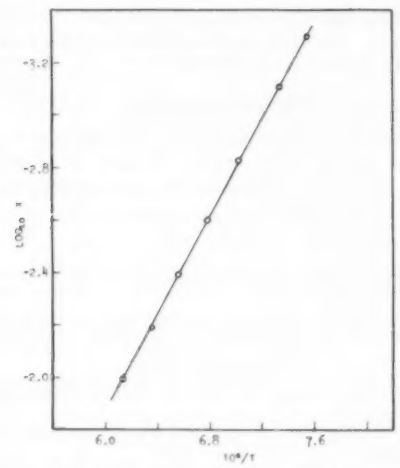

Fig. 1. Log_{10} x (cm) plotted as a function of 1/T for boron diffusion in silicon.

their corresponding X values. It was felt that the diffusion coefficients obtained assuming $C_s = 2 \times 10^{21}$ at./cm³ are closer to the true values which yield a D_o of 16. This D_o value is higher than 10.5 reported by Fuller and Ditzenberger (2) and approximately 5 reported by Kurtz and Yee (1). A surface concentration lower than 2×10^{21} at./cm³ would yield higher D_o values, but in order to have a diffusivity equal to that of either Fuller and Ditzenberger or Kurtz and Yee, the C_s value would have to be larger. Log D *vs.* 1/T plots of all three investigations are shown in Fig. 2. The D values obtained with a C_s equal to 2×10^{21} at./cm³ were used for the plot of this investigator's results. As can be seen from Fig. 2, the diffusivity obtained in this investigation is larger than one would expect on the basis of a field-aided diffusion theory. With a surface concentration less than that of Fuller and Ditzenberger, one would expect lower diffusivities.

The diffusion coefficients at 1250°C for boron diffusion in silicon where the concentration of the n-type impurity varied from 2×10^{13} to 8×10^{19} at./cm³ are given in Table II. These diffusion coefficients were calculated from Eq. [3] also assuming that $C_s = 2 \times 10^{21}$ at./cm³. Included in this table are the measured p-n junction depths, the resistivity of the sample, and their corresponding impurity concentrations. A plot of the log C, where C is the initial concentration of the impurity in the starting material, vs. log D is shown in Fig. 3. The points appear to fit a straight line, but if the surface concentration is considered to be less or greater than 2×10^{21} at./cm³, then the resulting points would fit a curve which would veer either to the right or to the left at the higher C values. Possibly, this is evidence in support of a C_s value near 10^{21} at./cm³. In any case, the diffusion coefficient of boron in silicon appears to increase as the concentration of the n-type impurity increases. This variation is similar to Millea's findings (6) for phosphorus and antimony diffusion in silicon. That is, the diffusion coefficients of the n-type impurities, phosphorus and antimony, in the heavily doped n-type silicon were twice their corresponding values in the intrinsic silicon. Since boron is a p-type material, one would expect the diffusion coefficient to change in a similar manner to that of indium, as reported by Millea where the diffusion coefficient in the heavily doped n-type silicon was only half its value in the intrinsic silicon.

Table II. Diffusion coefficients for boron in silicon of various impurity concentrations

Resistivity, ohm-cm	Junction depth, μ	Impurity density, at./cm³	Diffusion coefficient, cm²/sec
391	46	2×10^{13}	5.6×10^{-12}
79	45	7×10^{13}	5.8×10^{-12}
7.7	44.5	6×10^{14}	6.6×10^{-12}
0.6	42.5	2×10^{16}	8.0×10^{-12}
0.12	40	1×10^{17}	8.5×10^{-12}
0.024	36	2×10^{18}	10.0×10^{-12}
0.001	24	8×10^{19}	11.8×10^{-12}

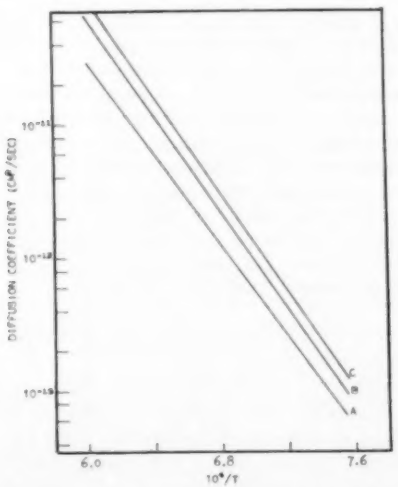

Fig. 2. Comparison of diffusion coefficients for boron diffusion in silicon. (A) Kurtz and Yee (1); (B) Fuller and Ditzenberger (2); (C) present investigation.

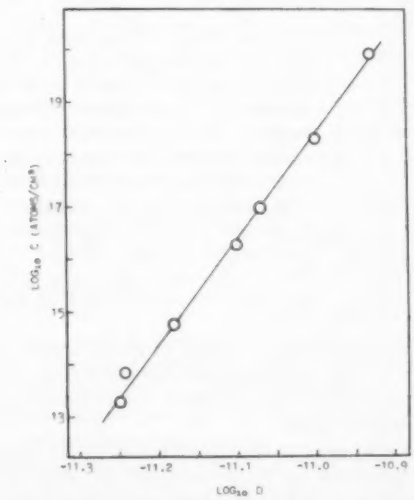

Fig. 3. Variation of the diffusion coefficient for boron diffusion in silicon as a function of the n-type impurity density, $\log_{10}$ C vs. $\log_{10}$ D.

An increase in D with an increase in impurity concentration could explain why the diffusivity of this investigation is larger than that of Fuller and Ditzenberger (2). They had used silicon of 10 ohm-cm resistivity, and in comparison to 0.1 ohm-cm material used in this investigation this means a lower bulk impurity concentration; thus one would expect a lower diffusivity. Although the resistivity of the bulk material was not given by Kurtz and Yee (1), it appears from their results that their bulk impurity concentration was even less than that of Fuller and Ditzenberger, so in view of this investigation their diffusivity also should be less. It has been shown (1, 4) that a built-in field could enhance the diffusivity by a factor of two, but it is doubtful that this field-aided theory alone could explain the difference between the diffusivity of Fuller and Ditzenberger and of Kurtz and Yee. The concentration of the diffusing boron falls off so rapidly from the surface to the p-n junction that only in part of the region between the surface and the junction does the boron concentration exceed 10^{19} at./cm^3. Therefore, only in the region nearer the surface would the field-aided theory apply so that the observed diffusivity would be twice its value in the intrinsic silicon only when the entire region has a boron concentration approximately equal to or greater than 10^{19} at./cm^3. This means that the bulk impurity concentration also would have to approach 10^{19} at./cm^3. It may be that the lower diffusivity found by Kurtz and Yee was due, at least partly, to a lower bulk impurity concentration instead of a lower surface concentration.

It is felt that more experimental work is needed concerning the effect on the diffusion coefficient of boron in silicon of a highly doped surface layer and of highly doped bulk silicon.

Acknowledgments

The author wishes to thank the members of the Sylvania group that were located at Northlake, Illinois, for many illuminating discussions and Mr. Homer Irwin who helped prepare many of the samples.

Manuscript received Dec. 19, 1960; revised manuscript received March 22, 1961.

Any discussion of this paper will appear in a Discussion Section to be published in the June 1962 JOURNAL.

REFERENCES

1. A. D. Kurtz and R. Yee, *J. Appl. Phys.*, **31**, 303 (1960).
2. C. S. Fuller and J. A. Ditzenberger, *ibid.*, **27**, 544 (1956).
3. H. Reiss, C. S. Fuller, and F. J. Morin, *Bell System Tech. J.*, **35**, 535 (1956).
4. F. M. Smits, *Proc. I. R. E.*, **46**, 1049 (1958).
5. F. J. Morin and J. P. Maita, *Phys. Rev.*, **96**, 28 (1954).
6. M. F. Millea, *Bull. Am. Phys. Soc.*, II, **3**, 102 (1958).
7. M. W. Valenta, *ibid.*, II, **3**, 102 (1958).
8. M. W. Valenta and C. Ramasastry, *Phys. Rev.*, **106**, 73 (1957).
9. J. Crank, "The Mathematics of Diffusion," p. 19, Clarendon Press, Oxford (1956).
10. G. Backenstoss, *Bell System Tech. J.*, **37**, 699 (1958).
11. W. L. Bond and F. M. Smits, *ibid.*, **35**, 1209 (1956).
12. D. R. Turner, *This Journal*, **106**, 701 (1959).
13. F. M. Smits, *Bell System Tech. J.*, **37**, 711 (1958).
14. M. B. Prince, *Phys. Rev.*, **93**, 1204 (1954).
15. G. Backenstoss, *ibid.*, **108**, 1416 (1957).
16. R. W. Berkstresser, Private communications.
17. W. C. Dunlap, Jr., H. V. Bohm, and H. P. Mahon, Jr., *Phys. Rev.*, **96**, 822 (1954).

Lead Dioxide Anode in the Preparation of Perchlorates

K. C. Narasimham, S. Sundararajan, and H. V. K. Udupa

Central Electrochemical Research Institute, Karaikudi, India

ABSTRACT

Lead dioxide deposited on graphite or carbon was used to make anodes suitable for the preparation of sodium perchlorate from sodium chlorate. This type of anode has been used successfully in the presence of certain addition agents as a replacement for platinum anode. The influence of anodic current density, temperature, pH, current concentration, and duration of electrolysis on the current efficiency of perchlorate formation was studied. Current efficiency was found to depend on anode surface transformation, which occurred with repeated use. Such changes could be observed visually and were confirmed by anode potential measurements. High current efficiency could be obtained even under slightly alkaline conditions of electrolysis, but addition of fluoride improved results. Addition of fluoride together with sulfate (as sulfuric acid) had the maximum effect on current efficiency under acidic conditions of pH.

This investigation is a result of preliminary studies carried out with the ultimate objective of setting up a pilot production unit to meet the requirements of perchlorates in India.

Use of platinum as anode material in the preparation of perchlorate from chlorate is well known. Many workers (1-6) have reported results obtained by using this anode in the preparation of perchlorates. The mechanism of anodic formation of perchlorates from chlorates, employing platinum anodes, has also been studied (7-10).

The high cost of platinum prompted several attempts to replace it by a cheaper material. In recent years, lead dioxide as the anode has been very much in evidence. This is seen in the considerable amount of work which has been carried out to obtain oxide deposits in a form suitable for use as anode in oxidation of chlorate to perchlorate.

Table I. Comparative statement of results obtained by different workers using lead dioxide anode

Conditions	Japanese workers (11-13)	Angel & Mellquist (17)	Grigger *et al.* (18)	Schumacher *et al.* (19)
Anode material	Lead dioxide coated over iron or nickel from lead nitrate bath	Lead dioxide coated on iron from tartrate bath	Lead dioxide on tantalum wire, rod or screen from lead nitrate bath	Lead dioxide deposited on platinum clad tantalum wires from lead nitrate bath
Electrolyte	Saturated solution of sodium chlorate at 20°C	Saturated solution of sodium chlorate	600 g/l of sodium chlorate	500 g/l of sodium chlorate
Addition agents	2 g/l NaF	2 g/l $K_2Cr_2O_7$	2.08 g/l $K_2S_2O_8$	0.5 g/l NaF
Cathode	Stainless steel	Mild steel	Stainless steel	Nickel or stainless steel
Bath voltage	4.5-5.0 v	4.9-6.2 v	5.0-6.5 v	4.75-5.1 v
Anode current density	20-31 amp/dm²	20 amp/dm²	30 amp/dm²	15.5 amp/dm²
Cathode current density	—	—	—	7.25 amp/dm²
Temperature	29°-30°C	20°-25°C	25°-35°C	30°-45°C
pH	—	—	—	6.0-6.9 (controlled by 18% HCl)
Current concentration	80 amp/l	—	—	—
Current efficiency	70-71%	72-79%	61.2-75%	83.0-91.5%
Energy consumption (DC)	3.18-3.3 kwh/kg of $NaClO_4$	—	—	1.04-1.23 kwh/lb of $NaClO_4$

Preparation of lead dioxide electrodes in various sizes and shapes by deposition on nickel or iron base materials for the preparation of perchlorates was reported by Japanese workers (11-16). Angel and Mellquist (17) reported the use of lead dioxide anode prepared from a tartrate bath for the electrolytic preparation of perchlorates. Recently, Grigger *et al.* (18) reported on the use of lead dioxide deposited on tantalum, with the addition of 2.08 g/l of potassium persulfate to the electrolyte to increase current efficiency of perchlorate formation. Schumacher *et al.* (19) employed a lead dioxide anode coated over platinum clad tantalum.

Although the optimum conditions for electrolysis of chlorate to perchlorate using lead dioxide anodes have been described by earlier workers (Table I), there does not appear to be good agreement in current efficiency and in operating conditions of the cell. Earlier methods for obtaining suitable electrodes are not considered to be practical. For this reason, conditions for electrolytic production of perchlorate on a laboratory scale using a lead dioxide anode prepared by a procedure developed in this laboratory (20, 21) were investigated. The influence of addition agents and pH also was studied in an attempt to arrive at optimum conditions for the process.

Lead dioxide anodes.—The lead dioxide anode used by earlier workers was prepared by deposition of the same from a lead nitrate bath using tantalum or platinum clad tantalum as base material (18, 19). The use of iron and nickel as base materials for deposition of lead dioxide also has been mentioned in the literature (11, 12, 16).

The lead dioxide anode used in this investigation was prepared by depositing the oxide in a smooth and adherent form on graphite or carbon base material from a lead nitrate bath. Either a rotating technique for cylindrical rods, or a to-and-fro motion technique for plate electrodes (20, 21), was used. A lead dioxide coating 0.5 to 1.0 mm thick proved to be just as effective as thick deposits, such as used by earlier workers (13, 18, 19). The graphite or carbon core acts as a support for deposited brittle lead dioxide and also serves as electrical contact for the same, thereby leading the current to the active anode. This type of anode allows preparation of light weight electrodes of desired dimensions to handle large currents on a commercial scale.

Experimental

Cell assembly.—The cell assembly consisted of a 250 ml tall-form beaker with a cell cover made of "perspex" with holes to introduce anode, cathode, and thermometer. The cell was placed in an outer vessel containing water and ice to control the temperature of the electrolyte in the cell. Two bent, perforated stainless steel plates (5.5 x 8.5 cm) acted as cathodes. Lead dioxide deposited on cylindrical graphite was used as anode (1.2 cm diameter x 8.0 cm long). Anode-cathode spacing was 1.5 cm.

Electrolyte.—The electrolyte was prepared by dissolving 600 g of sodium chlorate of A.R. quality in water to give 1000 ml of solution. The initial chlorate content of this solution was determined by the iodometric method (23).

Electrolysis.—In each electrolysis 200 ml of electrolyte was used. A selenium rectifier provided direct current. In each experiment the quantity of electricity theoretically required for complete conversion of chlorate to perchlorate (i.e., 2 Faradays) was passed unless otherwise stated.

Earlier it was established (6) that current efficiency calculated on the basis of perchlorate formed in an experiment by actual analysis with titanium trichloride (24) was within 1% of the value of current efficiency calculated by finding out the amount

Table II. Results of the preliminary investigation on perchlorate preparation

Anode, PbO_2; cathode, cobalt-tungsten alloy plated mild steel rods; volume of electrolyte, 850 ml; temperature, 35°-45°C; pH, 6.4-6.8 (maintained by the addition of hydrochloric acid)

Expt. No.	Motion of anode	Initial chlorate concentration, g/l	Final chlorate concentration after theoretical time, g/l	Addition agent	Current passed, amp	Anode current density, amp/dm²	Bath voltage, v	Current efficiency, %	
								Half the theoretical time	Theoretical time
1.	Stationary	582.2	250.3	2 g/l NaF	18	14.9	4.4	61.1	57.6
2.	Stationary	582.2	133.2	2 g/l NaF	32	26.6	4.8-5.2	80.1	76.5
3.	Stationary	593.2	147.4	2 g/l NaF	31	26.4	4.7-5.2	90.4	74.9
4.	Stationary	572.3	142.4	2 g/l NaF	32	26.8	4.9-5.2	88.5	74.9
5.	Stationary	491.9	261.3	2 g/l NaF	39	35.1	5.8	46.7	46.9
6.	Stationary	616.9	317.5	Nil	31	26.4	5.0-5.4	51.7	46.9
7.	Rotation 1000-1250 rpm	580.2	374.5	Nil	32	26.8	5.1-5.2	41.1	34.4

of chlorate used up employing iodometry. The latter method therefore was adopted. A known amount of electrolyte (5 ml) was pipetted out for analysis, after electrolysis for half the theoretical time and also after full theoretical time. Results of experiments showing the effect of addition agent, anodic current density, pH, current concentration, temperature, and duration of electrolysis on current efficiency of perchlorate formation are given in the attached tables. Experiments were carried out in duplicate, and results were found to be reproducible within experimental error.

Discussion of results.—Table II gives the results of preliminary experiments using a 1 in. diameter cylindrical lead dioxide anode. Experiments 2 to 4 show that 75% current efficiency could be obtained using cobalt-tungsten alloy deposited cathodes at an anodic current density of 26.6 amp/dm² at a pH of 6.4-6.8. Both higher and lower current density decreased current efficiency as seen by experiments 5 and 1. Rotation of the anode lowered current efficiency as seen by experiments 6 and 7. It has been confirmed that sodium fluoride in the electrolyte leads to an increase of current efficiency of perchlorate formation. Schumacher (19), after exhaustive investigation, found that nickel or stainless steel were the best cathodes for perchlorate preparation, but in these experiments cobalt-tungsten alloy plated (22) mild steel rods have been employed successfully. In subsequent experiments, however, stainless steel cathodes were employed.

Effect of addition agents.—Angel and Mellquist (17) reported that reasonable current efficiency (72-79%) for perchlorate formation could be obtained without any addition agent using lead dioxide anodes prepared by depositing from tartrate bath. Others (11-14) showed that practical efficiencies could be obtained only by adding 2 g/l sodium fluoride when lead dioxide anodes were prepared by depositing from a lead nitrate bath. Schumacher *et al.* (19) restudied that work and obtained best results with addition of only 0.5 g/l sodium fluoride to the electrolyte. The use of persulfate as addition agent instead of fluoride has been reported recently (18). Data in Table III indicate that without any addition agent current efficiency is very low. Normally electrolysis is carried out under acidic conditions (below pH 7) by the addition of either hydrochloric or perchloric acid (25). The addition of sulfuric instead of hydrochloric acid was tried and gave better results. This may be due to oxidation of $SO_4^{=}$ to $S_2O_8^{=}$ which in turn gives a better efficiency as found earlier by Bennett and Mack (8) and later by Grigger *et al.* (18) who employed persulfate as addition agent. The presence of both sodium fluoride and sulfuric acid gave still better results.

Under alkaline conditions current efficiency (Table III, experiment 5) was as good as that obtained

Table III. Effect of addition agents on current efficiency

Anode, PbO_2—stationary, previously used anodes; cathode, stainless steel; volume of electrolyte, 200 ml; anode current density, 23.2 amp/dm²; current concentration, 35.0 amp/l; temperature, 28°-30°C

Expt. No.	Initial chlorate concentration, g/l	Final chlorate concentration after theoretical time, g/l	Addition agents	pH	Bath voltage, v	Current efficiency, %	
						Half the theoretical time	Theoretical time
			(a) Acidic condition				
1.*	609.0	324.9	9 ml of 3.11*N* HCl	6.6-6.8	4.5	53.0	42.2
2.	609.0	233.3	3.1 ml of 3.11*N* H_2SO_4	6.6-6.8	4.4-4.5	70.1	57.6
3.	609.0	147.7	2 g/l NaF + 6.2 ml of 3.11*N* HCl	6.6-6.8	4.5	84.2	73.0
4. (a)	609.0	94.6	2 g/l NaF + 3.0 ml of 3.11*N* H_2SO_4	6.6-6.8	4.5	93.6	82.3
(b)	613.0	89.1	2 g/l NaF + 2.3 ml of 3.11*N* H_2SO_4	6.6-6.8	4.3	94.52	82.8
			(b) Alkaline condition				
5.	607.0	156.9	No addition agent	8-10.9	4.5-4.7	80.6	71.2
6.	607.0	88.5	2 g/l NaF	8-10.8	4.3-4.4	93.0	83.1
7.	599.5	237.3	3.35 g/l of Na_2SO_4	8.2-10.6	4.7-4.8	64.2	56.4
8.	599.5	124.8	3.35 g/l of Na_2SO_4 + 2 g/l NaF	8.2-10.5	4.2-4.5	86.5	76.7

* Fresh anode.

Table IV. Effect of pH on current efficiency

Anode, PbO_2—stationary, previously used anodes; cathode, stainless steel; volume of electrolyte, 200 ml; current density, 23.2 amp/dm²; current concentration, 35.0 amp/l; temperature, 28°-30°C

Expt. No.	Initial chlorate concentration, g/l	Final chlorate concentration after theoretical time, g/l	Addition agents	pH	Bath voltage, v	Current efficiency, %		Remarks
						Half the theoretical time	Theoretical time	
1.	609.0	147.7	2 g/l NaF	6.6-6.8	4.5	84.2	73.0	pH maintained by addition of 6.2 ml of 3.11*N* HCl.
2.	609.0	94.56	2 g/l NaF	6.6-6.8	4.5	93.6	82.3	pH maintained by addition of 3 ml of 3.11*N* H_2SO_4.
3.	599.5	128.7	—	6.0-10.4	4.5-4.6	85.1	74.4	After initial pH adjustment, no acid was added during electrolysis.
4.	607.0	116.6	—	6.9-10.7	4.5-4.6	83.7	78.6	
5. (a)	609.0	124.7	—	8.0-11.0	4.5-4.6	91.2	77.8	
(b)	599.5	119.3	—	8.0-10.9	4.3-4.6	88.8	77.7	
6.	599.5	115.4	—	9.0-10.7	4.4-4.6	85.0	77.8	
7.	607.0	112.7	—	10.0-10.8	4.3-4.5	89.0	79.8	
8.	599.5	116.6	2 g/l NaF	6.6-10.8	4.2-4.6	91.4	77.5	
9. (a)	607.0	88.5	2 g/l NaF	8.0-10.8	4.3-4.4	93.0	83.1	
(b)	607.0	96.5	2 g/l NaF	8.0-10.9	4.6-4.7	89.0	81.2	
10.	609.0	77.3	2 g/l NaF	8.5-11.0	4.5-4.7	91.7	84.9	

under acidic conditions by addition of hydrochloric acid (Table III, experiment 3) and was further improved by the addition of fluoride (Table III, experiment 6). Addition of sodium sulfate, however, was found to lower current efficiency slightly under alkaline conditions of electrolysis (compare experiments 6 and 8 as well as 5 and 7, respectively, in Table III).

Effect of pH.—The effect of pH alone does not appear to have been studied systematically by previous workers. It is taken for granted that oxidation should be carried out under acidic conditions. Using platinum anodes, several workers (7-9) reported low efficiencies for alkaline conditions of electrolysis although high current efficiency was reported by Hampel and Leppla (5). The authors noted that the pH of the bath becomes alkaline during electrolysis and the efficiency remains fairly high when using lead dioxide anodes under these conditions. If the starting pH is on the alkaline side (approximately pH 8), cell efficiency is improved and the presence of fluoride improves it even more.

When the starting pH was 8, it was observed that the pH of the electrolyte in the immediate vicinity of the anode was acidic (pH 2-3 as found by a few drops taken out with a glass rod and tested with pH indicator paper), but the final bath pH approached 11. Above this value of pH, disintegration as well as dissolution of the anode has been observed, leading sometimes to deposition of lead on the cathode.

Experiments in Table IV were all carried out with used lead dioxide anodes. Experiments 1 and 2 show the effect of maintaining pH during electrolysis by addition of hydrochloric acid or sulfuric acid with the addition of sodium fluoride also, a difference of nearly 9.3% in current efficiency being obtained. If the pH of the electrolyte is adjusted to 6.0 and then allowed to rise during electrolysis, as usually happens, the current efficiency was only 74.4%. Experiments 3 to 7 show the influence of starting pH on

Table V. Effect of current density and current concentration on current efficiency

Anode, PbO_2—stationary, previously used anodes; cathode, stainless steel; volume of electrolyte, 200 ml; addition agent, 2 g/l NaF; temperature, 30°C

Expt. No.	Initial chlorate concentration, g/l	Final chlorate concentration after theoretical time, g/l	Anode current density, amp/dm²	Current concentration, amp/l	Bath voltage, v	Current efficiency, %		Remarks
						Half the theoretical time	Theoretical time	
					(a) pH: 8.0-11.5			
1.	609.0	77.3	23.2	35.0	4.5-4.7	91.7	84.9	
2.	611.5	85.1	30.0	45.0	4.5-4.7	95.6	84.1	
3.	603.5	63.1	40.0	45.0	4.8-5.3	94.6	88.1	
4.	603.5	70.5	40.0	60.0	5.1-5.3	95.2	86.6	
5.	603.5	63.1	50.0	45.0	5.2-5.6	96.4	88.1	
6.	603.5	74.2	50.0	75.0	5.8-6.1	94.0	85.9	
					(b) pH: 6.6-6.8			
7.	613.0	89.5	15.3	23.0	3.9	94.3	82.9	2.1 ml of 3.11*N* H_2SO_4 added
8. (a)	597.5	66.8	23.2	35.0	4.3-4.6	93.4	86.8	2.7 ml of 3.11*N* H_2SO_4 added
(b)	613.0	89.0	23.2	35.0	4.3	94.5	82.8	2.3 ml of 3.11*N* H_2SO_4 added
9. (a)	597.5	155.7	30.0	45.0	4.5-4.9	77.2	71.3	3.0 ml of 3.11*N* H_2SO_4 added
(b)	613.0	137.4	30.0	45.5	4.5-4.8	76.4	74.8	3.1 ml of 3.11*N* H_2SO_4 added
10.	597.5	163.4	39.8	45.0	4.3-4.8	82.2	70.0	3.7 ml of 3.11*N* H_2SO_4 added

the current efficiency obtained. A starting pH of 7 or higher gave almost identical current efficiency. Acidic starting conditions (pH 6) give low efficiencies. The influence of pH is perhaps not as much evident with a used anode as with a fresh anode. This is seen from experiments 1, 3, and 5 in Table VII where the starting pH of the electrolyte with fresh anodes is 6.1, 7.0, and 8.0, respectively. The current efficiency figures under these conditions were 52.6%, 61.0%, and 71.2%. It also was observed that the surface transformation of the anode referred to below is favored by high pH. This explains why the influence of pH becomes less marked in the case of anodes which have already been used, as in the experiments in Table IV. Experiments 8, 9, and 10 again show the influence of starting pH, 6.6, 8.0, and 8.9; the corresponding current efficiencies being 77.5, 82.2 (average of two experiments), and 84.9%. It can be argued that the influence of pH is not very significant and trends are due only to experimental errors. The definite increase in current efficiency observed in the 3 sets of experiments referred to above in passing from acidic to alkaline starting condition cannot be just due to error or to chance alone. It can, therefore, be stated that the perchlorate formation at lead dioxide anode is influenced by the pH of the electrolyte used.

Effect of current density and current concentration.—Experiments 1, 2, 3, and 5 in Table V show that current efficiency is almost independent of current density employed in the range 23.2-50 amp/dm^2 under alkaline pH condition of electrolysis. Current concentration normally is not expected to affect this reaction which takes place at electrode surface. However, it has been observed that the pH at the immediate vicinity of the anode is highly acidic and different from that of the bulk pH and therefore is very much affected by the current concentration and hence the geometry of the cell. The comparatively small influence of pH on the current efficiency observed also has shown itself in current concentration studies under alkaline conditions of electrolysis. At 40 amp/dm^2 increase of current concentration from 40 to 65 amp/l decreased current efficiency from 88.1 to 86.6%. Similarly, at 50 amp/dm^2, increase of current concentration from 45 to 75 amp/l decreased current efficiency from 88.1% to 85.9%. The effect, although small, is definitely observed. The simultaneous increase of cell-voltage is also to be noted especially from the point of view of cell design and conditions for commercial scale production. In experiments under acidic conditions, the study was carried out with simultaneous change of both current density and current concentration. One point is obvious from this. The corresponding increase of current concentration resulting from an increase of current density in a given cell greatly contributes to the pH of the anode diffusion layer and the low pH developed is obviously detrimental in maintaining current efficiency so that it drops from 84.8% [average of experiments 8(a) and (b), to 70%, experiment 10]. This explains the influence of high current density on the current efficiency of perchlorate formation under acidic conditions of electrolysis. At low current densities, the anode potential does not attain a value high enough for the perchlorate formation to occur at an appreciable rate so that the efficiency is low. An optimum current density for highest current efficiency has thus been found under acidic conditions of electrolysis.

Effect of temperature.—Table VI shows that current efficiency is affected differently depending on whether acidic or alkaline pH conditions are used to start with. Thus it could be seen from experiments 1 to 4 in Table VI that, when the starting pH of the electrolyte is 8, current efficiency dropped from 88.1 to 85.8%, on increasing the bath temperature from 30° to 60°C (2.3% decrease for 30° increase) which is not very significant. However, increase of temperature to 75°C not only decreased current efficiency but also disintegrated the anode. When the pH is maintained by addition of acid at 6.6 to 6.8 as is done usually, it is observed that a maximum current efficiency is obtained for an optimum temperature condition (30°C), thereby making it imperative to maintain the temperature at this desired level to obtain this efficiency. Experiments 8 to 11 show a

Table VI. Effect of temperature on current efficiency

Anode, PbO_2—stationary, previously used anodes; cathode, stainless steel; volume of electrolyte, 200 ml; addition agent, 2 g/l NaF

Expt. No.	Initial chlorate concentration, g/l	Final chlorate concentration after theoretical time, g/l	Temp, °C	Bath voltage, v	Current efficiency, %		Remarks
					Half the theoretical time	Theoretical time	
(a) Alkaline condition: (pH: 8 to 11.5); anode current density, 40 amp/dm^2; current concentration, 45 amp/l							
1.	603.5	63.1	30	4.8-5.3	94.6	88.1	
2.	603.5	59.4	40	4.7-5.1	91.5	88.6	
3.	603.5	74.3	50	4.6-4.9	91.5	85.6	
4.	597.5	78.0	60	4.3-4.8	90.9	85.8	
5.	597.5	178.2	74	4.5-4.7	49.8	66.2	Electrode became intense brown in color and disintegrated
(b) Acidic condition: (pH: 6.6 to 6.8); anode current density, 23.2 amp/dm^2; current concentration, 35 amp/l							
6.	583.0	185.6	20	4.5-4.9	86.0	64.3	7.7 ml of 3.11*N* H_2SO_4 added
7.	614.5	147.7	25	4.2-4.4	94.7	74.2	2.5 ml of 3.11*N* H_2SO_4 added
8.	613.0	89.1	30	4.3	94.5	82.8	2.3 ml of 3.11*N* H_2SO_4 added
9.	583.0	106.5	35	4.0-4.2	81.0	79.3	2.9 ml of 3.11*N* H_2SO_4 added
10.	583.0	118.8	40	4.0	83.5	77.6	2.8 ml of 3.11*N* H_2SO_4 added
11.	604.5	154.5	60	3.9-4.1	88.6	71.5	3.2 ml of 3.11*N* H_2SO_4 added

Table VII. Effect of fresh and used anode on current efficiency

Anode, PbO_2—stationary; cathode, stainless steel; volume of electrolyte, 200 ml; anode current density, 23.2 amp/dm²; current concentration, 35 amp/l; temperature, 28°-30°C

Expt. No.	Nature of anode	Initial chlorate concentration, g/l	Final chlorate concentration, after theoretical time, g/l	Addition agents	pH	Bath voltage, v	Current efficiency, %	
							Half the theoretical time	Theoretical time
1.	Fresh	607	225.2	—	6.1-10.9	4.2-4.5	57.1	52.6
2.	Used	599.5	128.7	—	6.0-10.4	4.5-4.6	85.1	74.4
3.	Fresh	607	209.2	—	7.0-11.0	4.3-4.7	61.8	61.0
4.	Used	607	116.6	—	6.9-10.7	4.5-4.6	83.7	78.6
5.	Fresh	607	156.9	—	8.0-10.9	4.5-4.7	80.6	71.2
6.	Used	599.5	119.3	—	8.0-10.9	4.3-4.6	88.8	77.7
7.	Fresh	615.5	173.2	2 g/l NaF	8.0-10.9	4.5-4.75	77.7	70.6
8.	Used	607.0	88.5	2 g/l NaF	8.0-10.8	4.3-4.4	93.0	83.1
9.	Fresh	613.0	143.2	2 g/l NaF + 3.2 ml of 3.11*N* H_2SO_4	6.6	4.5-4.8	81.2	73.6
10.	Used	613.0	89.1	2 g/l NaF + 2.3 ml of 3.11*N* H_2SO_4	6.6	4.3	94.5	82.8

drop in current efficiency from 82.8 to 71.5% when the temperature was raised from the optimum level of 30°C to 60°C (11.3% drop for 30° increase).

The effect of temperature on perchlorate formation has been ascribed to various factors by early workers in this field. According to Oechsli (7), the decrease in perchlorate formation caused by the increase of temperature at a given current density may be due to the increase in hydroxyl ion concentration caused by the increased dissociation of water at higher temperatures. Bennett and Mack (8) state that an increase in electrolyte temperature tends to lower the active oxygen concentration and consequently gives a lower oxidizing power.

The effect of temperature on current efficiency can be explained perhaps on the basis of extent of decomposition of chloric acid at different temperatures. It is well known that all chemical reactions are accelerated by a rise in temperature due to activation energy effect. This is also true of the decomposition of chloric acid. Therefore, it is to be expected that a rise in temperature should bring about an increased rate of decomposition and lowering of current efficiency.

The rate of decomposition of chloric acid also depends on the anode layer pH. According to Oechsli (7), stability of chloric acid is favored greatly by diminished acidity. Therefore it is necessary to consider the effect of rise in temperature on anode layer pH. Due to electrode reaction, anode layer pH would be lower than bulk pH. The extent of lowering however would depend on diffusion which in turn is dependent on temperature. Higher temperatures would be expected to bring about a rise in anode pH due to increased rate of diffusion.

From the above discussion, it is clear that the rise in temperature has two opposite effects on current efficiency, *viz.*, (i) decrease in current efficiency due to higher rate of decomposition of chloric acid caused by activation energy effects and (ii) increase in current efficiency due to diminished instability of chloric acid caused by the rise in anode layer pH consequent on the increase of diffusion. The net effect would depend on which of the two would predominate. The rise of current efficiency with temperature up to the optimum is due presumably to the second factor predominating over the first, whereas above the optimum temperature the opposite trend is to be interpreted as due to the predominance of the first factor. The relatively low dependence of the current efficiency with temperature at a pH of 8.0 can be interpreted as due to an approximate compensation of the two opposing factors referred to above. In this connection, it is of interest to note that anode layer pH was found to be 1 to 2 when bath pH was 6.6 to 6.8, whereas it was 3 to 4 when bath pH was 8 at room temperature.

Effect of repeated use of anodes.—Results in Table VII show that current efficiency obtained with a fresh anode is lower than with an anode which has

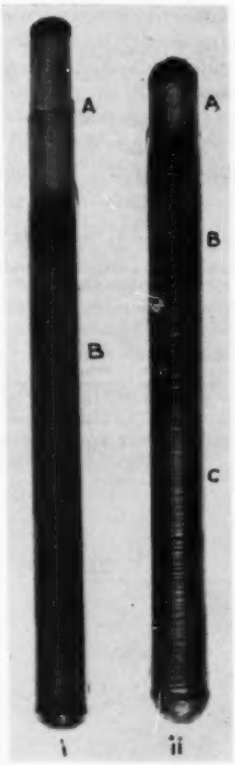

Fig. 1. Photograph showing fresh and used anodes (i) fresh anode, (ii) used anode. A, Graphite core; B, surface of deposited lead dioxide; C, surface of lead dioxide after use.

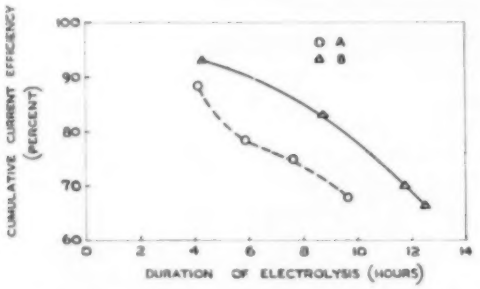

Fig. 2. Variation of current efficiency with duration of electrolysis. A, Acidic condition; B, alkaline condition.

been used before. A fresh lead dioxide anode has a smooth, black metallic sheen which soon changes to a brownish color on use. The addition of fluoride accelerates this change. Figure 1 is a photograph of the electrode showing the change that occurred during electrolysis. The development of the brown color always coincided with best anode performance. The cumulative current efficiency of perchlorate formation is shown in Fig. 2 and was found to decrease with duration of electrolysis to a greater extent under acidic than under alkaline conditions. This is more so with low chlorate concentrations.

Effect of chloride.—Table VIII shows the effect of the presence of chloride in the electrolyte. Concentrations of sodium chloride less than 8.1 g/l do not affect the final efficiency, whereas copious evolution of chlorine occurred when more chloride was present, leading to poor efficiency by oxygen evolution due to the highly alkaline conditions developed by electrolysis of sodium chloride and simultaneous formation of sodium hydroxide.

Anode potential measurements.—Attempts were made to measure the anode potential using a Heathkit vacuum tube voltmeter. It was observed that under any experimental conditions steady anode potential could not be obtained. Therefore it is possible to make only certain general observations. The anode potentials measured *vs.* SCE are expressed on the hydrogen scale by adding 0.2377 v (at 30°C). The potentials generally were higher under alkaline conditions (2.45-2.75 v) than under acidic conditions (2.1-2.3 v). The surface transformation occurring as a result of the use led to high fluctuations in anode potential. Addition of fluoride and sulfate under acidic conditions normally led to an increase in anode potential, especially with fresh anodes. The effect was erratic under alkaline conditions and was not great in extent.

The optimum conditions of electrolysis for perchlorate formation can be given as follows, although a fairly wide variation in conditions is possible when pH is alkaline.

	Alkaline condition	Acidic condition
pH	8 to start with	6.4-6.8
Anode current density	40 amp/dm²	23.2 amp/dm²
Current concentration	45 amp/l	35 amp/l
Addition agent	2 g/l NaF	2 g/l NaF + dil. H_2SO_4 for pH maintenance
Temperature	40°C	30°C
Energy consumption per kg of $NaClO_4$ (D.C.)	2.37 kwh	2.22 kwh

Conclusion

In any case, it is definitely to be considered that perchlorate formation is believed to occur at the anode surface as a result of adsorption of discharged

Table VIII. Effect of chloride addition on current efficiency

Anode, PbO_2—stationary; cathode, stainless steel; volume of electrolyte, 200 ml; addition agent, 2 g/l NaF; anode current density, 40 amp/dm²; current concentration, 45 amp/l; pH, 8.0 at the start and allowed to increase

Expt. No.	Initial chlorate concentration, g/l	Final chlorate concentration after theoretical time, g/l	Initial chloride concentration, g/l	Final chloride concentration, g/l	Duration, hr-min	Bath voltage, v	Current efficiency, %	Remarks
1.	614.5	—	50	39.20	1-20	4.1	—	Copious evolution of chlorine; pH turned alkaline rapidly, surface of lead dioxide changed; solution turned brown; Pb deposition on cathode—experiment stopped
2.	614.5	—	25	—	0-30	4.0	—	Copious evolution of chlorine; pH turned alkaline rapidly, surface of lead dioxide changed; solution turned brown; Pb deposition on cathode—experiment stopped
3.	614.5	199.3	12.3	4.06	6-50	4.1-4.2	65.2	Evolution of Cl_2 in the beginning; pH change gradual
4.	614.5	106.5	8.13	1.35	6-50	4.2	81.06	Cl_2 evolution only in the beginning; pH change gradual
5.	614.5	147.7	4.10	2.70	6-50	4.4-4.6	74.3	Cl_2 evolution in the initial stages (fresh PbO_2 anode was used); pH change gradual

chlorate radicals. This is assumed mainly because perchlorate formation takes place at a potential more positive than for oxygen evolution at a platinum anode (10). This is analogous to the Kolbe reaction which also occurs on platinum at a potential more positive than for oxygen evolution. We have also observed, by anode potential measurements on lead dioxide, that the reaction occurs at potentials more positive than the oxygen evolution potential on a lead dioxide anode. Further, anode potentials are more positive under alkaline conditions than under acidic condition during electrolysis. The formation of perchlorate probably occurs mainly as a result of the reaction of the discharged chlorate radical with water as indicated below.

$$ClO_3^- \rightarrow .ClO_3 + e$$

$$.ClO_3 + H_2O \rightarrow HClO_4 + H^+ + e$$

This reaction shows that high acidity should develop at the anode interface, and actually during electrolysis it was observed that the pH at the interface was lower than the bulk pH. High acidity at the anode leads to decomposition of chloric acid and to lowering of current efficiency. Experiments carried out at different current concentrations under acidic and alkaline electrolyte conditions confirm this. Use of a rotating lead dioxide anode lowers current efficiency especially when bulk pH is alkaline but the lowering is not as much when bath pH is 6.6-6.8 (26).

Whether bath pH is maintained alkaline or acidic it has been observed that anode layer pH is acidic and perchlorate formation occurs under an acidic environment. The degree of acidity determines the experimental conditions to give maximum current efficiency for perchlorate formation. This explains the varying current efficiency values reported by different workers (see Table I). The current density suggested by different workers therefore depends on the different pH conditions they employed. One factor which has been overlooked by earlier workers is the transformation of the lead dioxide anode surface which definitely appears to influence perchlorate formation. The authors are at present investigating this aspect further and the results will be reported in a later communication.

Acknowledgment

The authors express their grateful thanks to Professor K. S. G. Doss, Director of the Institute, for his keen interest and helpful discussions.

Manuscript received April 20, 1960; revised manuscript received April 17, 1961. This paper was prepared for delivery before the Chicago Meeting, May 1-5, 1960.

Any discussion of this paper will appear in a Discussion Section to be published in the June 1962 JOURNAL.

REFERENCES

1. F. Winteler, *Z. Elektrochem.*, **5**, 50 (1898); *ibid.*, **5**, 217 (1898); *ibid.*, **7**, 635 (1901).
2. J. G. Williams, *Trans. Faraday Soc.*, **15**, 134 (1919).
3. A. J. Allmand, "Applied Electrochemistry," p. 402, Edward Arnold, London (1912).
4. J. C. Schumacher, *Trans. Electrochem. Soc.*, **92**, 45 (1947); J. C. Schumacher, *Chem. Eng. Progr.*, **43**, 117 (1947); J. C. Schumacher, *Chem. & Met. Eng.*, **51**, No. 12, 108 (1944).
5. C. A. Hampel and P. W. Leppla, *Trans. Electrochem. Soc.*, **92**, 55 (1947).
6. K. C. Narasimham, A. Narayanaswami, and B. B. Dey, *J. Sci. Ind. Research (India)*, **16A**, 512 (1957).
7. W. Oechsli, *Z. Elektrochem.*, **9**, 807 (1903).
8. C. W. Bennett and E. L. Mack, *Trans. Am. Electrochem. Soc.*, **29**, 323 (1916).
9. V. S. Knibbs, *Trans. Faraday Soc.*, **16**, 424 (1920).
10. K. Sugino and S. Aoyagi, *This Journal*, **103**, 166 (1956); K. Sugino and S. Aoyagi, *Bull. Chem. Soc., Japan*, **26**, 185 (1953).
11. Y. Kato, K. Sugino, K. Koizumi, and S. Kitahara, *Electrotech. J. Japan*, **5**, 45 (1941).
12. S. Kitahara and T. Osuga, *J. Electrochem. Assoc., Japan*, **10**, 409 (1942).
13. K. Sugino, *Bull. Chem. Soc., Japan*, **23** (4), 115 (1950).
14. K. Sugino and Y. Shibazaki, *J. Electrochem. Soc., Japan*, **16**, 9 (1948).
15. Y. Kato and K. Koizumi, *ibid.*, **2**, 309 (1934).
16. T. Osuga and K. Sugino, *This Journal*, **104**, 448 (1957).
17. G. Angel and H. Mellquist, *Z. Elektrochem.*, **40**, 702 (1934).
18. J. C. Grigger, H. C. Miller, and F. D. Loomis, *This Journal*, **105**, 100 (1958).
19. J. C. Schumacher, D. R. Stern, and P. R. Graham, *ibid.*, **105**, 151 (1958).
20. K. C. Narasimham and H. V. K. Udupa, "Preparation of Lead Dioxide Electrodes—Part I." Presented at the symposium on "Electrolytic Cells" held at Karaikudi (India) in December 1958 (under publication).
21. H. V. K. Udupa and K. C. Narasimham, Indian Pat. No. 66,195, Dec. 22, 1958.
22. A. Brenner, P. Burkhead, and E. Seegmiller, *J. Research Natl. Bur. Standards*, **39**, 351 (1947).
23. Julius Grant, "Clowes and Coleman's Quantitative Analysis," p. 176, J. & A. Churchill Ltd., London (1947).
24. D. C. Eagles, *Chem. & Ind.*, 1002 (1954).
25. E. H. Karr, U.S. Pat. 2,772,229, Nov. 27, 1956.
26. K. C. Narasimham, S. Sundararajan, and H. V. K. Udupa, Unpublished work.

Electrolytic Production of Sintered Titanium from Titanium Tetrachloride at a Contact Cathode

R. B. Head[1]

School of Metallurgy, University of Melbourne, Melbourne, Australia

ABSTRACT

Titanium was deposited electrolytically from fused alkali chlorides by means of a contact cathode operating in an atmosphere of titanium tetrachloride and hydrogen. Owing to the heavy current used, the temperature of the cathode hot spot rose to about 1300°C while the graphite cell remained at a low temperature. Reduction of titanium tetrachloride and deposition of sintered metal took place simultaneously at the single cathode.

In depositing titanium metal from titanium trichloride-alkali chloride melts, powdery nonadherent metal usually is obtained at temperatures in the range 500°-800°C especially if high cathode current densities are used. It is impossible to leach all the entrained salt from such fine titanium powders with the consequence that the resulting ingots are contaminated with oxygen owing to the hydrolysis of lower titanium chlorides. Due to the large surface area of the powder, surface contamination is increased greatly.

While it is well known that coarsely crystalline adherent deposits can be obtained from melts to which fluoride additions have been made, attempts have been made to nucleate larger crystals from electrolytes containing alkali chlorides only. Hickman (1) deposited titanium crystals on a silver cathode at 550°C from a titanium trichloride-alkali chloride electrolyte at low current densities. The crystals initially formed were slender needles which became progressively smaller and more numerous during the growth of the cathode deposit.

Alpert *et al.* (2) have deposited ductile titanium from $SrCl_2$-NaCl-$TiCl_3$ melts. The trivalent titanium was, however, first reduced to the divalent state by a low current density pre-electrolysis. It has been noted that during the electrolytic refining of scrap titanium from alkali chloride melts, the cathode deposits are coarser and more crystalline than those obtained from melts containing $TiCl_3$.

When alkali chloride cells are operated at higher temperatures a certain amount of sintering of the cathode deposit takes place, and adherent deposits can be obtained although these are usually powdery. Elevated temperatures are known to shorten cell life and may be the cause of increased carbon pickup from graphite crucibles.

In a previous paper, Head (3) showed that if a thin cathode rod penetrated only a few millimeters into the melt it became surrounded by a high-temperature high-resistance zone when operated at a suitable current while the walls of the graphite cell remained at a low temperature. This form of cathode was termed a "hotspot" cathode. Further experiments have proved that titanium can be deposited at the boiling point of the electrolyte (≃1350°C), and that the cathode deposits obtained are sintered heavily so that they can be withdrawn from the cell in a manner similar to that used in depositing calcium. It was found that, when a mixture of titanium tetrachloride and hydrogen was passed over the cathode, reduction of the tetrachloride to trichloride and the deposition of titanium occur simultaneously. Recent experiments were made on a larger scale under conditions where the cell heating was maintained entirely by the hot zone to determine the quality of metal that could be produced and the highest degree of sintering obtainable. This method forms the basis of a continuous process and is described below.

[1] Present address: Division of Physical Chemistry, C.S.I.R.O. Chemical Research Laboratories, Melbourne, Australia.

Experimental

Cell design.—A graphite crucible (15 cm diameter by 18 cm) was sealed into a steel shell containing a Nichrome heater and provision for nitrogen flushing. A tungsten cathode rod, 6 mm x 6 mm x 25 cm, entered the cell through a flexible rubber seal and could be raised or lowered by means of a windlass. The upper part of the cathode rod passed through a fused silica dome through which the hot zone could be observed during operation of the cell. The graphite crucible was run about half full of electrolyte, and contact with the cathode rod was determined electrically. The cell and associated apparatus are shown in Fig. 1.

In the initial experiments, the cathode was operated within a thin graphite anode hood just touching the surface of the melt, and insulated from the anode by a steatite ring. It showed a tendency to crumble in contact with the hot mixture of tetrachloride and hydrogen and was discarded after two trials.

Hydrogen was bubbled through the $TiCl_4$ boiler, and the mixture of gases passed over the cathode and thence to the anode compartment via a circular hole in the anode hood. The excess $TiCl_4$ was condensed and returned to the boiler, while excess HCl and H_2 were allowed to exit to the atmosphere.

Preliminary experiments in air indicated that a current of approximately 250 amp at 15 v could be

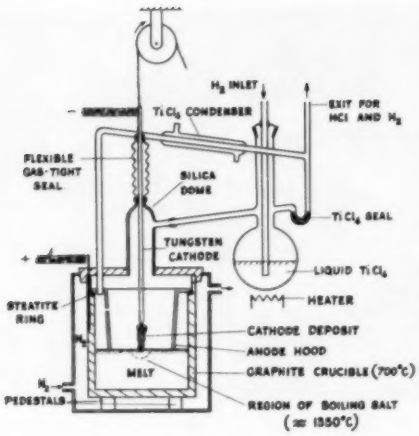

Fig. 1. Diagrammatic sketch of electrolytic cell for operation of contact cathode.

necessary to boil the electrolyte in the molten zone. A flexible d-c supply (0-350 amp at 0-24 v) was used in later experiments.

Operation of cell.—After the LiCl/NaCl/KCl electrolyte had been melted under purified hydrogen, the tip of the cathode was lowered into the melt, and an electrical indication of the contact with the melt was obtained. The cathode position was marked so as to provide a datum level during the withdrawal. The $TiCl_4$ used in these experiments was purified by refluxing over copper metal followed by fractional distillation after McTaggart (4). A mixture of $TiCl_4$ vapor and hydrogen was circulated rapidly through the cell by means of the boiler system and the cathode was lowered to its datum level. The cathode current was adjusted to 200 amp.

Since the quartz hood was initially cold, drops of condensed $TiCl_4$ ran down the cathode rod and reacted with the alkali metal liberated at the cathode producing a number of yellow flashes accompanied by small explosions. After about a minute the explosions ceased, and the cathode zone was observed to have reached a temperature of about 1200°C. The current quickly increased to 350 amp, indicating the growth of a cathode deposit, and at this point the cathode was withdrawn slowly by means of the windlass at a speed which limited the current to 300 amp. Under these conditions considerable vibration of the cathode rod occurred owing to the boiling electrolyte in the cathode zone. Salt smoke condensed on the cathode deposit forming a shroud, and a portion of the smoke was carried over with the exit gases and washed into the $TiCl_4$ boiler. No serious blockages of ventlines occurred. When the position of the cathode had risen to about 3 in. above the datum mark, corresponding to the limiting extension of the flexible seal, the top connection to the seal was slackened, and the cathode deposit drawn up into the silica dome and cooled in hydrogen.

The cathode deposits obtained were hard, strongly adherent columns of titanium sponge with a coke-like texture. After leaching, they contained about 0.5% of entrained salts. The microstructure of the sponge showed that dendrites were completely absent and that a considerable amount of sintering had taken place between adjacent areas of deposited metal. The microhardness of these areas was about 130 (V.H.N.), but after argon-arc-melting, the hardness of the vacuum annealed titanium ingots was not less than 200 (V.H.N.). The first portion of the cathode deposit always was assumed to be contaminated and was discarded prior to melting.

Table I. Typical analysis

Time of run	20 min
Temperature of cell wall	700°C
Temperature of tip of cathode	1350°C
Impressed voltage	9-15
Cathode current (amp)	200-350
Cathode current density (amp/cm²)	30
Anode current density (amp/cm²)	0.5
Weight of metal deposited	15
Percentage of entrained salt	0.5
Lower chlorides in melt ($TiCl_2$ + $TiCl_3$)	3%
Apparent cathode efficiency	27.5%
Energy consumption of cell	77 kwhr/kg

A typical analysis is shown in Table I.

Figure 2 shows the type of cathode deposit obtained. The cathode rod penetrates about 15 mm into the deposit.

During the first run the thin graphite anode hood partly disintegrated, resulting in a carbon content of 2% in the deposited metal. The hood was discarded in subsequent experiments, and the cell operated under conditions where the anode gases had access to the cathode. Attempts were made to sweep away the anode gases more rapidly by increasing the hydrogen flow.

The metal produced under these conditions had the following impurity content: C, 0.3%; O, 0.2-0.6%; N, 0.01%; Fe, trace; Mn, trace.

Owing to the relatively high carbon and oxygen content, the ductility was limited, and cracking usually occurred after two reductions by swaging.

Discussion

Production of lower titanium chlorides.—In previous work (3), $TiCl_3$ was formed directly in the melt either by means of a salt-vapor arc formed

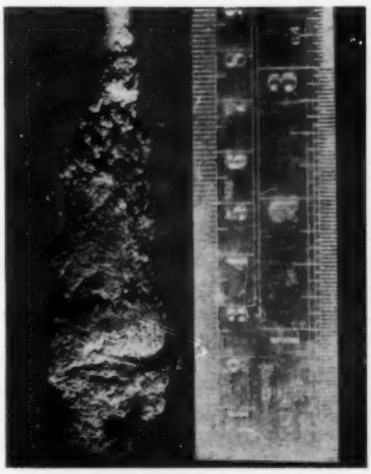

Fig. 2. Cathode deposit of Ti

between the tungsten cathode rod and the surface of the melt in an atmosphere of $TiCl_4$ and H_2, or by operating a "hotspot" cathode in a similar atmosphere. Where the cathode took the form of fine wires just touching the surface of the melt the energy expended in producing $TiCl_3$ was about 3.7 kwhr/kg of which 90% was dissipated at heat in the high resistance zone of the electrolyte. It is assumed that the major portion of the deposited metal reacted with $TiCl_4$ as follows

$$Ti + 3TiCl_4 \rightleftharpoons 4TiCl_3 \qquad [1]$$

$$1 \text{ kg } 11.9 \text{ kg } 12.9 \text{ kg} \qquad [2]$$

The trichloride can be produced by the hydrogen reduction of $TiCl_4$ at hot surfaces [a modification of the Sherfey (5) process] with a yield of only 6.6 kwhr/kg owing to freezing the equilibrium (6). Below 500°C, the reaction

$$2TiCl_4 + H_2 \rightleftharpoons 2HCl + 2TiCl_3 \qquad [3]$$

is extremely slow, but above this temperature only small yields of $TiCl_3$ can be expected owing to the unfavorable equilibria of reaction [3].

Since in the present apparatus a considerable area of incandescence surrounded the hot zone, both these reactions probably took place simultaneously. As the cathode was immersed to a finite depth, the major portion of the titanium did not react with tetrachloride.

No trouble was experienced from "anode effect," and it is evident that oxygen was present in the melt. The lack of separation between anolyte and catholyte was undoubtedly a cause of the low cathode efficiency observed. Hickman (1) showed that the anodic oxidation of $TiCl_3$ to $TiCl_4$ is suppressed largely where the anode is run under hydrogen owing to the conversion of chlorine to hydrogen chloride at the surface of the melt. The rate of production of $TiCl_3$ at the incandescent zone therefore must be depressed by additional HCl from the anode since it is limited by the back reaction

$$2HCl + 2TiCl_3 \rightleftharpoons H_2 + TiCl_4 \qquad [4]$$

Sintering of deposit.—Where the temperature of the cathode deposit approached the boiling point of the electrolyte a considerable amount of sintering took place resulting in relatively large areas of solid metal and the complete absence of dendrites. Often such deposits could be removed from the cathode rod only by sawing. A section through a deposit obtained at a hot zone temperature of about 1000°C is shown in Fig. 3.

Kroll (7) has stated that clean titanium metal sticks to itself and all other solids at temperatures in excess of 720°C. Solid metal was not, however, produced at the highest temperatures obtainable with the LiCl-NaCl-KCl melt, although it might have formed if a $BaCl_2$ melt had been used, (bp ≃ 1500°C). Hüttig (8) has found that the lowest temperature at which sintering starts is 0.37 to 0.53 Tf, where Tf is the temperature of melting on the absolute scale. Thus for titanium, sintering should begin between 650° and 930°C. The coherence of the deposits obtained at various temperatures is shown in Table II.

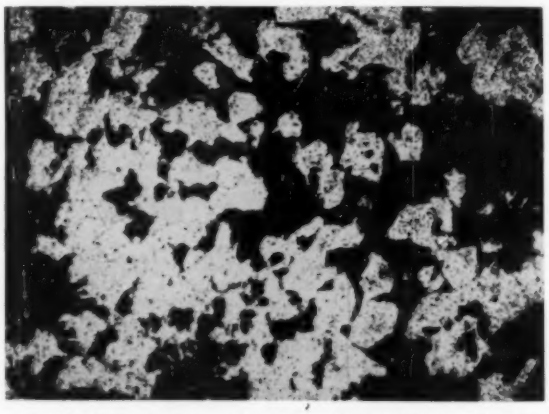

Fig. 3. Microstructure of cathode deposit showing sintered structure. Magnification 100X before reduction for publication.

Each zone of the cathode deposit is subjected to the maximum temperature of the moment of deposition. A certain rate of withdrawal is necessary for the maintenance of the hot zone, and consequently, the deposited metal only experiences a limited time-temperature cycle. Thus it is probable that solid metal completely free of inclusions can be obtained only if the hot zone temperature approaches the melting point of the deposited metal.

Energy consumption.—The major part of the energy required by the cell was that needed to maintain the hot zone and the cell heating. The high figure of 77 kwhr/kg of deposited metal is not markedly greater than that of small conventional cells if the energy expended in external heating is taken into account.

Conclusion

It has been shown that strongly sintered adherent deposits of titanium can be produced directly by the reduction of $TiCl_4$ vapor at a contact cathode operating at a temperature near the boiling point of an electrolyte containing only alkali chlorides while the cell walls remain at a relatively low temperature. This method of operation forms a basis for a continuous electrolytic process requiring only initial external heating.

Acknowledgments

The author wishes to thank Professor H. W. Worner, School of Metallurgy, University of Melbourne, for permission to publish this paper and

Table II. Coherence of deposits

Approximate temp	T/T_f	Form of deposit
600	0.45	Nonadherent black powder
900	0.6	Adherent, easily crushed gray sponge
1300	0.81	Hard gray sponge of high strength

gladly acknowledges the benefit of a Consolidated Zinc Pty. Ltd. Research Fellowship.

Manuscript received Dec. 9, 1960; revision received April 17, 1961.

Any discussion of this paper will appear in a Discussion Section to be published in the June 1962 JOURNAL.

REFERENCES

1. B. S. Hickman, M.Sc. Thesis, University of Melbourne (1955).
2. M. B. Alpert, F. J. Schultz, and W. F. Sullivan, *This Journal*, **104**, 555 (1957).
3. R. B. Head, *Proc. Australasian Inst. Mining & Met.*, **178**, 21 (1956).
4. R. B. Head, *Aust. J. Chem.*, **13**, 3, 332 (1960).
5. F. K. McTaggart, *J. Council Sci. Ind. Research, Australia*, **18**, 5 (1945).
6. J. M. Sherfey, *J. Research Nat. Bur. Standards*, **46**, 299 (1951).
7. R. B. Head, Ph.D Thesis, University of Melbourne (1955).
8. W. J. Kroll, *Metal Industry*, **84**, 17, 325 (1954).
9. Von G. F. Hüttig, *Kolloid-Zeits*, **98**, 3, 263 (1942).
10. W. J. Kroll, W. F. Hergert, and W. R. Carmody, *U.S. Bur. Mines Rept. Invest. No. 4752* (1950).

Technical Notes

Cordierite-Indialite; A New Manganese-Activated Phosphor

F. A. Hummel

Department of Ceramic Technology, College of Mineral Industries, The Pennsylvania State University, University Park, Pennsylvania

Crystals of the composition $2MgO \cdot 2Al_2O_3 \cdot 5SiO_2$, whether synthesized through the use of talc and clay, pure oxides, or by crystallization of glass, have long been spoken of as cordierite, although the natural mineral generally contains a considerable amount of Fe^{2+} as a replacement for the Mg^{2+} of the synthetic preparations.

Recently, as a result of detailed x-ray studies on natural minerals and synthetic preparations, Miyashiro (1) announced a hexagonal form of cordierite and suggested that it be called indialite. He further suggested that the term "cordierite" be reserved for the various structural states of the natural mineral, thus preserving their identity with the French geologist, Cordier. The structural states for both cordierite and indialite were distinguished by the use of a distortion index Δ, defined as follows:

$$\Delta = 2\theta_{131} - (2\theta_{511} + 2\theta_{421})/2 \text{ for CuK}\alpha_1 \text{ radiation}$$

Cordierites with the highest deviation from hexagonal symmetry had Δ values above 0.29°.

Further work by Schreyer and Schairer (2) on the distortion index of pure MgO-Al_2O_3-SiO_2 compositions heated in various ways showed that the structural states were considerably affected by the bulk composition of the mixture. They suggested that the name "cordierite" be retained as a collective term similar to plagioclase or mica.

It was discovered several years ago (3) that manganese-activated "cordierites" produced very good red luminescence when excited by cathode rays. The basic composition is the 2:2:5 ratio and the phosphor can be prepared by a molar substitution of MnO as follows:

$$\begin{matrix} 1.8MgO & & \\ & 2Al_2O_3 & 5SiO_2 \\ 0.2MnO & & \end{matrix}$$

introducing MnO as the carbonate or other suitable source of MnO. Without a flux to promote the reaction, firing temperatures of 1350°-1450°C are required. Introducing 0.2 of the Mg^{2+} as MgF_2 is very effective in promoting the synthesis at temperatures between 1200°-1300°C without damage to brightness. The compositions do not fluoresce under 2537 of 3650Å u.v. excitation.

There has been considerable discussion since the original work of Rankin and Merwin (4) as to whether the cordierite composition is variable and, particularly, whether it can accept silica in solid solution up to an approximate ratio of 2:2:8. Schreyer and Schairer (5) reported that no true equilibrium solid solution of silica in cordierite exists at high temperatures, but that metastable solid solutions of silica in indialite may form by crystallization of glass during short-time heating. Later, Schreyer and Schairer (2) found that, above 1320°C and particularly in the presence of liquid, cordierite may exhibit solid solution toward a hypothetical compound "Mg-beryl", $Mg_3Al_2Si_6O_{18}$.

Efficient phosphors with excess silica over the 5 required for the 2:2:5 ratio can be prepared as well

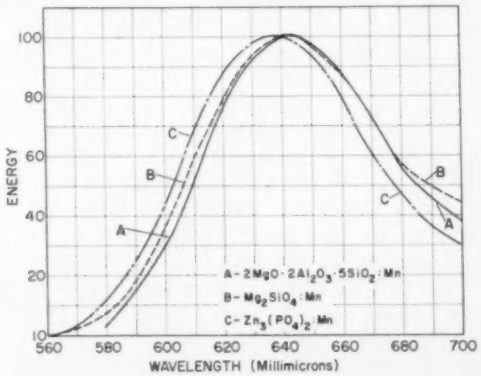

Fig. 1. Spectral distribution curves

as others which do not lie on the join between spinel and silica in the ternary system. Attempts to substitute Zn^{2+} for Mg^{2+} in the 2:2:5 composition showed that little or no solid solution is possible. On the other hand, small molar amounts of Ga^{3+} and Ge^{4+} will enter the lattice in place of Al^{3+} and Si^{4+}, but each type of substitution provides no increase in brightness of the phosphor.

It is obvious that a detailed study of the influence of Mn^{2+} on the relation of the structural states of various cordierites to the fluorescent brightness would be of great interest.

Spectral distribution curves showing the characteristics of $2MgO \cdot 2Al_2O_3 \cdot 5SiO_2$:Mn relative to Mg_2SiO_4:Mn and $Zn_3(PO_4)_2$:Mn are shown in Fig. 1.

Acknowledgment

The author wishes to thank the General Electric Company, Cleveland, Ohio, for financial assistance which made this work possible and for accumulation of the emission data.

Manuscript received March 17, 1961. This is Contribution No. 60-74 from the Department of Ceramic Technology, College of Mineral Industries, The Pennsylvania State University, University Park, Pa.

Any discussion of this paper will appear in a Discussion Section to be published in the June 1962 JOURNAL.

REFERENCES

1. Akiho Miyashiro, *Amer. J. Sci.*, **255** (1), 43 (1957).
2. W. Schreyer and J. F. Schairer, "Cordierite," Annual Report of the Director of the Geophysical Lab., pp. 85-96 (1959-1960).
3. U. S. Pat. No. 2,961,412, Nov. 22, 1960, F. A. Hummel to the General Electric Co., Cleveland, Ohio.
4. G. A. Rankin and H. E. Merwin, *Amer. J. Sci.* 4th ser., **45**, 301 (1918).
5. W. Schreyer and F. J. Schairer, "Anhydrous Cordierites and the System MgO-Al_2O_3-SiO_2," Annual Report of the Director of the Geophysical Lab., p. 98, (1958-1959).

Thermal Coefficients of EMF of the Silver (I) and the Silver (II) Oxide-Zinc-45% Potassium Hydroxide Systems

Stanley Hills

Research and Development Department, Yardney International Corporation, New York, New York

Recently increased research efforts on the silver oxide-zinc couple reflect the increasing importance of this system. Some thermodynamic data for this system have already been reported (1) but the reproducibility was too poor to indicate adequate reliability. This note presents additional electrochemical data and thermodynamic values derived therefrom.

Experimental

Four commercial silver oxide-zinc cells were used in this study. The cells initially were fully charged. Two cells were discharged partially to remove divalent silver and allowed to stand on open circuit until equilibrium was established as denoted by a constant and reproducible open-circuit potential. All four cells then were placed in a water bath and maintained at a specific temperature for 2 hr before potentials were taken with a K-3 potentiometer. Potentials were determined again after 30 min and, if found to be reproducible within a few tenths of a millivolt, the cells were brought to a new temperature. It was not possible to take special precautions to saturate the zincate electrolyte in the battery at each temperature because of the limited access to electrolyte between the planar electrodes which were under pressure.

The temperature range covered was 25°-65°C at intervals of 10°C. The bath was thermostated within ± 0.2°C. EMF readings were accurate to ± 0.0002 v. Individual cells displayed deviations about the observed mean potential which always were less than the accuracy of the potentiometer, a good indication that temperature stability was achieved. This was true also for the deviations between the two monovalent silver oxide cells, indicating that the electrodes had come to equilibrium. However, the two divalent silver oxide cells continuously differed by approximatley 1 mv.

Discussion

The thermal coefficients of EMF were found by the method of least squares to be −0.000169 and +0.0000570 v/°C, respectively, for silver-zinc cells containing monovalent and divalent silver oxide. Figures 1 and 2 depict the temperature dependence of EMF.

If it is assumed that the following reactions occur in the cell then the hydroxyl concentration of the 45% potassium hydroxide electrolyte need not be considered. This was supported by Bedwell (1) in a similar study.

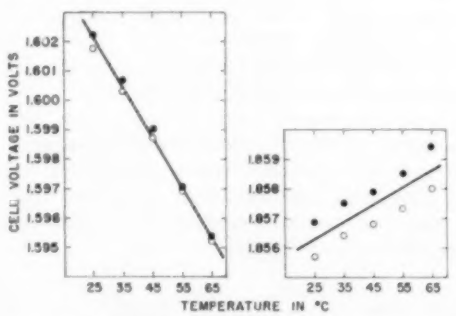

Fig. 1. (Left). dE/dT for $Ag_2O + Zn \rightarrow 2Ag + ZnO$

Fig. 2 (Right). dE/dT for $2AgO + Zn \rightarrow Ag_2O + ZnO$

$$Zn + Ag_2O \rightarrow 2Ag + ZnO \quad [1]$$

$$Zn + 2AgO \rightarrow Ag_2O + ZnO \quad [2]$$

The Gibbs-Helmholtz equation

$$\Delta H = n\mathbf{F}[T(dE/dT) - E]/4.184$$

yields ΔH terms of −76.2 kcal and −84.8 kcal for reactions [1] and [2] at 25°C. Agreement with corresponding ΔH values of −75.9 kcal and −84.5 kcal, calculated from Latimer (3), is within 0.5% for both reactions.

The relation between free energy and potential

$$F = -n\mathbf{F}E/4.184$$

yields ΔF terms of −73.90 kcal and −85.63 kcal for reactions [1] and [2] at 25°C. ΔF values for the same reactions, calculated from Latimer, are −72.46 kcal and −83.8 kcal respectively.

The enthalpy terms derived from the thermal coefficient of EMF are in closer agreement with those derived from National Bureau of Standards data (also used by Latimer) than the values obtained previously by Bedwell (1) in a study of both commercial and specially constructed cells. Bedwell not only had difficulty in reproducing results for chemically and electrolytically prepared silver oxides, but found that the coefficients for commercial and laboratory constructed cells were of opposite sign. There was a 22 mv difference between two supposedly identical commercial cells on the monovalent silver oxide plateau as compared to a maximum difference of 0.4 mv between two such cells in the present work. The coefficient found in this instance was opposite in sign to that found by the author.

Bedwell had better agreement among the commercial cells on the divalent silver oxide plateau. The voltage spread was approximately double the maximum 1.4 mv deviation found in the present study, and this coefficient was of the same sign but slightly larger than that found by the author.

Such thermodynamic data also prove useful for the solution of heat removal problems which arise in the high rate discharge of large cells. If dE/dT is negative, ΔH is greater than ΔF, and the cell in question evolves heat when undergoing a reversible discharge. If dE/dT is positive, the reverse occurs. Normal cell usage, however, does not even approach reversible conditions. The magnitude of the heat changes produced by the departure from reversibility (calories $= -n\mathbf{F}\eta/4.184 = 2.31$ kcal/0.1 v overvoltage/Faraday of current) is much larger than those associated with reversible discharge. Nevertheless, the latter should be included for precise work.

Acknowledgment

The author wishes to thank Yardney International Corporation for permission to publish this note.

Manuscript received Nov. 29, 1960; revised manuscript received March 29, 1961.

Any discussion of this paper will appear in a Discussion Section to be published in the June 1962 JOURNAL.

REFERENCES

1. M. E. Bedwell, ASTIA Report AD 200686-L.
2. National Bureau of Standards, "Selected Values of Chemical Thermodynamic Properties," (*a*) Table 35-1, March 31, 1949, (*b*) Table 31-1, December 31, 1948, (*c*) Table 8a, March 31, 1948.
3. W. M. Latimer, "Oxidation Potentials," 2nd ed., Prentice-Hall Inc., New York.

Brief Communication

Transport Numbers in Pure Fused Cesium Chloride

Edward D. Wolf

Institute for Atomic Research and Department of Chemistry, Iowa State University, Ames, Iowa

The chloride ion transport number in pure fused cesium chloride has been redetermined. Using a modified and more refined experimental procedure, an appreciably higher value for t_{Cl^-} was found than was previously reported (1); radiochloride was used to follow the movement of chloride ion.

Experimental.—Experimental materials, apparatus, and procedure were the same as previously used (1) with the following exceptions:

1. Spectroscopic graphite rods (⅛ x 12 in.) were used for both electrodes. The cell was suspended from a specially designed quartz cell holder in an upright tube furnace. This arrangement made it possible to maintain a dry inert gas over the salt during electrolysis. The dry gas flush was not essential in the present work, but becomes very important when working with hygroscopic salts (2). The control thermocouple was chromel-alumel which sensitized a Bristol Series 536 Freevane Electronic Controller. The measuring thermocouple was a standardized (with 99.99% Ag; agreed to ±0.5°C at melting point) platinum, platinum-13% rhodium thermocouple which was situated directly above the porous disk and in contact with the outer wall of the cell. This thermocouple was attached to a Rubicon Precision Potentiometer, Model 2745.

2. A silver coulometer was used in all experiments to determine the total equivalents of charge passed during electrolysis.

3. Three samples of AgCl were precipitated from each anolyte and catholyte. The precipitate was collected on 22 mm diameter filter paper, washed, vacuum dried, weighed, mounted on a card, and covered with cellophane. The 0.714 Mev β activity of Cl^{36} was counted using a Geiger-Müller end-window tube connected to a Nuclear Chicago 181A Decade Scaler and a Model T1 Dual Timer. Standard coincidence and self-absorption corrections were made. Sample holders were made of aluminum and constructed so as to expose a uniform center portion of the sample to the Geiger tube. This arrangement made it possible to obtain very precise reproducible geometry for successive samples.

Results and discussion.—The equation $t_{Cl^-} = C_A E_A / C_c Z$ can be derived, where t_{Cl^-} is the chloride ion transport number, E_A is the total equivalents of CsCl initially in the anolyte, C_A and C_c are the specific activities of CsCl in the anolyte and catholyte, respectively, after electrolysis, and Z is the number of faradays of charge passed.

The chloride ion transport number was found to be 0.435 ± 0.008 at 705°C. This compares with the previously reported value of 0.36 ± 0.04 at 685°C. No temperature dependence was found. The author feels that the modified experimental procedure and the precision indicated for the former value make the latter value erroneous.

Manuscript received April 24, 1961. Contribution No. 1012; work was performed in the Ames Laboratory of the U. S. Atomic Energy Commission.

Any discussion of this paper will appear in a Discussion Section to be published in the June 1962 JOURNAL.

REFERENCES

1. F. R. Duke and A. L. Bowman, *This Journal*, **106**, 626 (1959).
2. F. R. Duke and E. D. Wolf, Work on the Alkaline Earth Chlorides, to be published.

Detroit Meeting

THE ELECTROCHEMICAL SOCIETY

October 1, 2, 3, 4, and 5, 1961

Sunday through Thursday

CONDENSED TECHNICAL PROGRAM

Monday, October 2, 1961

Battery—Corrosion (Abstracts 32-44) 9:00 A. M.-12:15-P.M.; 2:00-5:10 P.M. (Tuller Room, Hotel Tuller, 14th floor)
Electrodeposition (Abstracts 69-77) 9:00 A.M.-12:05 P.M.; 2:00-4:45 P.M. (Wayne Room, Ballroom floor, Statler-Hilton Hotel)
Electronics-Semiconductors (Abstracts 113-130) 9:00 A.M.-12 M.; 1:30-5:00 P. M. (Grand Ballroom, Statler-Hilton Hotel)
Electro-Organic (Abstracts 158-165) 9:00 A. M.-12:00 M.; 2:00-5:30 P.M. (English Room, Ballroom floor, Statler-Hilton Hotel)
Electrothermics and Metallurgy (Abstracts 179-186) 9:00 A.M.-12 M.; 2:00-5:00 P. M. (Bagley Room, Ballroom Floor, Statler-Hilton Hotel)

Tuesday, October 3, 1961

Battery (Abstracts 1-14) 9:00 A.M.-12:00 M.; 2:00-4:55 P.M. (Tuller Room, Hotel Tuller, 14th floor)
Corrosion (Abstracts 45-56) 9:00-11:40 A.M.; 2:00-4:40 P.M. (Michigan Room, Ballroom floor, Statler-Hilton Hotel)
Electrodeposition (Abstracts 79-90) 9:00 A. M.-12:00 M.; 2:00-5:00 P.M. (Wayne Room, Ballroom floor, Statler-Hilton Hotel)
Electronics-Semiconductors (Abstracts 131-143) 9:00 A.M.-12:00 M.; 2:10-5:00 P.M. (Grand Ballroom, Statler-Hilton Hotel)
Electro-Organic (Abstracts 166-171) 9:00 A.M.-12:10 P.M.; 2:00-5:00 P.M. (English Room, Ballroom floor, Statler-Hilton Hotel)
Electrothermics and Metallurgy (Abstracts 187-194) 9:00-11:20 A.M.; 2:00-4:30 P.M. (Bagley Room, Ballroom floor, Statler-Hilton Hotel)

Wednesday, October 4, 1961

Battery (Abstracts 15-25) 9:00 A.M.-12:00 M.; 2:00-5:00 P.M. (Wayne Room, Ballroom floor, Statler-Hilton Hotel)
Corrosion (Abstracts 57-68) 9:00-11:15 A.M.; 2:00-4:40 P.M. (Michigan Room, Ballroom floor, Statler-Hilton Hotel)
Electrodeposition (Abstracts 91-106) 9:00 A.M.-12:00 M. (Tuller Room, Hotel Tuller, 14th floor); 9:00 A.M.-12:00 M.; 2:00-5:00 P.M. (Bagley Room, Ballroom floor, Statler-Hilton Hotel)
Electronics-Semiconductors (Abstracts 144-157) 9:00 A.M.-12:00 M.; 1:30-5:00 P.M. (Arabian Ballroom, Hotel Tuller)
Electro-Organic (Abstracts 172-178) 9:00 A.M.-12:00 M.; 1:30-5:00 P.M. (English Room, Ballroom floor, Statler-Hilton Hotel)
Electrothermics and Metallurgy (Abstracts 195-200) 9:00-11:45 A.M. (Italian Room, Hotel Tuller)

Thursday, October 5, 1961

Battery (Abstracts 26-31) 9:00-11:55 A.M. (Wayne Room, Ballroom floor, Statler-Hilton Hotel)
Electrodeposition (Abstracts 107-112) 9:00 A.M.-12:00 M. (Bagley Room, Ballroom floor, Statler-Hilton Hotel)

GENERAL INFORMATION

Convention Headquarters is the Statler-Hilton Hotel, Grand Circus Park at Washington Blvd., Detroit 31, Mich.

Rates per day for rooms with shower are: single, $7.50-12.00; tub and shower $12.50-14.00; double, with shower, $13.00-16.00; with tub and shower $16.50-17.50; twin, with shower $13.50-19.50; with tub and shower, $20.50-29.00; small suites, $25.00 for one, 30.00 for two; large suites for one or two $38.50.

Requests for room reservations should be mailed to the Statler-Hilton Hotel, Grand Circus Park at Washington Blvd., Detroit 31, Mich. If accommodations are not available at the Statler-Hilton, the hotel will make suitable reservations for you at a nearby hotel at a comparable price.

BE SURE to state that you will be attending The Electrochemical Society Meeting. If your wife will be attending, be sure to so indicate on your request for reservations.

The Office of the Secretary is Parlor B, Ballroom floor.
The Detroit Local Section Office is Parlor D, Ballroom floor.
Ladies' Headquarters is the Ivory Room, Ballroom floor.

REGISTRATION

The Registration Desk will be in the Foyer, Ballroom floor Sunday, October 1 through Thursday, October 5, 1961.
The registration schedule is:

Sunday, October 1—2:00-9:00 P.M.
Monday, October 2—7:30 A.M.-5:00 P.M.
Tuesday, October 3—8:00 A.M.-4:00 P.M.
Wednesday, October 4—8:00 A.M.-4:00 P.M.
Thursday, October 5—9:00 A.M.-12:00 M.

Registration fees are:

Technical Session Registration (Men and Women)	
Members	$ 7.00
Nonmember Speakers and Coauthors	7.00
Nonmembers	20.00*
Student Members	Complimentary
Student Nonmembers	2.00
Thursday Only	5.00
Ladies' Registration Fee for Social Events	5.00

* If a nonmember fills out an application form and subsequently is elected to membership in the Society, the difference between the nonmember and member registration fee will be applied to his first year's dues. If his membership begins on January 1 he is entitled to the entire differential; if his membership begins on July 1, he is entitled to half the differential.

Most of the technical sessions will be held in various rooms on the Ballroom floor of the Statler-Hilton Hotel; however several sessions are scheduled in the Hotel Tuller, Grand Circus Park, across the street from the Statler-Hilton.

INFORMATION ABOUT DETROIT

"The Detroit News" recently circulated a Sunday supplement on the City of Detroit. We have lifted some information therefrom. Detroit's population is about 3,762,000; it is a region with 6438 plants manufacturing everything from gelatin capsules and milk carton machinery to electronic computers, space missiles, and, of course, automobiles. Detroit's assets are considerable: available skilled labor, abundant water supply, and three sources of natural gas; it is one of a few cities whose electric utility is building an atomic reactor to investigate the cheap power hope of the future.

To quote from the News Editorial: "Detroit wasn't really the 'Arsenal of Democracy'; it just turned out more war-winning tools than any other city in the world. It probably isn't the nation's best sports town, though it does have more pleasure boats than any other and (from Ty Cobb to Joe Louis and Gordie Howe) has had its share of champions. While it is true that 55 per cent of its manufacturing employes and 10 per cent of those in non-manufacturing employment belong to unions, it truly doesn't rate the attention it gets when a strike that spreads from Newark, Del., to Los Angeles is reported from the negotiation table in Detroit. Actually, in 1959, all strikes cost Detroit a loss of 55/100ths of 1 per cent of work time."

Detroit is the "birthplace" of the modern shopping center with its Northland Center, the first (built in 1954) and still the largest major regional shopping center in the nation, 110 stores on 161 acres of land, providing parking for 9500 cars. Besides its 27 shopping centers, it boasts an excellent school system, both private and public and has 54 institutions of higher learning in its metropolitan area. There's always something to do in Detroit: Detroit Institute of Art, theaters, baseball, football, basketball, hockey, skiing within an hour's drive of downtown Detroit, "largest fresh-water beach in the world," for example.

SYMPOSIA

The Battery Division has scheduled a Fuel Cell Symposium, Wednesday morning on Fuel Electrodes, Wednesday afternoon on Oxygen Electrodes, and Thursday morning on Fuel Cells, in the Wayne Room, Ballroom floor, Statler-Hilton Hotel. On Tuesday morning and afternoon General Sessions are scheduled in the Tuller Room, Hotel Tuller, 14th floor.

The Battery and the Corrosion Divisions have scheduled a Joint Symposium on Fused Salt Corrosion Monday morning and afternoon in the Tuller Room, Hotel Tuller, 14th floor.

The Corrosion Division has scheduled sessions on Corrosion and Inhibition in Aqueous Solution Tuesday morning; High-Temperature Oxidation Tuesday afternoon; and Surface Structure vs. Corrosion Behavior Wednesday morning and afternoon, all in the Michigan Room, Ballroom floor, Statler-Hilton Hotel.

The Electrodeposition Division has scheduled a Symposium on Effects of Addition Agents in Electrodeposition on Monday, Tuesday, and Wednesday morning, in the Wayne Room, Ballroom floor, Statler-Hilton Hotel, as well as a Symposium on Electrodeposited Magnetic Films all day Wednesday and Thursday morning, in the Tuller Room, 14th floor, Hotel Tuller, in addition to a few general papers.

Electronics Division-Semiconductor Group has scheduled sessions on: Semiconductor Surfaces Monday morning; Fabrication Technology Monday afternoon; Expitaxial Films all day Tuesday; Intermetallic Semiconductors Wednesday morning; and Elemental Semiconductors Wednesday afternoon; Monday and Tuesday sessions are in the Grand Ballroom, Statler-Hilton Hotel, and the Wednesday sessions are in the Arabian Ballroom, Hotel Tuller.

The Electro-Organic Division has scheduled general sessions on Monday and Wednesday and a Symposium on Organic Electrochemistry in Nonaqueous Solvents on Tuesday; all sessions in the English Room, Ballroom floor, Statler-Hilton Hotel.

The Electrothermics and Metallurgy Division has scheduled a Symposium on Sintering of Refractory Metals and Materials, Tungsten Monday morning, Refractory Metals Monday afternoon, Oxides Tuesday morning, Refractory Compounds Tuesday afternoon, (these in the Bagley Room, Ballroom floor, Statler-Hilton Hotel) as well as a session on Anodic Films and Properties of Carbides Wednesday morning in the Italian Room, Hotel Tuller.

BOARD AND COMMITTEE MEETINGS

(Statler-Hilton Hotel)

Sunday, Oct. 1, 2:00 P.M.—**Board of Directors,** Michigan Room, Ballroom floor.

Monday, Oct. 2, 12:15 P.M.—Luncheon Meeting of the **Membership Committee,** Parlor E, Ballroom floor.

Monday, Oct. 2, 2:00 P.M.—**National Convention Committee,** Parlor E, Ballroom floor.

Monday, Oct. 2, 5:00 P.M.—**Editorial Staff of the Journal,** Parlor F, Ballroom floor.

Monday, Oct. 2, 5:00 P.M.—**Council of Local Sections,** Parlor E, Ballroom floor.

Wednesday, Oct. 4, 12:15 P.M.—Luncheon Meeting of the **General Chairman of Future Meetings,** Parlor E, Ballroom floor.

LUNCHEONS, SOCIAL AFFAIRS, AND BUSINESS MEETINGS OF DIVISIONS

Monday, Oct. 2, 5:30 P.M.—**Electrothermics and Metallurgy Division** Cocktail Hour, Bagley Room, Ballroom floor, Statler-Hilton Hotel.

Tuesday, Oct. 3, 12:15 P.M.—**Battery Division** Luncheon and Business Meeting, Arabian Room, Tuller Hotel.

Tuesday, Oct. 3, 12:15 P.M.—**Electrodeposition Division** Luncheon and Business Meeting, Wayne Room, Ballroom floor, Statler-Hilton Hotel.

Tuesday, Oct. 3, 12:15 P.M.—**Electro-Organic Division** Luncheon and Business Meeting, Parlor F, Ballroom floor, Statler-Hilton Hotel.

Wednesday, Oct. 4, 12:15 P.M.—**Corrosion Division** Luncheon and Business Meeting, Michigan Room, Statler-Hilton Hotel.

GENERAL FUNCTIONS

(Statler-Hilton Hotel)

Symposia Chairmen Breakfasts

Special breakfasts will be held for Symposia Chairmen on Monday through Thursday, October 2 through 5. On the day on which he presides at a technical session, each Symposium Chairman should be in the Cafe Rouge, Lobby floor at 7:45 A.M.

Sunday Evening Social Hour

There will be a Sunday evening social gathering in the Wayne Room, Ballroom floor, from 8 to 10 P.M. All those registered for The Electrochemical Society Meeting are invited to attend.

Monday Evening Mixer

There will be a Monday evening social get-acquainted gathering in the Wayne Room, Ballroom floor, from 8:00 to 10:00 P.M. All those registered for The Electrochemical Society Meeting are invited to attend.

Tuesday Palladium Medal Lecture

On Tuesday, October 3, at 5:00 P.M., Professor H. H. Uhlig will deliver the Palladium Medal Lecture in the Wayne Room, Ballroom floor.

Tuesday Palladium Medal Reception and Banquet

On Tuesday, October 3, a reception and banquet will be held for the Palladium Medalist, Professor H. H. Uhlig. Cocktails will be served from 6:45 to 7:15 in the Ballroom; dinner will be served at 7:15 in the Ballroom.

PLANT TRIPS

Monday afternoon.—Two trips are planned for Monday afternoon, one to Parke, Davis & Co., the other to the Phoenix Project of the University of Michigan, Ann Arbor, a nuclear energy research and development program. Buses will leave the Bagley St. Statler-Hilton Hotel entrance at 1:00 P.M.

Wednesday afternoon.—A trip is planned to the Enrico Fermi Reactor Project of the Detroit Edison Co., Monroe, Mich. No clearance is necessary to visit this plant which generates electricity from nuclear energy. Buses will leave the Bagley St. Statler-Hilton Hotel entrance at 1:00 P.M.

Wednesday evening.—A visit is planned to the International Salt Co.; this trip is for the men only; mining custom does not permit women underground. Buses will leave the Bagley St. Statler-Hilton Hotel entrance at 7:30 P.M.

1962 SPRING MEETING
at the
Statler-Hilton Hotel
LOS ANGELES, CALIFORNIA
May 6, 7, 8, 9, and 10, 1962

Sessions probably will be scheduled on:

Electric Insulation
Electronics-Luminescence and Semiconductors
Electrothermics and Metallurgy
Industrial Electrolytic
Theoretical Electrochemistry

Abstracts for the Los Angeles Meeting *(not exceeding 75 words in length)* must reach Society Headquarters, 1860 Broadway, New York 23, N. Y., *not later than* December 15, 1961 to be included in the Los Angeles program. Please indicate on abstract for which Division's symposium the paper is to be scheduled and underline the name of the author who will present the paper. No paper will be placed on the program unless one of the authors, or a qualified person designated by the authors, has agreed to present it in person. An author who wishes his paper considered for publication in the JOURNAL should send triplicate copies of the manuscript to the Managing Editor of the "JOURNAL," 1860 Broadway, New York 23, N. Y.

Presentation of a paper at a technical meeting of the Society does not guarantee publication in the "JOURNAL." However, all papers so presented become the property of The Electrochemical Society and may not be published elsewhere, either in whole or in part, unless permission for release is requested of and granted by the Editor. Papers already published elsewhere, or submitted for publication elsewhere, are not acceptable for oral presentation except on invitation by a Divisional program Chairman.

LADIES' PROGRAM

The ladies are cordially invited to make the Ivory Room, Ballroom floor, Statler-Hilton Hotel, their headquarters during the meeting. A coffee hour will be held from 9:00-10:00 A.M. Monday, Tuesday, and Wednesday.

Sunday, Oct. 1—Registration from 2:00 to 9:00 P.M.

Monday, Oct. 2—Coffee hour from 9:00 to 10:00 in the Ivory Room followed by a trip to Greenfield Village in Dearborn. Buses will leave the Bagley St. Hotel entrance at 10:30 A.M. Lunch will be served at Lovett Hall. If the weather should be extremely bad, the ladies will visit the Henry Ford Museum instead to see replicas of old shops, genuine antique cars and furniture. Monday evening the ladies may attend the mixer from 8:00-10:00.

Tuesday, Oct 3—Coffee hour from 9:00 to 10:00 A.M. Tuesday morning and afternoon are free to enjoy Detroit's many facilities. Ladies are invited to attend the Palladium Medal Reception and Banquet at 6:45 P.M.

Wednesday, Oct. 4—Coffee hour from 9:00 to 10:00 A.M., followed by a bus tour of Detroit's Cultural Center and downtown. Lunch will be served at J. L. Hudson's during a style show. Buses will leave the Bagley St. Hotel entrance at 10:30 A.M.

COST OF VARIOUS FUNCTIONS

(other than registration)

Please buy tickets as early as possible.

Symposia Chairmen Breakfasts	Standard menu prices
Sunday Evening Social Hour	Complimentary
Monday Electrothermics and Metallurgy Division Cocktail Hour	1.50
Monday Evening Mixer	Complimentary
Division Luncheons	$3.75
Tuesday Palladium Medal Reception and Banquet:	
Men	9.00
Ladies	7.00
Ladies' Social Functions:	
Monday	3.50
Wednesday	1.00
Plant Trips:	
Monday	1.50
Wednesday afternoon	1.75
Wednesday evening	1.25

JOURNALS

Copies of the July, August, and September issues of "The Journal of The Electrochemical Society" will be available at the Registration Desk. The price of a single copy of the "Journal" is $1.70 to members and $2.25 to nonmembers.

EXTENDED ABSTRACTS

The Battery Division is making available an extended abstract booklet containing 1000-word abstracts of most of the papers presented at the Division's Detroit Meeting. Copies of the booklet may be obtained from C. H. Clark, 34 Pleasant Way, Deal, N. J., after Sept. 15 for $2.00 each.

The Electrodeposition Division is preparing an extended abstract booklet containing 1000-word and 2000-word abstracts of the two symposia, Symposium on the Effect of Addition Agents in Electrodeposition and the Symposium on Electrodeposited Magnetic Films. Copies will be available at the Registration Desk or may be obtained by mail after Sept. 1 by sending an order **accompanied by check or money order** for $3.00 to Dan Trivich, Secretary-Treasurer of the Electrodeposition Division, Department of Chemistry, Wayne State University, Detroit 2, Michigan.

DISCUSSION

No recordings will be made of oral discussion. Those contributing to the discussion of a paper and desiring their remarks to be published will be supplied by the symposium chairman with a printed form on which any discussion may be written. These forms should be given to the symposium chairman or to the Managing Editor of the Journal after the session; or they can be mailed to the Managing Editor of the Journal, 1860 Broadway, New York 23, N. Y. The discussion will then be referred to the author for reply. Publication of the discussion and the comments of the author depends on publication of the article in the "Journal."

Written discussion of a published paper should be submitted within two months following publication of the article in the "Journal." A Discussion Section is published semi-annually in the "Journal."

EMPLOYMENT POSTERS

Companies which desire to recruit employees at the Detroit Meeting will have posters to this effect on a Bulletin Board adjacent to the Registration Desks (see Registration for location). Companies are requested to confine their announcements to this Bulletin Board.

NOTE

Photographing of lantern slides, charts, etc., will be permitted unless specifically prohibited by the speaker. Photo flash and photo floods are prohibited.

Technical Program—Detroit Meeting

Monday A.M., October 2, 1961

BATTERY-CORROSION

Joint Symposium on Fused Salt Corrosion, with Henry Leidheiser presiding

(TULLER ROOM, Hotel Tuller, 14th floor)

9:00 A.M.—Introductory Remarks

9:15 A.M.—"Solutions of Metals in Fused Salts" by Daniel Cubicciotti (Abstract No. 32)

10:00 A.M.—"The Formation Potential of Lithium Chloride" by R. D. Walker, Jr., and W. K. Smith (Abstract No. 33)

10:25 A.M.—"Etching of Silver Single Crystals in Fused Sodium Chloride" by K. H. Stern and Jerome Kruger (Abstract No. 34)

10:50 A.M.—Ten-minute intermission

11:00 A.M.—"Corrosion Associated with the ORNL Fused Salt Fluoride Volatility Process" by A. P. Litman and R. P. Milford (Abstract No. 35)

11:25 A.M.—"Corrosion Behavior of High-Temperature Alloys in Fused Fluoride Mixtures" by J. H. DeVan (Abstract No. 36)

11:50 A.M.—"Corrosion of Metals in Molten Sodium Polyphosphate" by L. F. Grantham, M. A. Hiller, and W. S. Ginell (Abstract No. 37)

ELECTRODEPOSITION

Effects of Addition Agents in Electrodeposition, with D. Trivich presiding

(WAYNE ROOM, Ballroom floor, Statler-Hilton Hotel)

9:00 A.M.—Introductory Remarks

9:05 A.M.—"The Role of Addition Agents in Bright Nickel Plating" by H. Brown (Abstract No. 69)

MEETING ROOM SCHEDULE

Meeting	Monday		Tuesday		Wednesday		Thursday	
	A.M.	P.M.	A.M.	P.M.	A.M.	P.M.	A.M.	P.M.
Battery			T	T	B	B	B	
Joint Battery—Corrosion	T	T						
Corrosion			D	D	D	D		
Electrodeposition	B	B	B	B	T			
					C	C	C	
Electronics—Semiconductors	A	A	A	A	F	F		
Electro-Organic	E	E	E	E	E	E		
Electrothermics and Metallurgy	C	C	C	C	G			

Statler Hilton Hotel
A—Grand Ballroom
B—Wayne Room
C—Bagley Room
D—Michigan Room
E—English Room

Hotel Tuller
G—Italian Room
F—Arabian Ballroom
T—Tuller Room, 14th floor

9:50 A.M.—"Kinetics of Electrode Processes in Relation to Electrodeposition" by B. E. Conway (Abstract No. 70)
10:35 A.M.—"Crystal Growth and the Structure of Electrodeposits" by S. C. Barnes, J. P. G. Farr, and H. J. Pick (Abstract No. 71)
11:20 A.M.—"Theories of Addition Agents in Electrodeposition" by Eugenio Bertorelle (Abstract No. 72)

ELECTRONICS-SEMICONDUCTORS

Semiconductor Surfaces, with Willis Adcock presiding

(GRAND BALLROOM, Statler-Hilton Hotel)

9:00 A.M.—"The Study of Some Uncommon Surface Treatments on Germanium" by W. A. Albers, Jr., and A. M. Rickel (Abstract No. 113)
9:20 A.M.—"An Impurity Surface State at the Germanium-Aqueous Electrolyte Interface" by P. J. Boddy and W. H. Brattain (Abstract No. 114)
9:40 A.M.—"Diffusion Masking of Silicon and Germanium by the Evaporation of Silicon Monoxide" by Bernard Kriegsman and Karabet Simonyan (Abstract No. 115)
10:00 A.M.—"Open Tube Diffusion of Phosphorus in Silicon" by W. J. Greig and J. C. Sarace (Abstract No. 116)
10:20 A.M.—"Evaluation of the Surface Concentration of Diffused Impurity Layers in Silicon" by O. N. Tufts (Abstract No. 117)
10:40 A.M.—"The Effect of Silicon Surface Treatment on Metallic Impurity Deposition" by G. B. Larrabee (Abstract No. 118)
11:00 A.M.—"Passivated Silicon Devices" by C. H. Li (Abstract No. 119)
11:20 A.M.—"Measurement of the Thickness and Refractive Index of Surface Oxide Films on Semiconductor Materials" by G. R. Booker and C. E. Benjamin (Abstract No. 120)
11:40 A.M.—"Hysteresis in the Large-Signal Field Effect in Semiconductor Surfaces" by D. R. Frankl (Abstract No. 121)

ELECTRO-ORGANIC

General Session, with Christopher Wilson presiding

(ENGLISH ROOM, Ballroom floor, Statler-Hilton Hotel)

9:00 A.M.—"Improvement in the Electrolytic Preparation of Iodoform" by R. Ramaswamy, M. S. Venkatachalopathy, and H. V. K. Udupa (Abstract No. 158)
9:30 A.M.—"Electrolytically Regenerated Manganic Sulfate for the Oxidation of Aromatic Hydrocarbons, II. Oxidation of Xylenes to Tolualdehydes" by R. Ramaswamy, M. S. Venkatachalapathy, and H. V. K. Udupa (Abstract No. 159)
10:00 A.M.—"Stereochemistry of Electrolytic Reductions of Butynediol and Cyclohexene-1,2-Dicarboxylic Acid" by George Brownell and C. L. Wilson (Abstract No. 160)
11:00 A.M.—"Electrolytic Formation of Oximes" by Tadao Hayashi and C. L. Wilson (Abstract No. 161)

ELECTROTHERMICS AND METALLURGY

Sintering of Refractory Metals and Materials, I. Tungsten, with W. W. Trainor presiding

(BAGLEY ROOM, Ballroom floor, Statler-Hilton Hotel)

9:00 A.M.—"Progress in Sintering," Keynote Address by D. L. Wilder (Abstract No. 179)
9:55 A.M.—"Some Effects of Powder Properties and Consolidation Technique on the Properties of Sintered Tungsten Compacts" by G. C. Bodine (Abstract No. 180)
10:30 A.M.—Twenty-minute intermission
10:50 A.M.—"Activated Sintering of Tungsten" by J. H. Brophy, H. W. Hayden, and J. Wulff (Abstract No. 181)
11:25 A.M.—"Sintering Characteristics of Ultrafine Tungsten Powder" by C. R. McKinsey (Abstract No. 182)

Monday P.M., October 2, 1961

BATTERY—CORROSION

Joint Symposium on Fused Salt Corrosion and High-Temperature Fuel Cells, with E. J. Ritchie presiding

(TULLER ROOM, Hotel Tuller, 14th floor)

2:00 P.M.—"The Thermally Regenerative Liquid Metal Cell" by B. Agruss (Abstract No. 38)
2:25 P.M.—"The Sodium|Tin Liquid-Metal Cell, A Preliminary Study" by R. D. Weaver, S. W. Smith, and N. L. Willmann (Abstract No. 39)
2:50 P.M.—"The Liquid-Metal Cell as an Energy Storage Device for Satellite Application" by E. H. Hietbrink and B. Agruss (Abstract No. 40)
3:15 P.M.—"The Lithium Hydride Electrode" by M. E. Indig and R. N. Snyder (Abstract No. 41)
3:40 P.M.—Ten-minute intermission
3:50 P.M.—"High-Temperature Fuel Cells" by M. L. Kronenberg (Abstract No. 42)
4:15 P.M.—"Electrical and Chemical Characteristics of a Hydrocarbon Fuel Cell of the Fused Carbonate Type" by Y. L. Sandler (Abstract No. 43)
4:40 P.M.—"Ionic Conduction in $(ZrO_2)_{.85}$ $(CaO)_{.15}$" by J. Weissbart and R. Ruka (Abstract No. 44)

ELECTRODEPOSITION

Effects of Addition Agents in Electrodeposition (cont'd), with Seward Beacom presiding

(WAYNE ROOM, Ballroom floor, Statler-Hilton Hotel)

2:00 P.M.—"Effects of Addition Agents on Physical and Mechanical Properties of Electrodeposits" by H. J. Read (Abstract No. 73)
2:45 P.M.—"X-Ray Determination of Residual Stresses in Electrodeposited Coatings" by G. W. Bush and H. J. Read (Abstract No. 74)
3:15 P.M.—"Electron Microscopic Observations of the Structure of Electroplated Nickel" by R. Weil and H. C. Cook (Abstract No. 75)
3:45 P.M.—"The Influence of Adsorbed Material on the Growth of the Metallic Lattice" by T. P. Hoar (Abstract No. 76)
4:15 P.M.—"Evidence for the Deposition of Very Complex Cations" by F. C. Mathers (Abstract No. 77)

ELECTRONICS-SEMICONDUCTORS

Fabrication Technology, with A. Rose presiding

(GRAND BALLROOM, Statler-Hilton Hotel)

1:30 P.M.—"Electrolytic Slicing of Germanium, II. Characteristics of the {110} and {100} n- and p-type Surfaces" by Sumner Sheff (Abstract No. 122)
1:50 P.M.—"Further Study by Electron Microscopy and Diffraction of Germanium Surfaces from Electrolytic Slicing" by J. J. Oberly (Abstract No. 123)
2:10 P.M.—"Spreading during Capillary Alloying" by Karl Busen, Kurt Lehovec, and Raynor Linzey (Abstract No. 124)
2:30 P.M.—"The Spreading of Molten Indium on Germanium" by A. A. Bergh (Abstract No. 125)
2:50 P.M.—"Characteristics of Porous Vycor as a Moisture Getter in Semiconductor Devices" by M. J. Rand (Abstract No. 126)
3:10 P.M.—"Fabrication of Ultra Fast Switching Tunnel Diodes" by H. C. Schindler (Abstract No. 127)
3:30 P.M.—"Automatic Custom Etching of Tunnel Diodes" by V. Vulcan (Abstract No. 128)
3:50 P.M.—"A Very Low Current Controlled Rectifier; Some Problems of Design and Fabrication" by C. W. Heath W. M. Robinson (Abstract No. 129)
4:10 P.M.—"Photolithography Applied to Silicon Transistor Technology" by J. Spanos (Abstract No. 130)
4:30 P.M.—Recent News Papers. Titles and short abstracts will be available at the meeting.

ELECTRO-ORGANIC

General Session, with Christopher Wilson presiding

(ENGLISH ROOM, Ballroom floor, Statler-Hilton Hotel)

2:00 P.M.—"New Study on the Electrolytic Reduction of Dicyandiamide. An Approach to the Essential Problem on Organic Electrode Process" by Kiichiro Sugino, Keijiro Odo, and Eiichi Ichikawa (Abstract No. 162)
2:30 P.M.—"A Continuous Flow Cell for Electrochemical Synthesis" by M. J. Allen (Abstract No. 163)
3:30 P.M.—"Voltammetric Study of the Kolbe Reaction" by M. J. Allen and W. W. Pierson (Abstract No. 164)
4:30 P.M.—"Anhydrous Voltammetry of the Acetate Ion at a Rotating Platinum Anode" by M. J. Allen and W. W. Pierson (Abstract No. 165)

ELECTROTHERMICS AND METALLURGY

Sintering of Refractory Metals and Materials, II. Refractory Metals, with E. M. Sherwood presiding

(BAGLEY ROOM, Ballroom floor, Statler-Hilton Hotel)

2:00 P.M.—"Fourth Plansee Seminar" by H. A. Johansen (Abstract No. 183)

2:40 P.M.—"Sintering of Pressureless Compacted Tungsten and Molybdenum" by H. H. Hausner and A. R. Poster (Abstract No. 184)
3:20 P.M.—"Sintering of Slip Cast Tungsten" by F. R. Charvat, and G. Reinhardt (Abstract No. 184A)
3:45 P.M.—"Plasma Spraying of Tungsten and Refractory Compounds and the Influence of Sintering on the Physical Properties of These Materials" by Irving Strauss and Robert Steinitz (Abstract No. 185)
4:25 P.M.—"Preparation of F48 Alloy by Means of Hydrostatic Pressing and Vacuum Sintering" by J. W. Pugh and J. F. Cerness (Abstract No. 186)
5:30 P.M.—Electrothermics and Metallurgy Division Cocktail Hour, Bagley Room, Ballroom floor, Statler-Hilton Hotel.

Tuesday A.M., October 3, 1961

BATTERY

General Session with Jeanne Burbank presiding

(TULLER ROOM, Hotel Tuller, 14th floor)

9:00 A.M.—Opening Remarks
9:05 A.M.—"The Operation and Use of Reference Cells" by N. C. Cahoon (Abstract No. 1)
9:25 A.M.—"Studies of Voltaic Cell Discharge by Polarization Oscillography" by R. E. Panzer, W. S. Harris, and W. C. Spindler (Abstract No. 2)
9:50 A.M.—"Determination of the Internal Resistance of Leclanche Cells by Square Wave Method" by Aladar Tvarusko (Abstract No. 3)
10:15 A.M.—"Alkaline Manganese Dioxide-Zinc Batteries" by J. L. S. Daley (Abstract No. 4)
10:40 A.M.—Ten-minute intermission
10:50 A.M.—"Solubility of Silver Oxides in Alkaline Solutions" by Stanley Hills (Abstract No. 5)
11:15 A.M.—"The AgO/Ag_2O Electrode in Alkaline Solutions" by T. P. Dirkse (Abstract No. 6)
11:40 A.M.—"A New Design for the Silver-Cadmium Battery" by P. L. Howard (Abstract No. 7)
12:15 P.M.—Battery Division Luncheon and Business Meeting, Arabian Room, Hotel Tuller.

CORROSION

Corrosion and Inhibition in Aqueous Solution, with R. Powers presiding

(MICHIGAN ROOM, Ballroom floor, Statler-Hilton Hotel)

9:00 A.M.—"Some Recent Developments in Inhibitor Theory" by Norman Hackerman (Abstract No. 45)
9:25 A.M.—"Corrosion Inhibition by Metallic Cations" by Henry Leidheiser, Jr. (Abstract No. 46)
9:50 A.M.—"Uniform and Pitting Corrosion of 3003 Aluminum in Aerated Citrate Buffer Solution" by E. L. Koehler and S. Evans (Abstract No. 47)
10:15 A.M.—Ten-minute intermission
10:25 A.M.—"The Polarization of Metals in Distilled Water" by F. E. DeBoer, J. E. Draley, and C. A. Youngdahl (Abstract No. 48)
10:50 A.M.—"Effect of Partial Dissolution of the Oxide Film on the Aqueous Corrosion Resistance of Zircaloy-2" by S. Kass and D. B. Scott (Abstract No. 49)
11:15 A.M.—"Corrosion and Electrochemical Behavior of Chromium-Noble Metal Alloys" by N. D. Greene, C. R. Bishop, and M. Stern (Abstract No. 50)

ELECTRODEPOSITION

Effects of Addition Agents in Electrodeposition (cont'd), with D. G. Foulke presiding

(WAYNE ROOM, Ballroom floor, Statler-Hilton Hotel)

9:00 A.M.—"The Growth of Zinc and Other Electrodeposits" by J. M. Keen and J. P. G. Farr (Abstract No. 79)
9:30 A.M.—"The Effect of Thio-Compounds on the Structure of Copper Electrodeposits" by S. C. Barnes (Abstract No. 80)
10:00 A.M.—"Rotating Disk Electrode Techniques for the Study of Addition Agents" by S. E. Beacom and R. N. Hollyer, Jr. (Abstract No. 81)
10:30 A.M.—"The Effect of Some Addition Agents on the Kinetics of Copper Electrodeposition from a Sulfate Solution, I. Cathode Potential-Current Density Relation" by D. R. Turner and G. R. Johnson (Abstract No. 82)
11:00 A.M.—"The Effect of Some Addition Agents on the Kinetics of Copper Electrodeposition from a Sulfate Solution, II. Rotating Disk Electrode Experiments" by G. R. Johnson and D. R. Turner (Abstract No. 83)
11:30 A.M.—"Some Structural Aspects of Nickel Electroplates" by L. P. Bicelli and G. Serravalle (Abstract No. 84)
12:15 P.M.—Electrodeposition Division Luncheon and Business Meeting, Bagley Room, Ballroom floor, Statler-Hilton Hotel.

ELECTRONICS-SEMICONDUCTORS

Epitaxial Films, with Pei Wang presiding

(GRAND BALLROOM, Statler-Hilton Hotel)

9:00 A.M.—"Epitaxial Silicon Thin Films" by K. J. Miller and R. C. Manz (Abstract No. 131)
9:20 A.M.—"Epitaxial Growth of Silicon" by C. H. Li and D. Scaringella (Abstract No. 132)
9:40 A.M.—"Epitaxial Deposition of Silicon in a Hot-Tube Furnace" by B. E. Deal (Abstract No. 133)
10:00 A.M.—"Properties of Epitaxially Grown Silicon Crystals" by C. J. Marlett and P. A. Newman (Abstract No. 134)
10:20 A.M.—"Impurity Control and Distribution in Epitaxial Silicon Films" by D. Kahng, R. C. Manz, M. M. Atalla, and C. O. Thomas (Abstract No. 135)
10:40 A.M.—"Methods for Measuring Resistivity Gradients and Thicknesses in Epitaxial Films" by J. E. McNamara and H. M. Robertson (Abstract No. 136)
11:00 A.M.—Recent News Papers. Titles and short abstracts will be available at the meeting.

ELECTRO-ORGANIC

Organic Electrochemistry in Nonaqueous Solvents, with S. Wawzonek presiding

(ENGLISH ROOM, Ballroom floor, Statler-Hilton Hotel)

9:00 A.M.—Introductory Remarks
9:10 A.M.—"Electrode Processes in Acetonitrile" by D. H. Geske (Abstract No. 166)
10:10 A.M.—"The Role of Proton Addition in the Polarographic Reduction of Aromatic Hydrocarbons and Carbonyl Compounds in Dimethylformamide" by P. H. Given (Abstract No. 167)
11:10 A.M.—"Polarography and Voltammetry in Dimethylsulfoxide" by I. M. Kolthoff and T. B. Reddy (Abstract No. 168)
12:15 P.M.—Electro-Organic Division Luncheon and Business Meeting, Parlor F, Ballroom floor, Statler-Hilton Hotel.

ELECTROTHERMICS AND METALLURGY

Sintering of Refractory Metals and Materials, III. Oxides, with Donald Hansen presiding

(BAGLEY ROOM, Ballroom floor, Statler-Hilton Hotel)

9:00 A.M.—"Sintering of Oxides" by G. C. Kuczynski (Abstract No. 187)
9:30 A.M.—"A Study of the Sintering Behavior of Some Uranium Dioxide Powders" by J. C. Clayton and L. Berrin (Abstract No. 188)
10:00 A.M.—Twenty-minute intermission
10:20 A.M.—"High-Temperature Electrical Conduction in the System UO_2-ZrO_2" by H. A. Johansen and J. G. Cleary (Abstract No. 189)
10:50 A.M.—"Sintering Kinetics of Linde A Al_2O_3" by C. A. Bruch (Abstract No. 190)

Tuesday P.M., October 3, 1961

BATTERY

General Session, with C. H. Clark presiding

(TULLER ROOM, Hotel Tuller, 14th floor)

2:00 P.M.—"The Runaway Condition in Sealed Nickel-Cadmium Cells and the Characteristics of Sealed Cells with Plastic Electrodes" by A. J. Salkind and J. C. Duddy (Abstract No. 8)
2:25 P.M.—"The 'Vicious Cycle' in Secondary Batteries, A Mathematical Approach" by W. G. Eicke, Jr. (Abstract No. 9)
2:50 P.M.—"Oxygen Evolution from Heavily Doped Nickel Oxide Electrodes" by H. N. Seiger and R. C. Shair (Abstract No. 10)
3:15 P.M.—Five-minute intermission
3:20 P.M.—"Variation of Microstructure in Storage Battery Plates with Method of Forming, I" by A. C. Simon and E. L. Jones (Abstract No. 11)
3:45 P.M.—"Variation of Microstructure in Storage Battery Plates with Method of Operation and Manufacture, II" by A. C. Simon and E. L. Jones (Abstract No. 12)

4:05 P.M.—"Porosity, Air Permeability, and Electrical Resistance of Storage Battery Separators" by W. S. Bundy (Abstract No. 13)
4:25 P.M.—"Battery Design-Current Density Distribution in a Cell" by C. M. Shepherd (Abstract No. 14)
5:00 P.M.—The Palladium Medal Address by H. H. Uhlig in the Wayne Room, Ballroom floor, Statler-Hilton Hotel.

CORROSION

High-Temperature Oxidation, with C. V. King presiding

(MICHIGAN ROOM, Ballroom floor, Statler-Hilton Hotel)

2:00 P.M.—"The Role of a Displacement Reaction in the Kinetics of Oxidation of Alloys" by R. L. Levin and J. B. Wagner, Jr. (Abstract No. 51)
2:25 P.M.—"Oxidation Kinetics of $ZrBe_{13}$ and $NbBe_{12}$" by Guy Ervin, Jr. (Abstract No. 52)
2:50 P.M.—"Corrosion of Zirconium Alloys in Superheated Steam" by R. D. Misch and Sherman Greenberg (Abstract No. 53)
3:15 P.M.—Ten-minute intermission
3:25 P.M.—"Oxidation of Refractory Metals as a Function of Pressure, Temperature, and Time: Tungsten in Oxygen" by J. N. Ong, Jr. (Abstract No. 54)
3:50 P.M.—"High-Temperature Oxidation of Fe-Cr Base Alloys, with Particular Reference to Fe-Cr-Y Alloys" by E. J. Felten (Abstract No. 55)
4:15 P.M.—"The Difference Effect and Anodic Behavior of Hafnium Dissolving in Hydrofluoric Acid" by W. J. James, M. E. Straumanis, and J. W. Johnson (Abstract No. 56)
5:00 P.M.—Palladium Medal Address by H. H. Uhlig in the Wayne Room, Ballroom floor, Statler-Hilton Hotel.

ELECTRODEPOSITION

Effects of Addition Agents in Electrodeposition (cont'd), with D. R. Turner presiding

(WAYNE ROOM, Ballroom floor, Statler-Hilton Hotel)

2:00 P.M.—"The Effect of Addition Agents on the Structure and Physical Properties of Gold Electrodeposits" by D. G. Foulke (Abstract No. 85)
2:30 P.M.—"Radiotracer Studies of the Uptake of Sulfur from Brightener Compounds by Copper and Nickel" by J. J. Hoekstra and Dan Trivich (Abstract No. 86)
3:00 P.M.—"A Study of Laminations in Bright Nickel Electrodeposits" by Nicholas Vanderkooi and Dan Trivich (Abstract No. 87)
3:30 P.M.—"The Effects of Organic Additives on the Kinetics of Tin Deposition" by Ernest Yeager, Frank Hovorka, and Stuart Meibuhr (Abstract No. 88)
4:00 P.M.—"Experimental Observations on the Behavior of Addition Agents in Bright Nickel Plating" by I. R. Bellobono and Eugenio Bertorelle (Abstract No. 89)
4:30 P.M.—"Effect of Addition Agents on the Formation of the Bright Deposit from Zn-, Cd-, and Ag-Cyanide Baths" by Tadao Hayashi and Takeo Ishida (Abstract No. 90)
5:00 P.M.—Palladium Medal Address by H. H. Uhlig, Wayne Room, Ballroom floor, Statler-Hilton Hotel.

ELECTRONICS-SEMICONDUCTORS

Epitaxial Films (cont'd), with C. O. Thomas presiding

(GRAND BALLROOM, Statler-Hilton Hotel)

2:10 P.M.—"Surface Effects and Autodoping in Epitaxial Germanium Layers" by E. Matovich and R. J. Andres (Abstract No. 137)
2:30 P.M.—"Evaluation of Germanium Epitaxial Films" by J. R. Biard and S. B. Watelski (Abstract No. 138)
2:50 P.M.—"Some Properties of Epitaxial Germanium" by A. B. Kuper and H. Christensen (Abstract No. 139)
3:10 P.M.—"Vapor Growth of GaAs" by V. J. Lyons and V. J. Silvestri (Abstract No. 140)
3:30 P.M.—"Mechanism for the Vapor Transport of Gallium Arsenide with Hydrogen Chloride" by F. V. Williams and R. A. Ruehrwein (Abstract No. 141)
3:50 P.M.—"An Open Tube Carrier Gas Method for the Epitaxial Growth of Gallium Phosphide" by C. J. Frosch and P. W. Foy (Abstract No. 142)
4:10 P.M.—"Vapor Phase Growth of GaAs and GaP" by R. R. Moest and B. R. Shupp (Abstract No. 143)
4:30 P.M.—Recent News Papers. Titles and short abstracts will be available at the meeting.
5:00 P.M.—Palladium Medal Address by H. H. Uhlig, Wayne Room, Ballroom floor, Statler-Hilton Hotel.

ELECTRO-ORGANIC

Organic Electrochemistry in Nonaqueous Solvents (cont'd), with S. Wawzonek presiding

(ENGLISH ROOM, Ballroom floor, Statler-Hilton Hotel)

2:00 P.M.—"Voltammetry in Liquid Sulfur Dioxide" by P. J. Elving and Elio Vianello (Abstract No. 169)
3:00 P.M.—"The Uses of Electrical Methods in Organometal Systems" by R. E. Dessy, Rudolf Salinger, and Richard Jones (Abstract No. 170)
4:00 P.M.—"Electrochemical Preparation of Polyfluoro Chemicals in Anhydrous HF" by R. D. Dresdner (Abstract No. 171)
5:00 P.M.—Palladium Medal Address by H. H. Uhlig, Wayne Room, Ballroom floor, Statler-Hilton Hotel.

ELECTROTHERMICS AND METALLURGY

Sintering of Refractory Metals and Materials, IV. Refractory Compounds, with A. C. Haskell presiding

(BAGLEY ROOM, Ballroom floor, Statler-Hilton Hotel)

2:00 P.M.—"Sintering of Hafnium Carbide with a Fugitive Metal Binder" by Charles Zalabak (Abstract No. 191)
2:30 P.M.—"Sintering of Pure SiC" by G. R. Watson and J. I. Fredriksson (Abstract No. 192)
3:00 P.M.—Half-hour intermission
3:30 P.M.—"Furnaces, Supports, and Atmospheres for the Sintering of Some Borides, Nitrides, and Silicides" by A. Blum (Abstract No. 193)
4:00 P.M.—"The Sintering of Dense, Fine-Grained Beryllides" by R. S. Truesdale, B. B. Lympany, and W. W. Beaver (Abstract No. 194)
5:00 P.M.—Palladium Medal Address by H. H. Uhlig, Wayne Room, Ballroom floor, Statler-Hilton Hotel.

Wednesday A.M., October 4, 1961

BATTERY

Fuel Cell Symposium: Fuel Electrodes, with Ernest Yeager presiding

(WAYNE ROOM, Ballroom floor, Statler-Hilton Hotel)

9:00 A.M.—Introductory Remarks
9:05 A.M.—"Chemisorption in Gas Electrode Reactions" by G. J. Young and J. R. Moser (Abstract No. 15)
9:35 A.M.—"The Electromotive Activity of Electrolytically Deposited Hydrogen at Carbon Electrodes" by H. F. Hunger (Abstract No. 16)
10:00 A.M.—"Chronopotentiometry of the Alcohol Fuel Electrode" by Manuel Shaw and W. J. Subcasky (Abstract No. 17)
10:25 A.M.—Ten-minute intermission
10:35 A.M.—"Voltammetric and Chronopotentiometric Study of the Anodic Oxidation of Methanol, Formaldehyde, and Formic Acid" by R. P. Buck and L. R. Griffith (Abstract No. 18)
11:05 A.M.—"The Electrochemical Oxidation of Methanol in Acid Electrolyte" by D. E. Icenhower and A. P. Bond (Abstract No. 19)
11:30 A.M.—"Raney Type Transition Metals as Fuel Electrode Catalysts" by H. Krupp, H. Rabenhorst, G. Sandstede, G. Walter, and R. McJones (Abstract No. 20)

CORROSION

Surface Structure vs. Corrosion Behavior, with F. W. Fink presiding

(MICHIGAN ROOM, Ballroom floor, Statler-Hilton Hotel)

9:00 A.M.—"The Nature of Oxide Films on Single Crystal Iron Whisker Surfaces" by J. V. Laukonis (Abstract No. 57)
9:25 A.M.—"The Isolation of Surface Films from Copper" by A. F. Beck and M. J. Pryor (Abstract No. 58)
9:50 A.M.—"Pitting Corrosion of Stainless Steels" by K. Hino (Abstract No. 59)
10:15 A.M.—Ten-minute intermission
10:25 A.M.—"A Comparative Study of the Morphology of Etched Aluminum Foils" by R. Bakish and E. Z. Borders (Abstract No. 60)
10:50 A.M.—"The Anodic Dissolution of Alloys" by R. F. Steigerwald and N. D. Greene (Abstract No. 61)
12:15 P.M.—Corrosion Division Luncheon and Business Meeting, Michigan Room, Statler-Hilton Hotel.

ELECTRODEPOSITION

Effects of Addition Agents in Electrodeposition (cont'd), with Heinz Gerischer presiding

(TULLER ROOM, Hotel Tuller, 14th floor)

9:00 A.M.—"Mechanism of Addition Agent Reaction in Bright and Leveling Nickel Deposition as Studied with Radioactively Tagged Compounds" by B. J. Riley and S. E. Beacom (Abstract No. 91)

9:30 A.M.—"Effect of Organic Additives on the Hydrogen Absorbed by Iron" by T. C. Franklin and Fujio Matsuda (Abstract No. 92)

10:00 A.M.—"Bismuth Electroplating" by J. G. Beach (Abstract No. 93)

10:30 A.M.—Round-Table Discussion

General Paper

11:30 A.M.—"A Cell for Plating Corrosion Test Panels with Varying Current Densities" by A. A. Johnson (Abstract No. 94)

ELECTRODEPOSITION

Electrodeposited Magnetic Films, with D. C. Wendell, Jr., presiding

(BAGLEY ROOM, Ballroom floor, Statler-Hilton Hotel)

9:00 A.M.—"Introduction to Magnetic Phenomena of Soft Magnetic Thin Films" by Rexford Alexander (Abstract No. 95)

9:30 A.M.—"A Method of Preparing Iron-Nickel Films and Some of Their Properties" by P. Kuttner and D. Clemson (Abstract No. 96)

10:00 A.M.—"Stress Reducing Organic Additives in the Sulfate-Chloride Bath for Iron-Nickel Deposition" by I. W. Wolf (Abstract No. 97)

10:30 A.M.—"A Discussion of Electrodeposited, Cylindrical Film Memory Elements" by T. R. Long (Abstract No. 98)

11:00 A.M.—"Magnetic Properties of a 97Fe-3Ni Thin Film Electroplate" by H. J. White and A. J. Kolk (Abstract No. 99)

11:30 A.M.—"Electrodeposited Magnetic Films for Computer Memories by Jet-Cell Plating in High Magnetic Fields" by J. H. Glaser and W. W. Richardson (Abstract No. 100)

ELECTRONICS-SEMICONDUCTORS

Intermetallic Semiconductors; with P. Pollack presiding

(ARABIAN BALLROOM, Hotel Tuller)

9:00 A.M.—"The Pseudobinary System Mg_2Si-Mg_2Ge" by R. J. LaBotz and D. R. Mason (Abstract No. 144)

9:20 A.M.—"Impurity Distribution in Single Crystal Indium Antimonide" by G. R. Cronin (Abstract No. 145)

9:40 A.M.—"Distribution of Sulfur Impurity in InSb Single Crystals" by M. D. Banus and H. C. Gatos (Abstract No. 146)

10:00 A.M.—"Correlation of Electrical Measurements and Chemical Analyses of Zinc- and Cadmium-Diffused GaAs" by J. F. Black (Abstract No. 147)

10:20 A.M.—"Correlation of Lattice Parameter Measurements and Electrical Measurements in Highly Doped GaAs" by J. F. Black and P. Lublin (Abstract No. 148)

10:40 A.M.—Recent News Papers. Titles and short abstracts will be available at the meeting.

ELECTRO-ORGANIC

General session, with M. J. Allen presiding

(ENGLISH ROOM, Ballroom floor, Statler-Hilton Hotel)

9:00 A.M.—"Polarographic Studies in Acetonitrile and Dimethylformamide, VII. Behavior of Benzyl Halides and Related Compounds" by S. Wawzonek and R. C. Duty (Abstract No. 172)

10:00 A.M.—"Polarographic Reduction of Some Diketones and Pyrones" by R. L. Flurry, R. H. Philp, and R. A. Day, Jr. (Abstract No. 173)

11:00 A.M.—"Electrochemical Reduction of the Benzene Ring" by H. W. Sternberg, Raymond Markby, and Irving Wender (Abstract No. 174)

ELECTROTHERMICS AND METALLURGY

Anodic Films and Properties of Carbides, with J. H. Westbrook presiding

(ITALIAN ROOM, Hotel Tuller)

9:00 A.M.—"Electrochemical Oxidation of Titanium Surfaces" by M. E. Sibert (Abstract No. 195)

9:25 A.M.—"Anodic Formation of Titanium Oxide Dielectric Films" by R. T. Lamoureux (Abstract No. 196)

9:50 A.M.—"A Study of the Anodic Film Formed on Titanium" by M. Tecotzky (Abstract No. 197)

10:15 A.M.—Fifteen-minute intermission

10:30 A.M.—"Silicon Carbide—An Electrolytic Capacitor Material" by B. J. Nicholson, W. Haas, and J. J. Flood (Abstract No. 198)

10:55 A.M.—"Characterization and Properties of UC Crystals Produced by Means of Electron-Beam Zone Melting" by Roger Chang and Harry Nadler (Abstract No. 199)

11:20 A.M.—"Mechanical Properties of Nearly Stoichiometric UC Polycrystals between 1500° and 2000°C" by Roger Chang (Abstract No. 200)

Wednesday P.M., October 4, 1961

BATTERY

Fuel Cell Symposium (cont'd): Oxygen Electrodes, with Donald Tuomi presiding

(WAYNE ROOM, Ballroom floor, Statler-Hilton Hotel)

2:00 P.M.—Introductory Remarks

2:10 P.M.—"Oxygen Transport and Reaction Rates at an Air-Depolarized Copper Cathode" by H. C. Weber, H. P. Meissner, and D. A. Sama (Abstract No. 21)

2:40 P.M.—"Characteristics of Oxygen Electrodes" by M. Barak, M. I. Gillibrand, and J. Gray (Abstract No. 22)

3:10 P.M.—"Polarization Behavior of the Oxygen Electrode for Fuel Cells" by P. V. Popat (Abstract No. 23)

3:35 P.M.—Discussion of the above papers

3:45 P.M.—Ten-minute intermission

3:55 P.M.—"The Oxygen Cathode Polarization Characteristics on Porous Carbon and Graphite" by Ernest Yeager, K. V. Rao, A. Kozawa, and Frank Hovorka (Abstract No. 24)

4:30 P.M.—"A Study of the Cathodic Reduction of Oxygen at Carbon Electrodes in Acid Electrolyte" by J. E. Wynn (Abstract No. 25)

CORROSION

Surface Structure vs. Corrosion Behavior (cont'd), with E. Koehler presiding

(MICHIGAN ROOM, Ballroom floor, Statler-Hilton Hotel)

2:00 P.M.—"On the Fundamentals of Etching of High-Purity Aluminum Foil for Capacitor Uses" by E. Borders, R. Kornhaas, and R. Bakish (Abstract No. 63)

2:25 P.M.—"Electron Diffraction and Electron Microscopy on Oxide Formed in Single Crystals of Iron at around 200°C" by P. B. Sewell, E. G. Brewer, and M. Cohen (Abstract No. 64)

2:50 P.M.—"The Surface Layer on Passive Iron" by J. L. Ord and J. H. Bartlett (Abstract No. 65)

3:15 P.M.—Ten-minute intermission

3:25 P.M.—"The Effect of Surface Structure on Subsequent Corrosion" by J. H. Greenblatt and J. T. N. Atkinson (Abstract No. 66)

3:50 P.M.—"Structure of Oxide Films Formed on Individual Crystal Grain of Stainless Steels" by Goro Shimaoka (Abstract No. 67)

4:15 P.M.—"Double Layer Capacities of Single Crystals of Gold in Perchloric Acid Solutions" by G. M. Schmid and Norman Hackerman (Abstract No. 68)

ELECTRODEPOSITION

Electrodeposited Magnetic Films (cont'd), with Herman Koretsky presiding

(BAGLEY ROOM, Ballroom floor, Statler-Hilton Hotel)

2:00 P.M.—"An Introduction to the Meaning of Fundamental Magnetic Terms and Their Significance in Magnetic Recording" by G. Bate (Abstract No. 101)

2:30 P.M.—"Magnetic Properties of Ferromagnetic Metals and Their Alloys Electrodeposited from Sulfamate Solutions" by V. Zentner (Abstract No. 102)

3:00 P.M.—"Magnetic Electrodeposits of Cobalt-Phosphorus" by J. S. Sallo and J. M. Carr (Abstract No. 103)

3:30 P.M.—"The Influence of Internal Stress on the Coercive Force of Thick Films of Cobalt and Nickel Electrodeposits" by R. D. Fisher (Abstract No. 104)

4:00 P.M.—"Further Studies of the Transition Region of a Cobalt Sulfate Electrolyte" by H. E. Quinn (Abstract No. 105)

4:30 P.M.—"An Investigation of the Crystal Structure and Magnetic Properties of Cobalt Nickel Platings from a Combination Sulfate/Chloride Bath with Saccharin as an Additive" by H. F. Quinn, M. Sulich, and J. Manley (Abstract No. 106)

Wednesday Evening Round-Table Discussion. Time and place to be announced.

ELECTRONICS-SEMICONDUCTORS

Elemental Semiconductors, with W. L. Dills presiding

(ARABIAN BALLROOM, Hotel Tuller)

1:30 P.M.—"Nondendritic Ribbon Crystals" by H. Norman, G. Russell, and M. Forney (Abstract No. 149)
1:50 P.M.—"Preparation of High-Purity Silicon from Silane" by C. H. Lewis, M. B. Giusto, H. C. Kelly, and Sidney Johnson (Abstract No. 150)
2:10 P.M.—"The Effect of Heat Treatment, Oxygen, and Structure on the Lifetime of Float Zoned Silicon Crystals" by M. D. Jordan and E. W. Stewart (Abstract No. 151)
2:30 P.M.—"Measurement Errors of Silicon Single Crystals and Slices" by J. S. Miller and V. E. Paulos (Abstract No. 152)
2:50 P.M.—"Resistivity Measurements at Microwave Frequencies" by G. L. Allerton and J. R. Seifert (Abstract No. 153)
3:10 P.M.—"Silicon Crystal Perfection Measurement and Grading" by M. R. Everingham (Abstract No. 154)
3:30 P.M.—"Horizontal Zone Leveling of Silicon" by J. L. Porter and D. M. Lamb (Abstract No. 155)
3:50 P.M.—"Iron-Boron Interactions in Silicon" by W. H. Shepherd and J. Turner (Abstract No. 156)
4:10 P.M.—"Trace-Plating" by W. Rindner and J. M. Lavine (Abstract No. 157)
4:30 P.M.—Recent News Papers. Titles and short abstracts will be available at the meeting.

ELECTRO-ORGANIC

General session, with M. J. Allen presiding

(ENGLISH ROOM, Ballroom floor, Statler-Hilton Hotel)

1:30 P.M.—"Kolbe and Crum Brown-Walker Syntheses with Perfluoroaliphatic Acids" by Sherlock Swann, Jr., and F. H. Baasted (Abstract No. 175)
2:00 P.M.—"Anodic Oxidation in a Heterogeneous System" by H. F. Conway, E. B. Lancaster, V. E. Sohns, and S. Dabic (Abstract No. 176)
3:00 P.M.—"Experimental Study of the Anode Effect in the Electrolysis of Fused Mixtures of Sodium Chloride and Zirconium Tetrafluoride" by C. M. Decroly and Rene Winand (Abstract No. 177)
4:00 P.M.—"Ionic Transference in Pure Molten Sodium Nitrate" by R. J. Labrie and V. A. Lamb (Abstract No. 178)

Thursday A.M., October 5, 1961

BATTERY

Fuel Cell Symposium (cont'd): Fuel Cells, with A. Fleischer presiding

(WAYNE ROOM, Ballroom floor, Statler-Hilton Hotel)

9:00 A.M.—Introductory Remarks
9:05 A.M.—"Internal Resistance in Cation-Membrane Fuel Cells" by E. A. Oster, A. P. Fickett, and P. Chludzinski (Abstract No. 26)
9:30 A.M.—"Transport Processes in Ion-Exchange-Membrane Fuel Cells" by Andrew Dravnieks and J. I. Bregman (Abstract No. 27)
9:55 A.M.—"Hydrogen-Halogen Fuel Cell" by R. M. Lurie and Carl Berger (Abstract No. 28)
10:25 A.M.—"Membrane Properties, Catalyst Type, Graphite Electrode Form—Their Effect on Ion-Membrane Fuel Cells" by R. M. Lurie, Carl Berger, and Ralph Schuman (Abstract No. 29)
10:50 A.M.—Ten-minute intermission
11:00 A.M.—"Radioisotope Activated Fuel Cell Electrodes" by Ricardo Salcedo y Gumucio and Maurice Lang (Abstract No. 30)
11:25 A.M.—"Fuel Cell Batteries with Carbon Electrodes" by E. A. Schumacher and R. J. Bennett (Abstract No. 31)

ELECTRODEPOSITION

Electrodeposited Magnetic Films (cont'd), with Abner Brenner presiding

(BAGLEY ROOM, Ballroom floor, Statler-Hilton Hotel)

9:00 A.M.—"A Method for the Study of Nucleation of Thin Films" by A. E. Cahill (Abstract No. 107)
9:30 A.M.—"Magnetic Properties of Electroless Cobalt Films and Their Application in High Density Digital Recording" by M. A. Foley (Abstract No. 108)
10:00 A.M.—"The Preparation and Magnetic Characteristics of Chemically Deposited Cobalt" by R. D. Fisher and W. H. Chilton (Abstract No. 109)
10:30 A.M.—"Electroless Ni-Co Films with Uniaxial Anisotropy" by J. Bagrowski and M. Lauriente (Abstract No. 110)

General Papers

11:00 A.M.—"The Effect of Pressure on the Electroless Deposition Process" by J. S. Sallo, J. I. Swenson, and J. M. Carr (Abstract No. 111)
11:30 A.M.—"Effect of Binary Alloy Plating on Delayed Brittle Failure of Ultra High Strength Steel" by Walter Beck and E. J. Jankowsky (Abstract No. 112)

Abstracts

BATTERY

Abstract No. 1

The Operation and Use of Reference Cells

N. C. Cahoon, Battery Development Lab., Union Carbide Consumer Products Co., Div. of Union Carbide Corp., P. O. Box 6056, Cleveland 1, Ohio

Reference cells are one of the important tools of the electrochemist, and it is surprising that the literature on the subject is so limited. A review of some of the limitations of reference cells is presented. Suggestions for their effective use in the laboratory are offered. A nomograph permitting the ready conversion of any potential, read against one reference electrode, to the equivalent potential against any one of seven other reference electrodes is described.

Abstract No. 2

Studies of Voltaic Cell Discharge by Polarization Oscillography

R. E. Panzer, W. S. Harris, and **W. C. Spindler,** Chemistry Div., Research Dept., U.S. Naval Ordnance Lab., Corona, Calif.

Investigation of cell polarization was done by direct display of cell potential-time curves on a Tektronix 535 oscilloscope. Utilizing simple circuitry incorporating Western Electric 275B relays, single pulses from voltaic cells were displayed at sweep speeds of 10^{-3} to 10^{-6} sec/cm. From Polaroid photographs delineation of polarization components may be done quite readily. The circuitry employed and examples of the data from cells of various types are shown and discussed.

Abstract No. 3

Determination of the Internal Resistance of Leclanché Cells by Square Wave Method

Aladar Tvarusko, Carl F. Norberg Research Center, Electric Storage Battery Co., Yardley, Pa.

The internal resistance of Leclanché cells was studied on shelf and during discharge by means of a square wave technique. A constant current square wave signal was passed through the test cell and the potential variation across the cell displayed on a high-sensitivity oscilloscope with differential input. The instantaneous voltage drop in the oscilloscope pattern, caused by the leading edge of the constant current square wave, indicated the pure resistance of the Leclanché cells. The internal resistance is independent of the amplitude and frequency of the applied square wave current and of the momentary d-c current. The type of manganese dioxide used in the cathode mix and the composition of the electrolyte influenced the internal resistance of D-size Leclanché cells on shelf and during 4Ω continuous discharge.

Abstract No. 4

Alkaline Manganese Dioxide-Zinc Batteries

J. L. S. Daley, Battery Development Lab., Union Carbide Consumer Products Co., Div. of Union Carbide Corp., P. O. Box 6056, Cleveland 1, Ohio

The MnO_2-Zn-KOH system will, in heavy drain applications, perform at far higher efficiency than its

Leclanché counterpart. Low freeze point electrolyte, stable low impedance, and excellent shelf properties, plus a number of novel safety features built into its commercial versions make the alkaline MnO_2-Zn cell potentially very useful.

Abstract No. 5

Solubility of Silver Oxides in Alkaline Solutions

Stanley Hills, Research and Development Dept., Yardney International Corp., 40 Leonard St., New York 13, N. Y.

The solubilities of both monovalent and divalent silver oxides, as determined polarographically over a KOH concentration range of 2-11.7M, vary between 4.5×10^{-4} and 7.5×10^{-4}M. Both oxides display a maximum solubility between 4 and 6M KOH. The solubility, in 45% KOH, of monovalent silver oxide is not affected by the presence of zincate (80 g ZnO/liter). Alkaline silver solutions were analyzed by a simple method, employing a dropping mercury electrode, which is as yet unreported in the literature. Silver, in a metastable valence state greater than one, was found to be soluble in concentrated alkali.

Abstract No. 6

The AgO/Ag_2O Electrode in Alkaline Solutions

T. P. Dirkse, Calvin College, Grand Rapids, Mich.

The standard potential of the AgO/Ag_2/OH^- electrode has been evaluated by direct measurement against a hydrogen electrode. The results appear to be somewhat dependent on the KOH concentration. Comparisons are made with voltages usually associated with the silver-zinc battery.

Abstract No. 7

A New Design for the Silver-Cadmium Battery

P. L. Howard, Yardney Electric Corp., 40 Leonard St., New York 13, N. Y.

For the past number of years the silver-cadmium battery has been designed for use as a normal low-rate charge system. During the past year requirements arose in which batteries would have to be completely charged and recharged with a 1-hr charging time. This has been accomplished. Test programs indicate that between 500 and 1000 cycles can be obtained in a 100-min cycle, of which 35 min is for discharge up to 65% of the cell capacity and the remaining 65 min is used to recharge the battery completely. Tests up to 50% discharge are now between 1500 and 2000 cycles and are still maintaining their total capacity. Other types of batteries are also reported on with the same type characteristics in both the sealed and open types.

Abstract No. 8

The Runaway Condition in Sealed Nickel-Cadmium Cells and the Characteristics of Sealed Cells with Plastic Electrodes

A. J. Salkind and **J. C. Duddy,** Carl F. Norberg Research Center. Electric Storage Battery Co., Yardley, Pa.

The discharge and overcharge performance characteristics of sealed nickel-cadmium cells with plastic (DP) electrodes are presented. These cells operated at high energy density levels on both a weight and volumetric basis. The thermal runaway condition which can occur in sealed nickel cells of all types on constant potential charging is reviewed and discussed.

Abstract No. 9

The "Vicious Cycle" in Secondary Batteries, A Mathematical Approach

W. G. Eicke, Jr., Electrochemistry Section, Electricity Div., National Bureau of Standards, Washington 25, D. C.

Equations relating voltage, temperature, heat capacity, time, and current have been derived for a cell on constant-potential charge. The equations have been derived assuming the cell to be fully charged and thermally isolated from its surroundings, thereby retaining all of the electrical energy supplied to it. The equations are of the form

$$1/i = A - Bt$$

and

$$1/T = C + D \ln (A - Bt)$$

where i is the current, t the time, T the absolute temperature, and A, B, C, and D are constants depending on the cell size, initial conditions, charging potential, etc. The case where cooling occurs is also considered.

Abstract No. 10

Oxygen Evolution from Heavily Doped Nickel Oxide Electrodes

H. N. Seiger and **R. C. Shair,** Research Lab., Alkaline Battery Div., Gulton Industries, Inc., Metuchen, N. J.

Nickel oxide electrodes were prepared in a nickel matrix. One set of electrodes was doped to 5 at. % with cobalt, and another set with 5 at. % barium. The oxygen evolved after interruption of charge was measured at 1 atm and 100°F. Analysis of data indicates at least three processes involved in the self-discharge mechanism. Doping affects the amounts of oxygen source materials and the evolution rate.

Abstract No. 11

Variation of Microstructure in Storage Battery Plates with Method of Forming, I.

A. C. Simon and **E. L. Jones,** U. S. Naval Research Lab., Washington 25, D. C.

This is a continuation of a previously reported investigation of the microscopy of the forming process. It was found that the microstructure of the plates varied significantly and markedly with changes in temperature, specific gravity, and current density, and that there appeared to be a relationship between the pre-existing sulfate crystal structure and the form of PbO_2 observed after forming.

Abstract No. 12

Variation of Microstructure in Storage Battery Plates with Method of Operation and Manufacture, II

A. C. Simon and **E. L. Jones,** U.S. Naval Research Lab., Washington 25, D. C.

An examination was made of the formed and unformed plates obtained from different manufacturers which revealed that significant differences occurred that could be identified with the source. Characteristics of some of these microstructures appeared to persist throughout certain types of operation and to relate to performance, although the investigation is too preliminary to substantiate this.

Abstract No. 13

Porosity, Air Permeability, and Electrical Resistance of Storage Battery Separators

W. S. Bundy, Research Labs., National Lead Co., 105 York St., Brooklyn 1, N. Y.

The porosity (void fraction) and pore size distribution of battery separators have been measured by an Aminco-Winslow porosimeter using mercury infusion. Air permeability of these separators has been measured by an Aminco-Frazier permeometer, two "Sheffield porosimeters," and by the Bendsten tester. Resistance measurements in various electrolytes were made with an a-c Kelvin bridge (L&N). By use of Darcy's law and Poisenille's law of fluid flow, the relationship of permeability, electrical resistance, and pore radius is found to be $8K(RA + pt) = r^2pt$, where K, p, R, A, t, and r are Darcy's constant, electrolyte specific resistance, separator electrical resistance, area, thickness, and pore radius, respectively.

Abstract No. 14

Battery Design–Current Density Distribution in a Cell

C. M. Shepherd, U.S. Naval Research Lab., Washington 25, D. C.

An uneven current density distribution in a battery may have a large number of undesirable effects. The current density distribution is a function of electrode height, grid resistance, electrolyte resistance, and polarization. Mathematical solutions have been obtained for those cases where the polarization curves are either linear, logarithmic, cubic, or inverse cubic. The results are presented in graphs which greatly simplify their use in practical battery design.

Abstract No. 15

Chemisorption in Gas Electrode Reactions

G. J. Young and **J. R. Moser,** Alfred University, Alfred, N. Y.

The requirement of rapid chemisorption equilibrium to attain readily reversible gas electrodes necessitates the proper selection of electrode catalysts. In the case of hydrogen, for example, those group VIII metals whose surfaces can be maintained in an active condition give approximately theoretical potentials and can support reaction rates corresponding to current densities of over 10^3 ma/cm^2. However, electrodes catalyzed with the Ib metals do not appear reversible and are strongly activation polarized. Hydrogen chemisorption equilibrium is established rapidly with the group VIII metals, but not with the group Ib metals. Similar considerations apply to hydrocarbon gas electrodes.

Abstract No. 16

The Electromotive Activity of Electrolytically Deposited Hydrogen at Carbon Electrodes

H. F. Hunger, Primary Battery Branch, Power Sources Div., U.S. Army Signal Research and Development Lab., Fort Monmouth, N. J.

The electromotive activation of hydrogen occurs in an appreciable degree only at electrodes which consist of or contain occluding metals. Further, electromotively active hydrogen can be produced by electrolytical deposition at an occluding or inert electrode. This active hydrogen can be stored in appreciable amounts at inert electrodes, like activated carbon electrodes. The storage capacity depends on the adsorption isotherm of the carbon which is related to the inner surface area.

Abstract No. 17

Chronopotentiometry of the Alcohol Fuel Electrode

Manuel Shaw and W. J. Subcasky, Electrochemical Research Div., Electric Autolite Co., Toledo 1, Ohio

The chronopotentiometric method is adapted to the study of electrochemical oxidation of alcohols. Conditions are described for obtaining well-defined potential-time curves giving reproducible transition times. The method permits the evaluation of transfer coefficients and heterogeneous rate constants, which are used to develop possible mechanisms for the rate-determining step. Interpretation of recovery curves gives additional information on the electrode reactions involved.

Abstract No. 18

Voltammetric and Chronopotentiometric Study of the Anodic Oxidation of Methanol, Formaldehyde, and Formic Acid

R. P. Buck and **L. R. Griffith,** California Research Corp., 200 Bush St., San Francisco 20, Calif.

The anodic oxidation of methanol, formaldehyde, and formic acid on a platinized-platinum electrode was studied by the technique of voltammetry at linearly changing potential at pH values from —1 to 16 and over a concentration range of 0.01-0.1M. The pH dependence of peak current, overpotential, and kinetic parameters was investigated for each of the three compounds. Mechanisms based on these results, and the supporting chronopotentiometric and product studies, are discussed.

Abstract No. 19

The Electrochemical Oxidation of Methanol in Acid Electrolyte

D. E. Icenhower and **A. P. Bond,** Ordnance Corps, Diamond Ordnance Fuze Labs., Washington 25, D. C.

The electrochemical oxidation of methanol was carried out in acid electrolytes at temperatures from 20° to 75°C using platinized platinum, platinized carbon, and other electrodes. Polarization data were obtained and reaction products were determined at current densities from 1 to 100 ma/cm^2. Most of the studies were carried out in sulfuric acid, but other electrolytes were investigated.

Abstract No. 20

Raney Type Transition Metals as Fuel Electrode Catalysts

H. Krupp, H. Rabenhorst, G. Sandstede, and **G. Walter,** Battelle Institut, Frankfurt, Germany, and **R. McJones,** Cummins Engine Co., Columbus, Ind.

Porous metal electrodes incorporating Raney catalysts are prepared by powder techniques from transition metals of the first and eighth groups. Half-cell performance is measured in various aqueous electrolytes at temperatures from 25° to 150°C. At 80°C in KOH, hydrogen yields current densities beyond 500 ma/cm^2, methanol yields well beyond 200 ma/cm^2, and hexane yields questionable values of a few ma/cm^2. The methanol reaction approaches complete oxidation.

Abstract No. 21

Oxygen Transport and Reaction Rates at an Air-Depolarized Copper Cathode

H. C. Weber, H. P. Meissner, and **D. A. Sama,** Dept. of Chemical Engineering, Massachusetts Institute of Technology, 77 Massachusetts Ave., Cambridge 39, Mass.

The physical processes by which oxygen is transported to an air-depolarized electrode and the importance of mass transport of oxygen through the electrolyte are discussed. A wiped, rotating, partially submerged cylindrical copper electrode was constructed to eliminate the resistance to oxygen transport posed by the electrolyte. The rate of oxidation of a smooth copper surface leaving a 20% KOH electrolyte was measured with this electrode. The measured oxidation rate is discussed in the light of the rate requirements of the oxygen electrode of a fuel cell.

Abstract No. 22

Characteristics of Oxygen Electrodes

M. Barak, M. I. Gillibrand, and **J. Gray,** Research and Development Labs., Chloride Electrical Storage Co., Ltd., Clifton, Manchester, England

Measurements are recorded of the polarization potentials of some oxygen electrodes at various temperatures and current densities. The effects on these characteristics of variations in the composition of the electrolyte are also noted. The reactions were followed by measurements of the consumption of oxygen, and possible reaction mechanisms have been deduced from these results.

Abstract No. 23

Polarization Behavior of the Oxygen Electrode for Fuel Cells

P. V. Popat, Aircraft Accessory Turbine Dept., General Electric Co., Lynn, Mass.

Polarization characteristics of the oxygen electrode in acidic and alkaline media at platinum black and other catalytically active materials for hydrogen-ox-

ygen fuel cells are presented. Experimental evidence strongly suggests that, in the cases studied, the polarization at steady state is associated with the pH changes at each electrode. Open-circuit voltage of the oxygen electrode apparently depends on a number of parameters associated with the electrode, electrolyte, and cell assembly. A tentative explanation for some of the anomalies of the oxygen electrode is advanced.

Abstract No. 24

The Oxygen Cathode Polarization Characteristics on Porous Carbon and Graphite

Ernest Yeager, K. V. Rao, A. Kozawa, and **Frank Hovorka,** Dept. of Chemistry, Western Reserve University, Cleveland, Ohio

The dependence of cathodic polarization on pressure as well as solution parameters has been established in alkaline solutions for various porous carbon and graphite electrodes. With relatively graphitic, low porosity electrodes, the activation polarization associated with the reduction of oxygen has been resolved and the Tafel slope found to be 0.11. Under most circumstances, however, mass transport, peroxide decomposition, and distributed I-R drops within the electrodes are controlling. These results are interpreted in terms of optimizing the performance of porous carbon, oxygen cathodes. [This research sponsored by the Office of Naval Research under Contract Nonr 2391(00)].

Abstract No. 25

A Study of the Cathodic Reduction of Oxygen at Carbon Electrodes in Acid Electrolyte

J. E. Wynn, Primary Battery Branch, Power Sources Div., U.S. Army Signal R and D Lab., Fort Monmouth, N. J.

Theoretical and experimental investigations were made on the oxygen dissolution reaction at porous activated carbon electrodes in acid electrolytes over the pH range 0-7 at 25°C. The current density range for accurate overpotential measurements was found to be 4.4×10^{-6} to 10^{-5} amp cm^{-2} using a Lugeen-Haber capillary to eliminate IR drop and agitation of the electrolyte to reduce concentration overpotential. At constant current density the mechanism of the complete reduction of molecular oxygen to water on carbon cathodes appeared to be limited by the formation of peroxide intermediates.

Abstract No. 26

Internal Resistance in Cation-Membrane Fuel Cells

E. A. Oster, A. P. Fickett, and **P. Chludzinski,** Aircraft Accessory Turbine Dept., General Electric Co., Lynn, Mass.

The contributions to total internal resistance of each of the cell components are measured and compared with computations for the G.E. cationic-reinforced-membrane fuel cell. On new cells of lower internal resistance, performance increases observed follow predictions.

Abstract No. 27

Transport Processes in Ion-Exchange-Membrane Fuel Cells

Andrew Dravnieks and **J. I. Bregman,** Armour Research Foundation, Technology Center, 10 W. 35th St., Chicago 16. Ill.

Performance of fuel cells utilizing ion-exchange membrane electrolytes depends not only on the polarization at the electrodes and the ionic transport through the membrane, but also on the processes of water metabolism in the cell system. Hence, wetting, electroosmotic, and capillary effects in the membrane and at the electrodes are important. Management of water metabolism is a necessary part in optimization of the membrane cell performance.

Abstract No. 28

Hydrogen-Halogen Fuel Cell

R. M. Lurie and **Carl Berger,** Ionics, Incorporated, Cambridge, Mass.

Cathodic electrolyte composition has been varied over a broad range of acid and halogen concentration. Experimental data, utilizing bromine as an oxidizing agent in this cell, have been obtained and indicate optimal concentration ranges for effective discharge characteristics. Some of the regeneration techniques studied involve electrical charging, heat, and radiation. Results of regenerative performance with respect to catalyst and membrane life are discussed. It appears that regenerable performance of this cell is satisfactory over a period of 1000 hr.

Abstract No. 29

Membrane Properties, Catalyst Type, Graphite Electrode Form—Their Effect on Ion-Membrane Fuel Cells

R. M. Lurie, Carl Berger, and **Ralph Schuman,** Ionics, Incorporated, Cambridge, Mass.

The water content, capacity, and thickness of polystyrene sulfonate membranes have been varied and resistance measurements made and related to ion-membrane fuel cell performance. Polarization data have been obtained for a number of hydrogen and oxygen electrode catalysts and related to potential improvements in catalyst type and electrode configuration in fuel cells. The data have indicated that the major losses in the system are a function of the polarization of the oxygen and hydrogen electrodes while the variation in the physical and chemical form of the membranes is of much less significance in cell performance.

Abstract No. 30

Radioisotope Activated Fuel Cell Electrodes

Ricardo Salcedo y Gumucio and **Maurice Lang,** Yardney Electric Corp., 40 Leonard St., New York 13, N. Y.

Much effort has been spent to develop fuel cell systems both for normal temperature and high-temperature operations. We have viewed the problem from a standpoint of determining the best electrodes and catalysts to reduce polarization to a minimum. To this end we have developed electrodes which incorporate isotopes. Such electrodes show the ability to deliver higher capacity at lower polarization values than the best heretofore prepared electrodes employing conventional catalysts. These electrodes function well at ambient temperatures of 20°-25°C. Experiments with C14 and Pm147 have been conducted using carbon and silver base materials. Concentrations of 10-50 microcuries/cm^2 have sustained currents up to 200 ma/cm^2 continuously with polarization values less than 0.2 of a volt. Results of various experiments are discussed.

Abstract No. 31

Fuel Cell Batteries with Carbon Electrodes

E. A. Schumacher and **R. J. Bennett,** Battery Dev. Lab., Union Carbide Consumer Products Co., Div. of Union Carbide Corp., P. O. Box 6056, Cleveland 1, Ohio

Progress in the development of low-temperature, hydrogen oxygen batteries with carbon electrodes is described. The influence of structural parameters and operating conditions on unit cell and multicell battery performance are discussed. Polarization data are given for anodes and cathodes divorced from battery design factors.

BATTERY—CORROSION

Abstract No. 32

Solutions of Metals in Fused Salts

Daniel Cubicciotti, Stanford Research Institute, Menlo Park, Calif.

Certain metals dissolve in their own fused salts. Metals that have been found to show such solubility

in their molten halides include the alkali metals, most of the alkaline earth metals, some of the rare earth metals, and certain transition and post-transition metals. Some of the properties of such solutions are reviewed, and their possible bearing on the corrosion of metals by fused salts is mentioned.

Abstract No. 33

The Formation Potential of Lithium Chloride

R. D. Walker, Jr., and **W. K. Smith,** Dept. of Chemical Engineering, University of Florida, Gainesville, Fla.

The standard formation potential of lithium chloride has been measured over the temperature range 615°-794°C in a fused salt galvanic cell using electrodes of lithium electroplated on tungsten and chlorine on graphite and found to be $E^\circ = 3.891\text{-}0.0006714t(^\circ C)$. Stable potentials were not attained for long periods because lithium dissolved in the melt and reacted with the container materials. Derived thermodynamic quantities are: $\Delta G_f^\circ = -89{,}758 + 15.488t$ cal/g mole; $\Delta S^\circ = 15.488$ cal/deg g mole.

Abstract No. 34

Etching of Silver Single Crystals in Fused Sodium Chloride

K. H. Stern and **Jerome Kruger,** National Bureau of Standards, Washington, D. C.

The etching of polycrystalline and single crystal silver surfaces of {100}, {110}, and {111} orientations has been studied in fused sodium chloride at 900°C. Topographies for the different surfaces obtained at 900°C in air and salt were compared. Both smooth electropolished and thermally etched crystals were exposed to the fused sodium chloride. Surface features observed in thermal etching differ from those in fused salt etching; previously thermally etched crystals exposed to fused salt alter their surface structure to that observed when electropolished crystals are exposed to salt alone.

Abstract No. 35

Corrosion Associated with the ORNL Fused Salt Fluoride Volatility Process

A. P. Litman and **R. P. Milford,** Oak Ridge National Lab., Operated by Union Carbide Corp. for the U.S. Atomic Energy Commission, Oak Ridge, Tenn.

Corrosive attack on the two major vessels used in the ORNL fluoride volatility process has often been severe. The process is being studied for recovering uranium from zirconium-uranium nuclear reactor fuel elements. First, the Zr-U is converted to the tetrafluorides in a $NaF\text{-}ZrF_4$ or $NaF\text{-}LiF\text{-}ZrF_4$ melt with HF. INOR-8, Inconel, copper, and nickel have been studied as construction materials for the hydrofluorinator, with INOR-8 preferred. Next, the UF_4 is fluorinated in a second vessel to volatile UF_6, further purified, and collected. 'L'-nickel, INOR-8, HyMu 80, and experimental nickel-rich binary alloys containing Mg, Al, Co, Fe, and Mn have been investigated as fluorinator materials, with 'L'-nickel now in use. Temperatures have ranged from 500°-750°C. Corrosion rate losses during early studies have sometimes exceeded 1 mil/hr as bulk metal losses and/or intergranular attack, pitting, and selective losses of chromium.

Abstract No. 36

Corrosion Behavior of High-Temperature Alloys in Fused Fluoride Mixtures

J. H. DeVan, Oak Ridge National Lab., Oak Ridge, Tenn. Operated for the U.S.A.E.C. by Union Carbide Corp.

The corrosion mechanisms of fused fluoride mixtures are being investigated in conjunction with the development of high-temperature nuclear reactors which employ such salts as fuels and coolants. Methods are presented for predicting corrosion rates in these systems based on the thermodynamic properties of the alloy container and fused salt system. The results of radiotracer studies conducted to demonstrate the proposed corrosion model also are reviewed.

Abstract No. 37

Corrosion of Metals in Molten Sodium Polyphosphate

L. F. Grantham, M. A. Hiller, and **W. S. Ginell,** Atomics International, Div. of North American Aviation, Inc., Canoga Park, Calif.

Corrosion tests of over 60 metals in molten sodium polyphosphate were conducted in connection with the fused oxide reaction program. The rates were determined as functions of alloy composition, metal pretreatment, and phosphate composition. In general, the corrosion rate decreased as the length of the test was increased. The corrosion rates were followed continuously during some tests by observing the intensity of a volatile corrosion product (P_2) with a mass spectrometer. The results of these examinations are interpreted in terms of diffusion to and through the metal phosphide film formed on the surface of the metal. (This work supported by the U.S.A.E.C.)

Abstract No. 38

The Thermally Regenerative Liquid Metal Cell

B. Agruss, Allison Div., General Motors Corp., Indianapolis 6, Ind.

A unique, thermally regenerative, direct conversion device is described, which is compact, silent, and requires no moving parts. It depends on the reaction of two liquid metals to furnish power and the subsequent thermal decomposition of the reaction product into its original constituents. The theory behind the operation of the system is developed. Laboratory data are given which corroborate the theory for both power production and regeneration. Probable applications are listed.

Abstract No. 39

The Sodium|Tin Liquid-Metal Cell, A Preliminary Study

R. D. Weaver, S. W. Smith, and **N. L. Willmann,** Delco-Remy, Div., General Motors Corp., Anderson, Ind.

The experimental results of investigations of cells based on a new concept in energy conversion, the thermally regenerative liquid-metal cell, are presented and compared with predicted performance. Charge-discharge data, electrolyte conductivity data, and life-test data are included. Descriptions of experimental techniques and materials employed are made. Several characteristics of these cells are presented, and recommendations for future work are suggested. It is concluded that these cell systems warrant further intensive study.

Abstract No. 40

The Liquid-Metal Cell as an Energy Storage Device for Satellite Application

E. H. Hietbrink and **B. Agruss,** Allison Div., General Motors Corp., Indianapolis 6, Ind.

Parametric equations were derived which define the minimum weight of an energy storage system operating in a circular orbit about the earth. The system consisted of three components: a liquid-metal cell for generating power during orbit dark time, the required inventory of liquid-metal alloy, and the solar cells necessary to supply power to recharge the cell during orbit light time. The equations define the cell operating voltage which corresponds to minimum system weight in terms of cell operating characteristics, other system component design constants, and orbit light and dark time. These equations were applied to various liquid metal cell systems to determine the optimum power to weight ratio for each case as a function of orbital altitude.

Abstract No. 41

The Lithium Hydride Electrode

M. E. Indig and **R. N. Snyder,** Delco-Remy, Div. of General Motors Corp., Anderson, Ind.

Results of electrochemical studies on the anodic character of a soluble LiH electrode in a fused LiCl-KCl electrolyte are presented for consideration as a possible high energy, low weight electrode material. Included are constant current polarization studies conducted with different grid materials, coulombic efficiencies based on a proposed two electron oxidation, and the effect of LiH concentration on potential. The experiments are described and possible electrode reactions are suggested with evidence for their justification.

Abstract No. 42

High-Temperature Fuel Cells

M. L. Kronenberg, Research Lab., Union Carbide Consumer Products Co., Div. of Union Carbide Corp., Parma 30, Ohio

Immobilized electrolyte, high-temperature fuel cells of nonconventional design were operated successfully on a wide variety of fuel gases. This design readily permits the incorporation of a working reference electrode and avoids gasketing problems for low-pressure operation. Galvanic utilization of carbon monoxide has been demonstrated whereas galvanic utilization of hydrocarbon fuels appears to depend on cracking or reforming operations.

Abstract No. 43

Electrical and Chemical Characteristics of a Hydrocarbon Fuel Cell of the Fused Carbonate Type

Y. L. Sandler, Research Labs., Westinghouse Electric Corp., Beulah Rd., Churchill Boro., Pittsburgh 35, Pa.

An experimental high-temperature fuel cell is described using alkali carbonates as an electrolyte. The chemical equilibria set up at the fuel electrode and the resulting electrical characteristics are discussed. The cells were operated on natural gas with good output (130 ma/cm^2 at 0.6 v) and at a relatively low temperature (~580°C). The low-temperature reforming reaction with water is used to convert methane almost quantitatively to hydrogen. Causes of instability, unwanted side reactions, and their prevention are discussed.

Abstract No. 44

Ionic Conduction in $(ZrO_2)_{.85}$ $(CaO)_{.15}$

J. Weissbart and **R. Ruka,** Research Labs., Westinghouse Electric Corp., Beulah Rd., Churchill Boro., Pittsburgh 35, Pa.

$(ZrO_2)_{.85}$ $(CaO)_{.15}$ is made the electrolyte of a high-temperature solid electrolyte galvanic cell. Oxygen transported through a cell of the general type Pt, O_2 (P_1) $\|$ $(ZrO_2)_{.85}$ $(CaO)_{.15}$ $\|$ O_2 (P_2), Pt is collected and weighed by a hot zirconium getter suspended from a quartz spring balance. The rate of oxygen transport is compared with current drawn by the cell. This method shows that the ionic conductivity is greater than 98% of the total conductivity at 1000°C.

CORROSION

Abstract No. 45

Some Recent Developments in Inhibitor Theory

Norman Hackerman, Dept. of Chemistry, University of Texas, Austin 12, Texas

The concept of the predominant influence of chemisorption in the inhibition process has been strengthened greatly in the last ten years by an accumulation of evidence which correlates potential shifts, heats of adsorption, and molecular structure with inhibitor efficiency. Specifically, recent experiments have shown a good correlation with pi-orbital character of amino nitrogens in two homologous series of compounds. This appears to strengthen the conclusion of other workers that inhibition by acetylenic compounds is traceable to the pi-orbital character of the electrons forming the triple bond. The important question which must be answered by future research is that of why chemisorption should lead to inhibition. At least two postulates can be made, but experimental proof of either will be quite difficult.

Abstract No. 46

Corrosion Inhibition by Metallic Cations

Henry Leidheiser, Jr., Virginia Institute for Scientific Research, 2820 Grove Ave., Richmond, Va.

Examples of the following types of inhibition by metallic cations are discussed: (*a*) formation of an inert solid solution alloy at the surface; (*b*) formation at the surface of a continuous, elemental coating with high hydrogen overvoltage; (*c*) formation of an inert intermetallic compound; and (*d*) induced formation of an oxide film. The important roles of diffusion in the solid-state and cathodic reactions involving intermetallic compound formation are stressed.

Abstract No. 47

Uniform and Pitting Corrosion of 3003 Aluminum in Aerated Citrate Buffer Solution

E. L. Koehler and **S. Evans** (present address: North American Aviation, Inc., Dept. 591-356, Canoga Park, Calif.), Central Research and Engineering Div., Continental Can Co., Inc., 7622 S. Racine Ave., Chicago 20, Ill.

In aerated citrate buffer solution, corrosion of 3003 aluminum may be either uniform or pitting. Polarization data indicate that uniform attack typically occurs below the limiting diffusion current for oxygen and is controlled by a limiting rate of anodic solution for the film-covered metal; pitting attack typically occurs at the limiting diffusion current for oxygen. With added chloride, pitting attack always occurs and at a rate which is greater than the oxygen limiting diffusion current. Although useful under anaerobic conditions, the polarization resistance method does not appear generally useful for determining corrosion rate under aerated conditions. However, anodic polarization data are useful for determining whether corrosion is of a uniform or pitting nature.

Abstract No. 48

The Polarization of Metals in Distilled Water

F. E. DeBoer, J. E. Draley, and **C. A. Youngdahl,** Argonne National Lab., 9700 S. Cass Ave., Argonne, Ill.

A method of determining the polarization behavior of metals in distilled water has been developed. Difficulties are encountered due to potential gradients in the water, double layer capacity effects, and the influence of the polarizing current on the corroding interface. The procedures used to overcome these difficulties are described, and representative polarization curves are presented.

Abstract No. 49

Effect of Partial Dissolution of the Oxide Film on the Aqueous Corrosion Resistance of Zircaloy-2

S. Kass and **D. B. Scott,** Bettis Atomic Power Lab., Westinghouse Electric Corp., Pittsburgh, Pa.

The aqueous corrosion resistance of corrosion-tested Zircaloy-2 was found to decrease markedly after vacuum heating to dissolve the oxide film partially. Although a complete explanation of the accelerated corrosion is not proposed, several possible mechanisms are presented.

Abstract No. 50

Corrosion and Electrochemical Behavior of Chromium-Noble Metal Alloys

N. D. Greene (present address: Dept. of Metallurgical Engineering, Rensselaer Polytechnic Institute, Troy, N. Y.) **C. R. Bishop,** and **M. Stern** (present

address: Speedway Labs., Linde Co., 1500 Polco St., Indianapolis 24, Ind.) Metals Research Labs., Union Carbide Metals Co., Div. of Union Carbide Corp., Niagara Falls, N. Y.

Alloying chromium with small amounts of platinum, palladium, iridium, rhodium, ruthenium, or osmium markedly improves its corrosion resistance to nonoxidizing acids such as sulfuric or hydrochloric acid. The presence of rhodium, palladium, or osmium has little influence on the resistance of chromium to an oxidizing acid such as nitric acid, while platinum, iridium, or ruthenium greatly increases corrosion rates in this medium. These phenomena can be explained in terms of the electrochemical and corrosion behavior of the metals involved, and are related to the passive and transpassive behavior exhibited by chromium.

Abstract No. 51

The Role of a Displacement Reaction in the Kinetics of Oxidation of Alloys

R. L. Levin and **J. B. Wagner, Jr.,** Hammond Metallurgical Lab., Yale University, New Haven, Conn.

The oxidation of some copper-zinc alloys and a copper-nickel alloy in pure oxygen at 700°C has been studied to determine the occurrence of a displacement reaction of the type.

$$B^{+s} + 2e^- + AO = A^{+s} + 2e^- + BO$$

as proposed by C. Wagner. The formation of BO in the displacement reaction has been shown to occur by observing a change in the oxide scale by metallographic examination and by noting a change in the rate of oxidation as given by the parabolic reaction rate constant. A change in the oxidation rate for several samples was further emphasized by observing the rates during two periods of oxidation which were separated by an isothermal annealing period in an inert gas.

Abstract No. 52

Oxidation Kinetics of $ZrBe_{13}$ and $NbBe_{12}$

Guy Ervin, Jr., Atomics International, Div. of North American Aviation, Inc., P. O. Box 309, Canoga Park, Calif.

A study of the oxidation of $ZrBe_{13}$ and $NbBe_{12}$ in the temperature range 700°-1500°C, using a volumetric technique, has given rates with parabolic time dependence above 800°C, but accelerating rates at 700°C due to fracture and consequent increase of the metal/gas surface area. In the range 1200°-1500°C the oxide coating is normal BeO and the kinetic behavior similar to that for Be metal oxidation, Below 1200°C the oxidation products and kinetics are more complex. (Work supported by U.S.A.E.C.)

Abstract No. 53

Corrosion of Zirconium Alloys in Superheated Steam

R. D. Misch and **Sherman Greenberg,** Argonne National Lab., 9700 S. Cass Ave., Argonne, Ill.

Zirconium alloys now available do not have adequate corrosion resistance for nuclear superheater conditions, such as 540°C and 600 psi steam. Three avenues of approach have been followed in an effort to produce alloys of adequate corrosion resistance: (*a*) compensating effects in the corrosion product; (*b*) promotion of electronic conductance of corrosion product without accompanying deleterious effects; and (*c*) catalysis of the combination of corrosion product hydrogen at the oxide surface. Although it is apparent that the actual situation is more complex than the above simplifications suggest, progress has in fact been made. Alloys have been produced which have corrosion rates of about 1 mil/year. Consideration must be given to the dependence of corrosion rate on heat treatment and to possible embrittlement of alloys by the absorption of corrosion product hydrogen. (Work performed under auspices of U.S.A.E.C.)

Abstract No. 54

Oxidation of Refractory Metals as a Function of Pressure, Temperature, and Time: Tungsten in Oxygen

J. N. Ong, Jr., Research Labs., Aeronutronic, Ford Rd., Newport Beach, Calif.

The rate of attack of tungsten in oxygen (cm/sec) can be represented by:

$$\text{Rate} = \frac{k_1 C_1^{1/2}}{t^{1/2}} + k_2 C_2 + k_3 C_3 + \frac{k_4 C_4^{1/2}}{t^{1/2}} + k_5 C_5$$

where each term in the equation represents the rate due to the following reactions, respectively:

(1) $W + O_2 \rightarrow WO_2$ (2) $WO_2 + \frac{1}{2} O_2 \rightarrow WO_3$ (3) $W + \frac{3}{2} O_2 \rightarrow WO_3$ (4) $W + O_2 \rightarrow WO_2$ (5) $WO_2 + \frac{1}{2} O_2 \rightarrow \frac{1}{3} (WO_3)_3$. The k's are rate constants and C's are concentrations of intermediate species which are functions of oxygen pressure. The experimental results of three workers are correlated in the temperature range 500°-1300°C and pressure range 34.0-0.0013 atm oxygen pressure.

Abstract No. 55

High-Temperature Oxidation of Fe-Cr Base Alloys, with Particular Reference to Fe-Cr-Y Alloys

E. J. Felten, Research Lab., General Electric Co., P. O. Box 1088, Schenectady, N. Y.

The oxidation kinetics of iron-chromium alloys containing 25 and 37.5% chromium and small additions of various Group III and IIIa metals have been measured between 700° and 1200°C. Agreement with the parabolic rate law is observed for all alloys. Iron-chromium binary alloys and those containing small amounts of aluminum or gallium have good oxidation resistance, but poor scaling resistance. Alloys containing yttrium, lanthanum, dysprosium, gadolinum, and erbium exhibit both good oxidation and scaling resistance. Enhanced scaling resistance for alloys containing the rare earth metals is attributed to the formation of internal as well as external oxide.

Abstract No. 56

The Difference Effect and Anodic Behavior of Hafnium Dissolving in Hydrofluoric Acid

W. J. James, M. E. Straumanis, and **J. W. Johnson,** Depts. of Chemical Engineering and Chemistry and of Metallurgical Engineering, School of Mines and Metallurgy, University of Missouri, Rolla, Mo.

Crystal bar hafnium dissolving in HF in the presence of HCl exhibited a positive difference effect, so pronounced as to overbalance completely the hydrogen volume developed by the internal polarization current and to reduce the rate of self-dissolution by an additional 3 $mm^3\ cm^{-2}\ mm^{-1}$ of H_2. The effect was accompanied by a strong shift of the hafnium electrode toward noble values. The results of the difference effect studies together with potential changes on addition of noble metal salts appear to confirm that the dissolution rate is brought about by direct chemical action of molecular HF.

Abstract No. 57

The Nature of Oxide Films on Single Crystal Iron Whisker Surfaces

J. V. Laukonis, Research Labs., General Motors Corp., Warren, Mich.

A topographic study of high-temperature oxidation on iron whiskers has been reported. Currently the oxide films are being removed from the whiskers and studied with an electron microscope. The oxide film replicas of the single crystal surfaces lend themselves to selected area diffraction and to both light and dark field transmission studies. The structure of the single

crystal surface and the structure and composition of oxide films formed at temperatures greater than or equal to room temperature are reported.

Abstract No. 58

The Isolation of Surface Films from Copper

A. F. Beck and **M. J. Pryor,** Metallurgical Labs., Olin Mathieson Chemical Corp., 275 Winchester Ave., New Haven 4, Conn.

A method for the isolation of oxide and sulfide films from copper has been developed. This depends on selective attack at the film-metal interface by a solution containing 3% ammonium acetate and 0.25% bromine in dried methanol. When stripping was performed in contact with dry air, no film dissolution or contamination was detected.

Abstract No. 59

Pitting Corrosion of Stainless Steels

K. Hino, Sumitomo Metal Industries Ltd., Central Research Labs., Amazasaki, Japan

Stainless steels have complicated properties for pitting corrosion. We studied the influencing factors such as heat treatment, working, surface condition, and welding process on pitting corrosion of various stainless steels in dilute solution of hydrochloric acid containing ferric chloride. Moreover, the effect of velocity of corrosion media and the relation between surface structure of metals and pitting corrosion were investigated.

Abstract No. 60

A Comparative Study of the Morphology of Etched Aluminum Foils

R. Bakish, Alloyd Corp., 35 Cambridge Parkway, Cambridge 42, Mass., and **E. Z. Borders,** Republic Foil Corp., Triangle St., Danbury, Conn.

Electron and optical microscopy data on the morphology and capacitance data on commercially available etched high-purity capacitor grade aluminum foils produced in the U.S. and abroad are presented. Attempts are made to establish correlation between morphology and useful capacitance per unit area for high and low voltage application. Related problems are also discussed.

Abstract No. 61

The Anodic Dissolution of Alloys

R. F. Steigerwald and **N. D. Greene,** Corrosion Research Lab., Dept. of Materials Engineering, Rensselaer Polytechnic Institute, Troy, N. Y.

Potentiostatic anodic polarization techniques are used to correlate the dissolution of alloys with their metallurgical structure and the dissolution behavior of their pure components. A broad range of alloys are studied including the systems Sn-Zn, Fe-Cr, Ti-Cr, and Cu-Ti. On the basis of the modern theory of electrode kinetics and modifications of Tammann's rules, general laws are developed for predicting the anodic behavior and corrosion resistance of alloys. The effect of solid-state interaction on dissolution is shown, and the dissolution of intermediate phases and intermetallic compounds is considered.

Abstract No. 62

There is no Abstract No. 62

Abstract No. 63

On the Fundamentals of Etching of High-Purity Aluminum Foil for Capacitor Uses

E. Borders and **R. Kornhaas,** Republic Foil Corp., Triangle St., Danbury, Conn., and **R. Bakish,** Alloyd Corp., 35 Cambridge Parkway, Cambridge 42, Mass.

Studies on the factors underlying morphology of etched foil structures are presented. The importance of coulomb input, current density, and heat treatment of the metal are evaluated for their contribution to morphological effects observed. Experimental results on studies conducted both with single crystals and polycrystals are presented.

Abstract No. 64

Electron Diffraction and Electron Microscopy on Oxide Formed in Single Crystals of Iron at around 200°C

P. B. Sewell, E. G. Brewer, and **M. Cohen,** Div. of Applied Chemistry, National Research Council, Ottawa, Canada

Large grain polycrystalline specimens and single crystals of iron were oxidized in the temperature range of 175°-260°C in 2 cm O_2. Both the amounts of total oxide and Fe_3O_4 formed were very dependent on the orientation of the iron. In general the thickness of Fe_3O_4 was low on surfaces of random orientation and high on surfaces of low index planes. In every case the Fe_3O_4 layer was highly oriented, as shown by electron diffraction and dark field electron microscopy. Particle size of the oxide was of the order of 50Å. At the lower temperature mainly cubic oxide was observed. The formation of α-Fe_2O_3 was dependent on surface preparation, orientation, and temperature.

Abstract No. 65

The Surface Layer on Passive Iron

J. L. Ord and **J. H. Bartlett,** Dept. of Physics, University of Illinois, Urbana, Ill.

The thickness of the layer on passive iron in 2*N* H_2SO_4 increases from about 20Å at the low potential end of the passive region to about 100Å at the upper end. Above the Flade potential the processes leading to activation do not produce an appreciable thinning of the layer. Under a constant current greater than the steady-state value, from which one starts, the rise of potential seems to be associated first with space charge effects and then with layer thickening.

Abstract No. 66

The Effect of Surface Structure on Subsequent Corrosion

J. H. Greenblatt and **J. T. N. Atkinson,** Naval Research Establishment, Dartmouth, Nova Scotia

Specimens of commercially pure aluminum and two special alloys containing iron and nickel have been examined by electron and optical microscope techniques after short periods of exposure to high-temperature pure water. Certain topographical and structural features of the corrosion films have been characterized and studied with particular reference to the presence of second phase particles in the metal. The specialized techniques developed for film examination are described, and the influence of structural features on corrosion behavior is discussed.

Abstract No. 67

Structure of Oxide Films Formed on Individual Crystal Grain of Stainless Steels

Goro Shimaoka, National Research Institute for Metals, 2-300 Nakameguro, Meguro-Ku, Tokyo, Japan

Electron microscope and selected-area diffraction studies were made on the oxide films produced on thin sections (prepared by electropolishing or chemical etching) of 18Cr-8Ni and 25Cr-20Ni stainless steels in the early stages of oxidation at 300°-600°C. The oxide films consisted of spinel-type oxide and some secondary phases. Complete parallel growth of the spinel oxides was observed on the austenitic single crystals.

Abstract No. 68

Double Layer Capacities of Single Crystals of Gold in Perchloric Acid Solutions

G. M. Schmid and **Norman Hackerman,** Dept. of Chemistry, University of Texas, Austin 12, Texas

The differential capacity of the 100 and 110 plane of of a single crystal of gold was measured in 1*N* to 10^{-3}*N*-$HClO_4$ using a single pulse method. No capacity minimum which could be associated with a zero point of charge was found between −1.0 v (~10 ma/cm² cathodic) and +1.4 v *vs.* SCE. The 100 plane shows an adsorption peak at −0.2 v which is absent on the 110 plane. Otherwise no difference in the behavior of the two planes could be detected.

ELECTRODEPOSITION

Abstract No. 69

The Role of Addition Agents in Bright Nickel Plating

H. Brown, The Udylite Research Corp., Warren, Mich.

The structure of various organic compounds used in aqueous electroplating baths is related to their functions in the baths. Principal attention is given to bright nickel plating and the effect on brightness and leveling of sulfonic, carbonyl, and amino groups, multiple bond carbon to carbon and carbon to nitrogen linkages. Possible mechanisms are considered for brightening and leveling based on adsorption and hydrogenation reactions on nickel as catalyst.

Abstract No. 70

Kinetics of Electrode Processes in Relation to Electrodeposition

B. E. Conway, Dept. of Chemistry, University of Ottawa, Ottawa, Ontario, Canada

Following a brief introduction of the basic concepts in electrode kinetics, the elementary processes in electrodeposition are reviewed, including diffusion, adsorption of ions in the double layer, Faradaic ion transfer at the metal interface, surface diffusion of ad-species, electrochemical crystal building steps, and the role of dislocations. Methods for studying ion transfer and diffusion at electrodes are given and the results of kinetic measurements in selected systems (Hg, Cu, Ag) are given. Possible rate-determining steps are discussed as are some fundamental factors determining the role of adsorption of additives at electrodes during electrodeposition.

Abstract No. 71

Crystal Growth and the Structure of Electrodeposits

S. C. Barnes, J. P. G. Farr, and **H. J. Pick,** Joseph Lucas Lab., Dept. of Industrial Metallurgy, The University, Birmingham 15, England

A comparison is made of published observations on the topography of growing electrodeposits and discussion given of the attempts made to correlate the structures produced with the state of the substrate and electrochemical parameters. Attention is drawn to the application of relaxation techniques. The effects of addition agents on crystal growth and the electrochemical reactions at a cathode are considered; the authors will summarize briefly their own experiences and compare these where possible with other published work.

Abstract No. 72

Theories of Addition Agents in Electrodeposition

Eugenio Bertorelle, Preside Instituto Chimico, RHO, Milan, Italy

Various aspects of the theories of addition agents and their influence on the mechanism of electrodeposition are examined fully and discussed. Particular attention is paid to the theory of inhibition, of complex formation and adsorption; the relation with experimentally observable quantities much as cathode polarization, codeposition of nonmetallic material deriving from addition agents or their decomposition products, is discussed. Some observations on the electrode reactions of addition agents are reported, and the different features concerning some of the industrially important metals are also mentioned.

Abstract No. 73

Effects of Addition Agents on Physical and Mechanical Properties of Electrodeposits

H. J. Read, Dept. of Metallurgy, Pennsylvania State University, University Park, Pa.

The physical properties to be discussed are density, magnetic behavior, and electrical resistivity. Emphasis is placed on the mechanical properties of hardness, tensile strength, ductility, and internal stress, but some attention is given to modulus of elasticity and to fatigue strength. Instances where addition agents are added intentionally to alter properties will be separated, so far as possible, from those cases where the addition agent serves another purpose, such as a brightener, but affects the physical or mechanical properties at the same time.

Abstract No. 74

X-Ray Determination of Residual Stresses in Electrodeposited Coatings

G. W. Bush, Research and Development Dept., National Steel Corp., Weirton, W. Va., and **H. J. Read,** Dept. of Metallurgy, The Pennsylvania State University, University Park, Pa.

Experimental and mathematical procedures were developed and tested for x-ray determination of stress in deposits from data secured with an x-ray diffractometer. The effects of deposit thickness, variations in elastic modulus, and stresses owing to differential thermal expansion between deposit and basis metal have been evaluated. Work on nickel deposits showed stress can be evaluated to ±4,000-6,000 psi and that stress was uniformly distributed over the area irradiated by the x-ray beam.

Abstract No. 75

Electron Microscopic Observations of the Structure of Electroplated Nickel

R. Weil and **H. C. Cook,** Dept. of Metallurgy, Stevens Institute of Technology, Hoboken, N. J.

Electron microscopy using thin films and replicas was employed to study the nature of various structural features due to addition agents, observed in electroplated nickel. The growth mechanisms were investigated by viewing the structure at successive stages in the deposition process. Selected-area diffraction was used to measure grain sizes and orientations. By observing samples annealed at several temperatures, the locations of foreign substances and their influences on the structure were determined.

Abstract No. 76

The Influence of Adsorbed Material on the Growth of the Metallic Lattice

T. P. Hoar, Dept. of Metallurgy, University of Cambridge, Cambridge, England

Addition agents, whether used for brightening, levelling, refining of grain size, or reduction of tensile stress in electrodeposits, are commonly held to act "by adsorption." The present paper attempts to discriminate between different kinds of adsorption according to the lattice structure and electrochemical characteristics of the metal being deposited, and the size, shape, and polarizability of the molecule being adsorbed. Empirical knowledge of the various kinds of addition agents can thereby be partially codified and explained. Outstanding problems in the field are reviewed briefly.

Abstract No. 77

Evidence for the Deposition of Very Complex Cations

F. C. Mathers, Chemistry Dept., Indiana University, Bloomington, Ind.

This paper gives experimental, but circumstantial, evidence that everything in the bath that has an effect on the nature and composition of the deposited metal must be in the bath in the form of complex cations, the metal itself, the acid ion, addition agents, and other things like "conducting salts," etc. What other explanation is there for the large quantities of tartaric acid and some iron in a silver deposit from the nitrate bath containing ferric nitrate and tartaric acid? The deposition potential of iron is so far from silver that it would seem impossible to deposit any iron otherwise. It is well known that there are many complex cations such as $CdCl^+$; therefore, it is logical that all metals and all acids form similar complexes. Ions are now known to be highly solvated so why cannot all the rest of the things in a bath be a part of the cations? How can the acid parts of the various salts get to the cathodes if they are not a part of the cations? Why is the deposit of tin from the fluoride bath always rough and crystalline but smooth from a similar sulfate bath? If bismuth chloride will be dissolved in molten metallic bismuth why not expect cathode deposits to be solutions of the things in the complex cations where the conditions for forming a solution in the metal could be better than when using molten materials?

Abstract No. 78

(There is no Abstract No. 78)

Abstract No. 79

The Growth of Zinc and Other Electrodeposits

J. M. Keen and **J. P. G. Farr,** Joseph Lucas Lab., Dept. of Industrial Metallurgy, The University, Birmingham 15, England

Zinc has been electroplated from acid sulfate solutions onto zinc polycrystalline and single crystalline cathodes, and onto copper single crystal surfaces. The surface features developed are described and are related to those observed on copper electrodeposits in terms of the supposed atomic structure of the substrate surface, of the bulk crystal structure of the deposited metal, and of the growth process. Some experiments on the deposition of lead cadmium and iron are also described and discussed.

Abstract No. 80

The Effect of Thio-Compounds on the Structure of Copper Electrodeposits

S. C. Barnes, Dept. of Industrial Metallurgy, The University, Birmingham, England

Active addition agents in acid copper plating solutions can be divided into two groups: those which increase cathodic overvoltage, and those which lower it. Thio-compounds are in the latter group. Their effects on the characteristics of epitaxial deposits formed on single crystal electrodes have been studied, in conjunction with measurements of cathodic polarization. It is found that pronounced habit changes occur when the addition agents are present in amounts sufficient to affect the overvoltage.

Abstract No. 81

Rotating Disk Electrode Techniques for the Study of Addition Agents

S. E. Beacom and **R. N. Hollyer, Jr.,** Research Labs., General Motors Corp., 12 Mile and Mound Rds., Warren, Mich.

The rotating disk electrode is used as a tool to study the effect of thiourea on the electrodeposition process. Rotating disk theory has been verified for deposition of copper from cupric sulfate solutions in the presence of certain ratios of cupric to inert electrolyte ions. The addition of thiourea produces measurable effects on the several parameters considered. Possible explanations for the role of thiourea are discussed.

Abstract No. 82

The Effect of Some Addition Agents on the Kinetics of Copper Electrodeposition from a Sulfate Solution, I. Cathode Potential-Current Density Relation

D. R. Turner and **G. R. Johnson,** Bell Telephone Labs., Inc., Murray Hill, N. J.

Thiourea, l-cystine, glycine, gelatin, and dextrin were used as addition agents in copper plating from a sulfate solution. Additions of dextrin up to 0.1 g/l have no effect on the kinetics of copper deposition. All the other addition agents inhibit the rate of copper deposition, and each one has a different behavior. Dextrin enhances the inhibiting effect of thiourea during copper plating. There is evidence that thiourea forms a stable complex with cuprous ions in the plating bath.

Abstract No. 83

The Effect of Some Addition Agents on the Kinetics of Copper Electrodeposition from a Sulfate Solution, II. Rotating Disk Electrode Experiments

G. R. Johnson and **D. R. Turner,** Bell Telephone Labs., Inc., Murray Hill, N. J.

A rotating disk electrode technique has been used to study the effect of thiourea, l-cystine, glycine, gelatin, and dextrin on the kinetics of copper electrodeposition from a sulfate solution. The results indicate that some addition agents function solely by means of an adsorption phenomenon whereas others involve an electrochemical reduction of either the addition agent or a cuprous ion-addition agent complex. The fraction of the total current consumed in reducing the addition agent, or a cuprous ion-addition agent complex, can be determined at any given cathode potential.

Abstract No. 84

Some Structural Aspects of Nickel Electroplates

L. P. Bicelli and **G. Serravalle,** Laboratori di Elettrochimica di Chimica Fisica E di Metallurgia del Politecnico di Milano, Piazza Leonardo da Vinci 32, Milan 132, Italy

Cathodic behavior of nickel polycrystalline and single crystal electrodes, oriented following the (100), (110), and (111) planes, has been investigated in perchlorate and sulfamate baths. The crystallization process of definite thickness deposits has been investigated particularly. X-rays were used to determine the basis and bath influence on the preferred orientations of the deposits, while the kinetic aspects of the electrodeposition processes are studied by means of current efficiency and overvoltage measurements. Some correlations between crystallographic results and overvoltage measurements have been established.

Abstract No. 85

The Effect of Addition Agents on the Structure and Physical Properties of Gold Electrodeposits

D. G. Foulke, Sel-Rex Corp., Nutley, N. J.

Bright gold processes in common use differ from the nonprecious metal baths in that the emphasis has been on the codeposition of metals with the gold, rather than on the use of organic addition agents. There are potent reasons for this divergent trend as compared to nickel and copper baths as can be shown by photomicrographs before and after heat treatment. Photomicrographs and x-ray diffractograms will indicate the structure of typical bright gold deposits now being plated and they will be related to the deposit analysis.

Abstract No. 86

Radiotracer Studies of the Uptake of Sulfur from Brightener Compounds by Copper and Nickel

J. J. Hoekstra (present address: Dow Chemical Co., Midland, Mich.) and **Dan Trivich,** Dept. of Chemistry, Wayne State University, Detroit 2, Mich.

The uptake of S-35 from thiourea by single crystal spheres of copper and nickel was found to increase with increasing concentration of thiourea in the solution, but

showed no preference for any particular crystal face. Allyl sulfonate labelled with S-35 was not taken up by nickel under simple immersion, but was included under condition of nickel electrodeposition. Dissolution of the electrodeposits caused the S-35 to be evolved as H_2S as shown by quantitative analysis and x-ray diffraction. (This work was made possible by a fellowship from the General Motors Research Labs. to J. J. H.)

Abstract No. 87

A Study of Laminations in Bright Nickel Electrodeposits

Nicholas Vanderkooi (present address: General Chemical Div. of Allied Chemical Corp., P. O. Box 405, Morristown, N. J.) and **Dan Trivich,** Dept. of Chemistry, Wayne State University, Detroit 2, Mich.

The laminated structure of bright nickel electrodeposits was studied as a function of current density, pH, cathode shape, and type and concentrations of brighteners, especially the system allyl sulfonate, N-allyl quinaldinium bromide. First-class brighteners (sulfonates) produce laminated electrodeposits; second-class brighteners alone do not, but they do enhance the laminated structure when used with the first-class type. On rough cathodes, equal numbers of laminations are produced on peaks and valleys. The significance of this in levelling is discussed. (This work was made possible by a fellowship from the General Motors Research Labs. to N. V.

Abstract No. 88

The Effects of Organic Additives on the Kinetics of Tin Deposition

Ernest Yeager, Frank Hovorka, and **Stuart Meibuhr** (present address: Applied Research Lab., U.S. Steel Corp., Monroeville, Pa.), Dept. of Chemistry, Western Reserve University, Cleveland 6, Ohio.

The electrode kinetics of tin deposition from simple acid solutions containing various organic substances have been studied by the measurement of the cathodic steady-state polarization as a function of current density. The experimental variables included temperature, concentration of stannous ion, concentration and type of addition agent and type of cathode, pure solid tin and liquid tin amalgam. The results indicate that the rate-determining step is charge transfer.

Abstract No. 89

Experimental Observations on the Behavior of Addition Agents in Bright Nickel Plating

I. R. Bellobono and **Eugenio Bertorelle,** Istituto Chimico, Rho, Milan, Italy

The cathode adsorption of addition agents plays a fundamental part in the studies on the mechanism of bright plating, of levelling, and similar phenomena. Using polarization measurements and the analytical determination of addition agents and their decomposition products at various electrodeposition times, it is possible to obtain important information about the relationship between adsorption and cathode polarization as well as about the influence of the decomposition products which may be present in solution. The experimental researches carried on examine these particular aspects of bright nickel electrodeposition in the presence of addition agents which behave as primary or secondary brighteners. An analytical method which makes use of a spectrophotometric technique for the determination of brighteners in electroplating solutions is also fully described.

Abstract No. 90

Effect of Addition Agents on the Formation of the Bright Deposit from Zn-, Cd-, and Ag-Cyanide Baths

Tadao Hayashi and **Takeo Ishida,** Dept. of Applied Chemistry, University of Osaka Prefecture, Sakai City, Osaka, Japan

Study was made of the effect of addition agents on the formation of bright Zn-, Cd-, and Ag-electrodeposits from cyanide baths. Cathode polarization measurements were carried out in the presence of various addition agents, and the deposits obtained from these baths were analyzed by the electron diffraction method and also by photomicrography in order to elucidate the characteristics of the crystal structure with respect to the formation of the bright deposit.

Abstract No. 91

Mechanism of Addition Agent Reaction in Bright and Leveling Nickel Deposition as Studied with Radioactively Tagged Compounds

B. J. Riley and **S. E. Beacom,** Research Labs., General Motors Corp., Warren, Mich.

Radioactively tagged sodium allyl sulfonate and N-allyl quinaldinium bromide have been used in a continuing study of the leveling phenomenon associated with the deposition of bright nickel. Further evidence has been obtained to support the previously stated concept of addition agent interaction which accounts for the synergistic effect in leveling brought about by combinations of addition agents.

Abstract No. 92

Effect of Organic Additives on the Hydrogen Absorbed by Iron

T. C. Franklin and **Fujio Matsuda,** Baylor University, Waco, Texas

A study was made of the effect of organic additives on the absorption of electrolytically generated hydrogen by small iron wires and the resultant effect on the embrittlement of the iron. A polarographic technique was used to analyze for the hydrogen, and the embrittlement of iron was studied by a bend test. A linear relationship was observed between the amount of hydrogen absorbed and the embrittlement.

Abstract No. 93

Bismuth Electroplating

J. G. Beach, Battelle Memorial Institute, 505 King Ave., Columbus 1, Ohio

Bismuth electrodeposits from bath containing "addition agents" were unsatisfactory toward answering an engineering need for a bismuth nickel-alloy coating. The desired results that were expected from the use of addition agents were obtained, and cogent problems were resolved by the use of periodic reverse-current plating.

Abstract No. 94

A Cell for Plating Corrosion Test Panels with Varying Current Densities

A. A. Johnson, Metal and Thermit Corp., 1700 E. Nine Mile Rd., Detroit 20, Mich.

To enable current density and thickness variations of the magnitude encountered on plated parts to be obtained on the standard flat 4 x 6 in. corrosion test panel, a new laboratory plating cell was designed. The use of the cell for corrosion testing is illustrated, and current density distribution profiles and other cell characteristics are given. The influence of current density and thickness of decorative chromium plate on its crack pattern and on the resulting corrosion protection is discussed.

Abstract No. 95

Introduction to Magnetic Phenomena of Soft Magnetic Thin Films

Rexford Alexander, Burroughs Lab. Research Center, Burroughs Corp., Paoli, Pa.

A simple model of the magnetic properties of ferromagnetic materials is presented for the description of terms of significance in magnetic thin films work. The anisotropy properties and the dynamics of thin films remagnetization are stressed.

Abstract No. 96

A Method of Preparing Iron-Nickel Films and Some of Their Properties

P. Kuttner and **D. Clemson,** Electronic Instruments Div., Burroughs Corp., Philadelphia, Pa.

Films of 1000Å thickness with excellent anisotropy (H_K = 1.2 oe), and coercivity of 0.5 oe have been made reproducibly from an aqueous bath of nickel and iron sulfate with addition agents. Plating is done in a magnetic field. The film composition is 95% Ni, 5% Fe. Without addition agents, the composition and magnetic properties of the films change. However, the magnetic properties cannot be explained on the basis of composition alone.

Abstract No. 97

Stress Reducing Organic Additives in the Sulfate-Chloride Bath for Iron-Nickel Deposition

I. W. Wolf, General Electric Corp., Syracuse, N. Y.

The sulfate-chloride bath has been used for the deposition of magnetic codeposits of nickel and iron. Of special interest have been the very thin films (approximately 1000Å) used for computer memory elements. Stress reduction in these codeposits was achieved by adding saccharin to the solution. However, the role of saccharin was not well understood. In this work, various organic molecules were added to baths in place of saccharin. Few were capable of reducing stress at all detectably and none as well as saccharin. There is strong evidence of a need for a very specific molecular form for stress reduction in this system.

Abstract No. 98

A Discussion of Electrodeposited, Cylindrical Film Memory Elements

T. R. Long, Bell Telephone Labs., Inc., Murray Hill, N. J.

A progress report is presented on a program of electrodepositing Ni-Fe films on a wire substrate for use in a nondestructive, cylindrical film memory. Permalloy films with uniaxial anisotropy are continuously deposited on a 5-mil diameter substrate. Experimental data on the process as well as on the magnetic character of the material are presented. The continuous nature of the process introduces some unique problems of control in the deposition of an alloy whose characteristics are strongly dependent on composition. These problems as well as some compensating advantages are discussed.

Abstract No. 99

Magnetic Properties of a 97Fe-3Ni Thin Film Electroplate

H. J. White and **A. J. Kolk,** Electronics Div., National Cash Register Co., Hawthorne, Calif.

The NCR "Rod" thin film computer memory element employs a 97Fe3Ni alloy deposited on a silvered-glass cane or a BeCu wire of approximately 10 mil diameter. The physical condition of the surface of the silver or the BeCu has been found to be of great importance in determining the magnetic properties of the overplate. The effects of current density, pH, plate thickness, and magnetic field applied during plating have been investigated. Unlike permalloy, the magnetic properties were not found to be sensitive to minor variations in alloy composition and were only slightly affected by the level of stress in the plate. The high-speed magnetic switching coefficient of the "Rod" is of a magnitude normally associated with the incoherent rotation mechanism.

Abstract No. 100

Electrodeposited Magnetic Films for Computer Memories by Jet-Cell Plating in High Magnetic Fields

J. H. Glaser and **W. W. Richardson,** Philco Corp., Willow Grove, Pa.

A new method has been developed for plating magnetic films by jet-cell plating technique (Philco propr.) which will allow monitoring of film properties during plating process and terminating operation at optimum condition. The technique allows plating in very high magnetic fields which results in dense films with high output and very good anisotropy. Individual monitored spot plating *vs.* etched film-matrix is evaluated.

Abstract No. 101

An Introduction to the Meaning of Fundamental Magnetic Terms and Their Significance in Magnetic Recording

G. Bate, Product Development Lab., Data Systems Div., International Business Machines Corp., Poughkeepsie, N. Y.

The paper covers terms used in describing the magnetic properties of the two principal types of magnetic memory materials. Those terms include saturation magnetization, remanence, squareness, coercive force, etc., and the physical significance of the parameters in the recording process is discussed.

Abstract No. 102

Magnetic Properties of Ferromagnetic Metals and Their Alloys Electrodeposited from Sulfamate Solutions

V. Zentner, Hughes Aircraft Co., Culver City, Calif.

The magnetic properties of nickel, iron, and cobalt electrodeposited from sulfamate solutions and their change with conditions of deposition were determined. Alloys of nickel-iron, cobalt-iron, and cobalt-nickel plated from sulfamate systems with systematic variations in bath composition were prepared. The dependence of alloy composition on electrodeposition variables was investigated and the relation between magnetic properties, alloy composition, and crystal structure of the deposits determined.

Abstract No. 103

Magnetic Electrodeposits of Cobalt-Phosphorus

J. S. Sallo and **J. M. Carr,** Honeywell Research Center, Hopkins, Minn.

Electrodeposited films of cobalt-phosphorus have been prepared having coercivities ranging from less than 50 oe to more than 1500 oe. The magnetic properties are independent of the substrate. Chemical composition, crystallographic orientation, and electron microscopy including Bitter Pattern studies are related to the observed coercive force. Conditions for preparing materials within this range of coercivity, including materials with stepped hysteresis loops, are described and related to the chemistry of the system.

Abstract No. 104

The Influence of Internal Stress on the Coercive Force of Thick Films of Cobalt and Nickel Electrodeposits

R. D. Fisher, Physical Research Dept., National Cash Register Co., Dayton 9, Ohio

Nickel and cobalt electrodeposits were prepared at low current density (15 ASF) from simple aqueous solution. The influence of the metal salt ($CoCl_2$ or $NiCl_2$) and saccharin solution concentration on the average stress and microstructure of the cobalt and nickel electrodeposits was investigated in conjunction with measurements of their magnetic properties. The coercive force and stress of the nickel and cobalt electrodeposits were determined and compared at thickness values of approximately 5μ. The results indicate that in certain instances the coercive force of the deposits can be directly correlated with the residual stress.

Abstract No. 105

Further Studies of the Transition Region of a Cobalt Sulfate Electrolyte

H. F. Quinn, Federal Systems Div., International Business Machines Corp., Owego, N. Y.

In conjunction with Croll, the author has previously reported the occurrence of a distinct change in the texture of cobalt electrodeposited from a dilute sulfate

bath. With all other parameters held constant, this transition was found to occur in the vicinity of pH 4. On repeating the experiments at smaller pH increments it has been observed that the texture (and the associated magnetic properties) changes smoothly throughout a transition region from 3.8 to 4.8 pH units. It has been shown that the change in coercivity of the plating is not directly associated with the textural changes. The nature of the alteration in the crystal growth process at the cathode is considered in terms of the theory of Willman and others. In particular, it is shown that the type and surface finish of the substrate are not significant controlling factors in the growth process.

Abstract No. 106

An Investigation of the Crystal Structure and Magnetic Properties of Cobalt Nickel Platings from a Combination Sulfate/Chloride Bath with Saccharin as an Additive

H. F. Quinn, M. Sulich, and **J. Manley,** Federal Systems Div., International Business Machines Corp., Owego, N. Y.

In order to obtain a specific recording characteristic and to provide data for process control we have investigated the crystal texture and magnetic properties of platings prepared in a cobalt chloride/nickel sulfate bath containing saccharin as the additive agent. The composition, texture, and magnetic properties of the platings as a function of varying a-c/d-c ratio for each of 4 pH values are reported.

Abstract No. 107

A Method for the Study of Nucleation of Thin Films

A. E. Cahill, General Electric Corp., Syracuse, N. Y.

Measurements of hydrogen overvoltage are used to determine what fraction of a surface consists of gold and what fraction consists of nickel-iron. When very thin layers of nickel-iron have been electroplated on a gold substrate, it is possible by this means to determine to what extent the nickel-iron is continuous. When the nickel-iron deposits in islands, the hydrogen overvoltage indicates that the solution is in contact with both gold and nickel-iron.

Abstract No. 108

Magnetic Properties of Electroless Cobalt Films and Their Application in High Density Digital Recording

M. A. Foley, Burroughs Lab., Research Center, Burroughs Corp., Paoli, Pa.

Electroless cobalt has been deposited on conductive and nonconductive substrates and the magnetic properties evaluated in respect to thickness, coercive force, and remanence. A coercivity range from 40-500 oe can be obtained by varying the plating conditions. The influence of various substrates on the magnetic properties together with bath pH, agitation, and rate of deposition has been determined. Crystallographic studies of films of low and high coercivity have been performed. The dynamic evaluation of thin magnetic films (2—100 μin.) in high density recording is discussed.

Abstract No. 109

The Preparation and Magnetic Characteristics of Chemically Deposited Cobalt

R. D. Fisher and **W. H. Chilton,** Physical Research Dept., National Cash Register Co., Dayton 9, Ohio

Chemically reduced cobalt films on Mylar have been prepared and their magnetic properties evaluated with respect to squareness, coercive force, remanent and saturation magnetization. The influence of deposition parameters and thickness on the microstructure (grain size and crystal orientation) of the cobalt films was investigated in conjunction with measurement of their magnetic properties. The coercive force may be varied from 200 to 600 oe depending on experimental conditions. The magnitude of the coercive force for a specific thickness is dependent on the grain development and grain size of the film. The squareness (Br/Bm) is dependent on the thickness and crystal orientation of the film. The average saturation flux density is 10,000 gauss.

Abstract No. 110

Electroless Ni-Co Films with Uniaxial Anisotropy

J. Bagrowski and **M. Lauriente,** Air Arm Div., Westinghouse Electric Corp., Baltimore 3, Md.

This study covers an extension of the work by Heritage and Walker on Ni-Co films produced by chemical reduction with uniaxial anisotropy. Of significance was the anomalously low coercive force disclosed for the Ni-Co films. The extension of this work involves an attempt to understand the basic mechanism for the anisotropy.

Abstract No. 111

The Effect of Pressure on the Electroless Deposition Process

J. S. Sallo, J. I. Swenson, and **J. M. Carr,** Honeywell Research Center, Hopkins, Minn.

Hydrostatic pressure is shown to alter the rate of electroless nickel deposition. Two classes of acid baths exist, depending on whether the rate is increased or decreased. This difference explains conflicting literature reports. One of these systems is shown to be diffusion controlled. In the other case, the results indicate that the rate is dependent on the active catalytic area which is exposed to the system and free of hydrogen gas.

Abstract No. 112

Effect of Binary Alloy Plating on Delayed Brittle Failure of Ultra High Strength Steel

Walter Beck and **E. J. Jankowsky,** Aeronautical Materials Lab., Naval Air Materials Lab., Philadelphia 12, Pa.

In a number of applications, involving high strength steel, tin-cadmium alloy plating has been substituted for cadmium plating. In this study, notched specimens of high strength steel were plated with tin-cadmium alloys, produced by codeposition of the components from a fluoborate bath, or by thermal interdiffusion of two separately plated metal layers from a stannate and a cyanide bath. The marked differences found in the susceptibility to delayed cracking were ascribed to differences in the hydrogen content of specimens plated from baths with different compositions, and discussed in the light of the kinetics of crack propagation in delayed failure, put forward by Troiano.

ELECTRONICS—SEMCONDUCTORS

Abstract No. 113

The Study of Some Uncommon Surface Treatments on Germanium

W. A. Albers, Jr., and **A. M. Rickel,** Research Labs., Bendix Corp., Southfield, Mich.

A number of uncommon surface treatments have been investigated on homogeneous germanium single crystals. Simultaneous measurements of a-c field effect and surface recombination velocity as functions of surface potential have been performed in order to evaluate the electrical nature of the resulting surfaces. The effect of surface preparation prior to treatment and crystallographic orientation effects have been included in the investigations. The characterization of a number of surface treatments which show potentialities as possible stabilization and/or passivation treatments is reported.

Abstract No. 114

An Impurity Surface State at the Germanium-Aqueous Electrolyte Interface

P. J. Boddy and **W. H. Brattain,** Bell Telephone Labs., Murray Hill, N. J.

Measurements of the capacity of the germanium-aqueous electrolyte interface in the region of pH 7 show negligible additional capacity due to surface states for properly cleaned solutions. Surface recombination velocity (s) is small (or zero) over a range of surface potential (ψ_s). Traces of Cu^{++} (ca. 10^{-6}M) added to the solution increase the capacity and s over certain ranges of ψ_s. These data indicate a recombination center about 50 mv below the center of the gap when Cu^{++} is present.

Abstract No. 115

Diffusion Masking of Silicon and Germanium by the Evaporation of Silicon Monoxide

Bernard Kriegsman and **Karabet Simonyan,** General Instrument Corp., Hicksville, N. Y.

A technique has been developed to mask the diffusion of impurities into silicon and germanium. This technique involves the vacuum evaporation of silicon monoxide onto the particular substrate. In silicon it offers the advantage of forming a continuous and a smooth diffusion mask at low temperatures. This avoids the necessity of thermally growing the mask which can cause an impurity redistribution at the silicon-silicon dioxide interface. In germanium it enables one to make double diffused and planar transistors.

Abstract No. 116

Open Tube Diffusion of Phosphorus in Silicon

W. J. Greig and **J. C. Sarace,** Semiconductor & Materials Div., Radio Corp. of America, Somerville, N. J.

Experimental data are presented for phosphorus diffusion in silicon employing an open tube carrier gas system. Using P_2O_5 as the diffusant source, the surface concentration is calculated in terms of the system parameters. namely, effects of source age, source temperature, silicon temperature, carrier gas, and carrier gas flow rate. Surface concentrations are calculated from sheet resistance and junction penetration measurements using the curves of Backenstoss. Data obtained from an evaluation of the diffusion coefficient calculated assuming a complementary error function distribution are given showing a dependence on the surface concentration and wafer surface condition. Anomalous results obtained from effects of source temperature on surface concentration and the diffusion coefficient as a function of surface concentration also are discussed.

Abstract No. 117

Evaluation of the Surface Concentration of Diffused Impurity Layers in Silicon

O. N. Tufts, Honeywell Research Center, Hopkins, Minn.

The relation between the surface concentration of a diffused layer and the electrical conductivity and Hall coefficient of the layer has been calculated for a complementary error function impurity distribution in silicon. The results show that the Hall coefficient is very nearly independent of the mobility values used in the calculation. This allows accurate values of the surface concentration to be determined without knowing exactly the variation of the mobility with impurity concentration. An experimental comparison of the surface concentration values obtained by the conductivity and Hall effect methods is made.

Abstract No. 118

The Effect of Silicon Surface Treatment on Metallic Impurity Deposition

G. B. Larrabee, Central Research Labs., Texas Instruments Inc., Dallas, Texas

Electrochemical studies of various silicon surfaces show differences in electrochemical potential which can be explained by the mode of formation of the oxide layer on the surface. Radiochemical studies substantiate the electrochemical findings and show why the condition of the silicon surface has such a pronounced effect on the extent of impurity contamination. Autoradiographic studies of the manner in which the metallic impurities are distributed over the various surfaces give additional evidence to explain this phenomenon.

Abstract No. 119

Passivated Silicon Devices

C. H. Li, Semiconductor Div., General Instrument Corp., 600 W. John St., Hicksville, N. Y.

Passivated surface is considered as a hermetic, large-area silicon-to-oxide joint or seal. The mechanical, electrical, and chemical requirements of this seal are discussed, with emphasis on oxide thickness, structure, and composition. Experimental data are given showing why and when on thermal cycling the oxide cracks and silicon deteriorates. A low-temperature passivating method has been developed giving units completely inert to ambient gases, organic solvents, or even various metallic and nonmetallic ions.

Abstract No. 120

Measurement of the Thickness and Refractive Index of Surface Oxide Films on Semiconductor Materials

G. R. Booker and **C. E. Benjamin,** Research Labs., Westinghouse Electric Corp., Beulah Rd., Churchill Boro., Pittsburgh 35, Pa.

The application of monochromatic-light interferometry to the measurement of the thickness and refractive index of surface oxide films on semiconductor materials is described. Interference fringe patterns may be obtained by comparing either the top surface or the bottom surface of a wedge-shaped step in the oxide film with an external reference plane, or by comparing the two surfaces of the wedge with one another. Capabilities and accuracies obtainable using these three systems are discussed. A novel method is described for the rapid measurement of oxide film thicknesses on silicon; the method uses simple equipment and is independent of surface roughness.

Abstract No. 121

Hysteresis in the Large-Signal Field Effect in Semiconductor Surfaces

D. R. Frankl, General Telephone and Electronics Labs., Inc., Bayside 60, N. Y.

The finite generation and recombination rates of excess minority carriers can lead to large hysteresis effects even at frequencies $<<(2\pi\tau)^{-1}$ in large-signal field effect measurements. The hysteresis loop occurs on the inversion-layer side of the conductance *vs.* field curve and widens with increasing frequency and with increasing minority carrier lifetime in the sample. The importance of this effect is that it may lead to appreciable errors in certain point-by-point measuring techniques. Experimental results on germanium and a simple theoretical treatment are presented.

Abstract No. 122

Electrolytic Slicing of Germanium, II. Characteristics of the {110} and {100} n- and p-type Surfaces

Sumner Sheff, Semiconductor Div., Raytheon Co., Newton, Mass.

A metallographic study was made of both sides of {110} and {100} n- and p-type germanium wafers produced by the electrolytic slicing technique. Etch pits were observed on the n-type surfaces which are closely related to those found on the {111} surfaces. These pits extend far into the germanium wafers in one of the <100> directions depending on the side being examined. An explanation of this observation is proposed. The effects of illumination, slice thickness, current density, electrolyte flow rate, and concentration are also discussed. Electron diffraction, electron micrographic, and field effect data for these surfaces are presented in the two following papers.

Abstract No. 123

Further Study by Electron Microscopy and Diffraction of Germanium Surfaces from Electrolytic Slicing

J. J. Oberly, Research Div., Raytheon Co., Waltham, Mass.

The study of germanium surfaces produced by electrolytic slicing has been extended to (100) and (110) surfaces. There is no indication of surface damage, and the surfaces of p-type Ge or of n-type Ge sliced under intense illumination are generally free from pits. The deep pits or "pipes" in unilluminated n-type Ge which have been attributed to avalanche breakdown are partially filled with particles identified as Ge. The randomly oriented Ge film previously observed on n-type (111) surfaces probably consisted of these particles.

Abstract No. 124

Spreading during Capillary Alloying

Karl Busen, Kurt Lehovec, and **Raynor Linzey,** Sprague Electric Co., North Adams, Mass.

This paper describes experiments carried out on (111) oriented germanium which were in contact with liquid indium. It was found that, in spite of a lateral restriction of the indium by the walls of a quartz capillary, there was spreading over the germanium surface, depending on the previous mechanical surface treatment. However, the maximum spreading is limited by the diffusion rate of dissolved germanium in radial direction toward the capillary.

Abstract No. 125

The Spreading of Molten Indium on Germanium

A. A. Bergh, Bell Telephone Labs., Inc., Allentown, Pa.

Factors influencing the spreading of molten indium on germanium oriented parallel to the <111> plane have been investigated. The surface tension of indium as a function of temperature and germanium content has been determined and the effect of the gaseous ambient and surface conditions of germanium studied. It was found that the latter has a more pronounced influence on spreading than the change in the surface tension of indium.

Abstract No. 126

Characteristics of Porous Vycor as a Moisture Getter in Semiconductor Devices

M. J. Rand, Bell Telephone Labs., Inc., Allentown, Pa.

The moisture adsorption capacities of porous Vycor are presented as adsorption isotherms at 30°-150°C with coverages up to 0.3 monolayers. The thermodynamics, kinetics, and mechanism of the adsorption are considered. Vacuum bakeout and hot gas flushing are compared as activation procedures. Equations are developed which predict the changes in an enclosed Vycor-containing ambient as a function of temperature.

Abstract No. 127

Fabrication of Ultra Fast Switching Tunnel Diodes

H. C. Schindler, General Instrument Corp., 600 W. John St., Hicksville, N. Y.

Tunnel diodes are finding increasing application as fast switching devices in control systems and computers. By optimizing the doping level and junction area, tunnel diodes have been prepared with unusually high peak current to capacity ratios which switch in as little as 0.5 manoseconds. 1 ma units of this type in a standard T018 package oscillate at frequencies up to 1.5 kmc. This paper presents a discussion of the manufacturing techniques employed to obtain these results as well as a correlation between doping level, junction area, and switching speed.

Abstract No. 128

Automatic Custom Etching of Tunnel Diodes

V. Vulcan, General Instrument Corp., 600 W. John St., Hicksville, N. Y.

An automatic electrolytic etching process has been invented for tunnel diodes capable of producing units with any peak current between 100 ma and 250 ma with a tolerance of ±2%. Any starting material may be used. Both analog and digital techniques have been employed in the design of the apparatus. Novel detector and feed-back circuitry forces the pulsed etching current to slave to the instantaneous sampled peak current, thus preventing overetching or burn-out. A tunnel diode gate automatically rejects high contact resistance units. High peak-to-valley ratios and low series resistances are preserved, resulting in desirable etch contours.

Abstract No. 129

A Very Low Current Controlled Rectifier; Some Problems of Design and Fabrication

C. W. Heath and **W. M. Robinson,** Electronics Components Div., General Electric Co., Auburn, N. Y.

The ZJ-203 very low current silicon controlled rectifier is housed in the standard JEDEC TO-5 transistor package. The device employs a welded case, glass-to-metal seals, hard solders for pellet mounting, and a painted external surface for maximum heat dissipation. Design objectives are discussed which have resulted in a PNPN device with very high gate sensitivity, blocking voltages up to 400 v, and extremely uniform characteristics. Some problems and unique features of design and fabrication are discussed. Among these are a relatively new ultrasonic method of bonding ohmic contacts to the silicon pellet, and the investigation of a forward voltage drop problem and its solution through a diffusion operation. Slides will be shown depicting devices construction and electrical characteristics.

Abstract No. 130

Photolithography Applied to Silicon Transistor Technology

J. Spanos, Hoffman Semiconductor Division, El Monte, Calif.

Photolithography as it applies to silicon technology is defined. The relationship of photolithography to device construction is specifically shown. Various techniques of mask making are compared as an auxiliary function. Specific problems in the use of photopolymeric materials are discussed from both a production and laboratory point of view. Device applications are shown.

Abstract No. 131

Epitaxial Silicon Thin Films

K. J. Miller and **R. C. Manz,** Bell Telephone Labs., Inc., Murray Hill, N. J.

The growth of epitaxial silicon films of controlled type, resistivity, and thicknesses for semiconductor devices is described. The surface texture, film crystal structure, and electrical properties are discussed and related to growth conditions.

Abstract No. 132

Epitaxial Silicon Thin Films

C. H. Li and **D. Scaringella,** Semiconductor Div., General Instrument Corp., Hicksville, N. Y.

An improved and reproducible method for epitaxial growth of silicon is described. The equipment is compact, simple, reproducible, and has an improved gas-mixing system. The process allows shorter time for preparing the first run and making each subsequent run. The layers produced are planar and uniform from center to edge. Under 500X magnification, they show no pits, oxides, pyramids, growth scales, or crystal structures. A description is given of the characteristics of diodes and transistors fabricated from this material.

Abstract No. 133

Epitaxial Deposition of Silicon in a Hot-Tube Furnace

B. E. Deal, Research and Development Dept., Rheem Semiconductor Corp., Mountain View, Calif.

A method has been developed for epitaxially depositing single crystal silicon in a conventional hot-tube

furnace. Silicon is deposited on a silicon substrate by the reduction of a silicon halide at temperatures in excess of 1200°C. A modification of the gas inlet system prevents decomposition of the silicon halide before contacting the silicon substrate. Several silicon slices can be treated simultaneously with good reproducibility of deposit thickness and resistivities.

Abstract No. 134

Properties of Epitaxially Grown Silicon Crystals

C. J. Marlett and **P. A. Newman,** United States Army Signal Research and Development Lab., Fort Monmouth, N. J.

Resistivity, Hall mobility, lifetime, and carrier concentration have been measured as a function of temperature from 80° to 500°K on a number of epitaxially grown n- and p-type silicon crystals having carrier concentrations between 10^{13} and 10^{20}/cm^3. Similar measurements have also been made on two layer structures of alternate p- and n-type material. The dislocation density of the samples was also observed.

Abstract No. 135

Impurity Control and Distribution in Epitaxial Silicon Films

D. Kahng, R. C. Manz, M. M. Atalla, and **C. O. Thomas,** Bell Telephone Labs., Inc., Murray Hill, N. J.

A study of the epitaxial growth of n-type silicon on n+-type substrates using a doped pedestal as a means of resistivity control in the film is described. Data are presented on the resistivity profiles obtained with the films and their relation to various parameters. Results are also presented on the diffusion of various impurities in epitaxial films and compared with diffusion in bulk silicon. The technique for obtaining the details of the doping profiles within the films also is described.

Abstract No. 136

Methods for Measuring Resistivity Gradients and Thicknesses in Epitaxial Films

J. E. McNamara and **H. M. Robertson,** Materials Research Dept., Semiconductor Products Div., Motorola, Phoenix, Ariz.

The orderly development of an epitaxial technology requires reliable experimental methods for the measurement of both film thicknesses and internal resistivity gradients. A general review of the possible methods is presented. Special consideration is given to the problem of measuring carrier concentration gradients in directions both normal and parallel to epitaxial growth planes.

Abstract No. 137

Surface Effects and Autodoping in Epitaxial Germanium Layers

E. Matovich and **R. J. Andres,** Hughes Products, P. O. Box 278, Newport Beach, Calif.

High-resistivity epitaxial germanium has been grown by using a catalytic reduction of $GeCl_4$ in an open-tube process, at temperatures intermediate to those used for pyrolytic decomposition of $GeCl_4$ (Bell Labs.) and disproportionation of GeI_2 (IBM). Surface structure of, and impurity distribution in, the epitaxial layers are shown to be a function of the growth conditions.

Abstract No. 138

Evaluation of Germanium Epitaxial Films

J. R. Biard and **S. B. Watelski,** Texas Instruments Inc., Box 5012, Dallas 22, Texas

A method has been developed for rapid and accurate determination of the resistivity of p-type epitaxial germanium films deposited on p+ germanium substrates. Determination of the resistivity is not dependent on a knowledge of film thickness. Data are presented for films with resistivities of 0.05-7.0 ohm-cm, deposited on 0.002 ohm-cm substrates; film thicknesses range from 0.15 to 0.6 mil.

Abstract No. 139

Some Properties of Epitaxial Germanium

A. B. Kuper and **H. Christensen,** Bell Telephone Labs., Inc., Murray Hill, N. J.

Germanium (111) epitaxial films have been deposited in an open tube system from H_2-$GeCl_4$ (undoped) at 850°C. Junction capacitance measurements suggest the principal impurity is copper (2.5×10^{14}/cc after 600°C anneal). After etch removal of the substrate one of these films was annealed at 550°C. Sheet resistance measurements as a function of annealing time suggested slow precipitation of copper characteristic of Ge with less than 10^5 dislocations/cm^2. Hall effect hole mobility *vs.* temperature was similar to that in high resistivity melt-grown Ge. Electron transmission diffraction shows no crystalline imperfections in these films.

Abstract No. 140

Vapor Growth of GaAs

V. J. Lyons and **V. J. Silvestri,** Research Center, International Business Machines Corp., Yorktown Heights, N. Y.

It has been demonstrated previously that synthesis and crystal growth of III-V compounds can be carried out at temperatures below the compound melting points by reacting a Group III halide with a Group V element. In this work single crystal films of GaAs have been grown from a vapor phase consisting of gallium iodides and arsenic. The material was deposited epitaxially on monocrystalline GaAs of various crystallographic orientations. The reactions were carried out in sealed quartz tubes under varying conditions of temperature and pressure. Measurements of the resistivity and mobility of the deposited GaAs are presented. Vapor pressure measurements for the system are discussed.

Abstract No. 141

Mechanism for the Vapor Transport of Gallium Arsenide with Hydrogen Chloride

F. V. Williams and **R. A. Ruehrwein,** Research and Engineering Div., Monsanto Chemical Co., Dayton, Ohio

Epitaxial layers of GaAs have been grown on GaAs substrates in an open system using hydrogen chloride as the transfer agent. The principal features of this process are: (*a*) reaction of GaAs with HCl at temperatures above about 750°C to yield a mixture of gaseous reaction products, and (*b*) reaction of the gaseous reaction products of step (*a*) at lower temperatures to redeposit GaAs. A mechanism for the first step has been deduced. Equilibrium data indicate that a lower chloride of gallium, GaCl, is formed. Thermodynamic constants for the reaction are given. The second step of the process is *not* a simple reversal of the first step. Disproportionation of the lower chloride of gallium occurs, along with redeposition of GaAs, in such a fashion that the theoretical fraction of GaAs which can be redeposited is two-thirds. Some effects of substrate orientation on epitaxial growth are discussed.

Abstract No. 142

An Open Tube Carrier Gas Method for the Epitaxial Growth of Gallium Phosphide

C. J. Frosch and **P. W. Foy,** Bell Telephone Labs., Inc., Murray Hill, N. J.

An open tube processing technique is described for growing epitaxial layers of gallium phosphide. The method is based on an appreciable volatility of a gallium containing vapor species which is believed to be GaP (g). Either undoped or doped epitaxial layers can be grown. Some of the structural and electrical characteristics of these layers are described. Epitaxial layers of gallium arsenide and gallium arsenide phosphide ($GaAs_xP_y$) also can be grown by this technique. It may also prove to be suitable for growing epitaxial layers of other multicomponent semiconductors.

Abstract No. 143

Vapor Phase Growth of GaAs and GaP

R. R. Moest and **B. R. Shupp,** Bell Telephone Labs., Inc., Murray Hill, N. J.

Gallium arsenide and GaP films have been grown in sealed systems charged with HCl gas. The growth rate on GaAs substrates from GaAs sources has been measured as a function of temperature, initial HCl pressure, and substrate orientation. Conductivity type of the films can be controlled by doping the source material. Epitaxial films of GaAs have been grown on Ge and GaP films on GaAs.

Abstract No. 144

The Pseudobinary System Mg_2Si-Mg_2Ge

R. J. LaBotz and **D. R. Mason,** Dept. of Chemical and Metallurgical Engineering, University of Michigan, Ann Arbor, Mich.

Thermal conductivity, electrical conductivity, Hall effect, x-ray diffraction, and differential thermal analysis data have been taken on the pseudobinary system Mg_2Ge—Mg_2Si. The data indicate that Mg_2Ge—Mg_2Si have complete solid solubility, as expected, because of the structural similarity between Mg_2Ge and Mg_2Si. The thermal conductivity, electrical conductivity, and Hall effect data are analyzed to determine relative variations in the properties as a function of composition.

Abstract No. 145

Impurity Distribution in Single Crystal Indium Antimonide

G. R. Cronin, Texas Instruments Inc., Dallas, Texas

The purpose of this work is to examine the anisotropic segregation of various impurities in InSb. Crystals oriented (111), (110), (311), and (100) were pulled from melts containing radioactive Zn, Sn, Fe, and Ag. Uniformity of distribution is evaluated parallel and perpendicular to the growth direction. The most striking result of this work is the nonuniformity of (111) crystals as compared with other orientations. All of the results are explained in terms of the facet effect.

Abstract No. 146

Distribution of Sulfur Impurity in InSb Single Crystals

M. D. Banus and **H. C. Gatos,** Lincoln Lab., Massachusetts Institute of Technology, Lexington 73, Mass.

Single crystals of InSb doped with inert or radioactive sulfur (δ35) were pulled from the melt using a Czochralski-type technique. The distribution of sulfur was studied by high resolution autoradiography and electrical measurements. In crystals grown along the <111> direction, a well-defined core with increased concentration of sulfur is associated with the {111} facet present at the liquid-solid interface. The effects of changing rotation rate during growth on the concentration "on-facet" and "off-facet" and on the effective distribution coefficients are presented. The results are discussed on the basis of crystal growth mechanisms.

Abstract No. 147

Correlation of Electrical Measurements and Chemical Analyses of Zinc- and Cadmium-Diffused GaAs

J. F. Black, General Telephone and Electronics Labs. Inc., Bayside 60, N. Y.

Thin rectangular slices of single-crystal GaAs were doped to degeneracy by indiffusing zinc or cadmium at 1100°-1200°C from arsenic-metal vapors in evacuated quartz capsules. The gradient of dopant concentration throughout the thickness of the slices was controlled over a wide range. In several cases the dopant concentration at the median plane of the slice was as an order of magnitude lower than at the surface of the slice. In all instances, however, the free hole concentration calculated from Hall effect measurements agreed with the average dopant concentration determined by chemical analysis. Data on measured Hall mobilities are presented and compared with data for melt-doped GaAs.

Abstract No. 148

Correlation of Lattice Parameter Measurements and Electrical Measurements in Highly Doped GaAs

J. F. Black and **P. Lublin,** General Telephone and Electronics Labs., Inc., Bayside 60, N. Y.

The variation in the lattice parameter of GaAs was studied as a function of doping with donor and acceptor elements, including Cd, Zn, Te, and Se. A modified precision lattice constant technique for powders was used; this can detect changes in the lattice constant of $\pm$0.0002Å in GaAs. On the basis of these lattice parameter measurements the solubility of the dopants could be determined. Data on Hall effect and resistivity are presented and correlated with the x-ray data.

Abstract No. 149

Nondendritic Ribbon Crystals

H. Norman, G. Russell, and **M. Forney,** Semiconductor Products Div., Motorola, 5005 E. McDowell Rd., Phoenix, Ariz.

A technique for growing single crystals of germanium by a nondendritic process is presented. The dependence of the process on crystallographic orientation of the seed and a restricted meniscus is discussed. The necessary temperature gradients to allow feasible growth rates are described and techniques for maintaining these gradients discussed.

Abstract No. 150

Preparation of High-Purity Silicon from Silane

C. H. Lewis, M. B. Giusto, H. C. Kelly, and **Sidney Johnson,** Metal Hydrides Inc., Beverly, Mass.

The preparation, purification, and thermal decomposition of silane, SiH_4, were investigated for the purpose of preparing high-purity silicon. Quantitative yields of silane were obtained by the reduction of silicon tetrachloride with various hydrides. The reactivity of silane with various purifying agents was studied. Variables in the thermal decomposition of silane were evaluated with regard to purity of the elemental silicon produced, and the efficiency of dissociation and deposition rate. Silane was dissociated on an inductively heated single crystal silicon substrate to yield high-purity silicon. Neutron activation analyses for microcrystalline high-purity silicon as deposited are indicated below:

Impurities in Silicon Metal from Thermal Decomposition of Silane

Neutron activation analyses (ppb)

Fe	17.0*	As	1.0	Zn	0.41*	Ga	0.0062*
Cu	11.0	P	1.0*	Ni	0.27*	Sb	0.0037*
Bi	1.6*	Tl	0.91*	In	0.032*	Mn	0.00062*

* Not detected. Value shown is limit of detection in ppb.

Abstract No. 151

The Effect of Heat Treatment, Oxygen, and Structure on the Lifetime of Float Zoned Silicon Crystals

M. D. Jordan and **E. W. Stewart,** E. I. du Pont de Nemours & Co., Brevard, N. C.

Lifetime of float zoned silicon crystals is shown to be independent of oxygen content, crystal structure, and initial lifetime values after heat treatment at diffusion temperatures. Samples have been analyzed by copper decoration techniques and neutron activation in an attempt to explain these results. The data obtained are compared to previous work, and the effect of these phenomena on device production are postulated.

Abstract No. 152

Measurement Errors of Silicon Single Crystals and Slices

J. S. Miller, and **V. E. Paulos,** Materials and Sensors Quality Assurance, Texas Instruments Inc., P. O. Box 312, Dallas 21, Texas

One of the most important aspects connected with the measurement of any parameter for practically all

products is the amount of error involved when making such a measurement. If this error is not determined or estimated, then the accuracy and precision of the measurement is unknown. The use of such information, when the error is unknown, could be extremely expensive by causing excessive rejection of products which otherwise might have been acceptable. This is especially true of silicon single crystals and slices used in the manufacture of semiconductor devices.

At Texas Instruments, there are many parameters which are used to determine the quality of silicon single crystals and slices such as the grade of silicon used, its boron and phosphorus content, the lifetime of the crystal, dislocation density, diameter, resistivity, general appearance, etc. However, for the purpose of this discussion we will deal only with crystal and slice resistivity and slice thickness.

Abstract No. 153

Resistivity Measurements at Microwave Frequencies

G. L. Allerton and **J. R. Seifert,** Western Electric Co., 555 Union Blvd., Allentown, Pa.

Resistivity measurements can be made at microwave frequencies with less damage to the material than obtained by a conventional four point probe and in a faster and more accurate manner. A high Q resonant circuit has been developed for low resistivity ranges of 0.002 to 1.0 ohm-cm. A second method of measuring the transmission loss through thin slices is used to cover the resistivity range from 0.1 to 40 ohm-cm.

Abstract No. 154

Silicon Crystal Perfection Measurement and Grading

M. R. Everingham, E. I. du Pont de Nemours & Co., Inc., Brevard, N. C.

Several sample preparation and etching techniques to reveal structural defects in silicon crystals are compared. One method is described which provides excellent reproducibility in a reasonable period of time. A system of numerical grading to designate the relative severity of lineage and slip is outlined. This system has proven useful in standardizing perfection measurements between various laboratories.

Abstract No. 155

Horizontal Zone Leveling of Silicon

J. L. Porter, Sylvania Electric Products Inc., Woburn, Mass., and **D. M. Lamb,** Sylvania Electric Products Inc., Towanda, Pa.

A method for the horizontal zone leveling of silicon is described. Maintaining the walls of the vessel at a temperature below the melting point of silicon prevents adhesion of the silicon upon solidification. Such a technique facilitates the formation of large, heavily doped silicon crystals for microwave application.

Abstract No. 156

Iron-Boron Interactions in Silicon

W. H. Shepherd and **J. Turner,** Research Labs., The Plessey Co. Ltd., Caswell, Towcester, Northants, England

Time dependent resistivity changes in p-type silicon, saturated with iron and quenched from above 900°C, are shown to be due to pairing between iron and boron. At 45°C more than 50% of the boron may be paired. Precipitation of the iron has also been studied. Below 200°C the iron solubility after precipitation is strongly influenced by pairing and electron hole equilibria. Analysis of these data gives the true solubility of iron at these temperatures.

Abstract No. 157

Trace-Plating

W. Rindner and **J. M. Lavine,** Research Div., Raytheon Co., Waltham, Mass.

The observation of nucleation of plated metals on lines scribed on semiconductors using hard stylus materials had led to investigations showing that preferential plating can also be obtained on thin films traced with soft styli on semiconducting and insulating materials. Trace and plating materials may be either doping elements or carrier metals. Ohmic and rectifying contacts to Ge and Si as well as mesa transistors have been fabricated by trace-plating in conjunction with conventional alloying techniques.

ELECTRO-ORGANIC

Abstract No. 158

Improvement in the Electrolytic Preparation of Iodoform

R. Ramaswamy, M. S. Venkatachalapathy, and **H. V. K. Udupa,** Central Electrochemical Research Institute, Karaikudi 3, S. Rly., India

Use of a lead dioxide anode with a graphite substrate in the electrolytic preparation of iodoform is described. Influence of bath composition, temperature, and pH on the current efficiency has been investigated. Results are compared with those obtained with the conventional anodes like platinum and graphite. Effect of rotation of the anode in the preparation is discussed.

Abstract No. 159

Electrolytically Regenerated Manganic Sulfate for the Oxidation of Aromatic Hydrocarbons, II. Oxidation of Xylenes to Tolualdehydes

R. Ramaswamy, M. S. Venkatachalapathy, and **H. V. K. Udupa,** Central Electrochemical Research Institute, Karaikudi 3, S. Rly., India

The electrolytic oxidation of p-xylene to p-tolualdehyde has been investigated both by a single stage process as well as by a two-stage process using lead dioxide anode. The single stage process using manganous sulfate as "oxygen carrier" gave a low current efficiency ($<30\%$), whereas the two-stage process gave an overall current efficiency of 40-45%. Manganous sulfate as a suspension in 55% H_2SO_4 could be oxidized anodically to a manganic sulfate paste which could be used in the controlled oxidation of xylenes to tolualdehydes. Results obtained in this cyclic process are presented.

Abstract No. 160

Stereochemistry of Electrolytic Reductions of Butynediol and Cyclohexene- 1,2- Dicarboxylic Acid

George Brownell and **C. L. Wilson,** Phillips-Foscue Corp., Box 1306, High Point, N. C.

(No abstract received)

Abstract No. 161

Electrolytic Formation of Oximes

Tadao Hayashi, Dept. of Applied Chemistry, University of Osaka Prefecture, Mozu-Umeno-cho, Sakai City, Osaka, Japan and **C. L. Wilson,** Phillips-Foscue Corp., Box 1306, High Point, N. C.

(No abstract received)

Abstract No. 162

New Study on the Electrolytic Reduction of Dicyandiamide. An Approach to the Essential Problem on Organic Electrode Process

Kiichiro Sugino, Keijiro Odo, and **Eiichi Ichikawa,** Tokyo Institute of Technology, Ookayama Meguro-ku, Tokyo, Japan

Although dicyandianide gave no distractive polarographic wave, it was reduced at a mercury cathode at −1.05 v (*vs.* S.C.E.) to give a 4 hydrogen addition compound; at a palladium-black cathode dicyandiamide was reduced at −0.10 v (*vs.* S.C.E.) with 100% current efficiency to give a 2 hydrogen addition compound. Thus the observed difference in reduction potentials and products indicates the essential difference between reduction by direct electron transfer (Hg electrode) and reduction by chemisorbed hydrogen (Pd-black electrode).

Abstract No. 163

A Continuous Flow Cell for Electrochemical Synthesis

M. J. Allen, Chemical Research Dept., Electro-Optical Systems, Inc., Pasadena, Calif.

One of the major drawbacks to the use of electrochemical techniques in the production of synthetic organic chemicals is the unavailability of an efficient, readily fabricated continuous flow cell. A pilot plant cell has been developed which consists of thin polysterene compartments. The odd numbered compartments are separated from the next higher even numbered compartments by an ion-exchange membrane. Located between the even numbered compartments and the next higher odd numbered compartments are floating electrodes. The terminal electrodes at each end of the cell are connected to a d-c source. Each compartment has an inlet and outlet through which the catholyte and anolyte flow into alternate cell sections. A study of the reduction of p-hydroxybenzaldehyde has been made utilizing this cell.

Abstract No. 164

Voltammetric Study of the Kolbe Reaction

M. J. Allen, Chemical Research Dept., Electro-Optical Systems, Inc., Pasadena, Calif., and **W. W. Pierson,** Dept. of Chemistry, Seton Hall University, South Orange, N. J.

Various acids such as acetic, caproic, heptanoic, isocaproic, isovaleric, octanoic, and valeric acid were investigated as their sodium salt in a methanolic medium at a rotating platinum anode. The data obtained are discussed and correlated with free radical formation at the electrode surface. A comparison is also made with the data obtained on sodium acetylglycinate, which is known not to undergo the typical Kolbe dimerization.

Abstract No. 165

Anhydrous Voltammetry of the Acetate Ion at a Rotating Platinum Anode

M. J. Allen, Chemical Research Dept., Electro-Optical Systems, Inc., Pasadena, Calif., and **W. W. Pierson,** Dept. of Chemistry, Seton Hall University, South Orange, N. J.

The most commonly accepted theory on the mechanism of the Kolbe reaction is the discharged ion theory of Brown and Walker whereby the acetate loses one electron to the anode resulting in an acetate radical which spontaneously splits off CO_2 and produces a methyl radical which is free to react with a second methyl radical to give the Kolbe dimer, ethane. If this theory is correct, the discharge of acetate ion should give an irreversible voltammetric step where the diffusion current varies linearly with acetate ion concentration. The acetate ion was investigated in a methanolic medium in concentrations of from 0.08M to 1.0M. The half-wave potentials (corr.) *vs.* Ag, AgCl electrode varied from +1.64 v for the lower concentration to +1.25 v for the higher concentration. The diffusion current varied linearly from 0.32 to 3.28 ma.

Abstract No. 166

Electrode Processes in Acetonitrile

D. H. Geske, Dept. of Chemistry, Cornell University, Ithaca, N. Y.

The properties of acetonitrile make it a uniquely suitable media for the investigation of organic electrode processes. In particular, resistance of the solvent itself to electro-oxidation is important. Recent electrochemical investigations are discussed.

Abstract No. 167

The Role of Proton Addition in the Polarographic Reduction of Aromatic Hydrocarbons and Carbonyl Compounds in Dimethylformamide

P. H. Given, Pennsylvania State University, University Park, Pa.

The electrochemical reduction of a neutral molecule requires addition of protons as well as electrons, and proton addition may well be irreversible. By working in a suitable organic solvent, protonation can be made so slow that electron addition by itself can be studied. The addition of weak acids to solutions in such solvents alters the polarographic behavior in a variety of ways, which throw light on polarographic mechanisms; phenol is particularly useful as a protonating agent since it is not reducible at the dropping mercury electrode within the accessible range of potentials, nor does it give a hydrogen discharge wave in dimethylformamide. Experimental data for several systems are discussed to illustrate the above generalities. Evidence is presented that in dimethylformamide the effective protonating agent is the undissociated acid and not the solvated proton.

Abstract No. 168

Polarography and Voltammetry in Dimethylsulfoxide

I. M. Kolthoff and **T. B. Reddy,** (present address: Bell Telephone Labs. Inc., Murray Hill, N. J.) University of Minnesota, Minneapolis 14, Minn.

A polarographic study of several acids, some representative metal ions, a few quinones and oxygen has been made in the solvent dimethylsulfoxide (DMSO). Perchloric, sulfuric, and hydrochloric acids were found to be strong, monoprotic acids in DMSO. Cobalt(II) and nickel(II) are reduced irreversibly at the dropping mercury electrode with large overpotentials indicating strong solvation. Polarograms of quinones gave two cathodic waves of unequal height in the absence of proton donor. The effect of proton donor on the polarograms of quinones was studied. The mechanism of the reduction of quinones in DMSO is discussed. A rotated platinum and rotated mercury pool electrodes can be used to advantage in DMSO.

Abstract No. 169

Voltammetry in Liquid Sulfur Dioxide

P. J. Elving and **Elio Vianello,** Dept. of Chemistry, University of Michigan, Ann Arbor, Mich.

Although numerous excellent studies of voltammetry in nonaqueous solvents and, more particularly, in nonprotonic-releasing solvents have been reported, liquid sulfur dioxide is apparently the first nonprotonic solvent to be investigated as a medium for voltammetry. Sulfur dioxide has an interesting possible advantage in investigating the mechanisms of organic electrode reactions because of its effectiveness as a reaction medium in stabilizing free radicals. The experimental principles of voltammetry in sulfur dioxide are described: use of vacuum line technique for preparing solutions and maintaining them during measurement, usable indicating and reference electrodes, and available background electrolytes. Attention is given to the implication of the possible reaction of the solvent with indicating and reference electrodes and the minimization of the solution resistance. Results obtained in the cathodic and anodic voltammetry of various inorganic and organic depolarizers are discussed.

Abstract No. 170

The Uses of Electrical Methods in Organometal Systems

R. E. Dessy, Rudolf Salinger, and **Richard Jones,** Dept. of Chemistry, University of Cincinnati, Cincinnati, Ohio

During recent years considerable effort has been expanded on the elucidation of the structure of the Grignard reagent, "RMgX," resulting from the reaction of RX and Mg in ether. A combination of tracer techniques and electrolysis experiments, along with conductivity experiments, indicates that there are two distinct types of Mg in the compound, and that an empirical formula R_2Mg, MgX_2 is a better representation than RMgX. Recent kinetic investigations on the reactions with Schiff bases involving measurement of dielectric constant show that two distinct types of R group are present during reaction, confirming the above hypothesis.

Abstract No. 171

Electrochemical Preparation of Polyfluoro Chemicals in Anhydrous HF

R. D. Dresdner, University of Florida, Gainesville, Fla.

Many organic materials are ionogens in anhydrous HF providing conducting solutions. When a direct current at (4-6 v) voltages is passed through such solutions, hydrogen is evolved at the cathode and a myriad of products containing fluorine are found. In many of these the hydrogen has been completely replaced by fluorine. Organic materials containing groups such as carboxyl, acyl halide, sulfonyl halide, ether, sulfide, amine, and sulfoxide lend themselves to this process to varying degrees. The products formed in the process depend to a large extent on the many variables that require a degree of control, but because of the high energies involved, structure retention is the frequent exception rather than the rule. Fragmentation, cyclization of acyclic starting materials, acyclization of branched starting material, and polymerization are encountered along with a high degree of fluorination of the starting structures. Elements in the products are generally found in their highest oxidation states. The process is still an art in many respects and any degree of predictability of products is still a hazard. This paper attempts to review the results of the current literature in the field.

Abstract No. 172

Polarographic Studies in Acetonitrile and Dimethylformamide, VII. Behavior of Benzyl Halides and Related Compounds

S. Wawzonek and **R. C. Duty,** Dept. of Chemistry, State University of Iowa, Iowa City, Iowa

Polarographic studies of benzyl chloride, benzyl bromide, benzyl iodide, benzylmercuric iodide, dibenzylmercury, mercuric iodide, ethyl chloracetate and ethyl bromoacetate have been made in acetonitrile and dimethylformamide containing tetrabutylammonium salts. Benzyl chloride and ethyl chloracetate were found to undergo a facile displacement reaction with bromide ion. Benzyl chloride and bromide react with iodide ion to form benzyl iodide which reacts rapidly with mercury and forms benzylmercuric iodide. The latter compound, upon standing, slowly forms mercuric iodide.

Abstract No. 173

Polarographic Reduction of Some Diketones and Pyrones

R. L. Flurry, R. H. Philip, and **R. A. Day, Jr.,** Dept. of Chemistry, Emory University, Atlanta 22, Ga.

Additional studies on the polarographic reduction of benzil, benzoin, and several diketones have been carried out. A mechanism is proposed to account for the differences in the ease of rearrangement of the intermediate dienol assumed to be formed in the reduction of the diketone. This ease of rearrangement is related to the pH at which the second wave is observed for certain diketones. Preliminary results on the reduction characteristics of γ-pyrone and several substituted pyrones are reported.

Abstract No. 174

Electrochemical Reduction of the Benzene Ring

H. W. Sternberg, Raymond Markby, and **Irving Wender,** U.S. Dept. of the Interior, Bureau of Mines, Pittsburgh 13, Pa.

Application of electrolytic methods to coal chemistry has been restricted by the fact that the benzene ring, which represents a large portion of the coal structure, could not be reduced electrolytically. We now have found that electrolysis of tetralin in methylamine saturated with lithium chloride gives hexalin and octalin. The possibility of direct electron transfer from cathode to tetralin is discussed, and the implications of this reaction for the polarographic determination and electrolytic reduction of the benzene ring are pointed out.

Abstract No. 175

Kolbe and Crum Brown-Walker Syntheses with Perfluoroaliphatic Acids

Sherlock Swann, Jr., and **F. H. Baastad** (Fellow of the Royal Norwegian Council for Scientific and Industrial Research, 1952-53, Present address: Finn Baastad, Grandeveien 5, Bygdoy, Oslo, Norway), Dept. of Chemistry and Chemical Engineering, University of Illinois, Urbana, Ill.

The Kolbe electrolytic synthesis of tetradecafluorohexane from free heptafluorobutyric acid has been carried out in excellent yield. It has been found possible to prepare the half fluorinated hexane by electrolysis of a mixture of the potassium salts of butyric acid and heptafluorobutyric acid. Similarly, ethyl heptafluorododecanoate has been obtained from the potassium salts of monoethyl sebacate and heptafluorobutyric acid. Electrolyses of the potassium salts of nonanoic and pentadecafluoroöctanoic acids have also been carried out.

Abstract No. 176

Anodic Oxidation in a Heterogeneous System

H. F. Conway, E. B. Lancaster, V. E. Sohns, and **S. Dabic,** Northern Regional Research Lab., Peoria, Ill. (This is a Laboratory of the Northern Utilization Research and Development Div., Agricultural Research Service, U.S. Dept. of Agriculture)

In-cell oxidation of starch to dialdehyde starch by electrolytically generated periodic acid is a pseudo electro-organic reaction. Possible reactions of starch and dialdehyde starch with components of the reaction mixture under conditions in the cell are reviewed. The mechanical features of the cell that can influence starch oxidation and the engineering problems encountered in the initial pilot-scale production are discussed.

Abstract No. 177

Experimental Study of the Anode Effect in the Electrolysis of Fused Mixtures of Sodium Chloride and Zirconium Tetrafluoride

C. M. Decroly and **René Winand,** Lab. of Metallurgy and Electrochemistry, University of Brussels, 50 Ave. F. D. Roosevelt, Brussels 5, Belgium

An experimental investigation has been made of the anode effect when electrolyzing mixtures of fused sodium chloride and zirconium tetrafluoride. Factors which have been studied were: composition of the melt, diameter of the graphite cylindrical anode, temperature, speed of rotation of the anode, and addition of zirconium dioxide. It can be shown that there exists a critical current density under which it is impossible to observe any anode effect. At a given temperature, these critical current densities depend on the composition of the melt and on the diameter of the anode. No marked effect of temperature, rotation of the anode, and addition of zirconium dioxide could be observed. A preliminary explanation of the facts observed is given.

Abstract No. 178

Ionic Transference in Pure Molten Sodium Nitrate

R. J. Labrie and **V. A. Lamb,** Metallurgy Div., National Bureau of Standards, Washington 25, D. C.

Transference numbers of sodium and nitrate ions in pure molten sodium nitrate have been measured in "H-shaped" cells containing a porous diaphragm between anode and cathode compartments. The cells differ from those used in previous researches in that legs made of sodium-ion-conductive porcelain served to carry the current of sodium ions into and out of the cell. This design allows repeated observations with high experimental precision. Transference number values depended on the material of the diaphragm. Diaphragms were of porcelain, alundum, and fritted Pyrex.

ELECTROTHERMICS AND METALLURGY

Abstract No. 179

Progress in Sintering

D. L. Wilder, Ames Lab., University of Iowa, Ames, Iowa

(No abstract received)

Abstract No. 180

Some Effects of Powder Properties and Consolidation Technique on the Properties of Sintered Tungsten Compacts

G. C. Bodine, Fansteel Metallurgical Corp., North Chicago, Ill.

The initial phase of the Bureau of Naval Weapons Tungsten Sheet Rolling Program included the evaluation of candidate tungsten powders with respect to the effect of particle distribution, density, and chemistry on consolidation to sintered billets. The relationship between compaction pressure and sintering cycle was also studied. The results of this investigation are presented.

Abstract No. 181

Activated Sintering of Tungsten

J. H. Brophy, H. W. Hayden, and **J. Wulff,** Dept. of Metallurgy, Massachusetts Institute of Technology, Cambridge 39, Mass.

Small additions of nickel to tungsten permit the strengthening and densification of both powder compacts and plasma-sprayed deposits at relatively low temperatures while maintaining a relatively high melting point. Theoretically, the mechanism appears to be a kinetic intermediate between current theories of solid and liquid phase sintering. Several other activating agents have been employed successfully, and in each case the densification is kinetically similar.

Abstract No. 182

Sintering Characteristics of Ultrafine Tungsten Powder

C. R. McKinsey, Union Carbide Metals Co., Niagara Falls, N. Y.

(No abstract received)

Abstract No. 183

4th Plansee Seminar

H. A. Johansen, Research Labs., Westinghouse Electric Co., Beulah Rd., Churchill Boro., Pittsburgh 35, Pa.

(No abstract received)

Abstract No. 184

Sintering of Pressureless Compacted Tungsten and Molybdenum

H. H. Hausner, Adjunct Professor, Polytechnic Institute of Brooklyn, and Consulting Engineer, 730 5th Ave., New York 19, N. Y., and **A. R. Foster,** Sylvania Electric Products Inc., Towanda, Pa.

The densification rate during sintering of a mass of powder can be expressed in an equation consisting of three components, dealing with the density before sintering, powder particle size, and particle activity. The methods of sintering tungsten and molybdenum powders compacted under pressure are well known. These powders, however, can be sintered also as loose particles or as slip cast, and the rate of sintering in this case depends to a large extent on the particle characteristics. The "activity" of the powder particles is discussed. Surprisingly high densities of tungsten and molybdenum can be obtained by sintering these pressureless compacted powders. Explanation of this effect is given.

Abstract No. 184A

Sintering of Slip Cast Tungsten

F. R. Charvat, Union Carbide Metals Co., 4625 Royal Ave., Niagara Falls, N. Y. and **G. Reinhardt,** National Aeronautics and Space Administration, Lewis Research Center, Cleveland 35, Ohio

The effect of sintering variables including temperature in the range 1500°-2250°C, and time from 0.5 to 4 hr with vacuum and hydrogen atmosphere are characterized for slip-cast tungsten. The results of the analysis are presented graphically with densification parameter as dependent variable. The use of the curves to calculate linear shrinkage and density is illustrated. An indication of the degree to which dimensional tolerances may be controlled in the slip-casting and sintering processes is obtained by statistical analysis of green and sintered dimensions.

Abstract No. 185

Plasma Spraying of Tungsten and Refractory Compounds and the Influence of Sintering on the Physical Properties of These Materials

Irving Strauss and **Robert Steinitz,** General Telephone & Electronics Labs. Inc., Bayside 60, N. Y.

The preparation of parts from tungsten and refractory compounds, such as tantalum carbide, by plasma spraying is described. The behavior of the deposited material during sintering at various temperatures is studied and compared with that of the same material produced by standard powder metallurgy techniques. The rate of densification of the sprayed material during sintering is compared with that of cold pressed material, and the influence of sintering on some physical properties, such as strength, microstructure, and electrical resistivity, is reported.

Abstract No. 186

Preparation of F48 Alloy by Means of Hydrostatic Pressing and Vacuum Sintering

J. W. Pugh and **J. F. Cerness,** Lamp Metals and Components Dept., General Electric Co., 21800 Tungsten Rd., Cleveland 17, Ohio

The experiments described were designed to prove the feasibility of the powder metallurgy approach to the manufacture of F48 Alloy (Cb-15W 5Mo 1Zr). Both pre-alloyed powders and elemental blends were hydrostatically pressed and vacuum sintered. The effect of sintering time and temperature on density, grain size, purity, hardness, and homogeneity was evaluated and analyzed. A two step sintering cycle was designed, and experimental samples were made and tested for fabricability by forging and rolling at room temperature as well as at elevated temperatures. Sheet made from these samples was evaluated for recrystallization temperature, hardness, purity, microstructure, and tensile properties both at room temperature and at 2200°F. Results indicate that F48 billets produced by this method are more fabricable than those produced by arc-casting. Properties of the sheet produced were generally equivalent to those of sheet made by arc-casting, except that the tensile strength was slightly higher and the elongation was usually lower. These deviations are attributed to differences in purity.

Abstract No. 187

Sintering of Oxides

G. C. Kuczynski, Metallurgy Dept., University of Notre Dame, Notre Dame, Ind.

(No abstract received)

Abstract No. 188

A Study of the Sintering Behavior of Some Uranium Dioxide Powders

J. C. Clayton and **L. Berrin,** Bettis Atomic Power Lab., Westinghouse Electric Corp., Pittsburgh 30, Pa.

The sintering behavior of some 35 well-characterized uranium dioxide powders was studied. Pressing pres-

sures and sintering time, temperature, and atmosphere were varied. Definite relationships were found between the sinterability of the powders and their preparation method, surface texture, particle size and shape, and aggregate size and distribution.

Abstract No. 189

High-Temperature Electrical Conduction in the System UO_2-ZrO_2

H. A. Johansen and **J. G. Cleary,** Research Labs., Westinghouse Electric Corp., Beulah Rd., Churchill Boro., Pittsburgh 35, Pa.

Present knowledge of the phase relationships and electrical properties is briefly reviewed and discussed. Examination is made of the dependence of the electrical conduction on density, composition, temperature, and atmosphere. The nature of the electrical conduction is investigated.

Abstract No. 190

Sintering Kinetics of Linde A Al_2O_3

C. A. Bruch, Research Lab., General Electric Co., Schenectady, N. Y.

(No abstract received)

Abstract No. 191

Sintering of Hafnium Carbide with a Fugitive Metal Binder

Charles Zalabak, NASA, Lewis Research Center, Cleveland, Ohio

Hafnium carbide powder mechanically mixed with cobalt powder has been cold compacted and sintered in such manner as to remove the cobalt by vaporization. Densities of 95% of theoretical have been achieved with surface connected porosity of about 2%. Observations are made of the variations in grain size and microhardness obtained over the range of process variables. The variables and range covered were: added cobalt, 0.5 to 5% by weight; maximum temperature, 3500° to 4500°F; time at maximum temperature, 1/10 and 1/2 hr; and heating cycle.

Abstract No. 192

Sintering of Pure SiC

G. R. Watson and **J. I. Frederiksson,** Norton Co., Niagara Falls, Canada

The process of manufacture, properties, and uses of a new slip-cast pure SiC refractory (U.S. Pat. 2,964,823) are described. Previous attempts to make such bodies failed. The finished articles can be made with controlled porosities between about 20 and 50% and may be permeable or impermeable to fluids, as desired. The physical properties for representative types are illustrated. Practical applications include: rocket nozzle throats, permeable filters for corrosive gases or liquids, resistors, and various refractory specialties.

Abstract No. 193

Furnaces, Supports, and Atmospheres for the Sintering of Some Borides, Nitrides, and Silicides

A. Blum, Borolite Corp., 3113 Forbes Ave., Pittsburgh 30, Pa.

In the sintering of borides, nitrides, and silicides of high purity, furnace equipment, supports, and the atmosphere must be chosen so as to minimize contamination of the charge during the sintering process. This choice must be made on the basis of the thermodynamic properties of the respective materials as well as of the kinetics of the reaction between the charge and the materials with which it may be in contact. Illustrations of the sintering conditions for some borides, nitrides, and silicides are given.

Abstract No. 194

The Sintering of Dense, Fine-Grained Beryllides

R. S. Truesdale, B. B. Lympany, and **W. W. Beaver,** The Brush Beryllium Co., Cleveland, Ohio

Fabrication of the intermetallic compounds of beryllium is normally accomplished through hot pressing or sintering. The standard ceramic process of cold pressing and sintering has been successfully applied to these materials. The results of sintering studies on the compound Nb_2Be_{17} and other beryllide compounds are presented. The effect of particle size, stoichiometry, sintering atmosphere, temperature, time on density, grain size, and modulus of rupture of the materials are described.

Abstract No. 195

Electrochemical Oxidation of Titanium Surfaces

M. E. Sibert, Missiles and Space Div., Lockheed Aircraft Corp., Palo Alto, Calif.

Films produced on titanium depend on nature and concentration of electrolyte, forming voltage, current density, and temperature. In most cases, dense films of limited thickness are produced, but in some cases thick porous films result. Physical, chemical, and electrical nature of the coatings are discussed, together with their relation to the surface character. Evidence indicates that films prepared in aqueous electrolytes are not of the rutile structure. These coatings are highly uniform, insulating, and adherent.

Abstract No. 196

Anodic Formation of Titanium Oxide Dielectric Films

R. T. Lamoureux, Missiles and Space Div., Lockheed Aircraft Corp., Palo Alto, Calif.

Equipment is described which was employed for continuous measurement of dielectric properties of electrochemically produced films on titanium sheet. Data obtained using this equipment are discussed in relation to the process parameters of dielectric film formation. Effects of time, temperature, and humidity on the titanium oxide dielectrics prepared are also described.

Abstract No. 197

A Study of the Anodic Film Formed on Titanium

M. Tecotzky, Missiles and Space Div., Lockheed Aircraft Corp., Palo Alto, Calif.

A physical and chemical study has been made of the anodic film formed on titanium. The thin films studied were prepared by anodizing titanium in an aqueous solution of monoethyl and diethyl hydrogen phosphate, A study was made of film thickness. The physical and chemical form of the film was examined using x-ray and electron diffraction techniques, as well as chemical investigation.

Abstract No. 198

Silicon Carbide—An Electrolytic Capacitor Material

B. J. Nicholson, W. Haas, and **J. J. Flood,** Research Div., Philco Corp., Blue Bell, Pa.

Solid electrolytic capacitors have been developed which have for dielectric a thin film of silica grown by thermal oxidation on silicon carbide. Use of a silicon carbide foam permits construction of units with large capacity per unit volume. After oxidation, the foam is anodically "formed" in an electrolyte of KNO_3 in N-methylacetamide; this is only possible when impurities

in the foam are very small. MnO_2 counterelectrodes are then applied. Parameters of these capacitors are described.

Abstract No. 199

Characterization and Properties of UC Crystals Produced by Means of Electron-Beam Zone Melting

Roger Chang and **Harry Nadler,** Atomics International, Div. of North American Aviation, Inc., Canoga Park, Calif.

The preparation of UC single crystals in dimensions up to 10 cm in length and ½ cm in diameter by means of electron beam zone-melting is described. Orientation control was accomplished by seeding. The zone-melted crystals were slightly hyperstoichiometric in C, and methods of removal of the excess C are presented. Reduction in impurities by zone-refining and microstructural studies of the nature of imperfections in UC crystals made by this technique are also reported. (This work was supported by the U.S.A.E.C.)

Abstract No. 200

Mechanical Properties of Nearly Stoichiometric UC Polycrystals between 1500° and 2000°C

Roger Chang, Atomics International, Div. of North American Aviation, Inc., Canoga Park, Calif.

The creep, flow, and recovery behavior of nearly stoichiometric arc-cast polycrystalline UC in the temperature range 1500°-2000°C is reported. Deformation of UC in this temperature range is shown to be diffusion-controlled and has almost all the characteristics of a metal. Analysis of the experimental data in terms of current dislocation theories is also presented. (This work was supported by the U.S.A.E.C.)

INDEX TO AUTHORS

(The number in the right-hand column is the abstract number used in the Technical Program and in the Abstracts)

	Abstract No.
Agruss, B.	38, 40
Albers, W. A., Jr.	113
Alexander, Rexford	95
Allen, M. J.	163, 164, 165
Allerton, G. L.	153
Andres, R. J.	137
Atalla, M. M.	135
Atkinson, J. T. N.	66
Baasted, F. H.	175
Bagrowski, J.	110
Bakish, R.	60, 63
Banus, M. D.	146
Barak, M.	22
Barnes, S. C.	71, 80
Bartlett, J. H.	65
Bate, G.	101
Beach, J. G.	93
Beacom, S. E.	81, 91
Beaver, W. W.	194
Beck, A. F.	58
Beck, Walter	112
Bellobono, I. R.	89
Benjamin, C. E.	120
Bennett, R. J.	31
Berger, Carl	28, 29
Bergh, A. A.	125
Berrin, L.	188
Bertorelle, Eugenio	72, 89
Biard, J. R.	138
Bicelli, L. P.	84
Bishop, C. R.	50
Black, J. F.	147, 148
Blum, A.	193
Boddy, P. J.	114
Bodine, G. C.	180
Bond, A. P.	19
Booker, G. R.	120
Borders, E.	60, 63
Brattain, W. H.	114
Bregman, J. I.	27
Brewer, E. G.	64
Brophy, J. H.	181
Brown, H.	69
Brownell, George	160
Bruch, C. A.	190
Buck, R. P.	18
Bundy, W. S.	13
Busen, Karl	124
Bush, G. W.	74
Cahill, A. E.	107
Cahoon, N. C.	1
Carr, J. M.	103, 111
Cerness, J. F.	186
Chang, Roger	199, 200
Charvat, F. R.	184A
Chilton, W. H.	109
Chludzinski, P.	26
Christensen, H.	139
Clayton, J. C.	188
Cleary, J. G.	189
Clemson, D.	96
Cohen, M.	64
Conway, B. E.	70
Conway, H. F.	176
Cook, H. C.	75
Cronin, G. R.	145
Cubiciotti, Daniel	32
Dabic, S.	176
Daley, J. L. S.	4
Day, R. A., Jr.	173
Deal, B. E.	133
DeBoer, F. E.	48
Decroly, C. M.	177
Dessy, R. E.	170
DeVan, J. H.	36
Dirkse, T. P.	6
Draley, J. E.	48
Dravnieks, Andrew	27
Dresdner, R. D.	171
Duddy, J. C.	8
Duty, R. C.	172
Eicke, W. G., Jr.	9
Elving, P. J.	169
Ervin, Guy, Jr.	52
Evans, S.	47
Everingham, M. R.	154
Farr, J. P. G.	71, 79
Felten, E. J.	55
Fickett, A. P.	26
Fisher, R. D.	104, 109
Flood, J. J.	198
Flurry, R. L.	173
Foley, M. A.	108
Forney, M.	149
Foulke, G. D.	85
Foy, P. W.	142
Frankl, D. R.	121
Franklin, T. C.	92
Fredriksson, J. I.	192
Frosch, C. J.	142
Gatos, H. C.	146
Geske, D. H.	166
Gillibrand, M. I.	22
Ginell, W. S.	37

	Abstract No.
Giusto, M. B.	150
Given, P. H.	167
Glaser, J. H.	100
Grantham, L. F.	37
Gray, J.	22
Greenberg, Sherman	53
Greenblatt, J. H.	66
Greene, N. D.	50, 61
Greig, W. J.	116
Griffith, L. R.	18
Haas, W.	198
Hackerman, Norman	45, 68
Harris, W. S.	2
Hausner, H. H.	184
Hayashi, Tadao	90, 161
Hayden, H. W.	181
Heath, C. W.	129
Hietbrink, E. H.	40
Hiller, M. A.	37
Hills, Stanley	5
Hino, K.	59
Hoar, T. P.	76
Hoekstra, J. J.	86
Hollyer, R. N., Jr.	81
Hovorka, Frank	24, 88
Howard, P. L.	7
Hunger, H. F.	16
Icenhower, D. E.	19
Ichikawa, Eiichi	162
Indig, M. E.	41
Ishida, Takeo	90
James, W. J.	56
Jankowsky, E. J.	112
Johansen, H. A.	183, 189
Johnson, A. A.	94
Johnson, G. R.	82, 83
Johnson, J. W.	56
Johnson, Sidney	150
Jones, E. L.	11, 12
Jones, Richard	170
Jordan, M. D.	151
Kahng, D.	135
Kass, S.	49
Keen, J. M.	79
Kelly, H. C.	150
Koehler, E. L.	47
Kolk, A. J.	99
Kolthoff, I. M.	168
Kornhaas, R.	63
Kozawa, A.	24
Kriegsman, Bernard	115
Kronenberg, M. L.	42
Kruger, Jerome	34
Krupp, H.	20
Kuczynski, G. C.	187
Kuper, A. B.	139
Kuttner, P.	96
LaBotz, R. J.	144
Labrie, R. J.	178
Lamb, D. M.	155
Lamb, V. A.	178
Lamoureux, R. T.	196
Lancaster, E. B.	176
Lang, Maurice	30
Larrabee, G. B.	118
Laukonis, J. V.	57
Lauriente, M.	110
Lavine, J. M.	157
Lehovec, Kurt	124
Leidheiser, Henry, Jr.	46
Levin, R. L.	51
Lewis, C. H.	150
Li, C. H.	119, 132
Linzey, Raynor	124
Litman, A. P.	35
Long, T. R.	98
Lublin, P.	148
Lurie, R. M.	28, 29
Lympany, B. B.	194
Lyons, V. J.	140
Manley, J.	106
Manz, R. C.	131, 135
Markby, Raymond	174
Marlett, C. J.	134
Mason, D. R.	144
Mathers, F. C.	77
Matovich, E.	137
Matsuda, Fujio	92
McJones, R.	20
McKinsey, C. R.	182
McNamara, J. E.	136
Meibuhr, Stuart	88
Meissner, H. P.	21
Milford, R. P.	35
Miller, J. S.	152
Miller, K. J.	131
Misch, R. D.	53
Moest, R. R.	143
Moser, J. R.	15
Nadler, Harry	199
Newman, P. A.	134
Nicholson, B. J.	198
Norman, H.	149
Oberly, J. J.	123
Odo, Keijiro	162
Ong, J. N., Jr.	54
Ord, J. L.	65
Oster, E. A.	26
Panzer, R. E.	2
Paulos, V. E.	152
Philip, R. H.	173
Pick, H. J.	71
Pierson, W. W.	164, 165
Popat, P. V.	23
Porter, J. L.	155
Poster, A. R.	184
Pryor, M. J.	58
Pugh, J. W.	186
Quinn, H. F.	105, 106
Rabenhorst, H.	20
Ramaswamy, R.	158, 159
Rand, M. J.	126
Rao, K. V.	24
Read, H. J.	73, 74
Reddy, T. B.	168
Reinhardt, G.	184A
Richardson, W. W.	100
Rickel, A. M.	113
Riley, B. J.	91
Rindner, W.	157
Robertson, H. M.	136
Robinson, W. M.	129
Ruehrwein, R. A.	141
Ruka, R.	44
Russell, G.	149
Salcedo y Gumucio, Ricardo	30
Salinger, Rudolf	170
Salkind, A. J.	8
Sallo, J. S.	103, 111
Sama, D. A.	21
Sandler, Y. L.	43
Sandstede, G.	20
Sarace, J. C.	116
Scaringella, D.	132
Schindler, H. C.	127
Schmid, G. M.	68
Schumacher, E. A.	31
Schuman, Ralph	29
Scott, D. B.	49
Seifert, J. R.	153
Seiger, H. N.	10
Serravalle, G.	84
Sewell, P. B.	64
Shair, R. C.	10
Shaw, Manuel	17
Sheff, Sumner	122
Shepherd, C. M.	14
Shepherd, W. H.	156
Shimaoka, Goro	67
Shupp, B. R.	143

Sibert, M. E. 195
Silvestri, V. J. 140
Simon, A. C. 11, 12
Simonyan, Karabet 115
Smith, S. W. 39
Smith, W. K. 33
Snyder, R. N. 41
Sohns, V. E. 176
Spanos, J. 130
Spindler, W. C. 2
Steigerwald, R. F. 61
Steinitz, Robert 185
Stern, K. H. 34
Stern, M. 50
Sternberg, H. W. 174
Stewart, E. W. 151
Straumanis, M. E. 56
Strauss, Irving 185
Subcasky, W. J. 17
Sugino, Kiichiro 162
Sulich, M. 106
Swann, Sherlock, Jr. 175
Swenson, J. I. 111

Tecotzky, M. 197
Thomas, C. O. 135
Trivich, Dan 86, 87
Truesdale, R. S. 194
Tufts, O. N. 117
Turner, D. R. 82,83
Turner, J. 156
Tvarusko, Aladar 3

Udupa, H. V. K. 158, 159

Vanderkooi, Nicholas 87
Venkatachalapathy, M. S. 158, 159
Vianello, Elio 169
Vulcan, V. 128

Wagner, J. B., Jr. 51
Walker, R. D., Jr. 33
Walter, G. 20
Watelski, S. B. 138
Watson, G. R. 192
Wawzonek, S. 172
Weaver, R. D. 39
Weber, H. C. 21
Weil, R. 75
Weissbart, J. 44
Wender, Irving 174
White, H. J. 99
Wilder, D. L. 179
Williams, F. V. 141
Willmann, N. L. 39
Wilson, C. L. 160, 161
Winand, René 177
Wolf, I. W. 97
Wulff, J. 181
Wynn, J. E. 25

Yeager, Ernest 24, 88
Young, G. J. 15
Youngdahl, C. A. 48

Zalabak, Charles 191
Zentner, V. 102

Current Affairs

Candidates for Society Offices, 1962

Frank L. LaQue

Arthur C. Haskell, Jr.

Martin F. Quaely

The Board of Directors of The Electrochemical Society, in accordance with the provisions of our Constitution, has approved the following Report of the Nominating Committee.

Report of Nominating Committee

We are pleased to report that the Nominating Committee has selected the following nominees for offices in The Electrochemical Society:

For President (One-Year Term, 1962-1963)—
Frank L. LaQue

For Vice-President (Three-Year Term, 1962-1965)—
Arthur C. Haskell, Jr.
Martin F. Quaely
Ernest B. Yeager

For Secretary (Three-Year Term, 1962-1965)—
Ivor E. Campbell

All nominees have been contacted and have signified that they would accept the offices if elected.

The Nominating Committee recommends for consideration that the office of Secretary be limited to two terms for any one individual.

(Signed) W. C. Gardiner, *Chairman*
F. W. Fink
A. E. Middleton
R. R. Rogers
C. W. Tobias

The above slate will be voted on in the fall ballot-by-mail election, and the successful candidates will assume office in the spring of 1962 at the Los Angeles Meeting of the Society.

The two other Vice-Presidents, Walter J. Hamer and Lyle I. Gilbertson, since they were elected for three-year terms, will automatically become first and second Vice-President, respectively.

Frank L. LaQue

Presidential Candidate

F. L. LaQue has been vice-president of The International Nickel Co., Inc., and manager of the Development and Research Division since June 1954. He previously had served as head of the Corrosion Engineering Section of that Division since 1945. A native of Gananoque, Ont., Canada, Mr. LaQue received the degree of Bachelor of Science in chemical and metallurgical engineering from Queen's University, Kingston, Ont., in 1927.

He joined International Nickel that same year and, since, has specialized in the field of corrosion and corrosion-resisting materials. Under his leadership, Inco's well-known corrosion testing stations were established at Kure Beach and Harbor Island, N. C.

Active in many technical societies, Mr. LaQue has served as President of the American Society for Testing Materials and of the National Association of Corrosion Engineers. He is a member of the Society of Automotive Engineers, is on the 1961 Technical Board Executive Committee, and is Chairman of the SAE General Materials Council. He also is a member of the Executive Committee of the Welding Research Council and a past Chairman of the Corrosion Research Council. He was appointed one of three ASTM representatives on the Standards Council of the American Standards Association for a term expiring in 1963.

Mr. LaQue was presented with the Frank Newman Speller Award in 1949 by the National Association of Corrosion Engineers, and delivered the ASTM Edgar Marburg Lecture in 1951.

Ernest B. Yeager

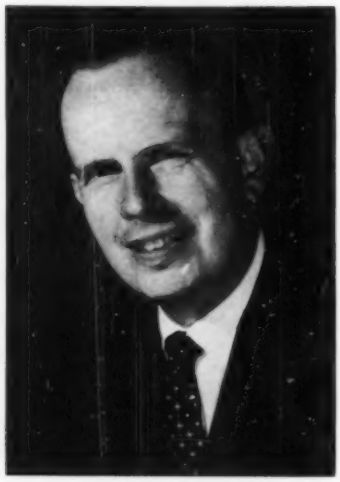

Ivor E. Campbell

He is a member of the Advisory Committee on Engineering and Related Standards of the National Bureau of Standards of the United States Department of Commerce, and Chairman of the Advisory Panel for the Division of Metallurgy. He is associated with the National Research Council of the National Academy of Sciences as Chairman of the Subcommittee on Corrosion. He also serves as an advisor to the Metallurgical Departments of Case Institute of Technology and the University of Pennsylvania.

Currently, Mr. LaQue is a Vice-President of The Electrochemical Society. In the past, he has held the posts of Business Manager of the JOURNAL and Chairman of the Sustaining Membership Committee.

A well-known speaker, he is the author of well over 100 articles and publications on corrosion and other topics. His book "Corrosion in Action," published in 1955, was the basis for a film of the same title which has been shown to hundreds of student and technical society audiences throughout the world.

Arthur C. Haskell

Vice-Presidential Candidate

Arthur Haskell, 42, is a native of New England, having been born in Cambridge, Mass. He was educated at Boston's Northeastern University. At present, he is chief of the Process Metallurgy Division of the Research Department at the TAM Division of the National Lead Co. in Niagara Falls, N. Y.

His professional career, for the most part, has been devoted to research and development and, to a lesser extent, production of reactive metals and their alloys, hydrides, carbides, etc. After receiving his degree in chemical engineering from Northeastern in 1942, he joined Metal Hydrides Inc. in Beverly, Mass. Following work here on the Manhattan Project on the first commercial production of uranium metal, he headed the "special metals" group which was concerned with zirconium, titanium, calcium, barium, and other metals. On completion of the Project, he received awards from the U. S. Army Engineers and the AEC.

In the early fall of 1945, Mr. Haskell accepted a position with Burke Products Inc., Marblehead, Mass., where he had been consulting on powder metallurgy. Here, he was in charge of metallurgical development, primarily investment casting.

In the fall of 1946, he commenced his present affiliation as associate metallurgist and advanced to his present position in late 1954. In addition to metals and metalloids, previously mentioned, the work of his group involves research and pilot development of ferroalloys and fused oxides. Processing methods include not only standard induction or arc furnacing but also high-vacuum furnacing, and aluminothermic reactions. He has authored or coauthored papers on the vacuum induction melting of reactive metals, adsorbed gases on powdered metals and titanium carbide, safety in handling zirconium powder, and electric furnace production of oxides and metalloids.

Mr. Haskell joined The Electrochemical Society in 1952. He has taken an active part in the Niagara Falls Section, including their representation on the Council of Local Sections. He has chaired or been a member of various nominating committees for the Local Section, the Electrothermics and Metallurgy Division, and the Society. He also has served on the Society's Membership Committee.

During 1953, he was elected to the office of Secretary-Treasurer of the Electrothermics and Metallurgy Division. On completion of the two-year term, he was elected Chairman of the Division and, simultaneously, a member of the Board of Directors. He then served a two-year term on the Division's Executive Committee. He currently is serving another term on the Becket Award Committee, and was instrumental in formulating the original rules for the Award. At present and for the past three years, he has been a member of the Board of Directors' Ways and Means Committee.

He is a member of the American Society for Metals, the American Institute of Chemical Engineers, and American Institute of Mining, Metallurgical, and Petroleum Engineers. He also is a member of the Metallurgical Advisory Board of the Erie County Technical Institute in Buffalo.

Martin F. Quaely

Vice-Presidential Candidate

Martin F. Quaely was born in Hartford, Conn., in 1913. He graduated from Trinity College, Hartford, specializing in chemistry and physics. Further advanced studies in chemistry were carried out at Fordham University.

Mr. Quaely served as a research chemist from 1935 to 1944 with the Guggenheim Brothers Laboratories in New York City, where he worked on chemical and metallurgical problems involving corrosion of metals, purification of water, recovery and refining of metals, etc. From 1944 to 1946, he was a senior engineer with the Federal Telecommunications Laboratories in New York City, where his chief fields of study were gas-metal reactions, thermionic cathodes, grid emission, and metallurgy of vacuum-tube materials.

For the next four years, 1946-1950, he was chief chemist for the Amperex Division of North American Philips Co., where he was advisor on chemical and metallurgical problems and operations pertaining to the development and production of radio, transmitting, x-ray, and Geiger tubes. Studies were continued on gas-metal reactions, gas contents of tube materials, getter materials, etc. Mr. Qualey joined Westinghouse Electric Corp. in 1950. He is, at present, senior re-

search engineer in the Research Department of the Lamp Division at Bloomfield, N. J. He has been involved at one time or another in the chemistry and metallurgy of zirconium, tungsten, thorium, titanium, vanadium, uranium, and chromium. He has made numerous studies on the role of gases in metals and other lamp materials. In 1954, he was awarded the Chromium Plating Award of the American Electroplaters' Society for his work in the field of chromium plating.

Since joining The Electrochemical Society in 1941, Mr. Quaely has been quite active in its affairs. He has been a member of the Executive Committee of the New York Metropolitan Section since 1949, and was Vice-Chairman of the Section in 1953-1954 and Chairman in 1954-1955. He also has been a Councilor from the Section on the Council of Local Sections and its predecessor, the Local Section Advisory Committee, since 1952. As a member of the Electronics Division, he has served as Secretary-Treasurer of the Division 1955-1959, and as Chairman 1959-1961. As a member of the Council of Local Sections, he served as Vice-Chairman 1957-1958, Chairman 1958-1959, and Council Representative on the Board of Directors of the Society 1959-1961. In addition to being a member of the Electronics Division, he belongs to the Corrosion Division and to the Electrothermics and Metallurgy Division. Mr. Quaely has served on the Convention Committees for Society meetings held in New York City in 1953 and 1958; he is General Chairman for the Fall 1963 Meeting of the Society. He has been a member of the Admissions Committee of the Society since 1955 (term expires 1963), and of the Ways and Means Committee since 1958. He served on the Board of Directors 1959-1961. At present, he is Chairman of the special Subcommittee on Extended Abstracts, established by the Publication Committee.

In addition to The Electrochemical Society, Mr. Quaely is a member of the American Chemical Society, Faraday Society, American Society for Metals, American Vacuum Society, and the American Association for the Advancement of Science.

Ernest B. Yeager

Vice-Presidential Candidate

Ernest Yeager, professor of chemistry at Western Reserve University, Cleveland, was born in Orange, N. J., in 1924. He received his B.A. degree (*summa cum laude*) from New Jersey State College at Montclair in 1945, his M.S. from Western Reserve University in 1946, and his Ph.D. in physical chemistry from the same University in 1948. While a graduate student at Western Reserve University, he held a Coffin Fellowship (General Electric).

After receiving his Ph.D., Dr. Yeager stayed on as an instructor in the Department of Chemistry at Western Reserve University. He became an assistant professor in 1951, an associate professor in 1953, and a professor in 1957. Dr. Yeager is also technical director of the Ultrasonics Research Laboratory at Western Reserve. He is Chairman of the Frontiers in Chemistry lecture series at Western Reserve University.

His research interests include the properties of electrolytes, electrode kinetics, applications for ultrasonic techniques in physical chemistry, and emission spectroscopy. He and his graduate students at Western Reserve University are credited with the initial development of the sodium amalgam-oxygen fuel cell. In addition to many published articles in electrochemistry and ultrasonics, Dr. Yeager is editor of the forthcoming Electrochemical Society Monograph on "Electrode Processes."

In 1954, Dr. Yeager received the Technical Award of the Cleveland Technical Societies Council, in 1956 the Biennial Award of the Acoustical Society of America for his research on ultrasonics, and in 1959 the Annual Award of the Chemical Professions in Cleveland.

Dr. Yeager has been active as a member of The Electrochemical Society since 1949. He served as Vice-Chairman of the Theoretical Electrochemistry Division from 1953 to 1954, and Chairman from 1955 to 1957. He is currently a member of the Executive Committee of the Battery Division. In addition, Dr. Yeager was Vice-Chairman of the Cleveland Section of the Society from 1953 to 1954, and Chairman from 1954 to 1955.

Other societies in which Dr. Yeager has been active include the Acoustical Society of America, of which he is a Fellow, Sigma Xi, the Optical Society of America, the Society for Applied Spectroscopy (past Chairman of the Cleveland Section), the American Chemical Society, and the American Association of University Professors. He has presented lectures before 45 local sections of the American Chemical Society. Dr. Yeager also has been active on various Government committees, including the Committee on Undersea Warfare and the Primary Battery Panel of the National Academy of Sciences.

Ivor E. Campbell

Secretarial Candidate

Ivor E. Campbell is director of research and development of the National Steel Corp. at Weirton, W. Va. He was born in Kenton, Ohio, in 1919, and received his undergraduate training in chemistry and mathematics at Evansville College in Evansville, Ind., and his graduate training at the Ohio State University, from which he received his Ph.D. degree in inorganic chemistry in 1943.

Dr. Campbell joined the staff of the Battelle Memorial Institute in 1943 as a research chemist, became assistant supervisor of the Division of Nonferrous Metallurgy and chief of the Division of Inorganic Chemistry and Chemical Engineering in 1950, which position he held until leaving Battelle in 1959 to assume his present position.

He is the author of over 35 papers in various scientific and trade journals. His papers deal principally with physical chemistry, vapor plating, preparation of high-purity metals, and super refractories. He is coauthor of The Electrochemical Society's monograph "Vapor Plating" published in 1955, and editor of "High Temperature Technology" published in 1956.

Dr. Campbell joined The Electrochemical Society in 1944. He served as Secretary-Treasurer of the Electrothermics Division from 1949 to 1953, Chairman of the Division from 1953 to 1955, and as a member of the Executive Committee of the Division from 1955 to 1957. He was Chairman of the Bylaws Committee of the Society in 1954 and 1955, and Chairman of the Becket Memorial Award Committee in 1956.

Dr. Campbell was elected Secretary of The Electrochemical Society in 1959 for a three-year term. He became Interim Secretary by Board appointment in January 1959 to fill the term ensuing between his election and his term of office.

Committees of The Electrochemical Society, Inc., 1961-1962

Admissions Committee

	Term Expires
Louis Weisberg, Chairman	Spring 1964
L. I. Gilbertson	Spring 1962
M. F. Quaely	Spring 1963

Finance Committee

	Term Expires
E. G. Enck, Chairman	Treas.'s Term
I. E. Campbell	Secy.'s Term
F. L. LaQue	Spring 1962
L. I. Gilbertson	Spring 1962
R. F. Bechtold	Spring 1962

National Convention Committee

	Term Expires
E. G. Enck	Treas.'s Term
I. E. Campbell	Secy.'s Term
Fielding Ogburn	Spring 1962
Oliver Osborn	Spring 1962
E. L. Koehler	Spring 1962

Honors and Awards Committee

	Term Expires
Hans Thurnauer, Chairman	Spring 1963
H. C. Froelich	Spring 1962
Sherlock Swann, Jr.	Spring 1962
L. O. Case	Spring 1963
E. F. Kiefer	Spring 1964
A. U. Seybolt	Spring 1964
John Convey	Spring 1965
Stanley Wawzonek	Spring 1965

Investment Advisory Panel

	Term Expires
Hans Thurnauer	Spring 1962
G. W. Heise	Spring 1963
R. A. Schaefer	Spring 1964
N. M. Winslow	Spring 1965
R. M. Hunter	Spring 1966

Membership Committee (Contributing)

J. C. Schumacher, Chairman—Term expires Spring 1962

Membership Committee (Personal)

F. W. Koerker, Chairman—Term expires Spring 1962

Nominating Committee

	Term Expires
Sherlock Swann, Jr., Chairman	Spring 1962
M. L. Holt	Spring 1962
E. B. Yeager	Spring 1962
Morris Feinleib	Spring 1962
R. R. Rogers	Spring 1962

Perkin Medal Award Committee

	Term Expires
H. B. Linford, Chairman	Spring 1963
R. A. Schaefer	Spring 1962
F. A. Lowenheim, Alternate	Spring 1962
C. V. King, Alternate	Spring 1962

Publication Committee

	Term Expires
C. L. Faust, Chairman	Spring 1964
H. A. Laitinen	Spring 1962
Norman Hackerman	Spring 1963
C. V. King	Spring 1964
I. E. Campbell	Secy.'s Term

Committee on Protocol

	Term Expires
L. O. Case	Spring 1962
Sherlock Swann, Jr.	Spring 1962
Paul Delahay	Spring 1962

Tellers Committee

	Term Expires
G. D. Stendahl, Chairman	Spring 1962
Carl Lang	Spring 1962
P. A. Crispino	Spring 1962
Paul Howard, Alternate	Spring 1962
H. W. Salzberg, Alternate	Spring 1962
Charles Sanborn	Spring 1962

Ways and Means Committee

	Term Expires
F. L. LaQue, Chairman	Spring 1962
R. A. Schaefer	Spring 1962
M. F. Quaely	Spring 1962
W. J. Hamer	Spring 1962
E. F. Kiefer	Spring 1962
F. P. Peters	Spring 1962
L. I. Gilbertson	Spring 1962

Committee for Administration of the Corrosion Handbook Fund

F. L. LaQue, Board Representative

Representatives of The ECS to Other Societies

American Association for the Advancement of Science

G. W. Heise—Term expires Spring 1962
F. A. Lowenheim—Term expires Spring 1963

American Standards Association

	Term Expires
Y-10 and Y-32—L. O. Case	Spring 1962
C-67—U. B. Thomas	Spring 1962
C-40—Eugene Willihnganz	Spring 1962
R. C. Shair, Alternate	Spring 1962

National Academy of Sciences—National Research Council—Advisory Board for the Office of Critical Tables

E. B. Yeager—Term expires Spring 1962

National Research Council—Division of Chemistry and Chemical Technology

Norman Hackerman—Term expires Spring 1962

American Society for Testing Materials

C-25—A. Gunzenhauser—Term expires Spring 1962

Instrument Society of America

C-96—Thermocouple Sectional Committee American Standards Association organized by Instrument Society

E. M. Sherwood—For duration of project, estimated completion end of 1961

American Electroplaters' Society—Representative to Electrodeposition Division

D. G. Foulke—Term expires June 1962

A Pictorial Return to Indianapolis

Row A—Mrs. H. B. Linford, H. B. Linford (Society President-Elect), R. A. Schaefer (Society President), and Mrs. Schaefer; M. F. Quaely, L. I. Gilbertson (Society Treasurer, and Vice-President-Elect), and E. G. Enck (Society Treasurer-Elect); T. D. Callinan and D. R. Stearn; N. J. Johnson and R. M. Burns. **Row B**—Richard Longini, Sidney Barnartt, and Rolf Haberecht (Indianapolis Committee—Registration); R. K. Iler and John Bugosh; J. A. Brown, Mastaro Fukuda, and C. L. Rulfs. **Row C**—E. M. Sherwood, Samuel Korman, and Charles Sheer; M. Booe (Co-Chairman Indianapolis Meeting); Maurice Indig and John Keralla; M. Fleischmann, A. J. deBethune, B. D. Cahan, and Dr. and Mrs. H. H. Bode. **Row D**—I. E. Campbell (Society Secretary), W. E. Kuhn, A. C. Haskell, S. R. Kresses, and F. W. Koerker; Mrs. A. M. Max and A. M. Max (General Chairman Indianapolis Meeting); Ambrose Smith (Indianapolis Committee—Publicity); Group at Tuesday Evening Reception honoring Dr. and Mrs. Ralph Schaefer. **Row E**—Paul Delahay, Hans Strehlow, R. A. Robinson, L. G. Longsworth (back to camera), and R. C. Bates; C. W. Tobias and A. F. Daniel; Fumio Hine; Mr. and Mrs. S. W. Smith and Mr. and Mrs. Richard Wilson. **Row F**—E. C. Heubschmann, A. K. Hagenlocker, F. A. Shirland, and H. E. Hinterman; T. S. Dewoody (back to camera) and N. H. Nix; Group snapshot; Stanislaw Szpak, D. E. Swonberg, N. J. Johnson, and R. F. Bechtold.

Electrochemical Society Awards

A. C. Makrides

R. E. Meyer

P. C. Milner

Young Author's Prize for 1960

At the Annual Banquet held on Tuesday, May 2, during the Indianapolis Meeting of The Electrochemical Society, A. C. Makrides, of the Research Dept., Socony Mobil Oil Co., Inc., Dallas, Texas, was announced as the winner of the 1960 Young Author's Prize of $100. His prize-winning paper, "Dissolution of Iron in Sulfuric Acid and Ferric Sulfate Solutions," appeared in the November 1960 issue of the JOURNAL.

Dr. Makrides received his B.A. and Ph.D. degrees from the University of Texas, Austin. During 1954-1955, he was a Union Carbide Research Fellow at the Institute for the Study of Metals of the University of Chicago, and, from 1955 to 1957, he was a research chemist with the American Petroleum Institute at the Dept. of Chemistry of the University of Texas. From 1958 to 1960, he was with the Metals Research Laboratories of Union Carbide Metals Co. In September 1960, he joined the Field Research Lab. of Socony Mobil Oil Co. at Dallas, Texas.

Dr. Makrides' research has been concerned with dissolution of metals, hydrogen overpotential, and corrosion inhibition. He also has done work on the heat of wetting of solids and on the surface properties of silicon dioxide.

He is a member of The Electrochemical Society, the Faraday Society, the American Chemical Society, Phi Beta Kappa, and Sigma Xi.

Turner Memorial Award for 1960

Robert E. Meyer, Chemistry Division, Oak Ridge National Lab., Oak Ridge, Tenn., and Paul C. Milner, Bell Telephone Labs., Inc., Murray Hill, N. J., are the winners of the Francis Mills Turner Memorial Award, Sponsored by the Reinhold Publishing Corp., in recognition of their papers which appeared in the JOURNAL during the past year. Dr. Meyer's paper, "Cathodic Processes on Passive Zirconium," was published in the October 1960 JOURNAL; Dr. Milner's paper, "Interpretation of Measurements of Potential Decay on Open Circuit," appeared in the April 1960 JOURNAL.

Announcement of their selection as co-winners of the award, consisting of $100 worth of scientific and technical publications to be divided between them, was made at the Society's Annual Banquet on May 2 in Indianapolis.

Dr. Meyer studied at Valparaiso University, Valparaiso, Ind., from 1947 to 1950, and at the University of Chicago from 1950 to 1954. He received his M.S. degree in 1952 and his Ph.D. in 1954 from the latter institution.

During 1954-1956, he was employed as an instructor of organic chemistry, and carried on research on the self-diffusion of liquid metals. In 1956, he took his present position as chemist with the Chemistry Division at Oak Ridge National Lab. His work has dealt with the electrochemistry of zirconium and its alloys, including studies of film growth and cathodic processes.

Paul C. Milner received his B.S. degree in 1952 from Haverford College, and the M.A. and Ph.D. degrees from Princeton University in 1954 and 1956, respectively.

After two years of service in the Navy, he joined the technical staff of Bell Telephone Labs. in 1957. His work has been in the field of electrochemical research and he has been interested particularly in electrode kinetics.

Dr. Milner is a member of the American Chemical Society, The Electrochemical Society, Phi Beta Kappa, and Sigma Xi.

Honorable Mention

Dr. M. J. Morant, Dept. of Applied Physics, University of Durham, Durham, England, has received Honorable Mention for his paper entitled "Equilibrium Space Charge at the Contact of a Metal and a Pure Highly Insulating Liquid and Its Influence on High-Field Conductivity," which was published in the August 1960 issue of the JOURNAL.

ECS Summer Assistance Awards and Weston Fellowship Award Announced for 1961

On recommendation of the Honors and Awards Committee, the Board of Directors of the Society voted on October 9, 1960 to approve the issuance of three Summer Assistance Awards for the year 1961, in the amount of $800 each, to cover the period June-September, one of which shall be designated as the Edward Weston Fellowship. The funds for these awards are derived from income from investments in the Consolidated Fellowship Fund and the Edward Weston Fellowship Fund.

The Committee responsible for the selection of the recipients consisted of H. A. Laitinen, Chairman, Lee O. Case, Charles W. Tobias, Norman Hackerman, Cecil V. King, and L. B. Rogers (two each from the West, Midwest, and East).

R. L. Brubaker

M. J. Schaer

R. E. Visco

The Summer Assistance Award is made "without regard to sex, citizenship, race, location, or financial need to a fellow or teaching assistant pursuing work between the degree of B.S. and Ph.D. on a subject in the field of interest to The Electrochemical Society. The recipient must be the possessor of a nine-month grant in this field of interest for the academic year 1961-1962 and must have been the holder of a similar grant for the academic year 1960-1961."

The following are the recipients of the Assistance Awards for 1961:

Ronald L. Brubaker, a graduate student at the Dept. of Chemistry, Princeton University, Princeton, N. J. Mr. Brubaker has been designated as the recipient of the Edward Weston Fellowship.

Michael J. Schaer, a graduate student at the Dept. of Chemical Engineering, Oregon State College, Corvallis, Ore.

Robert E. Visco, a graduate student at the Dept. of Chemistry and Chemical Engineering, University of Illinois, Urbana, Ill.

Mr. Brubaker is working for a Ph.D. degree in analytical chemistry. His main interests are in electrochemistry and the application of electrochemical methods in instrumental analysis. His research, under the direction of Dr. Christie G. Enke, consists of a study of the formation and properties of electrode surface films and the characteristics of systems in which the reactant species is adsorbed on the electrode surface.

Mr. Schaer is working for a Ph.D. degree in chemical engineering with a minor in mathematics. His present research project, under the direction of Professor Robert E. Meredith, consists of a study of the effects associated with streaming potential under a high-pressure gradient.

Mr. Visco is working for a Ph.D. degree in analytical chemistry with minors in physical chemistry and mathematics. His research director is Dr. Arnold M. Hartley, and the general field of research is organic electrochemistry. The particular problem is an electrochemical investigation of nitroferrocene, including polarography and coulometry. The purpose is to compare the behavior of this type of aromatic nitro-compound with those which already have been reported in the literature.

The reports on these awards will appear in a later issue of the JOURNAL. The report on the first Summer Assistance Award, for 1960, appeared on page 88C of the April 1961 JOURNAL.

Division News

Electric Insulation Division

The Electric Insulation Division of The Electrochemical Society held its business meeting on Monday, May 1, 1961, with A. Sherburne, Chairman, presiding. C. Houtz, Secretary-Treasurer, read the minutes of the May 1960 meeting and presented the Treasurer's Report.

The Chairman of the Nominating Committee presented the names of candidates for office during the period 1961-1962. One ballot was cast and accepted for the following offices:

Chairman—T. D. Callinan, IBM Research Lab., Yorktown Heights, N. Y.

Vice-Chairman—C. C. Houtz, Bell Telephone Labs., Inc., Murray Hill, N. J.

Secretary-Treasurer—B. R. Eichbaum, Aeronutronic Div., Ford Motor Co., Newport Beach, Calif.

Executive Committee—A. H. Sharbaugh, General Electric Co., Schenectady, N. Y.; H. Thurnauer, Minnesota Mining & Manufacturing Co., St. Paul, Minn.

The new Bylaws state that the officers will be in office for a period of two years and all can be re-elected except the Chairman.

At the 1962 Spring Meeting in Los Angeles, the Electric Insulation Division will have three days of sessions on: (*a*) paper, (*b*) ceramics, (*c*) capacitors, and (*d*) thin film and microcircuit insulation.

Chairman A. Sherburne presented his farewell address thanking the Executive Committee and members of the Division for their cooperation which contributed to the good attendance and success of the meetings during the last two years.

B. R. Eichbaum, *Secretary-Treasurer*

Electronics Division

The annual business meeting of the Electronics Division of The Electrochemical Society was held immediately following the Division luncheon on Monday, May 1, 1961.

The Chairman of the Nominating Committee, Charles T. Lattimer, presented the names of the nominees chosen by the Nominating Committee. The incumbent Division Chairman, Martin F. Quaely, then asked for additional nominations from the floor. Since there were no additional nominations, the following slate of officers for the 1961-1963 term was accepted:

Chairman—Robert J. Ginther, Solid State Div., Naval Research Lab., Washington 25, D. C.

Vice-Chairman (Luminescence)—Henry F. Ivey, Research Dept., Lamp Div., Westinghouse Electric Corp., Bloomfield, N. J.

Vice-Chairman (Instrumentative/

Head table at Theoretical Electrochemistry Division Luncheon held on Wednesday, May 3, 1961, at the Indianapolis Meeting of the Society. Left to right—Standing: W. J. Hamer, A. J. deBethune, M. Fleischmann, A. Disteche, Sigmund Schuldiner, and A. Watanabe. Seated: Paul Ruetschi, E. Raub, C. W. Tobias, Hans Strehlow, and L. G. Longsworth.

General)—Charles P. Marsden, Electron Devices, National Bureau of Standards, Washington 25, D. C.

Vice-Chairman (Semiconductors)—F. Hubbard Horn, Semiconductor Studies Section, Research Lab., General Electric Co., P. O. Box 1088, Schenectady, N. Y.

Secretary-Treasurer—Austin E. Hardy, Radio Corp. of America, New Holland Pike, Lancaster, Pa.

Each of the newly elected officers was introduced and said a few words of acceptance. The retiring Chairman thanked his staff for their dedicated effort and support during the past two years.

The Secretary-Treasurer then reported briefly on the Enlarged Abstracts operation. He announced that the 1961 edition had been a "sellout" and that no more copies were available.

A. E. Hardy, *Secretary-Treasurer*

Electro-Organic Division

Members of the Electro-Organic Division are advised that, in order for the election of officers to comply with the new Bylaws, it will be necessary for elections to be held at the same time as the Divisional meeting. Therefore, Article 5 of the new Bylaws will be inactivated for a period of one year retroactive to the Fall Meeting of 1960 and the election of new officers will take place during the Fall Meeting of 1963.

M. J. Allen, *Chairman*
R. A. Day, Jr., *Vice-Chairman*
E. C. Olson, *Secretary-Treasurer*

Electrothermics and Metallurgy Division

The business meeting of the Electrothermics and Metallurgy Division was held at Indianapolis on Wednesday, May 3, 1961, under the Chairmanship of E. M. Sherwood. The following slate of officers was elected unanimously for the 1961-1963 term:

Chairman—J. H. Westbrook, Ceramic Studies Section, Research Dept., General Electric Co., P. O. Box 1088, Schenectady, N. Y.

Vice-Chairman—W. E. Kuhn, Carborundum Co., P. O. Box 337, Niagara Falls, N. Y.

Vice-Chairman—L. H. Juel, Great Lakes Carbon Corp., P. O. Box 637, Niagara Falls, N. Y.

Secretary-Treasurer—L. M. Litz, Research Lab., National Carbon Co., P. O. Box 6116, Cleveland 1, Ohio

Members-at-Large (four required)—T. D. McKinley, Pigment Dept., Experimental Station, E. I. du Pont de Nemours & Co., Wilmington 98, Del.; C. A. Hampel, 8501 Harding Ave., Skokie, Ill.; R. R. Rogers, Mines Branch, Dept. of Mines & Technical Surveys, 551 Booth St., Ottawa, Ont., Canada; M. C. Udy, Strategic-Udy Processes, Inc., 3986 Royal Ave., Niagara Falls, N. Y.

The Treasurer's Report showed the Division to be in excellent financial condition. It was reported by E. M. Sherwood that the F. M. Becket Memorial Award Committee is taking immediate action to permit the Becket Award to be granted during the academic year 1961-1962.

It was reported also that monographs covering the Iron Ores Symposium, the Rhenium Symposium, and the Fine Particle Symposium were in preparation or under consideration. Various symposia subjects were considered in line with intentions to plan the national meeting programs over a longer range.

The major E & M seminar at the Detroit Meeting will cover Sintering of High-Temperature Refractory Materials. An E & M Executive Committee meeting was scheduled for May to detail future programs.

L. M. Litz, *Secretary-Treasurer*

Theoretical Electrochemistry Division

At the business meeting held on May 3, 1961, during the Indianapolis Meeting of the Society, the following were elected officers of the Theoretical Electrochemistry Division for the 1961-1963 term:

Chairman—Paul Rüetschi, Carl F. Norberg Research Center, Electric Storage Battery Co., Yardley, Pa.

Vice-Chairman—Sidney Barnartt, Westinghouse Research Labs., Pittsburgh 35, Pa.

Secretary-Treasurer — Sigmund Schuldiner, Code 6160, U. S. Naval Research Lab., Washington 25, D. C.

Member Executive Committee—David A. Vermilyea, Research Lab., General Electric Co., Schenectady, N. Y.

Member Executive Committee—Paul C. Milner, Bell Telephone Labs., Inc., Murray Hill, N. J.

S. Schuldiner, *Secretary-Treasurer*

Section News

Philadelphia Section

The annual spring meeting of the Philadelphia Section of The Electrochemical Society was held on Saturday, May 20, 1961. It included a visit to the Carl F. Norberg Research Center of the Electric Storage Battery Co. in Yardley, Pa., and a social hour and dinner at the nearby Washington Crossing Inn.

This was a very successful meeting, with an attendance of over 60, attracting some members from the New York Metropolitan Section. The Electric Storage Battery Co. provided a tour of their new Research Center, including demonstrations in electrochemistry, physical chemistry, organic chemistry, and solid state

physics. They also demonstrated and gave rides in their small fuel-cell powered car.

The following were elected officers of the Section for 1961-1962:

Chairman—Harry C. Mandell, Jr., Pennsalt Chemicals Corp., P. O. Box 4388, Philadelphia 18, Pa.

Vice-Chairman—E. Charles Evers, Harrison Lab. of Chemistry, University of Pennsylvania, Philadelphia 4, Pa.

Treasurer—Albert A. Ware, Ware Brothers Co., 317 N. Broad St., Philadelphia 7, Pa.

Secretary—Henry C. Miller, Pennsalt Chemical Corp., P. O. Box 4388, Philadelphia 18, Pa.

Local Section Councilors—G. F. Temple, Foote Mineral Co., P. O. Box 796, Paoli, Pa.; G. W. Bodamer, Electric Storage Battery Co., Yardley, Pa.

Executive Committee Members—R. A. Schaefer, Electric Storage Battery Co., Yardley, Pa.; G. F. Nordblom, R. D. 4, West Chester, Pa.; R. Kunin, Rohm & Haas Co., 5000 Richmond St., Philadelphia 37, Pa.; F. X. McGarvey, 107 Seventh St., Haddon Heights, N. J.; P. Rüetschi, Electric Storage Battery Co., Yardley, Pa.

H. C. Miller, *Secretary*

Theoretical Division Enlarged Abstract Booklet Spring 1961

The Theoretical Electrochemistry Division has available a number of copies of the "Enlarged Abstract" booklet containing 1000-word abstracts of papers presented before the Theoretical Division symposia during the Indianapolis Spring Meeting of the Society, April 30 to May 3, 1961.

The booklet contains about 100 pages and includes the abstracts of the Symposium on Electrochemical Instrumentation which was sponsored by the National Science Foundation. Six foreign speakers participated at this meeting.

The price is $2.50 per copy. Checks should be made payable to: Theoretical Division, The Electrochemical Society. Booklets are available from:

P. Rüetschi
Electric Storage Battery Co.
Research Center
Yardley, Pa.

New Members

In July 1961, the following were elected to membership in The Electrochemical Society by the Admissions Committee:

Active Members

J. C. Angus, Minnesota Mining & Mfg. Co.; Mail add: 1750 E. Larpenteur, St. Paul 9, Minn. (Electronics—Semiconductors, Electro-Organic, Electrothermics & Metallurgy, Theoretical Electrochemistry)

S. L. Bass, Dow Corning Corp., Midland, Mich. (Electric Insulation, Electronics—Semiconductors)

R. L. Baughman, Fansteel Metallurgical Corp.; Mail add: 2811 Elizabeth, Zion, Ill. (Electrothermics & Metallurgy)

J. A. Brown, Sinclair Research Lab. Inc.; Mail add: 1222 S. Harold, Palos Heights, Ill. (Battery, Theoretical Electrochemistry)

K. M. Busen, Sprague Electric Co.; Mail add: 74 Spring St., Williamstown, Mass. (Electronics—Semiconductors)

E. J. Cairns, General Electric Research Lab.; Mail add: 17 B1 Sheridan Village, Schenectady, N. Y. Theoretical Electrochemistry)

Chang-Kwei Chu, Westinghouse Semiconductor Div.; Mail add: 308 S. Pennsylvania Ave., Greensburg, Pa. (Electronics—Semiconductors)

J. A. Cunningham, Chemistry Branch, Research Engineering, Texas Instruments, Inc., Dallas, Texas (Electronics—Semiconductors)

P. C. Douglass, Bausch & Lomb, Inc.; Mail add: 31 Pickford Dr., Rochester, N. Y. (Electrodeposition)

J. R. Driear, Westinghouse Electric Corp.; Mail add: 210 Brinton St., Monroeville, Pa. (Electronics, Electrothermics & Metallurgy)

A. K. Dube, Automation Alloys, Inc., E. State St., Morocco, Ind. (Electronics—Semiconductors, Electrothermics & Metallurgy)

K. E. Fleming, Allegheny Electronic Chemicals Co.; Mail add: Box 529, Bradford, Pa. (Electronics—Semiconductors)

F. R. Flood, General Electric Co., John St., Hudson Falls, N. Y. (Battery)

R. G. Frieser, Bell Telephone Labs., Inc., Murray Hill, N. J. (Electronics—Semiconductors)

Adolf Goetzberger, Shockley Transistor, Unit of Clevite Corp.; Mail add: 524 Kendall Ave., Palo Alto, Calif. (Electronics—Semiconductors)

P. M. Gross, Daystrom, Inc., Weston Instruments Div., 614 Frelinghuysen Ave., Newark 12, N. J. (Electrothermics & Metallurgy)

W. T. Grubb, General Electric Co.; Mail add: 1800 Hillside Ave., Schenectady 9, N. Y. (Battery, Industrial Electrolytic, Theoretical Electrochemistry)

W. H. Hall, Sarkes Tarzian, Inc.; Mail add: 704 Ladd Ave., Bloomington, Ind. (Electronics-Semiconductors)

E. J. Havlena, Jr., Detroit Edison Co.; Mail add: 4762 Second Ave., Detroit 1, Mich. (Battery)

D. C. Jillson, Semiconductor Products, General Electric Co.; Mail add: 4 Wheeler Rd., Fayetteville, N. Y. (Electronics—Semiconductors, Electrothermics & Metallurgy)

E. W. Justi, Braunschweig Institute of Technology; Mail add: 4 Pockelstrasse, Braunschweig, West Germany (Battery, Electronics—Semiconductors, Industrial Electrolytic, Theoretical Electrochemistry)

W. A. Kagdis, Martin Co.; Mail add: 4202 Prince George Rd., Baltimore 16, Md. (Electronics—Semiconductors)

Edward Kantner, Gulton Industries Inc., Metuchen, N. J. (Battery, Electronics—Semiconductors)

C. C. Kirkpatrick, Electric Storage Battery Co., Rising Sun & Adams Ave., Philadelphia 20, Pa. (Battery)

D. L. Kendall, Texas Instruments, Inc.; Mail add: 624 Greenleaf Dr., Richardson, Texas (Electronics—Semiconductors)

D. J. Klein, Atomics International, Div. of North American Aviation, Inc., Dept. 790, P. O. Box 309, Canoga Park, Calif. (Electronics—Semiconductors)

P. H. Landolt, Brown Boveri Corp.; Mail add: West Trail, Conn. (Electric Insulation)

S. H. Langer, American Cyanamid Co., Stamford, Conn. (Electro-Organic)

J. K. Lee, R.C.A. Tube Div.; Mail add: 315 W. Highland Ave., Marion, Ind. (Corrosion, Electric Insulation, Electronics, Electrothermics & Metallurgy, Theoretical Electrochemistry)

W. M. Lenard, Bendix Corp.; Mail

By action of the Board of Directors of the Society, all prospective members must include first year's dues with their applications for membership.

Also, please note that, if sponsors sign the application form itself, processing can be expedited considerably.

add: 8350 Evangeline, Dearborn 6, Mich. (Electronics)

George Lozar, Sprague C.R.E.A.S., S.p.A.; Mail add: Piazza 4, Novembre No. 1, Milan, Italy (Corrosion, Electric Insulation, Electrothermics & Metallurgy, Theoretical Electrochemistry)

J. R. Luck, Minneapolis Honeywell Regulator Co.; Mail add: 5536-15th Ave., Minneapolis 17, Minn. (Electrodeposition, Theoretical Electrochemistry)

Bruce McDonald, Shockley Transistor, Unit of Clevite Corp.; Mail add: 2549 Kirk Rd., San Jose 24, Calif. (Electronics—Semiconductors)

D. M. Mohilner, Louisiana State University; Mail add: 1001 Aster St., Baton Rouge, La. (Electrodeposition, Electro-Organic, Theoretical Electrochemistry)

R. A. Munson, General Electric Research Labs.; Mail add: 1019 Wendall Ave., Schenectady, N. Y. (Battery, Theoretical Electrochemistry)

H. J. H. Perry, Onan Div., Studebaker-Packard Corp.; Mail add: 9150 Colfax Ave. S., Minneapolis 20, Minn. (Battery, Electrodeposition, Electro-Organic, Industrial Electrolytic, Theoretical Electrochemistry)

R. B. Nealon, Ronson Corp. of Pennsylvania, Delaware Water Gap, Pa. (Electrodeposition)

R. W. Pierce, Union Carbide Olefins Co.; Mail add: 1004-2¾ Mile Creek Rd., St. Albans, W. Va. (Electronics—Semiconductors, Electrothermics & Metallurgy)

P. I. Pollak, Merck Sharp & Dohme Research Labs, Div. of Merck & Co., Inc., Rahway, N. J. (Electronics—Semiconductors and Luminescence)

John Renner, Solvay Process Div., Allied Chemical Corp., Syracuse 1, N. Y. (Industrial Electrolytic)

E. W. Riggs, Sarkes Tarzian Inc.; Mail add: 1033 S. Hawthorne Dr., Bloomington, Ind. (Electronics—Semiconductors)

Harry Rosenberg, Transistor Electronics Corp.; Mail add: 128 Burley St., Danvers, Mass. (Electronics—Semiconductors, Theoretical Electrochemistry)

Martin Rubenstein, Westinghouse Electric Corp.; Mail add: 1365 Hillsdale Dr., Pitcairn, Pa. (Electronics—Semiconductors and Luminescence)

J. C. Sarace, R.C.A. Semiconductor Div.; Mail add: Ten Eyck Rd., R.D. 5, Somerville, N. J. (Electronics—Semiconductors)

C. R. Smith, Dow Corning Corp.; Mail add: 1511 W. Carpenter St., Midland, Mich. (Electronics—Semiconductors)

R. N. Snyder, Delco-Remy Div., General Motors Corp.; Mail add: 420 W. 37 St., Anderson, Ind. (Battery)

Vincent Sussman, Epoxy Products, Inc.; Mail add: 20 Martha Rd., Roseland, N. J. (Electric Insulation)

C. D. Thurmond, Bell Telephone Labs., Inc.; Mail add: 22 Lidgerwood Parkway, Morristown, N. J. (Electronics—Semiconductors)

Gino Tovazzi, Istituto Int. Studio Sviluppo Relazioni Umane; Mail add: Villa Olanda, Mira-Porte, Venice, Italy (Electro-Organic)

L. A. Vander Lugt, Calvin College; Mail add: 1818 Newark S. E., Grand Rapids, Mich. (Theoretical Electrochemistry)

T. R. Waite, Atomics International; Mail add: 10440 Plainview Ave., Tujunga, Calif. (Electronics)

George Wertwijn, Hoffman Electronics, Inc.; Mail add: 479 Burton Ave., Highland Park, Ill. (Electronics—Semiconductors)

H. K. Willcox, I.B.M. Development Lab.; Mail add: Clover Hill Rd., Poughkeepsie, N. Y. (Electronics—Semiconductors and Luminescence)

Associate Members

Albert Adler, Clevite Transistor Products; Mail add: 53 Alton Place, Brookline 46, Mass. (Electronics—Semiconductors)

J. R. Chabria, Ohio Semiconductors; Mail add: 1158 Elmwood Ave., Columbus 12, Ohio (Electronics—Semiconductors and Luminescence)

Barbara E. McDaniel, P. R. Mallory & Co., Inc.; Mail add: 4836 E. 19 St., Indianapolis 18, Ind. (Electric Insulation)

J. R. Moser, Pratt & Whitney Aircraft Co.; Mail add: 142 Plain Dr., East Hartford 8, Conn. (Battery)

R. L. Newman, R. C. A., Advanced Development Dept., Somerville, N. J.

W. D. Richardson, Jr., Sprague Electric Co.; Mail add: 669 Barbour St., North Adams, Mass. (Electronics—Semiconductors)

R. J. Rothlein, Patterson-Moos, Inc.; Mail add: 7803—79th Place, Glendale 27, N. Y. (Theoretical Electrochemistry)

N. L. Willmann, Delco-Remy Div., General Motors Corp.; Mail add: 411 S. Cherry St., Hartford City, Ind. (Battery)

Student Members

S. J. Angelovich, Massachusetts Institute of Technology; Mail add: 6 Amackassin Terrace, N. Y. (Battery)

S. L. Phillips, Chemistry Dept., University of Wisconsin, Madison 6, Wis. (Electrodeposition, Electro-Organic, Theoretical Electrochemistry)

D. S. Polcyn, Chemistry Dept., University of Wisconsin, Madison 10, Wis. (Electronics—Semiconductors, Theoretical Electrochemistry)

Student Members—Cleveland Section Award Winners

D. G. Barnes, College of Wooster; Mail add: Kenarden 2, Wooster, Ohio

J. S. Dodge, Case Institute of Technology; Mail add: 10904 Euclid Ave., Cleveland 6, Ohio (Battery)

R. A. Leuenberger, Fenn College; Mail add: 1265 Inglewood Dr., Cleveland Heights 21, Ohio (Battery)

R. K. Nibert, Baldwin-Wallace College; Mail add: 191 E. Center St., Berea, Ohio (Theoretical Electrochemistry)

F. E. Stickland, Jr., Hiram College;

December 1961 Discussion Section

A Discussion Section, covering papers published in the January-June 1961 JOURNALS, is scheduled for publication in the December 1961 issue. Any discussion which did not reach the Editor in time for the June 1961 Discussion Section will be included in the December 1961 issue.

Those who plan to contribute remarks for this Discussion Section should submit their comments or questions in triplicate to the Managing Editor of the JOURNAL, 1860 Broadway, New York 23. N. Y., *not later than September 1, 1961.* All discussion will be forwarded to the author(s) for reply before being printed in the JOURNAL.

Mail add: Box 352, Hiram, Ohio (Electrothermics & Metallurgy)

B. B. Wayland, Western Reserve University; Mail add: 17459 Northwood Ave., Lakewood 7, Ohio (Electrothermics & Metallurgy)

Reinstatement to Active Membership

M. R. Hatfield, Union Carbide Consumer Products Co.; Mail add: 4 Southview Rd., Chappaqua, N. Y. (Battery)

Transfers from Associate to Active Membership

R. L. Bleutge, Union Carbide Consumer Products Co.; Mail add: 2207 Atkins Ave., Lakewood 7, Ohio (Battery)

S. P. Carbone, Sprague Electric Co.; Mail add: 11 Doncaster Rd., Lynnfield, Mass. (Electric Insulation, Electronics—Semiconductors, Theoretical Electrochemistry)

Transfer from Student to Active Membership

Jonathan Booker, Brush Beryllium Co.; Mail add: 1122 E. 98 St., Cleveland 8, Ohio (Corrosion, Electrothermics & Metallurgy)

Deceased

J. H. Brennan, Niagara Falls, N. Y.
Stanford Essig, Fort Wayne, Ind.
Arthur Linz, New York, N. Y.

Personals

William T. Dunlap, credited with major contributions to high-carbon ferrochrome smelting and electrolytic processes for chromium and manganese, retired on July 1 from Union Carbide Metals Co., Niagara Falls, N. Y., after 38 years of active service. Mr. Dunlap, senior engineer on the technology department staff, was honored at a luncheon at the LaSalle Yacht Club, during which his many accomplishments were reviewed. He was not only a major contributor in metallurgical developments, but also was a pioneer in statistical and economic studies. His excellent teaching ability contributed to the development of many of the company's engineers.

Mr. Dunlap became well versed in all phases of the company's business during a long and varied career, dating back to 1923. He joined the company as an analytical chemist and, three years later, was appointed a research assistant. In 1947, he advanced to assistant manager. He was appointed senior engineer of the technology department economic appraisal group when it was organized in 1959.

Mr. and Mrs. Dunlap plan to settle in Hickory, N. C., in the fall.

He has been a member of The Electrochemical Society since 1927.

Maurice Friedman has been elected a vice-president of General Instrument Corp., Newark, N. J. Mr. Friedman, formerly executive vice-president of the company's Semiconductor Div., also will serve in the newly created post of executive assistant to the president, and will be responsible, under president Moses Shapiro, for "coordinating activities of General Instrument's 18 divisions and subsidiaries and for development of the company's long-range acquisition program." Mr. Friedman, who has spent over 20 years in the electronics industry in development and production of electronic and electrochemical components, holds 19 U.S. and foreign patents in these fields.

James P. Hoare transferred, in October 1960, from Ford Motor Co., Dearborn, Mich., to General Motors Corp., Warren, Mich., where he is in the Electrochemistry Dept. at the Technical Center.

Herbert Matare recently became a staff physicist at the Research Labs. Div. of Bendix Corp., Southfield (Detroit), Mich.

Samuel Piken has been appointed chemical supervisor of Brooks & Perkins, Inc., Detroit, Mich. Previously, he was methods development engineer with the Chrysler Corp., Detroit.

Wayne J. Subcasky, formerly with the Chrysler Corp., Detroit, has joined the staff of the Electrochemical Research Dept. of the Electric Autolite Co. in Toledo, Ohio.

John K. Taylor, research chemist, whose entire 32-year professional career has been with the National Bureau of Standards, Washington, D. C., has been appointed chief of the Applied Analytical Research Section of the Bureau's Analytical and Inorganic Chemistry Div. The Section is concerned with the development and application of methods for the analysis and characterization of solids, liquids, and gases.

A major part of Dr. Taylor's work at the Bureau has been concerned with the application of physical methods to chemical analysis, including the polarographic method and the limitations of voltammetric processes. Recently, he has conducted research in high-precision coulometric methods of analysis. This involved analysis by means of electrolysis in which analytical results are based on the physical standards of current and time. Dr. Taylor has written numerous papers on these subjects and, in 1960, was awarded the Dept. of Commerce Silver Medal in "recognition of his contributions to accurate electrochemical methods of analysis."

James M. Breckenridge

When The Electrochemical Society held its Spring Convention in Nashville, Tenn., in 1942, Dr. James M. Breckenridge was General Chairman of the Meeting. Dr. Breckenridge died on April 13, 1961 in Nashville, after an illness of several years. He was 80 years old.

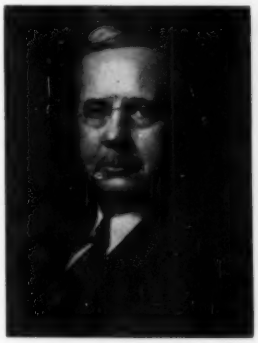

J. M. Breckenridge
1880-1961

When Dr. Breckenridge retired as head of the Chemistry Dept. at Vanderbilt University in 1949, he was presented with a scroll honoring him as having taught more students than any other Vanderbilt professor. He joined Vanderbilt as head of the Chemistry Dept. in 1919.

Dr. Breckenridge was born in 1880 in Jamestown, Ont., Canada. He received his B.A. degree from Albion (Mich.) College in 1903, and the Ph.D. degree from the University of Wisconsin in 1910.

He was a research chemist for the Welsbach Gas Mantle Co. of Gloucester, N. J., from 1910 to 1912. For the next two years, he was professor of chemistry at Carroll College in Waukesha, Wis., and he was head of the Chemistry Dept. at Wabash College, Crawfordsville, Ind., from 1914 to 1916. During World War I, Dr. Breckenridge was head of the Experimental Station of the Hercules Powder Co.

He is listed in the "International Who's Who in America." His research interests were in paints, electrodeposition, alloys, beryllium, forensic chemistry, and explosives.

—Allen G. Gray

Book Reviews

Extractive Metallurgy, by Joseph Newton. Published by John Wiley & Sons, Inc., New York, 1959. 532 pages; $9.75.

Professor Newton's book has been written to fill a great need in teaching—a descriptive text in extractive metallurgy for students taking no other courses in the subject. The book is arranged from a unit-operations viewpoint with chapters on ore dressing, pyrometallurgy, hydrometallurgy, and electrometallurgy, along with chapters on sources of metals, chemical principles, fuels and refractories, ingots, and a rather lengthy chapter on the structure of metals and alloys.

The author has handled the problem of jargon quite well, keeping it to a minimum, and introducing it in a free-flowing style by the use of italics. Thus, the index may be used instead of a separate glossary to find rapidly the definitions of the terminology. The use of worked examples in the text and the problem lists at the end of the chapters will prove to be a help to the student and remove some of the burden from the teacher.

There are aspects of the book, however, which seem somewhat less desirable. The author devotes 43 pages to chemical principles and 88 pages to the structure of metals and alloys. This emphasis on structure of metals instead of chemical and thermodynamic principles seems unfortunate in a treatment of extractive metallurgy, where thermodynamic and chemical principles could be so fruitfully used. In other respects, too, the balance in treatment of the subject may be disappointing to some. Of the 514 pages of text, only slightly over 200 pages are devoted to the actual operations used in extracting metals from their ores. Also, after devoting a liberal amount of space to an explanation of phase diagrams, he hardly uses them in the discussion of the extraction processes. Instructors who emphasize iron and steelmaking will undoubtedly find insufficient the single page devoted to coke production.

The author has a tendency to introduce new material in the summaries, possibly resulting in some confusion to the student.

In summation, it may be said that the author has achieved his stated objective by writing a clear exposition of the material he has chosen to present. As in any subject, the exact topics and their order of presentation are a matter of individual preference. However, this text is sure to appeal to many teachers.

Carl J. Alstetter

Organic Coating Technology, Vol. II. Pigments and Pigmented Coatings, by Henry Fleming Payne. Published by John Wiley & Sons, Inc., New York, 1961. 724 pages; $17.50.

This volume covers the fundamentals of pigmented coatings with descriptions of pigments, binders, and other paint ingredients, and includes the manufacturing methods, preparation of surfaces to receive coatings, and the methods of application. The book contains many excellent sketches and photographs. Corrosion-resistant and chemical-resistant paint systems are very well described. The book will be of particular value to those interested in corrosion prevention.

Henry S. Myers

Progress in Dielectrics, Vol. II. Edited by J. B. Birks and J. H. Schulman. Published in Great Britain by Heywood and Co., Ltd., and in the United States by John Wiley & Sons, Inc., New York, 1960. 225 + V pages, 75 figures; $9.50.

Theory and practice concerning the general subject of dielectric behavior have grown so vigorously in recent years that the appearance of another "progress" sequence of books in this field is warranted. This particular series provides a common meeting place for chemists, physicists, electrical engineers, and, to a lesser extent, for biologists and technicians who have an interest in dielectric theory of materials.

The interaction of dielectric materials with weak electric fields is stressed. This is in contrast to Vol. I, in which the emphasis was on strong-field phenomena such as breakdown corona, etc. As before, an assembly of capable authors has been selected, five being from Great Britain and two from the United States. The subject matter is divided evenly between the theoretical and practical aspects of the subject, three chapters being devoted to each.

In the first chapter, Wiley appropriately surveys the general theory of dielectric polarization and absorption and sets the stage for an appreciation of the later chapters. He emphasizes work since 1956, when a comprehensive review article appeared in another series of books. This chapter alone requires an elementary knowledge of vector analysis, differential equations, and statistical analysis for proper appreciation. Curtis follows with a detailed and thorough review of the dielectric properties of organic polymers. His lucid presentation makes this chapter a very valuable text for both the specialist and nonspecialist, and he achieves a noteworthy systematization of this extensive subject. Bloch and Charlesby, who have pioneered in the subject of polymer irradiation, discuss the physicochemical effects of radiation of dielectric materials.

The concluding three chapters deal with the more practical aspects of the subject. Sutton describes the origin and nature of the dielectric properties of glass, including the d-c behavior and breakdown theories. Plessner and West discuss the science and technology of high-permittivity ceramics for capacitors, and cover the composition of materials as well as chemical and manufacturing processes. In recent years, the use of microwave frequencies has led to the use of optical techniques for transmission of power through space. Hence, increased emphasis has been placed on the fabrication of lightweight composite plastics which may be used as dielectric lens, and so forth. In the concluding chapter, Brown covers both the theory and construction of such two-phase systems of dielectrics with a minimum of mathematics.

The authors, as well as editors Birks and Schulman, are to be commended for the excellent and readable account of low-field phenomena presented in Vol. II of "Progress in Dielectrics." Interested workers in this field will look forward to the continuance of this series.

A. H. Sharbaugh

Contributi Teorici e Sperimentali di Polarografi, Vol. V. Edited by Giovanni Semerano. Published by Centro di Polarografia, Via Loredan 4, Padova, Italy, 1960. 315 pages, 17 x 24 cm. Price: 2500 Lire.

Notice to Members and Subscribers

(Re Changes of Address)

To insure receipt of each issue of the JOURNAL, please be sure to give us your old address, as well as your new one, when you move. Our records are filed by states and cities, not by individual names. The Post Office does not forward magazines.

We should have this information *by the 16th of the month* to avoid delays in receipt of the next issue.

The fifth volume of this serial publication is a collection of lectures and reports presented at two scientific meetings at Bressanone, Italy, in August 1959, organized by the Center of Polarography of the Italian National Research Council and by the Institute of Physical Chemistry of the University of Padua.

The first part of this volume is in Italian and deals with the "Relationship between constitution and physicochemical behavior." Each paper has a very brief summary in French, German, and English. Papers in this section deal with chemical kinetics, quantum mechanics, spectroscopy dipole moments, coordinating power, valency shell of sulfur, organic N-O-derivatives, and physical biochemistry.

The second part of this volume is on the "Relationships between polarographic constants and molecular structure" and is of considerable interest to the polarographer. This section is polylingual; the papers are in either Italian (2), English (6), French (1), or German (1). Eight of these papers are review articles by experts in this field; two represent original work. The review articles are excellent summaries of the correlations between polarographic reduction potentials and structure (Semerano, Zuman, Tirouflet, Berg, Rigatti), the effect of structure on the mechanism of reduction (Elving), polarography of aromatic hydrocarbons and related substances (Hoijtink), and interpretations of polarographic current-voltage curves for irreversible electrode reactions (Randles).

On the basis of the second part, this volume is recommended to both the expert and the beginner in organic polarography.

Stanley Wawzonek

News Items

Carl Wagner Receives Bunsen Medal

Carl Wagner, director of the Max-Planck-Institut für Physikalische Chemie, Göttingen, Germany, was awarded the Bunsen Medal on May 12 at the 60th annual meeting of the Deutsche Bunsengesellschaft held at Karlsruhe. This distinction was conferred for his many researches on properties of solids, especially on semiconductors, alloys, and their surface behavior, and his contributions to the modern views on physics of solids and corrosion science. He also was recognized for his contributions to the teaching of thermodynamics through his text on this subject, written with Walter Schottky and Hermann Ulich, which has been used as a standard book by a generation of students in Germany.

Professor Wagner was professor of metallurgy at the Massachusetts Institute of Technology from 1949 to 1958, where he taught thermodynamics and kinetics, and also carried out many researches with the aid of students who came from many countries.

He was the first recipient of the Palladium Medal conferred by The Electrochemical Society, at the Fall Meeting in Detroit in 1951.

Professor Herbert H. Uhlig of the Massachusetts Institute of Technology represented the Society at the Karlsruhe meeting.

Allen G. Gray Appointed Editor of ASM Periodical Publications

Allen G. Gray has been appointed editor of periodical publications for the American Society for Metals. While retaining editorship of *Metal Progress*, ASM's magazine of materials and process engineering, he now will have general editorial supervision of all society periodicals, including *Metals Review*, *Review of Metal Literature*, *Metals Engineering Quarterly*, and *Transactions Quarterly*.

Dr. Gray specialized in materials engineering and chemical aspects of metalworking and metal processing during 12 years of research and development with the Du Pont Co. During World War II, on loan from Du Pont, he directed a group working on materials and corrosion problems for the Manhattan atomic bomb project at the University of Chicago. He also worked with General Electric at its Knolls Atomic Power Lab. on problems of the Savannah River Atomic Energy Plant.

He is a member of the Advisory Committee to the U.S. Atomic Energy Commission on Industrial Information, and holds a number of patents relating to metallurgical treatment of uranium for atomic energy applications. He also has presented a number of articles on aerospace materials and processes along with the everyday uses for metals in conventional manufacturing.

After receiving his bachelor's and master's degrees in metallurgy from Vanderbilt University, Nashville, he earned his Ph.D. degree at the University of Wisconsin, where he served on the teaching staff before joining Du Pont. He had served *Steel* magazine on a part-time basis as Consulting Editor, 1942-1952, and joined the magazine's staff as Technical Editor from 1952 to 1957. When the late Ernest E. Thum was named Editor-in-chief of *Metal Progress* in 1958, Dr. Gray was appointed Editor.

He is Editor-in-Chief of The Electrochemical Society monograph "Modern Electroplating," and has been lecturer for an advanced course at Western Reserve University, Cleveland, dealing with metallurgy, electroplating, and corrosion. He is author of the section on steel technology in the "Encyclopedia Americana."

OiS Club Scheme

The Optical Society of America has been translating *Optika i Spektroskopiya* and distributing this monthly journal free, under a grant from the National Science Foundation, to all OSA members and subscribers to the *Journal of the Optical Society of America*. This free distribution was an experiment for three years, so that the individual reader might become accustomed to reading a translation journal not as an oddity but as a publication that is looked for each month in the same manner as is *J. Chem. Phys.*, *J. Am. Chem. Soc.*, etc. In December of this year the NSF grant ends, but the interest in *Optics and Spectroscopy* is now too lively for OSA to discontinue the translation, so they have evolved the OiS Club Scheme.

This is a special subscription rate for members of those societies who wish to take part in the OiS Club Scheme, *viz.*: To OSA members—$7.50; To members of the OiS Club—$11.00; To nonmembers and libraries—$15.00.

OSA states that if a translation journal is to be of real use (as is the case with any scientific journal), it should be read widely by all the people working in the field, and that these research results should be made available in the shortest possible time. *Optics and Spectroscopy* is published in English translation within three months of the Russian edition coming out, *e.g.*, the March 1961 issue was published in English on June 10. OSA is making this special offer to members of some 60 scientific societies across the English-speaking world, and it asks the members of those societies to write to the Assistant Secretary, OSA, 1155 16th St., N.W., Washington 6, D. C., for further details or to send in their orders.

One thing that has been learned from *Optics and Spectroscopy* is that the majority of the references cited are to English-language journals!

Third Seminar on Electrochemistry

The Third Seminar on Electrochemistry will be held at the Central Electrochemical Research Institute, Karaikudi-3, Madras State, India, sometime during the third week of December 1961, the exact date to be announced.

Papers on original work are solicited for presentation at the Seminar. Also invited are contributions relating to personal experiences and data collected in the operation of electrochemical plants.

Three copies of detailed abstracts of papers (not exceeding 300 words in length) should be submitted to the Convener of the Seminar, Mr. V. Aravamuthan, Assistant Director, Central Electrochemical Research Institute, Karaikudi-3, Madras State, India, not later than September 15, 1961, and *two copies* of the full papers by November 15, 1961. Arrangements will be made for the presentation of papers of authors unable to attend the Seminar.

Abstracts will be printed and copies supplied in advance of the meeting.

Conference on Magnetism and Magnetic Materials

The seventh annual International Conference on Magnetism and Magnetic Materials will be held November 13-16, 1961 in the Thunderbird Room of the Westward Ho Hotel in Phoenix, Ariz. The conference is being sponsored jointly by the American Institute of Electrical Engineers and the American Institute of Physics, in cooperation with the Office of Naval Research, the Institute of Radio Engineers, and the Metallurgical Society of the A.I.M.E.

More than 1000 scientists and engineers are expected to attend. Invited speakers include representatives from Russia, Japan, England, France, and the United States.

Papers on basic theoretical and experimental investigations, potential engineering applications, and apparatus and techniques which utilize recent advances in magnetism are being solicited. Authors should submit abstracts by August 18 to Dr. F. E. Luborsky, General Electric Co., Research Lab., P. O. Box 1088, Schenectady, N. Y.

As in past years, an exhibit of magnetic products and instrumentation is being sponsored.

Separation and Determination of Fe, Al, Ti, and Zn

Titanium, zirconium, iron, and aluminum now can be effectively separated and quantitatively determined by an analytical method (1) developed for the Diamond Ordnance Fuze Labs. by T. J. Murphy, W. S. Clabaugh, and R. Gilchrist of the inorganic chemistry staff of the National Bureau of Standards.

By starting with a half-gram sample of mixed oxides and by following this procedure, workers with proper technical training can determine the amount of each of the metals present within ± 0.2 mg.

The method was developed as part of a continuing program to develop analytical techniques and to produce purer reagent chemicals (2). Although originally designed for the quantitative analysis of barium titanate dielectrics, it is applicable to the analysis of alloys and other materials containing the four metals.

References

1. For further technical information, *see* "Method for the Separation of Titanium, Zirconium, Iron, and Aluminum from One Another and for Their Subsequent Determination," T. J. Murphy, W. S. Clabaugh, and R. Gilchrist, *J. Research Nat. Bur. Standards* **64** (Phys. and Chem.), 535 (1960).
2. Specifications of the American Chemical Society for Reagent Chemicals, Revised Ed. (1961).

Separation of Hf from Zn

Hafnium and zirconium, ordinarily very difficult to distinguish chemically, now can be separated by a single-step anion-exchange procedure (1) developed by the National Bureau of Standards. The separation for analysis is obtained by using a strong quaternary-amine anion-exchange resin column with diluted sulfuric acid as eluting solution. After separation of a mixture containing approximately 100 mg each of hafnium and zirconium, a spectrochemical examination showed only a few ppm cross contamination.

The separation procedure was developed by J. L. Hague and L. A. Machlan of the Bureau staff.

Reference

1. For further information, *see* "Separation of Hafnium from Zirconium by Anion Exchange," J. L. Hague and L. A. Machlan, *J. Research Nat. Bur. Standards*, **65A** (Phys. and Chem.), 75 (Jan.-Feb. 1961).

Battelle Research on Refractory Metals

Protective coatings to safeguard tungsten, tantalum, molybdenum, and columbium alloys from the destructive effects of oxidation must be developed before these refractory metals can assume a prominent role

Manuscripts and Abstracts for Spring 1962 Meeting

Papers are now being solicited for the Spring Meeting of the Society, to be held at the Statler Hilton Hotel in Los Angeles, Calif., May 6, 7, 8, 9, and 10, 1962. Technical Sessions probably will be scheduled on Electric Insulation, Electronics (including Luminescence and Semiconductors), Electrothermics and Metallurgy, Industrial Electrolytics, and Theoretical Electrochemistry.

To be considered for this meeting, triplicate copies of abstracts (*not exceeding 75 words in length*) must be received at Society Headquarters, 1860 Broadway, New York 23, N. Y., *not later than December 15, 1961. Please indicate on abstract for which Division's symposium the paper is to be scheduled and underline the name of the author who will present the paper.* No paper will be placed on the program unless one of the authors, or a qualified person designated by the authors, has agreed to present it in person. An author who wishes his paper considered for publication in the JOURNAL should send triplicate copies of the manuscript to the Managing Editor of the JOURNAL, 1860 Broadway, New York 23, N. Y.

Presentation of a paper at a technical meeting of the Society does not guarantee publication in the JOURNAL. However, all papers so presented become the property of The Electrochemical Society, and may not be published elsewhere, either in whole or in part, unless permission for release is requested of and granted by the Editor. Papers already published elsewhere, or submitted for publication elsewhere, are not acceptable for oral presentation except on invitation by a Divisional program Chairman.

in nuclear and space technology. This is the opinion of Dr. C. A. Krier, Battelle Memorial Institute, Columbus, writing in the June *Battelle Technical Review*.

According to Dr. Krier, these principal refractory metals, which are highly rated for their other properties, are among the least resistant to destructive oxidation at high temperatures. Unlike most oxidation-resistant metals, the principal refractory metals do not form their own protective oxide coatings.

Present research and development efforts are concentrated in two areas: (*a*) finding materials which are both oxidation resistant and compatible with the metal to be protected; (*b*) developing processes to apply the coatings. In his article, Dr. Krier discusses a number of coatings and methods of application for various metals and environmental conditions.

Copies of the article are available on request from Publications Dept., Battelle Memorial Institute, 505 King Ave., Columbus 1, Ohio.

Powder Metallurgy Process for Producing Zircaloy 2

The Metallurgical Products Dept. of the General Electric Co., Detroit 32, Mich., has announced the commercial availability of Zircaloy 2 as produced by a unique powder.metallurgy process—a modified vacuum hot-pressing technique which is also a superior technique for producing finished or semifinished shapes in refractory metals such as columbium, tantalum, or their carbides.

The Zircaloy 2 produced by the process will meet all nuclear specifications. The material possesses outstanding physical characteristics that are normally associated with a wrought product. For instance, the density is 6.57 g/cc, which is 100% of theoretical. Another advantage is that the properties are nondirectional. Also, two metals which may be dissimilar can be bonded together by diffusion, producing a joint as strong as or stronger than the parent metal.

BeO Coating Process

A breakthrough in the application of beryllium oxide protective coatings to nuclear fuel materials has been announced by Nuclear Materials and Equipment Corp. (NUMEC) of Apollo, Pa. Successful deposition of a coating of nonporous beryllia on small particles of uranium dioxide in layers—up to 100 μ on 100 μ diameter particles—has been achieved for the first time.

NUMEC has led in the development of processes for both single and multilayer coatings of spherical particles. Included in the list of coatings successfully applied are zirconium oxides, alumina, molybdenum, niobium, vanadium, chromium, pyrolytic graphite, beryllium, and tungsten. Duplex and multilayer coatings of molybdenum and niobium metal and alloys also have been applied to spherical particles. Commercial production capability for these coatings now is available at the Apollo plant.

Sapphires to Protect Phone Satellites from Space Hazards

Thousands of pieces of man-made sapphire will cover the surface of the communications satellites now being developed by Bell Telephone Laboratories, company president James B. Fisk said recently. The sapphires are expected to protect

CATALYST CHEMIST

WANTED: To operate in fuel cell area, physical chemist skilled in the measurement of physical and chemical parameters of solid catalysts. Either university or industrial background acceptable provided there is good knowledge of absorption processes and chemical kinetics.

Resume should include educational background and complete details of previous experience.

All qualified applicants will receive consideration for employment without regard to race, creed, color, or national origin.

Onan-Division of Studebaker-Packard Corporation

Minneapolis 14, Minnesota

Prime career openings in California for

PHYSICAL CHEMISTS
ELECTROCHEMISTS
ELECTROANALYTICAL CHEMISTS

with experience in electrochemistry, surface chemistry or photochemistry.

Present programs include fundamental research on phenomena related to fuel cells and other galvanic systems and investigations of electrode kinetics, polarization phenomena, catalysis and electroanalytical techniques.

Astropower, Inc. is an expanding research and development organization located close to the watersport vacationland of Newport Beach. This community is fast becoming one of the nation's leading research centers and is adjacent to a future site of a major University of California campus. It is only 40 miles from Los Angeles.

Qualified applicants are invited to submit resumes to Dr. George Moe, Vice-President Research, at the address below. Qualified applicants will receive consideration without regard to race, creed, color or national origin.

ASTROPOWER, INC.

A subsidiary of The Douglas Aircraft Company, Inc.

2968 Randolph Avenue Costa Mesa, California

solar cells from space radiation, enabling "working" telephone satellites to endure the rigors of space for 10 years or more.

The Bell System previously has announced plans to develop a satellite communication system and put it into operation as soon as possible. A ground station in Maine will be ready early next year. The first test satellite will be ready at the same time if the Government designates a launching vehicle soon. The Bell System has offered to pay costs of the rocket and launching.

The first experimental phone satellite will be roughly spherical, but may have as many as 60 flat surfaces or gem-like facets. The solar cells on each facet would receive an equal amount of light. The solar cells, invented at Bell Labs., are small silicon wafers mounted on the outside surface to convert sunlight to electricity. The sapphire sheathing will protect the solar cells from the deteriorating effects of electron bombardment in space, and will reduce the effects of proton bombardment.

Protective materials other than sapphire are not being ignored, although sapphire appears most promising. The cost is not prohibitive; sapphire will convey heat away; it overcomes the effects of very rapid and extreme changes of temperature in space; being hard, it will resist erosion by micrometeorites.

Bell Labs. engineers plan to use their first experimental satellite both to take additional measurements of space radiation and to serve as a first "real-life test" of components planned for a working satellite system.

Meetings of Other Organizations

Oct. 4-6—National Association of Corrosion Engineers, Western Regional Conference, Hotel Multnomah, Portland, Ore.

Oct. 9-11—National Association of Corrosion Engineers, North Central Regional Conference, Chase-Park Plaza Hotel, St. Louis, Mo.

Oct. 9-13—American Rocket Society, Space Flight Report to the Nation, New York Coliseum, New York, N. Y.

Oct. 30-Nov. 2—National Association of Corrosion Engineers, Northeast Regional Conference, Hotel Statler, New York, N. Y.

Literature from Industry

Engelhard Industries Technical Bulletin (Vol. I, No. 4). This 56-page issue summarizes precious metals reaches in six fields by scientists of Engelhard Industries, Inc. Copies of the bulletin are available from Technical Service Dept., Engelhard Industries, Inc., 75 Austin St., Newark 2, N. Y.

Employment Situations

Positions Available

Four challenging research positions for experienced surface chemists, in fully-equipped laboratory devoted to research and development on aluminum and copper alloys, involving: A. Electrochemical kinetics, adsorption, and oxide film structure investigations related to finishing processes. B. Studies of interfacial surface reactions between polymeric resins and metal oxide surfaces relating to strength and permanence of joints in the adhesive bonding of metals. C. Mechanisms relating to surface phenomena, associated with liquid metal-solid metal inter-action as applied to soldering and brazing. D. Surface and electrochemical reactions effecting the kinetics of general, localized, and stress corrosion processes. Pleasant living, with access to major university. Send reply to R. H. Endriss, Personnel Manager, Olin Mathieson Chemical Corp., 125 Munson St., New Haven, Conn.

Advertiser's Index

Astropower, Inc., Div. of Douglas Aircraft Co. 201C
Eagle-Picher Company 149C
Great Lakes Carbon Corp., Electrode Division ..... Cover 2
Onan—Div. of Studebaker-Packard Corporation 201C
Rowe Products Inc. 152C-153C
Sandia Corporation 202C
E. H. Sargent & Company 154C
Stackpole Carbon Company 151C

ELECTROCHEMIST

PhD or MS with sound theoretical background and experience in electrodeposition. For research studies and consultation on electrodeposition problems, especially those concerned with electrical contacts.

Sandia Corporation, located in Albuquerque, N. M., is engaged in research and development of nuclear weapons and other projects for the AEC. Albuquerque is a modern city of about 225,000; has an excellent climate and many cultural and recreational attractions. Winters are mild, summer nights are cool, and there's plenty of year-round sunshine. Liberal employee benefits include generous vacations, retirement and insurance plans and an educational assistance program. Paid relocation allowance.

Send resume to: **Professional Employment Section 531.**

SANDIA CORPORATION
ALBUQUERQUE, NEW MEXICO

The Electrochemical Society

Patron Members

Aluminum Co. of Canada, Ltd., Montreal, Que., Canada
International Nickel Co., Inc., New York, N. Y.
Olin Mathieson Chemical Corp., Chemicals Div., Industrial Chemicals Development Dept., Niagara Falls, N. Y.
Union Carbide Corp.
Divisions:
Union Carbide Metals Co., New York, N. Y.
National Carbon Co., New York, N. Y.
Westinghouse Electric Corp., Pittsburgh, Pa.

Sustaining Members

Air Reduction Co., Inc., New York, N. Y.
Ajax Electro Metallurgical Corp., Philadelphia, Pa.
Allen-Bradley Co., Milwaukee, Wis.
Allied Chemical Corp.
Solvay Process Div., Syracuse, N. Y.
General Chemical Div., Morristown, N. J.
Alloy Steel Products Co., Inc., Linden, N. J.
Aluminum Co. of America, New Kensington, Pa.
American Metal Climax, Inc., New York, N. Y.
American Potash & Chemical Corp., Los Angeles, Calif. (2 memberships)
American Smelting and Refining Co., South Plainfield, N. J.
American Zinc Co. of Illinois, East St. Louis, Ill.
American Zinc, Lead & Smelting Co., St. Louis, Mo.
American Zinc Oxide Co., Columbus, Ohio
M. Ames Chemical Works, Inc., Glens Falls, N. Y.
Armco Steel Corp., Middletown, Ohio
Basic Inc., Maple Grove, Ohio
Bell Telephone Laboratories, Inc., New York, N. Y. (2 memberships)
Bethlehem Steel Co., Bethlehem, Pa. (2 memberships)
Boeing Airplane Co., Seattle, Wash.
Burgess Battery Co., Freeport, Ill. (4 memberships)
Canadian Industries Ltd., Montreal, Que., Canada
Carborundum Co., Niagara Falls, N. Y.
Catalyst Research Corp., Baltimore, Md.
Columbian Carbon Co., New York, N. Y.
Consolidated Mining & Smelting Co. of Canada, Ltd., Trail, B. C., Canada (2 memberships)
Continental Can Co., Inc., Chicago, Ill.
Cooper Metallurgical Associates, Cleveland, Ohio
Corning Glass Works, Corning, N. Y.
Diamond Alkali Co., Painesville, Ohio
Dow Chemical Co., Midland, Mich.
Wilbur B. Driver Co., Newark, N. J. (2 memberships)
E. I. du Pont de Nemours & Co., Inc., Wilmington, Del.
Eagle-Picher Co., Chemical Div., Joplin, Mo.
Eastman Kodak Co., Rochester, N. Y.
Thomas A. Edison Research Laboratory, Div. of McGraw-Edison Co., West Orange, N. J.
Electric Auto-Lite Co., Toledo, Ohio
C & D Division, Conshohocken, Pa.
Electric Storage Battery Co., Yardley, Pa.
Engelhard Industries, Inc., Newark, N. J. (2 memberships)
The Eppley Laboratory, Inc., Newport, R. I. (2 memberships)
Exmet Corp., Tuckahoe, N. Y.
Fairchild Semiconductor Corp., Palo Alto, Calif.
Food Machinery & Chemical Corp.
Becco Chemical Div., Buffalo, N. Y.
Westvaco Chlor-Alkali Div., South Charleston, W. Va.
Foote Mineral Co., Paoli, Pa.
Ford Motor Co., Dearborn, Mich.
General Electric Co., Schenectady, N. Y.
Chemistry & Chemical Engineering Component, General Engineering Laboratory
Chemistry Research Dept.
General Physics Research Dept.
Metallurgy & Ceramics Research Dept.
Aircraft Accessory Turbine Dept., West Lynn, Mass.
General Instrument Corp., Newark, N. J.
General Motors Corp.
Allison Div., Indianapolis, Ind.
Delco-Remy Div., Anderson, Ind.
Guide Lamp Div., Anderson, Ind.
Research Laboratories Div., Warren, Mich.

(Sustaining Members cont'd)

General Telephone & Electronics Laboratories Inc., Bayside, N. Y. (2 memberships)
Gillette Safety Razor Co., Boston, Mass.
Globe-Union, Inc., Milwaukee, Wis.
Gould-National Batteries, Inc., Minneapolis, Minn.
Grace Electronic Chemicals, Inc., Baltimore, Md.
Great Lakes Carbon Corp., New York, N. Y.
Hanson-Van Winkle-Munning Co., Matawan, N. J. (2 memberships)
Harshaw Chemical Co., Cleveland, Ohio (2 memberships)
Hercules Powder Co., Wilmington, Del.
Hewlett-Packard Co., Palo Alto, Calif.
Hill Cross Co., Inc., West New York, N. J.
Hoffman Electronics Corp., Semiconductor Div., El Monte, Calif. (2 memberships)
Hooker Chemical Corp., Niagara Falls, N. Y. (3 memberships)
Hughes Aircraft Co., Culver City, Calif.
International Business Machines Corp., Yorktown Heights, N. Y.
International Minerals & Chemical Corp., Skokie, Ill.
ITT Federal Laboratories, Div. of International Telephone & Telegraph Corp., Nutley, N. J.
Jones & Laughlin Steel Corp., Pittsburgh, Pa.
K. W. Battery Co., Skokie, Ill.
Kaiser Aluminum & Chemical Corp.
Div. of Chemical Research, Permanente, Calif.
Div. of Metallurgical Research, Spokane, Wash.
Kawecki Chemical Co., Boyertown, Pa.
Kennecott Copper Corp., New York, N. Y.
Libbey-Owens-Ford Glass Co., Toledo, Ohio
Lockheed Aircraft Corp., Missiles & Space Div., Sunnyvale, Calif.
Mallinckrodt Chemical Works, St. Louis, Mo.
P. R. Mallory & Co., Indianapolis, Ind.
Merck & Co., Inc., Rahway, N. J.
Metal & Thermit Corp., Detroit, Mich.
Miles Chemical Co., Div. of Miles Laboratories, Inc., Elkhart, Ind.
Minnesota Mining & Manufacturing Co., St. Paul, Minn.
Monsanto Chemical Co., St. Louis, Mo.
Motorola, Inc., Chicago, Ill.
National Cash Register Co., Dayton, Ohio
National Lead Co.. New York, N. Y.
National Research Corp., Cambridge, Mass.
National Steel Corp., Weirton, W. Va.
North American Aviation, Inc., Rocketdyne Div., Canoga Park, Calif.
Northern Electric Co., Montreal, Que., Canada
Norton Co., Worcester, Mass.
Ovitron Corp., Long Island City, N. Y.
Peerless Roll Leaf Co., Inc., Union City, N. J.
Pennsalt Chemicals Corp., Philadelphia, Pa.
Phelps Dodge Refining Corp., Maspeth, N. Y.
Philco Corp., Research Div., Blue Bell, Pa.
Philips Laboratories, Inc., Irvington-on-Hudson, N. Y.
Pittsburgh Plate Glass Co., Chemical Div., Pittsburgh, Pa.
Potash Co. of America, Carlsbad, N. Mex.
Radio Corp. of America
Tube Div., Harrison, N. J.
RCA Victor Record Div., Indianapolis, Ind.
Ray-O-Vac Co., Madison, Wis.
Raytheon Co., Waltham, Mass.
Reynolds Metals Co., Richmond, Va.
Rheem Semiconductor Corp., Mountain View, Calif.
Schering Corporation, Bloomfield, N. J.
Shawinigan Chemicals Ltd., Montreal, Que., Canada
Speer Carbon Co.
International Graphite & Electrode Div., St. Marys, Pa.
Sprague Electric Co., North Adams, Mass.
Stackpole Carbon Co., St. Marys, Pa.
Stauffer Chemical Co., New York, N. Y.
Tennessee Products & Chemical Corp., Nashville, Tenn.
Texas Instruments, Inc., Dallas, Texas
Metals and Controls Corp., Attleboro, Mass.
Three Point One Four Corp., Yonkers, N. Y.
Titanium Metals Corp. of America, Henderson, Nev.
Tung-Sol Electric Inc., Newark, N. J.
Udylite Corp., Detroit, Mich. (4 memberships)
Universal-Cyclops Steel Corp., Bridgeville, Pa.
Upjohn Co., Kalamazoo, Mich.
U. S. Steel Corp., Pittsburgh, Pa.
Victor Chemical Works, Chicago, Ill.
Western Electric Co., Inc., Chicago, Ill.
Wyandotte Chemicals Corp., Wyandotte, Mich.
Yardney Electric Corp., New York, N. Y.